Report

Experiment analysis; the relation between wave loading and resulting strain in an asphaltic concrete revetment

Master Thesis

By M.P. Davidse

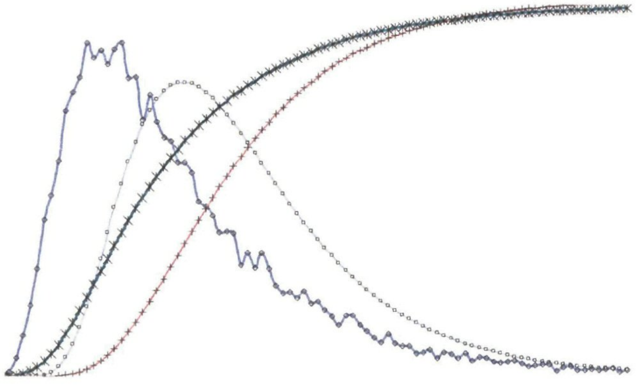

Delft University of Technology
Faculty of Civil Engineering
Section Hydraulic Engineering

March, 2009

Graduation committee:

Prof. drs. ir. J.K. Vrijling
Hydraulic Engineering, TU Delft

Ir. H.J. Verhagen
Hydraulic Engineering, TU Delft

Ir. M.F.C. van de Ven
Road and Railway Engineering, TU Delft

Ing. A.K. de Looff
KOAC • NPC

KOAC • NPC
we keep you moving

TU Delft
Delft University of Technology

Preface

This report is the result of the research performed for my master thesis at the faculty of Civil Engineering and Geosciences of Delft University of Technology.

The research is concentrated on finding the relation between wave loading and strain at the underside of an asphalt revetment constructed in the Delta flume experiment in the year 1991. In the experiment the loading on the asphalt revetment is measured in combination with the resulting deformation of the asphalt layer. By simulation with a Monte Carlo analysis, the strain is recalculated trying to bring together the measurements and calculations earlier performed by others.

This research has been performed in conjunction with KOAC•NPC, research and consultancy company on asphaltic revetments. I am very grateful to KOAC•NPC for making available the facilities, the knowledge and support while writing the thesis. My gratitude especially goes to Arjan de Looff whose door was never closed when I had some questions, for the support and guidance he gave me in the research progress.

Also I like to thank my wife Coralien and my parents for the support they gave me during my study at Delft University of Technology.

Rien Davidse,

March, 2009

Summary

This report describes the analysis of a Delta flume experiment on an asphaltic concrete revetment performed in the year 1991. In the experiment the strain at the underside of the revetment is measured together with the deflection of the revetment and the wave impact pressure which causes the strain. In the years after the experiment some researchers analyzed the experiment aiming to model and calculate the relation between the wave impact and the strain. In this thesis the model used by these researchers is used in a statistic approach recalculating the strain.

In the year 1991 the Technical Advisory Commission (TAW-A4) ordered a full scale investigation on wave impacts on an asphaltic concrete revetment. The goal of the experiment was to gain insight into the mechanisms which would lead to failure, cracking of the revetment. Also the behaviour of the revetment after failure (residual strength) was studied. To gain inside in the behaviour of the revetment strain measuring devices and pressure transducers are placed into the revetment. The measured strains are compared with calculated strains by several researchers. One of the researchers concluded that there was almost no resemblance between the measured and calculated strain and recommended to perform a sensitivity analysis on the calculations. This conclusion and recommendation is what resulted into the subject of this thesis.

Due to extensive testing of materials in the last fifteen years a better understanding of material behaviour is achieved. This concerns in particular the modulus of elasticity of asphaltic concrete and the modulus of subgrade reaction. This knowledge is used in this thesis to get new results, by recalculation, from the same model.

To perform a sensitivity analysis a stochastic simulation is used. A choice is made for using the Monte Carlo method for simulation of the strains and the results of the simulations are compared with the measured strains.

The conclusions are divided into conclusions regarding the recalculation and conclusions regarding the Monte Carlo simulation. In the recalculation a better agreement between the measured and calculated strain is obtained. The model describes the calculated dynamic strain in a good way. This is also concluded by Ruygrok, one of the researchers who also investigated this Delta flume experiment. The simulated strains calculated with the Monte

Carlo method are not in agreement with the measured strains. The difference between the calculation and the measurements are assigned to the differences between the quasi-static and the dynamic strain. Another reason for the differences is that the information of the wave impacts stored in the impact factor distribution cannot be divided into time and space, which leads to a too rough approach in the simulation.

It is recommended to investigate the relation between the quasi-static or dynamic strain with the total strain. If the quasi-static strain adds extra damage to the revetment this part should be taken into account when a safety assessment is performed.

Samenvatting

Dit rapport beschrijft een analyse van een experiment uitgevoerd in the Deltagoot in het jaar 1991. In de Deltagoot een asfaltbeton bekleding is belast onder golfaanval waarbij de rekken en de doorbuiging van de bekleding zijn gemeten. In de jaren na het experiment hebben een aantal onderzoekers het experiment geanalyseerd en gemodelleerd met de bedoeling de relatie tussen gemeten en berekende rekken vast te leggen. In dit afstudeerrapport hetzelfde model als de onderzoekers is gebruikt in een statistische benadering waarmee de rekken opnieuw berekend zijn.

In het jaar 1991 gaf de Technische Adviescommissie voor Waterkeringen (TAW-A4) opdracht tot het uitvoeren van een experiment waarbij een taludverdediging van asfaltbeton aangebracht op een dijklichaam is belast onder golfaanval. Het doel van het experiment was om inzicht te krijgen in welk faalmechanisme tot bezwijken van de bekleding zou leiden. Ook het gedrag van de bekleding na falen (reststerkte) is bestudeerd. Om inzicht te krijgen in het gedrag van de bekleding zijn rekopnemers en drukopnemers in het asfalt geplaatst. De gemeten rekken zijn vergeleken met de berekende rekken door verschillende onderzoekers. Eén van de onderzoekers concludeerde dat er nauwelijks sprake was van overeenkomst tussen gemeten en berekende rekken. Deze onderzoeker gaf ook de aanbeveling om een gevoeligheidsanalyse uit te voeren naar de berekeningen. Deze conclusie en aanbeveling samen met andere heeft geleid tot het onderwerp van dit afstudeerrapport.

Doordat er in de laatste vijftien jaar veel aan het testen van materialen is gedaan is er meer kennis over het materiaalgedrag. Dit betreft vooral kennis over de elasticiteits modulus en de modulus van de reactie van de ondergrond. Deze kennis is gebruikt in dit afstudeerrapport om nieuwe resultaten te verkrijgen van hetzelfde model. Met deze kennis zijn de eerder berekende rekken opnieuw berekend.

Om een gevoeligheidsanalyse uit te voeren is een statistische simulatie uitgevoerd. Er is een keuze gemaakt om de Monte Carlo methode te gebruiken om de rekken te simuleren en deze te vergelijken met de berekende rekken.

De conclusies zijn opgedeeld in een deel betreffende de herberekening van de rekken en een deel betreffende de Monte Carlo simulatie. In de herberekening is een goede relatie tussen de berekening en de metingen verkregen. Dit geeft aan dat het model de gemeten dynamische

rekken goed benaderd. Dit is ook eerder geconcludeerd door Ruygrok, één van de onderzoekers die eerder een analyse van het Deltagoot experiment heeft uitgevoerd. De gesimuleerde rekken berekend met de Monte Carlo simulatie komen niet overeen met de gemeten rekken. Het verschil tussen beide word toegeschreven aan het verschil tussen quasistatische en dynamische rek. Een andere reden voor de verschillen kan liggen in de kansdichtheidsverdeling van de stootfactor. Deze verdeling van de kansdichtheid is gegeven voor verschillende drukopnemers tegelijk en voor maximale golfklappen. Hierdoor kan geen verdeling in ruimte en tijd gemaakt worden waardoor er verschillen kunnen optreden met de gemeten rekken die op een andere positie zijn gemeten dan de positie van de drukopnemers.

Er wordt aanbevolen om het verschil tussen quasistatische en dynamische rek te onderzoeken samen met de verhouding van deze twee met de totale rek. Mocht blijken dat de quasistatische rek zorgt voor extra vermoeiingsschade dan moet deze worden meegenomen in de berekening op falen volgens de toetsingsmethode.

Table of Contents

1 List of symbols and used trademarks

b	base of the prismatic load	(m)
c, k	modulus of subgrade reaction	(Pa(/m))
C_p	pressure wave propagation speed (in unsaturated soil)	(m/s)
C_s	shear wave propagation speed	(m/s)
E	modulus of elasticity	(Pa)
D_r	relative density of the subsoil	(-)
g	acceleration of gravity	(m/s^2)
G_a	shear modulus of asphalt	(Pa)
h	layer thickness	(m)
h_a	layer thickness	(m)
H	wave height	(m)
H_s	significant wave height	(m)
L_p	peak wave length	(m)
T	wave period	(s)
T_p	peak period	(s)
p_{max}	maximum pressure impact	(Pa)
p(q)	probability of occurrence of impact factor q	(-)
q, S, S_f	impact factor $q = \frac{p_{max}}{\rho g H}$	(-)
q_α	impact factor for slope α	(-)
q_{gem}	the mean impact factor	(-)
$q_{n\%}$	impact factor with frequency of exceedance of n%	(-)
q_r	impact factor for slope 1:4	(-)
z	half of the base of the prismatic load (b/2)	(m)
α	slope angle	(-)
$\xi_0 = \frac{\tan(\alpha)}{\sqrt{H_0 / L_0}}$	surf similarity parameter based on deep water wave height (H_0)	(-)
$\xi_b = \frac{\tan(\alpha)}{\sqrt{H_b / L_0}}$	surf similarity parameter based on breaking water wave height (H_b)	(-)
φ	pressure height with respect to the slope	(m)
σ	the tension at underside of the revetment	(Pa)
ν	Poisson's contraction coefficient for asphalt	(-)
ρ_w	density water	(kg/m^3)
ρ_n	density saturated soil	(kg/m^3)
ρ_a	density of air	(kg/m^3)

$\chi = \frac{H}{gT^2}$	wave steepness parameter	(-)
p_{max}	highest measured impact pressure during wave impact measured by one pressure transducer	
$P_{max.max}$	highest measured impact pressure during wave impact measured by all pressure transducers	
DRO	pressure transducer number used in the Delta flume experiment	
VLP	number 1 till 8; strain measuring device, number 9 till 12; deflection measuring device, used in the Delta flume experiment	
x-direction	direction in wave direction (length of the flume) (see section 3.2)	
y-direction	perpendicular (horizontal) to x-direction (width of the flume)	
z-direction	vertical direction, height with respect to the bottom of the flume	

Here a list of Dutch words is given with there translations:

klap	-	impact
goot	-	flume
bodem	-	bottom
niveau	-	level
meting	-	measurement
afstand	-	distance
tijd	-	time
overschrijdingspercentega	-	exceedance precentage
stootfactor	-	impact factor
(rek)amplitude	-	(strain) amplitude
(deflectie)amplitude	-	(deflection) amplitude
verdeling	-	distribution
golven	-	waves
(on)regelmatig	-	(ir)regular
proef	-	test, run
druk	-	pressure
berekend	-	calculated

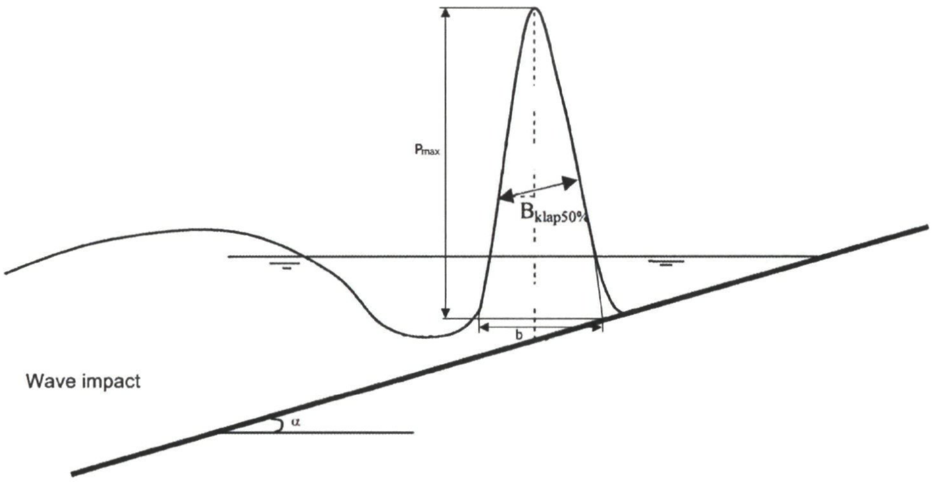

Figure 1-1 Used symbols and definitions

The use of trademarks in any publication of Delft University of Technology does not imply any endorsement or disapproval of this product by the University.

2 Introduction and problem description

2.1 Introduction

In the final stage of the master programme Hydraulic Engineering an investigation is executed. This report is the result of this investigation where the relation between occurring strain due to wave loading and calculated strain is studied. To increase knowledge about the relation between wave loading and occurring strain a full scale experiment is performed in the year 1991 ordered by the technical advisory committee on water defences. In the experiments the wave loading is measured by pressure transducers and the behaviour of the asphalt revetment is measured by deflection meters and strain measuring devices.

The experiment is described by Derks and Klein Breteler (1992). Also an analysis is done by de Waal (1993) where an attempt is made to calculate the measured strain. It appeared to be difficult to recalculate the strain because of the many uncertainties involved in the calculation. Because of these uncertainties a recommendation done by de Waal is to recalculate the occurring strain by statistical analysis. This recalculation is the subject of this master thesis.

In chapter five the calculation done by de Waal (1993) is described and in chapter seven the formula used by de Waal is derived. The research done by de Waal can be schematized in a flow chart.

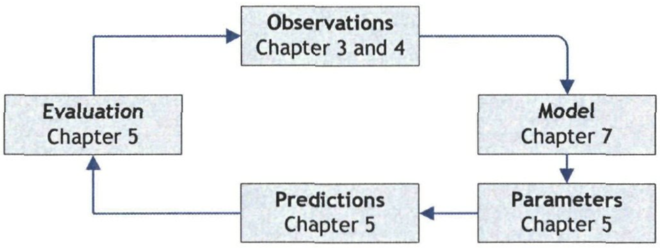

Figure 2-1 Flow chart of the research done by de Waal

The result of the analysis of de Waal (1993) was disappointing so in this thesis a reanalysis is performed where other descriptions for the input parameters of the model are used.

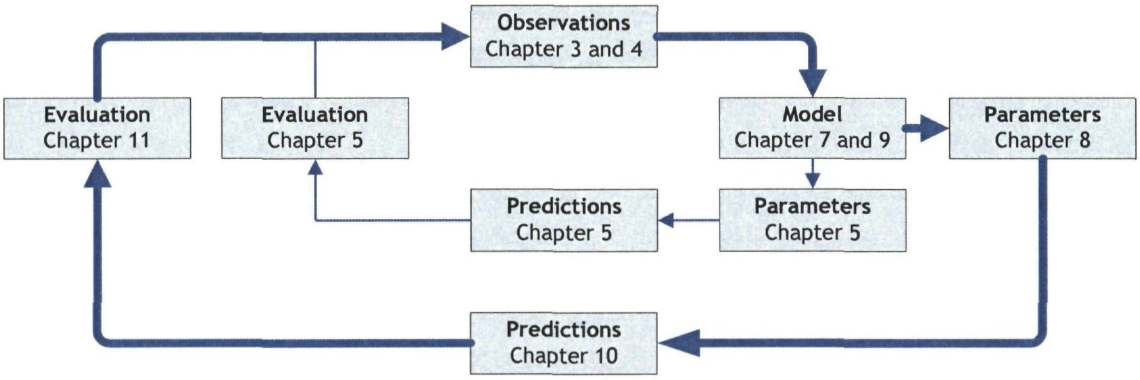

Figure 2-2 Flow chart used in this thesis

In the next three sections the problem is summarized, the assignment is formulated and the conditions for this study are given. In the chapters three, four and five the experiment that was carried out in 1991 is described. In the chapters three and four the report of Derks and Klein Breteler is summarized. In chapter five the analysis of de Waal is summarized. Chapter six describes the conditions under which the Monte Carlo simulation is executed. In this chapter some of the conditions described by de Waal are used or discussed. In this study the problem is analyzed using a Monte Carlo simulation. Chapter seven describes the function of the Monte Carlo simulation. Also in this chapter the formula for calculating the strain is derived with the use of a report produced by 't Hart (2008). In chapter eight the probability functions for the different parameters that are needed for calculating the strain are constructed. In this chapter results from measurements, knowledge obtained by KOAC•NPC and advice from the graduation committee is used for the construction of the probability functions. Chapter nine describes the simulation set-up. This chapter gives the reader insight in the procedure that is followed to get the simulation results. The result of the simulation is presented in chapter ten. These results are compared with the measurements and a sensitivity analysis is executed. Chapter eleven gives the final conclusions with the recommendations for both practical use and further investigation.

2.2 Problem description

In practise asphalt dike revetments are designed and evaluated with the computer program GOLFKLAP. In the program the revetment is schematized as an elastic beam supported by springs (Winkler foundation). De Waal (1993) used this principle to calculate strains and compared these with the measured strain in the Delta flume. When the report of de Waal (1993) is studied one finds a disappointing conclusion in which is stated that no good relation between measured and calculated strain could be found. Because of this conclusion the question arose how to come to a better relation or how to quantify the relation between the measured and calculated strain. Also a lot of uncertainties in the used parameters were recognized.

2.3 The assignment

To recalculate the strain information about the waves, the resulting pressure on the slope and information about the revetment and the subsoil should be known. Also the relation between the wave load and the resulting reaction of the construction should be known. In this investigation all the available information of the waves is used to set up a probability distribution function. Also information about the material properties and the subsoil properties are searched for. The probability functions are used to recalculate the strains and are compared with the measured strains.

2.4 Conditions for this study

The first obvious condition is the (limited) material that is available. The report produced by Derks and Klein Breteler, de Waal, Ruygrok and the report with the laboratory results of the asphalt cores is the only available information about the Delta flume experiment there is. No data sets of measurements are available so the figures and tables presented in these report are used to determine what the wave conditions, the spacing of the measuring devices etc. were. In chapter six the conditions for the simulation and calculations are stated.

2.5 References

DE WAAL, J.P. (1993) Gedrag van asfaltbekleding onder golfaanval, Relatie tussen belasting en rek (in Dutch)(Report H 1702), *DWW Rijkswaterstaat, Delft*

DERKS, H. AND KLEIN BRETELER, M. (1992) Gedrag van asfaltbekleding onder golfaanval, verslag modelonderzoek in Deltagoot, with annexes (in Dutch)(Report H 1480), *DWW Rijkswaterstaat, Delft*

RUYGROK, P.A. (1991) Parameterbepalingen voor het zand en de asfaltbekleding van het TAW A4 Dijkmodel in de Deltagoot (in Dutch)(Report CO-324970/7), *Grondmechanica Delft, Delft*

RUYGROK, P.A. (1994) Dimensioneren van asfaltbekledingen op golfklappen, analyse van de relatie tussen golfbelasting en rekken, with annexes (in Dutch)(Report CO-347160/17), *Grondmechanica Delft, Delft*

'T HART, R (2008) Scheur ten gevolge van golfbelasting in een al gescheurde asfaltbekleding (Report 435340-0004 v01) (in Dutch), *Stowa, Utrecht*

VERSLUIS, A. (1991) 3-puntsbuigproeven aan balken van boorkernen uit de deltagoot (Report 91523-2 or DWW-504)(In Dutch), *Netherlands Pavement Consultants, Hoevelaken*

3 Background information of the Delta flume experiment

3.1 Introduction

In this chapter and the next the experiment and set-up and the measurements are described. The information described in these chapters is gained from the report composed by Derks and Klein Breteler in the year 1992. The figures found in these chapters are also copied from this report (Derks and Klein Breteler (1992)) although relevant words in these figures are translated for the foreign reader.

3.2 The dike body

The experiment is performed in the Delta Flume. The body of the dike consisted of two types of sand. The inner part consisted of sand coming from a depot. The outer part of the body, at least 4m, normally measured, consisted of sand from the Delta Flume itself. The sand is carefully placed in the flume in a 1:4 slope measuring the humidity and the condensation.
After installing the sand body, the asphalt layer is constructed. The layer thickness was 0,15 m at the left side and 0,25 m at the right side of the flume (looking in wave direction)(see figure below). These sides are separated by a hollow steel casing which is used to place the measuring devices (the measuring beam).

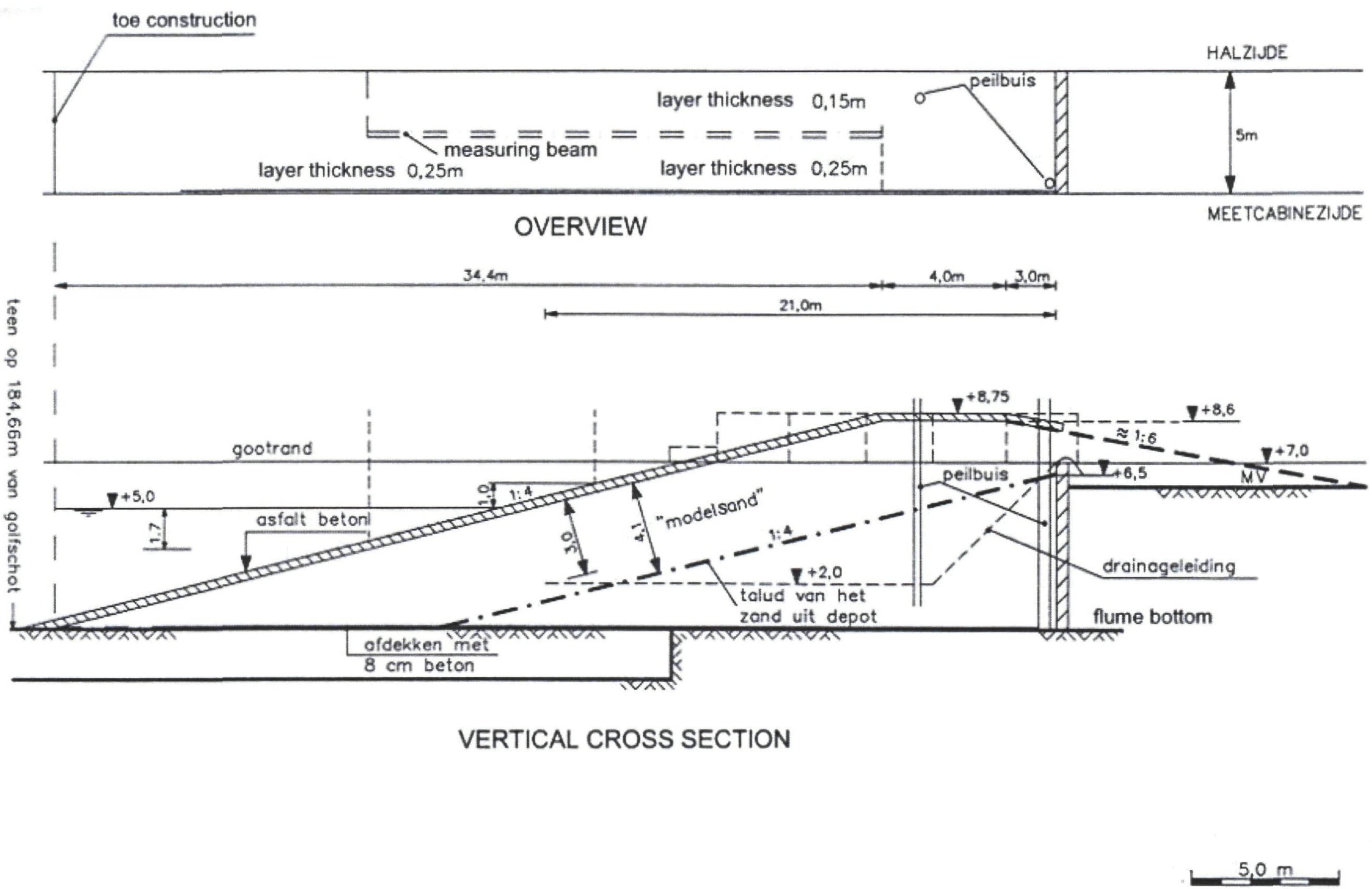

Figure 3-1 Vertical cross section and overview of the dike body

To place the measurement devices like the pressure transducers and deflection meters which are not in the measuring beam, cores are sawed out of the revetment. These cores are used to determine the properties of the asphalt revetment.

3.3 Instruments used

The following instruments are used:

- pressure transducers, to determine the wave pressure
- water pressure meters, to determine the water pressure in the sand body
- deflection meters, to measure the displacement of the asphalt revetment under wave loading are placed inside the revetment measuring the deflection of the top
- strain measuring devices, to determine the deformation of the asphalt revetment under wave loading are placed inside the revetment about 1.5 - 2.5 cm from the bottom of the revetment

The measuring beam is placed in the axis of the flume at +3.31 m till +5.13 m from the bottom of the flume. The measuring beam contained 25 pressure transducers.

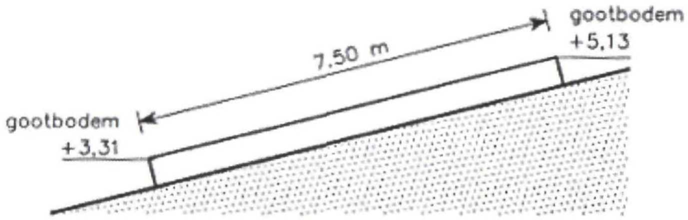

SIDEVIEW MEASURING BEAM

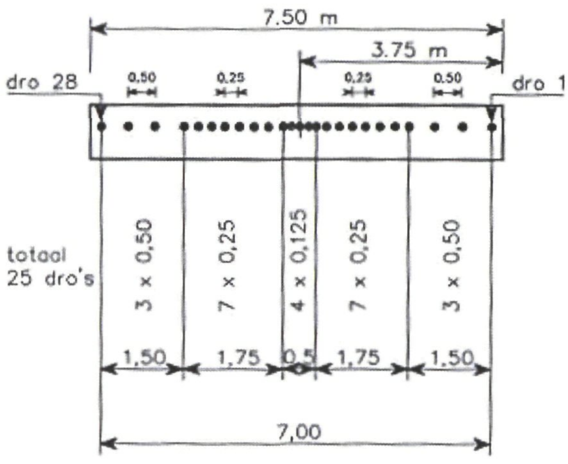

POSITION PRESSURE TRANSDUCER IN MEASURING BEAM

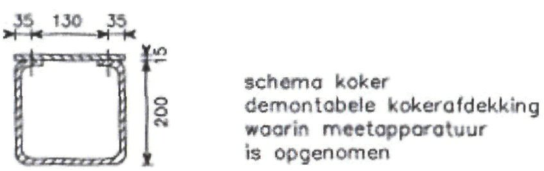

CROSS SECTION MEASURING BEAM

Figure 3-2 Measuring beam details

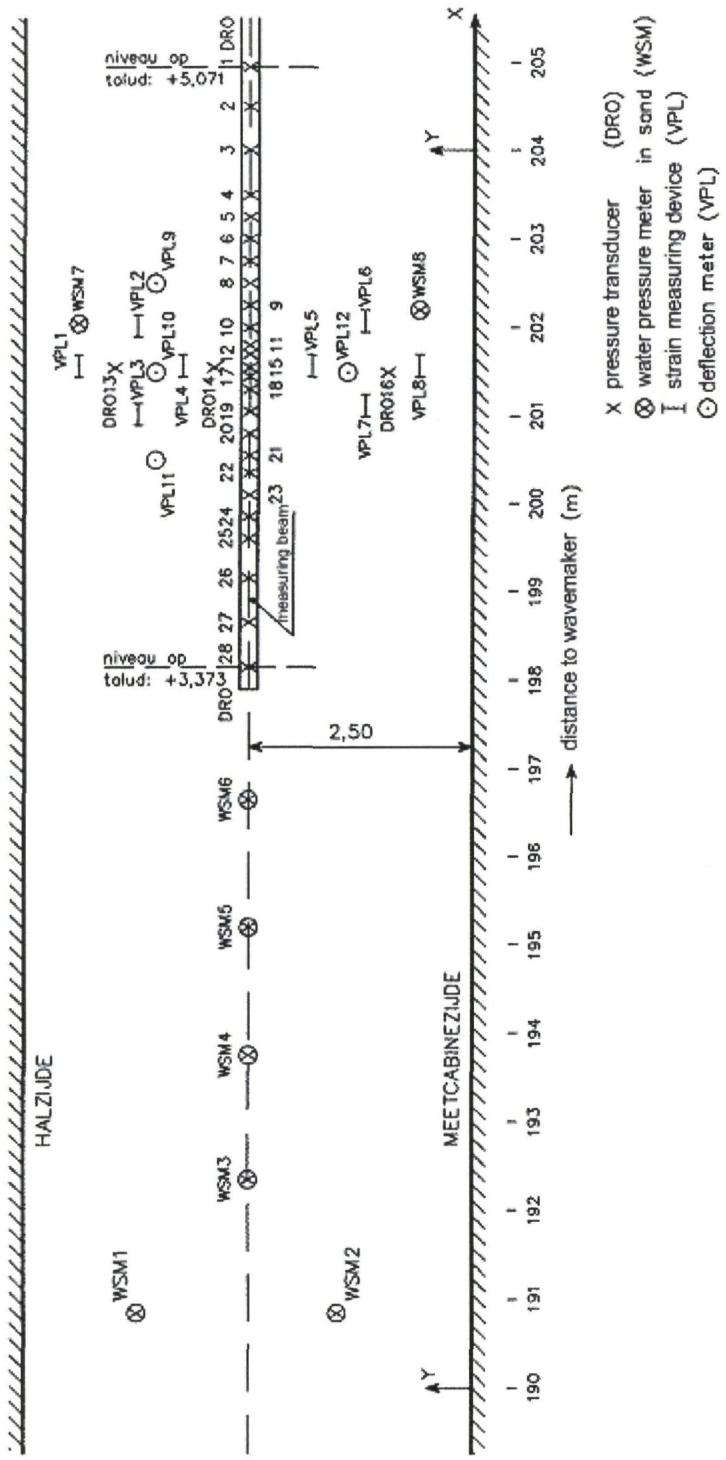

Figure 3-3 Top view of the Delta flume, location of the measuring devices

The connection between the asphalt layer and the measuring beam is made sandtight, watertight and flexible by using rubber mastic. This rubber mastic made the measuring beam and the asphalt revetment stick together. Also at the connection between the revetment and the flume wall this rubber mastic is used although first for protection of the flume wall triplex plates are glued to the flume wall at the connection spot. Both connections appeared to be sand- and watertight.

To record the data a sampling frequency of 100 Hz is used. For 10 measuring devices a sampling frequency of 1000 Hz is used.

3.4 The test runs

First a test run is performed to check whether the strain measuring devices and the deformation meters were functioning. Two concrete blocks were placed on a wooden beam and the defection and strain was measured (test run AS001 till AS012). Next some tests runs are performed to check all the measuring devices. Each day a series of runs are performed. The first three series were executed manly with regular waves, the fourth and the fifth also with a Pierson-Moskowitz spectrum. The duration of most of the runs was 900 s, where the part in the spectrum with the highest waves was chosen. This is important to know for statistical analysis. The series with the executed dates are given in Table 3-1.

Table 3-1 Experiment conditions

Datum	Test number	Spectrum type or Regular waves	H_s,H (m)	T_p,T (s)	Waterlevel in flume (m)	Waterlevel in sand (m)	Duration measurement (s)	$\frac{H}{gT^2}$ (-)	Δh (m)
10/9	**Testing the devices with concrete blocks Slope measurement number 1**								
11/9	AS 021	R	0,97	4,0	+4,68	+2,0	900	0,0062	0,33
	AS 022	R	1,05	5,0	+4,71	+2,0	900	0,0042	0,51
	AS 023	R	1,06	6,0	+4,69	+2,0	900	0,0030	0,69
	AS 024	PM	1,23	4,72	+4,68	+2,0	900		
12/9	AS 104	R	1,17	7,0	+4,90	+2,0	900	0,0024	0,95
	AS 106	R	1,54	5,0	+4,89	+2,0	900	0,0063	0,59
	AS 107	R	1,61	6,0	+4,88	+2,0	900	0,0046	0,82
	AS 108	R	1,75	7,0	+5,11	+2,0	600	0,0036	1,04
	AS 111	R	1,69	6,0	+5,09	+2,0	900	0,0048	0,78
13/9	AH 108	R	1,45	7,0	+5,28	+2,0	900	0,0030	0,99
	AS 105	R	1,07	8,0	+5,27	+2,0	900	0,0017	1,19
	AS 109	R	1,47	8,0	+5,37	+2,0	900	0,0023	1,46
	AS 113	R	1,60	8,0	+5,40	+2,0	900	0,0026	1,17
16/9	AS 025	PM	0,89	7,6	+5,21	+2,0	900		
	AS 202	PM	1,43	7,14	+5,01	+2,0	5400		
17/9	AS 203	PM	1,52	8,65	+5,10	+2,0	5400		
	AS 117	R	1,80	5,0	+4,89	+2,1	900	0,0073	0,65
	AS 116	R	1,73	4,0	+4,81	+2,3	900	0,0110	0,52
	AS 118	R	1,47	4,0	+4,76	+2,7	900	0,0094	0,52
18/9	**Slope measurement number 2 and 3**								
20/9	AS 301	R	1,52	6,0	+5,11	+5,0	900	0,0043	0,74
	AS 401	PM	1,51	8,65	+5,10	+5,0	5400		
	AS 402	Duits	1,34	7,8	+4,74	+4,75	727		
23/9	**Slope measurement number 4**								
23/9	AS 501	PM	1,48	8,65	+5,08	+4,2	5400		
	AS 502	PM	1,48	8,65	+5,08	+4,2	5400		
24/9	AS 503	PM	1,49	8,65	+5,08	+4,2	5400		
	AS 504	PM	1,49	8,65	+5,08	+4,2	5400		
25/9	**Slope measurement number 5**								
25/9	AS 601	PM	0,76	2,98	+4,65	+3,3	3600		
	AS 602	PM	1,49	8,65	+4,97	+3,4	5300		
26/9	**Slope measurement number 6**								
27/9	AS 603	PM	1,49	8,65	+5,10	+3,4	4480		
27/9	**Slope measurement number 7**								
30/9	**Slope measurement number 8 and 9**								

This table shows the differences between the run. The freatic line was kept low during the first five series, no real damage occurred. The slope measurements show maximum displacements of 0.01 m which is between the boundaries of measurement errors. The series six and seven were executed with a heightened freatic level. This level was about the same as the water level in the flume. The asphalt revetment was deformed after these series. The maximum deformation was about 0.03 - 0.04 m.

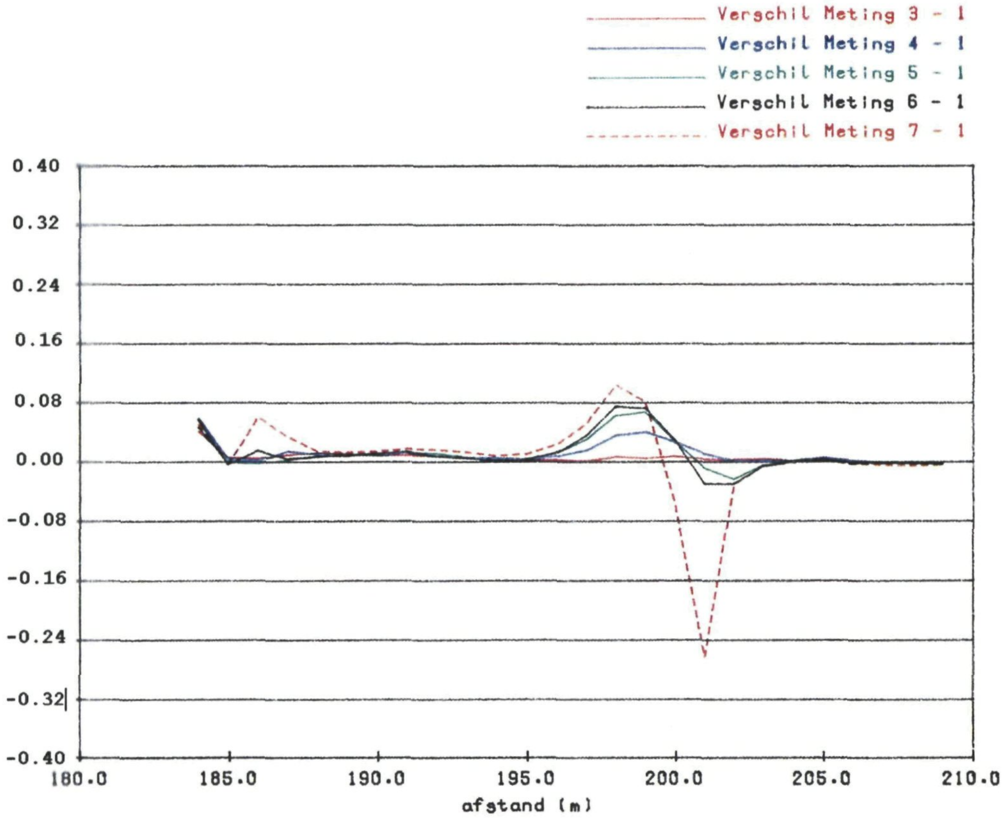

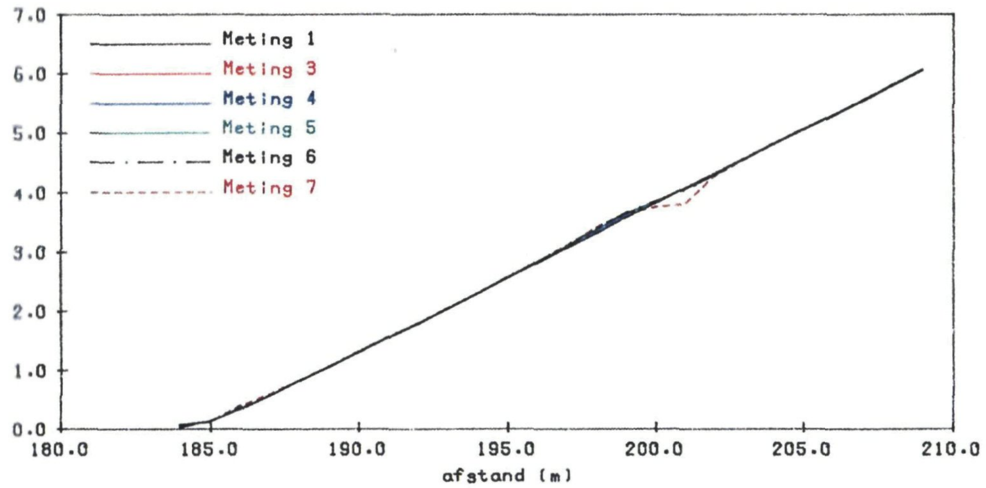

Figure 3-4 Slope deformations measured after several runs

Measurement five and six and seven are performed on an artificially damaged slope and will not be treated in this thesis.

3.5 References

Derks, H. and Klein Breteler, M. (1992) Gedrag van asfaltbekleding onder golfaanval, verslag modelonderzoek in Deltagoot (in Dutch)(Report H 1480), *DWW Rijkswaterstaat, Delft*

4 Measurements in the Delta flume experiment

4.1 First approach

In the analysis of the experiment at first the extreme wave impacts with the resulting deflection and strain is studied. The relation between the local measured pressure loads and deflection/ strain within a measurement run is first studied. Initially the pressure and the measured deflection/ strain were coupled. This revealed the problem that some wave impacts caused permanent deformations and had positive and negative deformation/ strain at different heights as result.

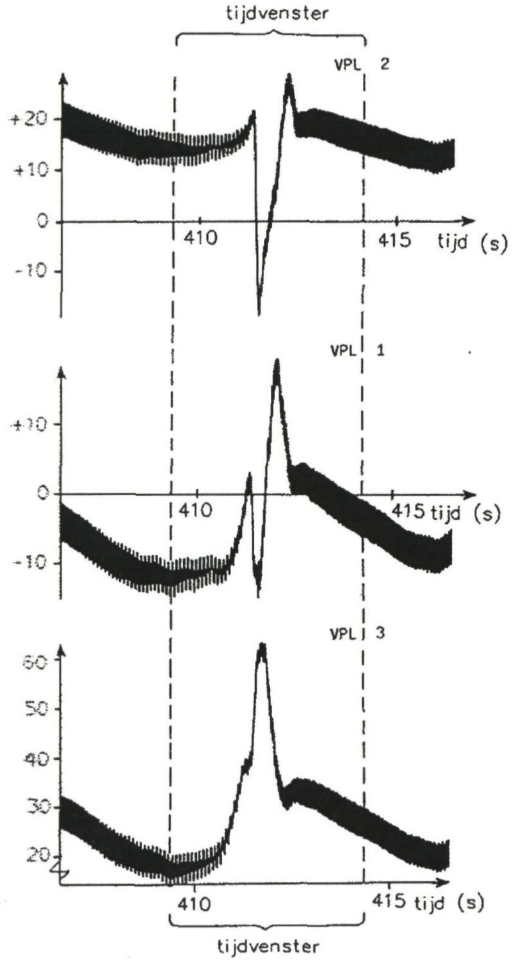

Figure 4-1 Measured strain (in μm) at different heights upslope (run AH108, 406.5<t<416.5 s)

This figure shows the difference in strain at different heights in the same time interval. To cope with this problem of positive and negative strain, a choice is made to use the amplitude of the deformation/ strain which corresponds with the occurred wave impact. To make the measured deformation and strain correspondent with a wave impact a time frame around the time of maximum impact is chosen. The time frame has a length of 0.7 times the wave period T and starts at 0.3T before maximum impact. The amplitude is chosen to be the difference between the maximum and minimum within this time frame. With this as starting point the influence of the surroundings to the measurements are analyzed. Other analyzed aspects are the distribution of the wave heights and the distribution of the place of the wave impacts. The results in the report are presented as a wave pressure with respect to the still water level.

4.2 Set-up of the system of analysis of the Delta flume experiment

In the set-up of the system a division in steps is made. In this section the different steps are described.

4.2.1 Evaluation wave pressure measurements

- evaluation of the reliability of the wave pressure maxima in the measurement beam. These measurements are compared with the measurements of transducers placed in the slope

4.2.2 Tests with regular waves

- incoming wave height
- statistical distribution of the wave impact place
- statistical distribution of the impact factor, related to the incoming wave height
- for the wave impacts on the strain measuring devices, the statistical distribution of the maximum amplitude of strain and deformation, and also the maximum of the wave impacts
- per wave height for the maximum wave impact above the central strain measurement device: the values, the amplitude of the strain, the deformation and water pressures.

4.2.3 Tests with irregular waves

- statistical distribution of the wave impact place
- statistical distribution of the impact factor, related to the incoming significant wave height
- for the five maximum wave impact recordings on the central strain measurement devices, a combined analysis is made of the: wave height, pressure recording in time, maximum wave pressure recording with respect to place, strain development in time, deformation development in time and, if possible, water pressure development.

As mentioned before the maximum amplitude is used. This amplitude is the difference between maximum and minimum within a time frame at moment of impact. This time frame is 0.7 times the wave period T, starting at 0.3T before the impact.

4.3 Result of the analysis of the Delta flume experiment

4.3.1 The measuring devices

Derks and Klein Breteler (1992) concluded that the measuring frequency of 100 Hz and 1000 Hz were sufficient for measuring the wave impacts and the strain and deflection measurements. This because almost no differences in extreme values were measured between the sampling rate of 100 Hz and 1000 Hz. The most common forms of the measuring signals are given in Figure 4-2.

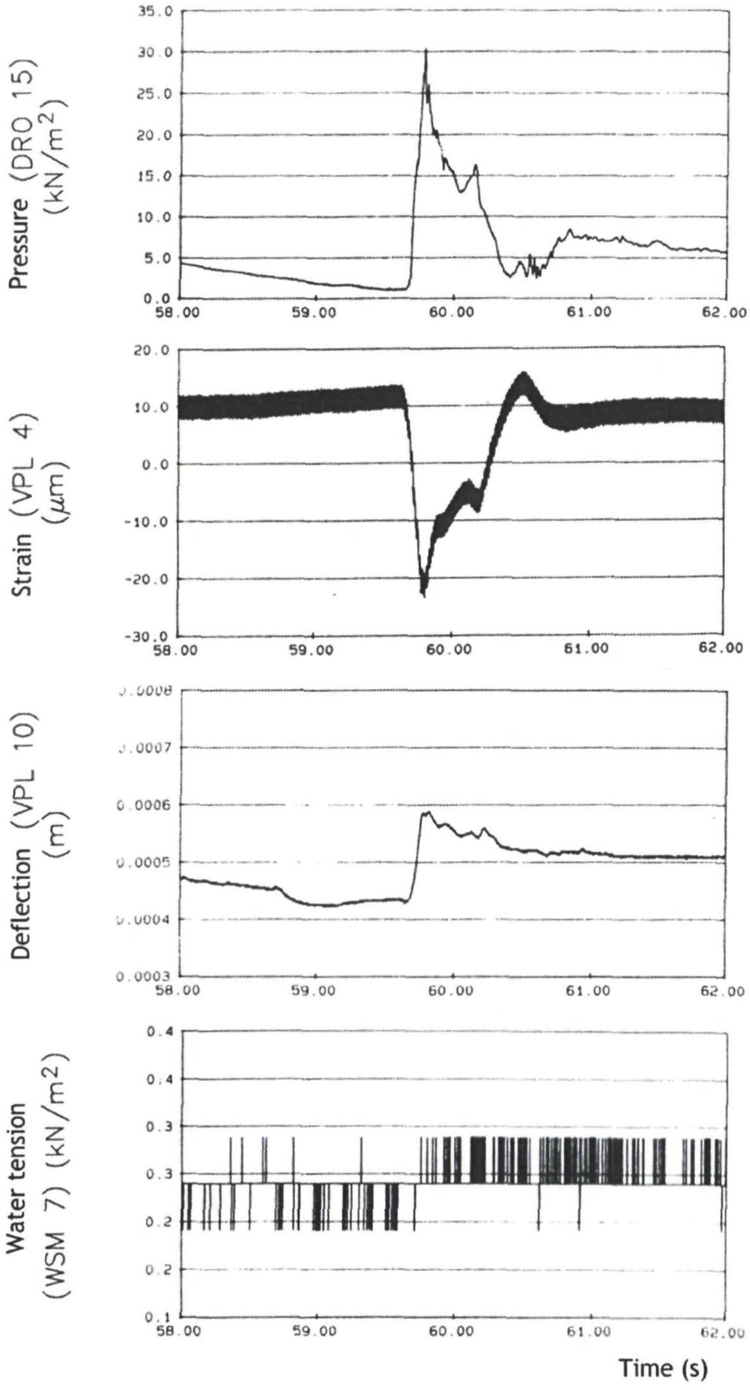

Figure 4-2 Measuring signal examples

In the approach on the relation between the measured pressure, the strain and the deflection, it was not useful to look for the maximum and minimum strain and deflection and find the belonging wave impact. It was more useful to look for the maximum impact pressure and then find the belonging strain and deflection. This because the maximum and minimum strain and deflection can be positive and negative, depending on the distance to the load, and the strain and deflection can be caused by a wave impact which is not investigated. A negative value of the strain means an extension (stretch) and a positive value shortening (compression). For the deflection a displacement downwards is positive and a displacement upwards is negative.

While measuring it was surprising that the impact pressure of one transducer could differ a factor 5 with the neighbouring transducer. This shows there was a substantial spatial spread of the extreme impact pressures.

4.3.2 Results regular wave tests

For tests AS022, with regular waves, the impact factor, the strain amplitude and deflection amplitude is plotted with respect to the exceedance frequencies. The strain amplitude is given as the maximum amplitude for the chosen time frame belonging to the wave which is causing the strain. The same counts for the deflection amplitude.

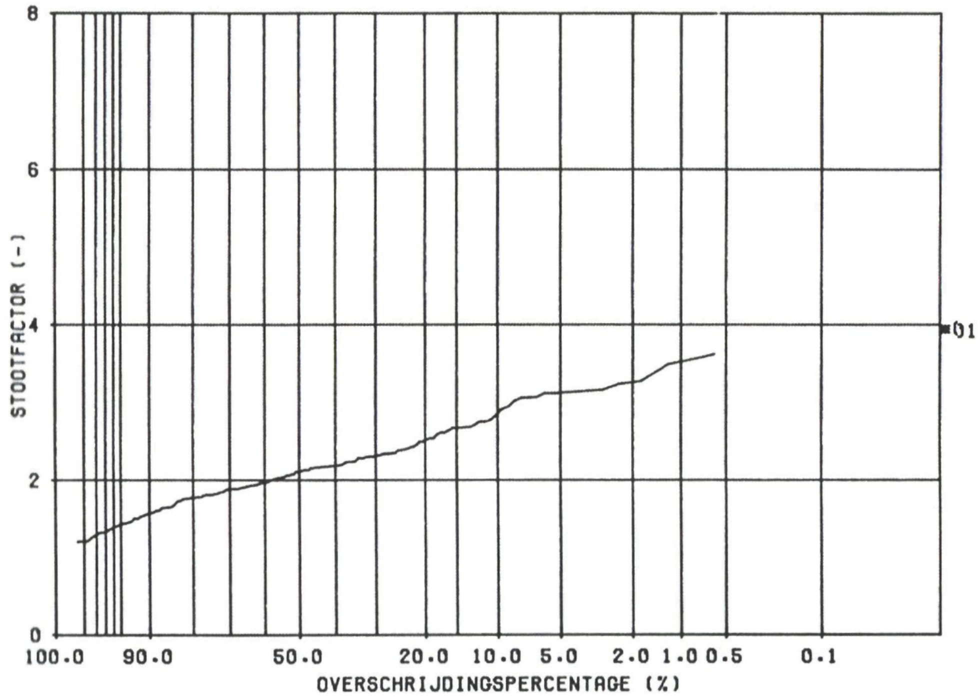

Figure 4-3 Exceedance percentage of the impact factor (Run AS022, DRO 11-19)

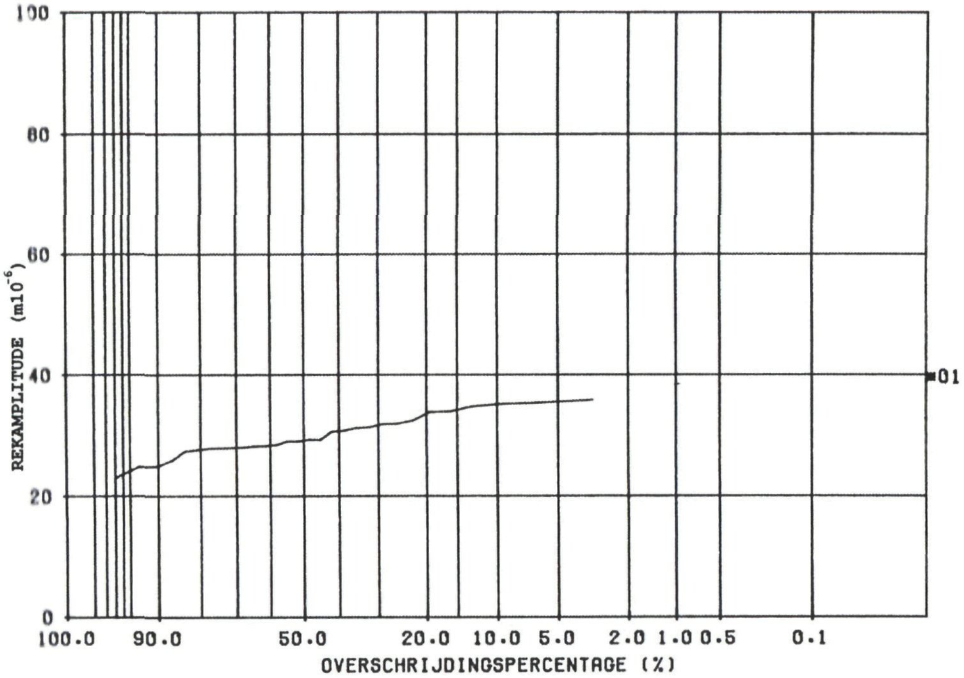

Figure 4-4 Exceedance percentage of the strain amplitude (Run AS022, VPL 4, for maximum wave impacts at DRO 11-19)

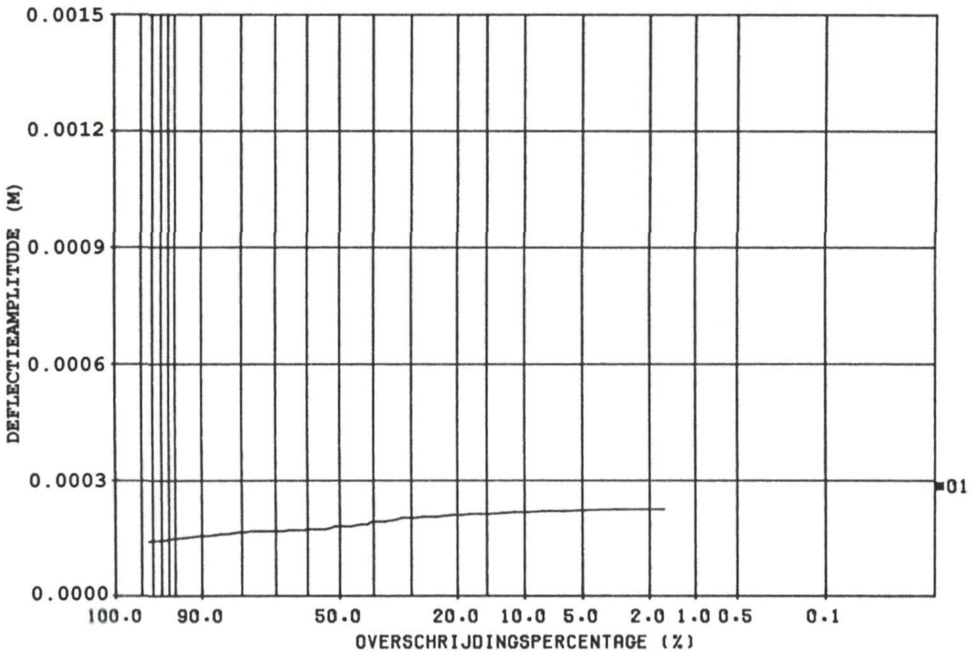

Figure 4-5 Exceedance percentage of the deflection amplitude (Run AS022, VPL 10, for maximum wave impacts at DRO 11-19)

On the x-axis a Rayleigh distribution is chosen, $P(x) = 1 - e^{\frac{-x^2}{2\sigma^2}}$. The graphs show that the distribution is indeed stochastic and also that the deviation is different for every parameter. The deviation of the strain and the deflection is less than the deviation of the impact factor. In the next figure the relation of the strain and deflection with the impact factor are shown, this for the same test AS022.

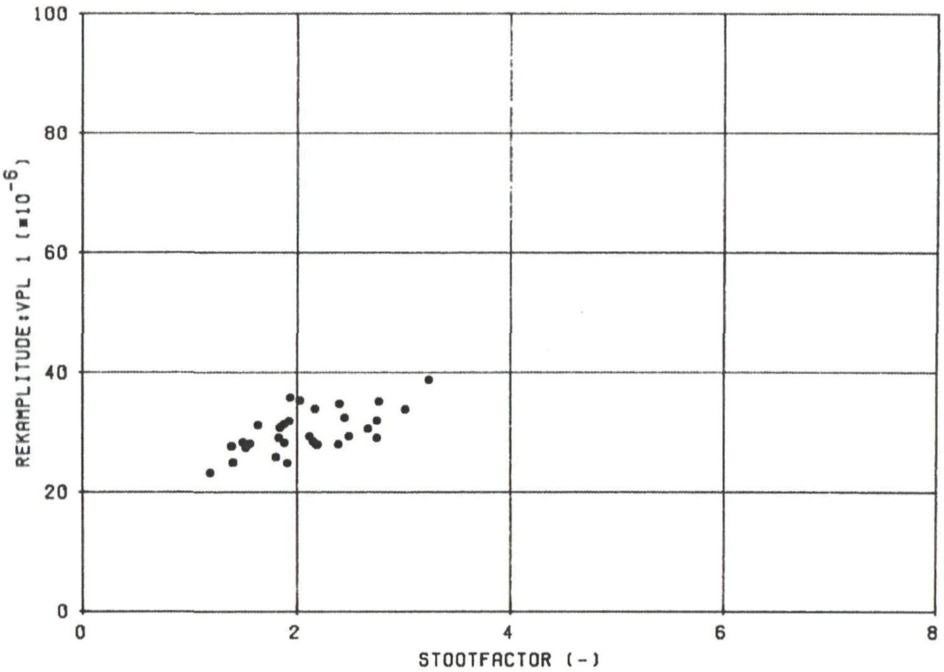

Figure 4-6 Relation between the strain amplitude and the impact factor (Run AS022, measured at DRO 11-19)

In the tests with regular waves there is not much deviation in the place of impact. Only in the test with a high wave period the area of impact is very wide. For the test run AS021 with wave height H=0.97 m and T=4.0 s the distribution in comparison with the still water line is given in Figure 4-7.

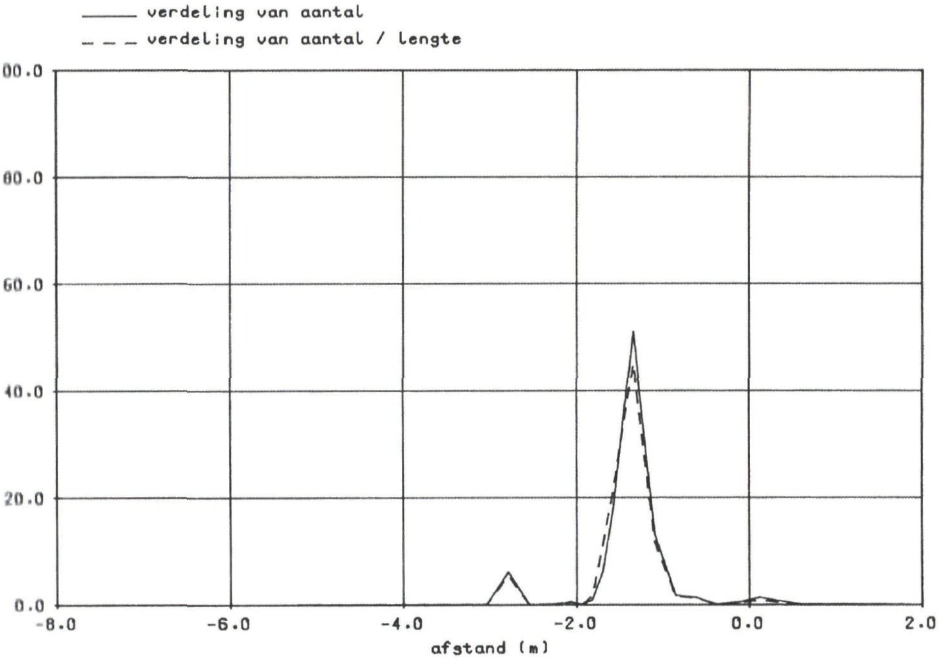

Figure 4-7 Distribution of the maximum wave impacts on the revetment with respect to still water level

The measured data is compared with data of research done by others in Figure 4-8. It was found that the relation between the places of impact, the wave height and wave steepness can be approximated with:

$$\frac{\Delta h}{H} = 0.0085\left(\frac{H}{gT^2}\right)^{-0.75} \qquad \text{if } \tan(\alpha) = 0.25$$

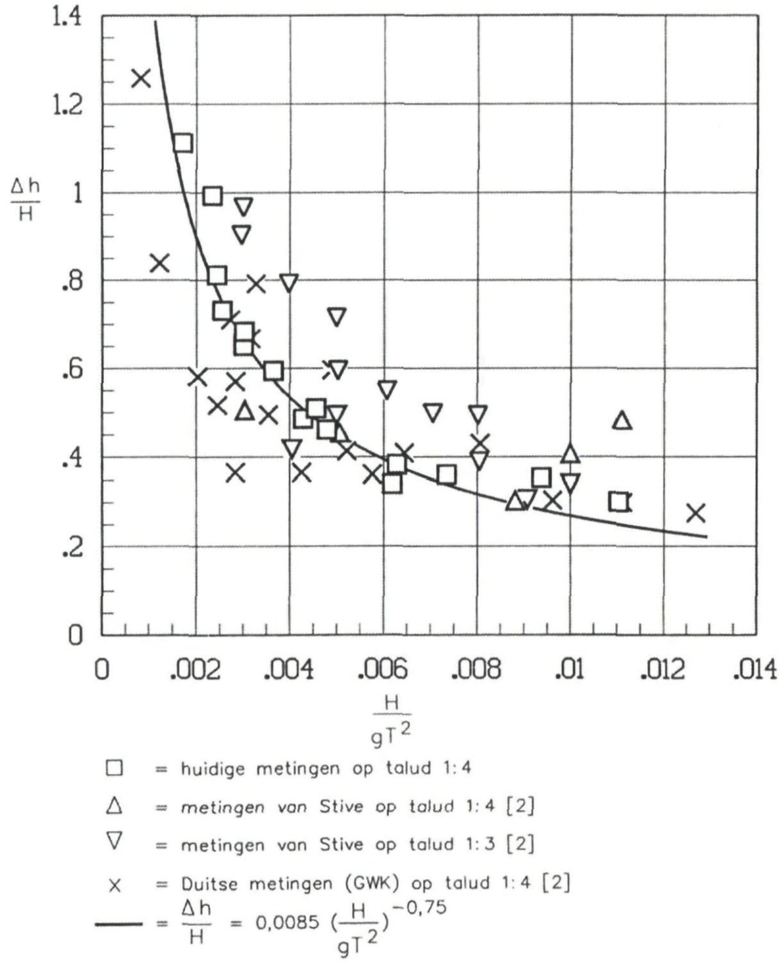

Figure 4-8 Place of impact in different experiments (regular waves)

The value of the impact factor is dependent on the wave steepness.

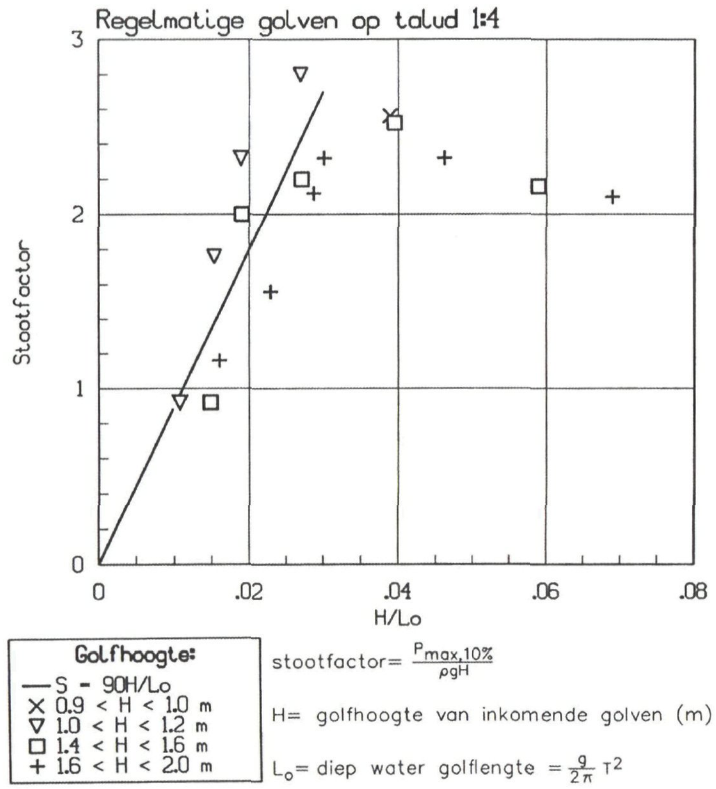

Figure 4-9 Measured impact factor as function of the wave steepness (regular waves, slope 1:4)

The impact factor increases linearly till a wave steepness of 3% after which it will decrease. Based on van Vledder (1990) it is concluded that:

$$q_{10\%} = \frac{P_{max.10\%}}{\rho g H} = c \cdot \tan\alpha \qquad \text{with c= 10 a 14}$$

4.3.3 Tests with irregular waves

The results of measurements of a test with irregular waves (AS025) will be given in some figures:

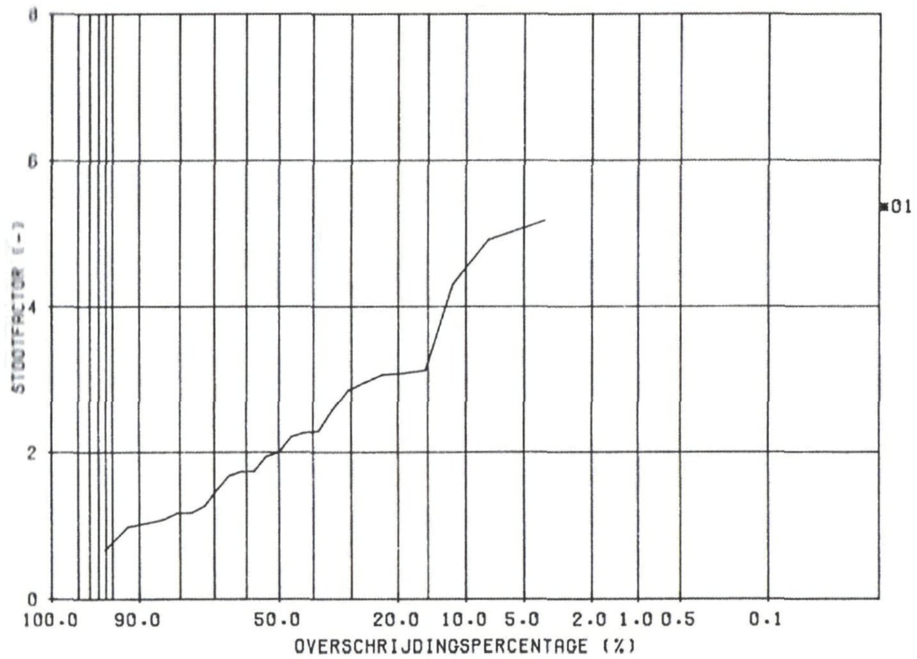

Figure 4-10 Exceedance percentage of the impact factor (Run AS025, DRO 9-17)

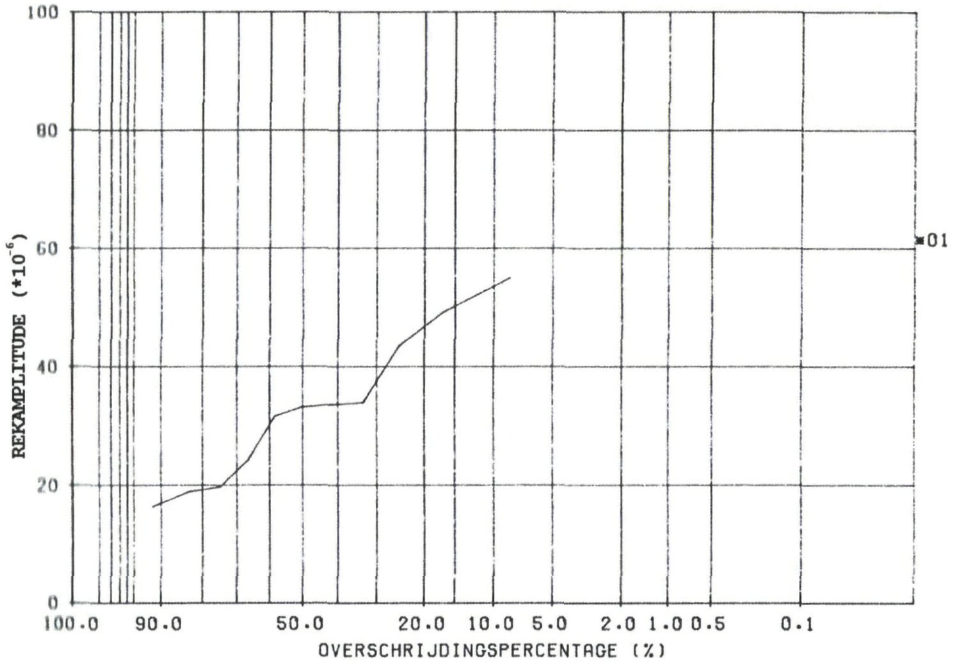

Figure 4-11 Exceedance percentage of the strain amplitude (Run AS025, VPL 3, for maximum wave impacts at DRO 9-17)

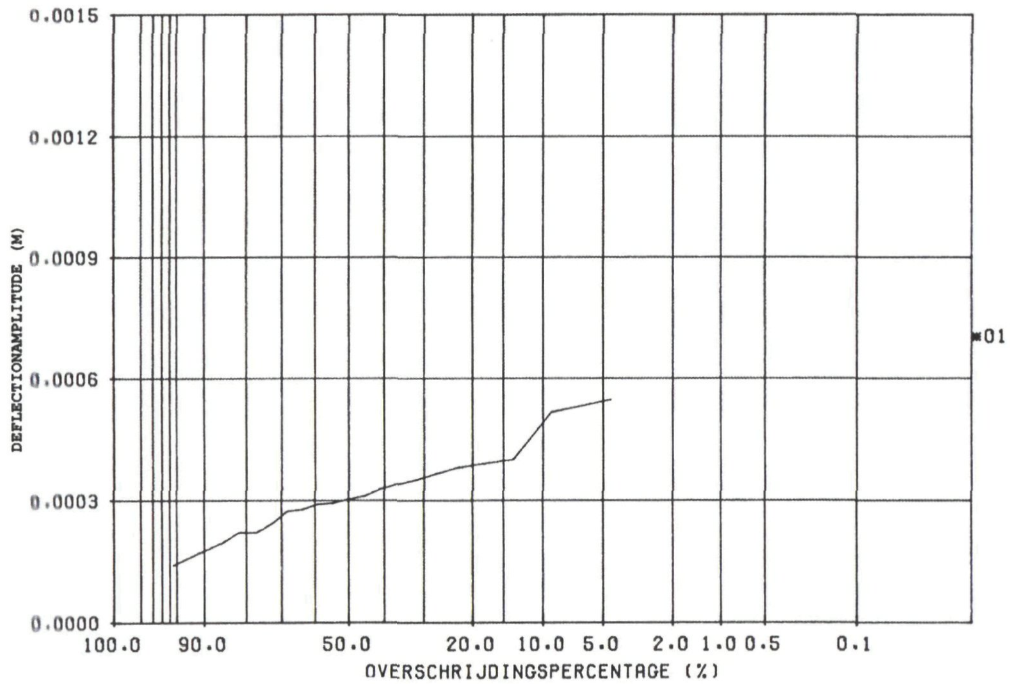

Figure 4-12 Exceedance percentage of the deflection amplitude (Run AS0252, VPL11, for maximum wave impacts at DRO 9-17)

The difference between these graphs for tests with irregular waves and the graphs for tests with regular waves is mostly in the deviation. Also the highest impact pressure for irregular waves is a factor 1.5 higher than the highest impact pressure of regular waves. It should be noted that the peak wave period in test AS025 is 7,6 seconds while in test AS022 the wave period is 5,0 seconds.

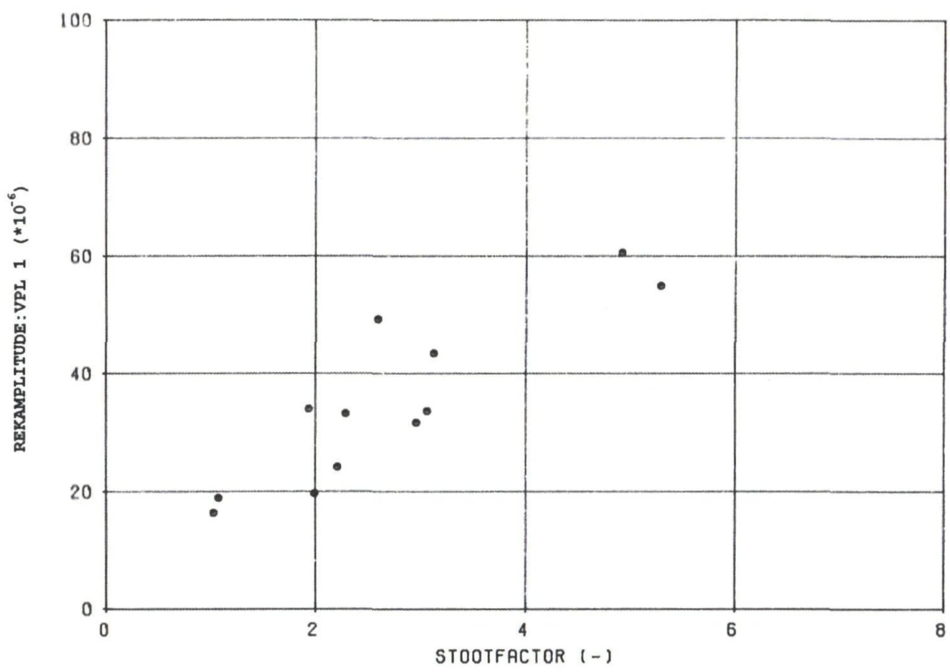

Figure 4-13 Relation between the strain amplitude and the impact factor (Run AS025, measured at DRO 9-17)

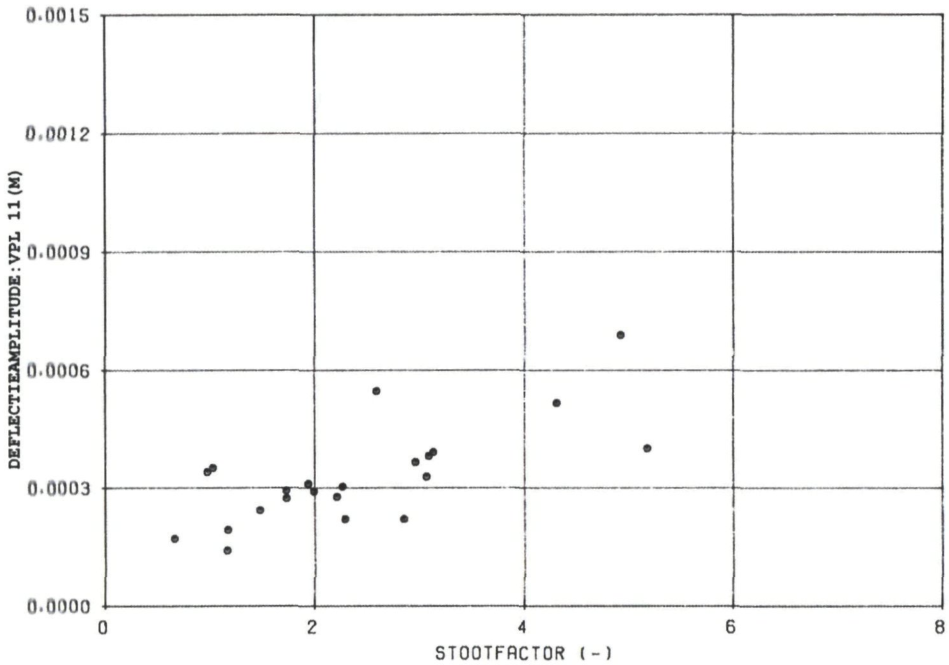

Figure 4-14 Relation between the deflection amplitude and the impact factor (Run AS025, measured at DRO 9-17)

4.4 References

DERKS, H. AND KLEIN BRETELER, M. (1992) Gedrag van asfaltbekleding onder golfaanval, verslag modelonderzoek in Deltagoot (in Dutch)(Report H 1480), *DWW Rijkswaterstaat, Delft*

VAN VLEDDER, G. PH. (1990) Literature survey to wave impacts on dike slope (Report H976), *Delft hydraulics, Delft*

5 Relation between loading and strain in the Delta flume experiment

5.1 Introduction

In this chapter the results and the conclusions of de Waal (1993) are summarized. In de Waal (1993) the calculated relation between the (prismatic) loading and the strain of the asphaltic revetment constructed in the Deltagoot 1991 experiment, is treated. Because of the conclusions and recommendations de Waal (1993) made, part of this thesis is to quantify the sensitivity of the assumed parameters in the calculation.

5.2 Selection of tests and waves

5.2.1 Selection of the tests

In de Waal (1993) a choice is made for using some tests with regular and some tests with irregular waves. The criteria for choosing these tests are:

- the pressure transducers outside the measuring beam should have functioned. So only the test run one and two can be considered
- the wave impact point should be in the heart of the measuring section
- the breaker parameter should have a value of about 1 so the impact factor will be high
- the tests should have different wave heights
- remarks in the measuring report could lead to excluding the test

The following selection has been made:

Tests with regular waves:

- AH108
- AS117
- AS022

Tests with irregular waves:

- AS025
- AS202
- AS203

5.2.2 Selection of the waves

In the search for the relation between load and strain the individual wave impacts are considered. A choice is made to select 3 waves per test with regular waves and 5 per test with irregular waves. The criteria for the selection:

- the instantaneous pressure distribution for the width of the flume (DRO 13 t/m 16) has to be as constant as possible
- the point of impact should be as close as possible to the heart of the measuring

section (DRO 15)

- the maximum impact pressure should be relatively large. The probability of exceedance should be less than 40%

The selected waves are given in Table 5-1:

Table 5-1 The selected waves

Proef	h_t (m)	H (m)	T (s)	t (s)
AS022	4.71	1.05	5.0	769
AS022	4.71	1.05	5.0	744
AS022	4.71	1.05	5.0	594
AH108	5.28	1.45	7.0	411
AH108	5.28	1.45	7.0	75
AH108	5.28	1.45	7.0	453
AS117	4.89	1.80	5.0	374
AS117	4.89	1.80	5.0	219
AS117	4.89	1.80	5.0	309
AS202	5.01	1.43	7.1	3695
AS202	5.01	1.43	7.1	3560
AS202	5.01	1.43	7.1	5605
AS202	5.01	1.43	7.1	5483
AS202	5.01	1.43	7.1	3539
AS203	5.10	1.52	8.7	4828
AS203	5.10	1.52	8.7	1319
AS203	5.10	1.52	8.7	3540
AS203	5.10	1.52	8.7	1227
AS203	5.10	1.52	8.7	51
AS025	5.21	.89	7.6	81
AS025	5.21	.89	7.6	151
AS025	5.21	.89	7.6	771
AS025	5.21	.89	7.6	207
AS025	5.21	.89	7.6	728

It should be noted that the first criteria could not be fulfilled. As shown in the previous chapter the differences between the impacts over the width of the flume are relatively large. Because the point of impact should be close to DRO 15, the maximum impact pressure at this point is almost 30% higher than the, over the width of the flume, mean impact. More to the border of the flume (DRO 13 and 16) the impact pressure is about 15% lower than the mean impact. However the standard deviation of these 30% and 15% is about 20% and these values are only valid for the impacts at the DRO 15.

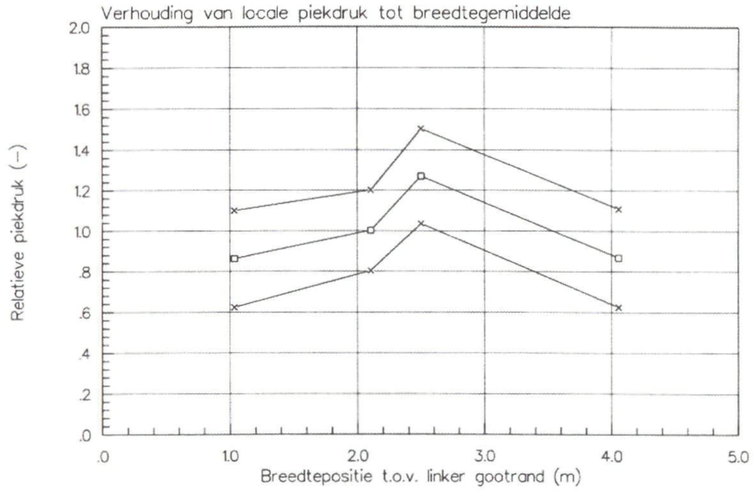

Figure 5-1 Pressure distribution over the width of the flume compared to the mean distribution

5.3 Analysis of the wave impacts

To analyze the wave impacts the measured pressures on the slope are converted into pressure height with respect to the slope by:

$$\varphi = \frac{p}{\rho_w g}$$

with:

φ	pressure height on the slope	(m)
p	pressure on the slope	(N/m^2)
ρ_w	mass density of water	(kg/m^3)
g	acceleration of gravity	(m/s^2)

An example of the course of the pressure height, for test AH108, with wave height H=1.45 meter and a period of T=7.0 seconds, is given in the next figure. On the horizontal axis the distance in meters is given with respect to the wave generator and on the vertical axis the pressure height in meters. Every graph represents a time interval of 0.05 seconds starting at 75.30 seconds which is time with respect to the starting point of the experiment run AH108.

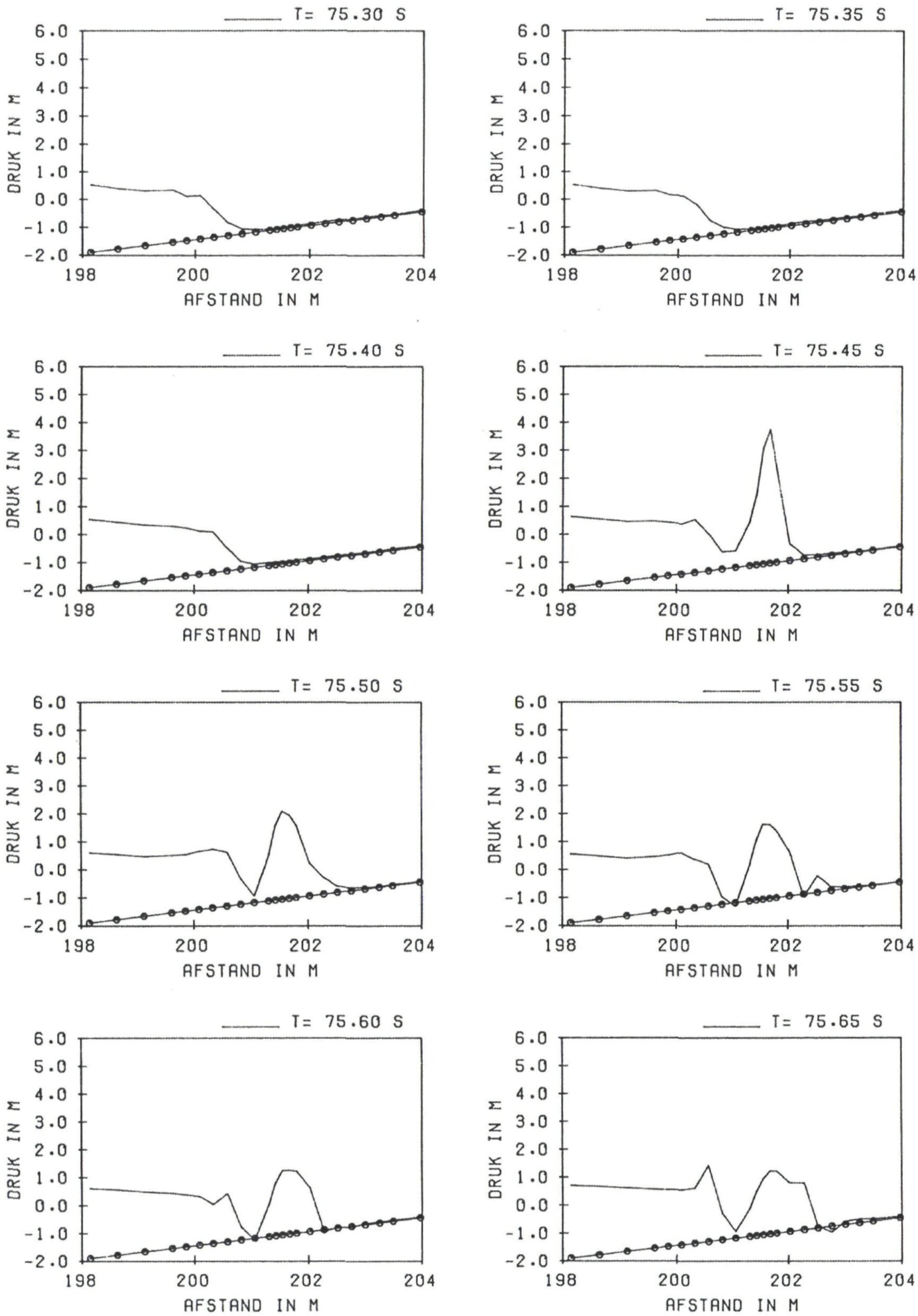

Figure 5-2 Example of the pressure course in time (Run AH108)

The fourth graph chosen to be the maximum wave impact and this value of maximum impact pressure is used in the calculation. The parameters of the prismatic load are determined like in the figure below.

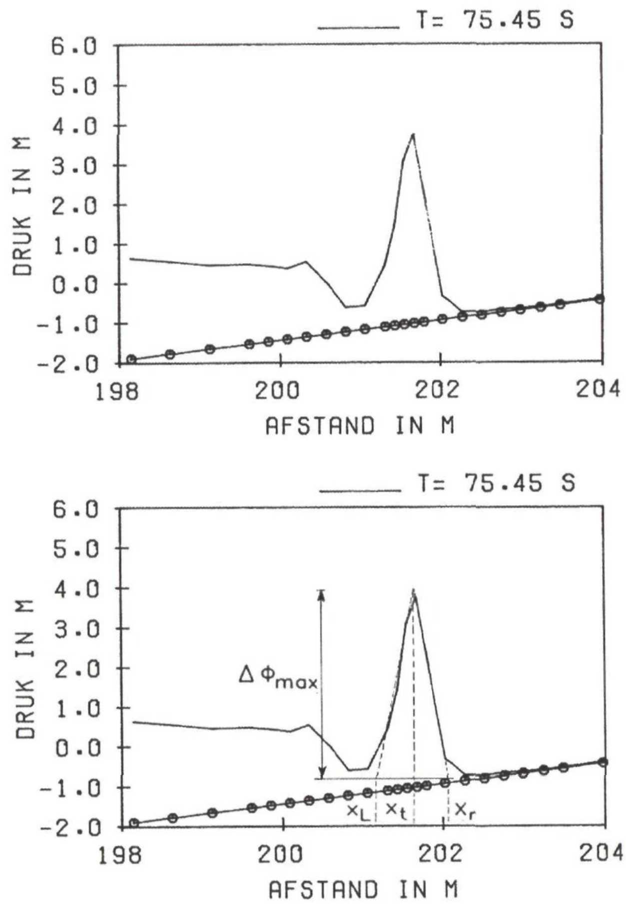

Figure 5-3 Example of the schematization of the impact (Run AH108)

While searching for the maximum wave impact the following was discovered:

- the pressure variation in time can vary very quickly
- the wave impact can most of the time be approximated by a prismatic load
- most of the time the prismatic load is not symmetric but the top is located more to the sea side
- the choice of the reference line is arbitrary within the limits of 10%-15% of $\Delta\varphi_{max}$. It is tried to choose such a value that $\Delta\varphi_{max}$ is relatively large

An example of the quick change in the pressure height is given in Figure 5-4 for a significant wave height H_s=1.43 m and a peak wave period of T_p=7.14 s.

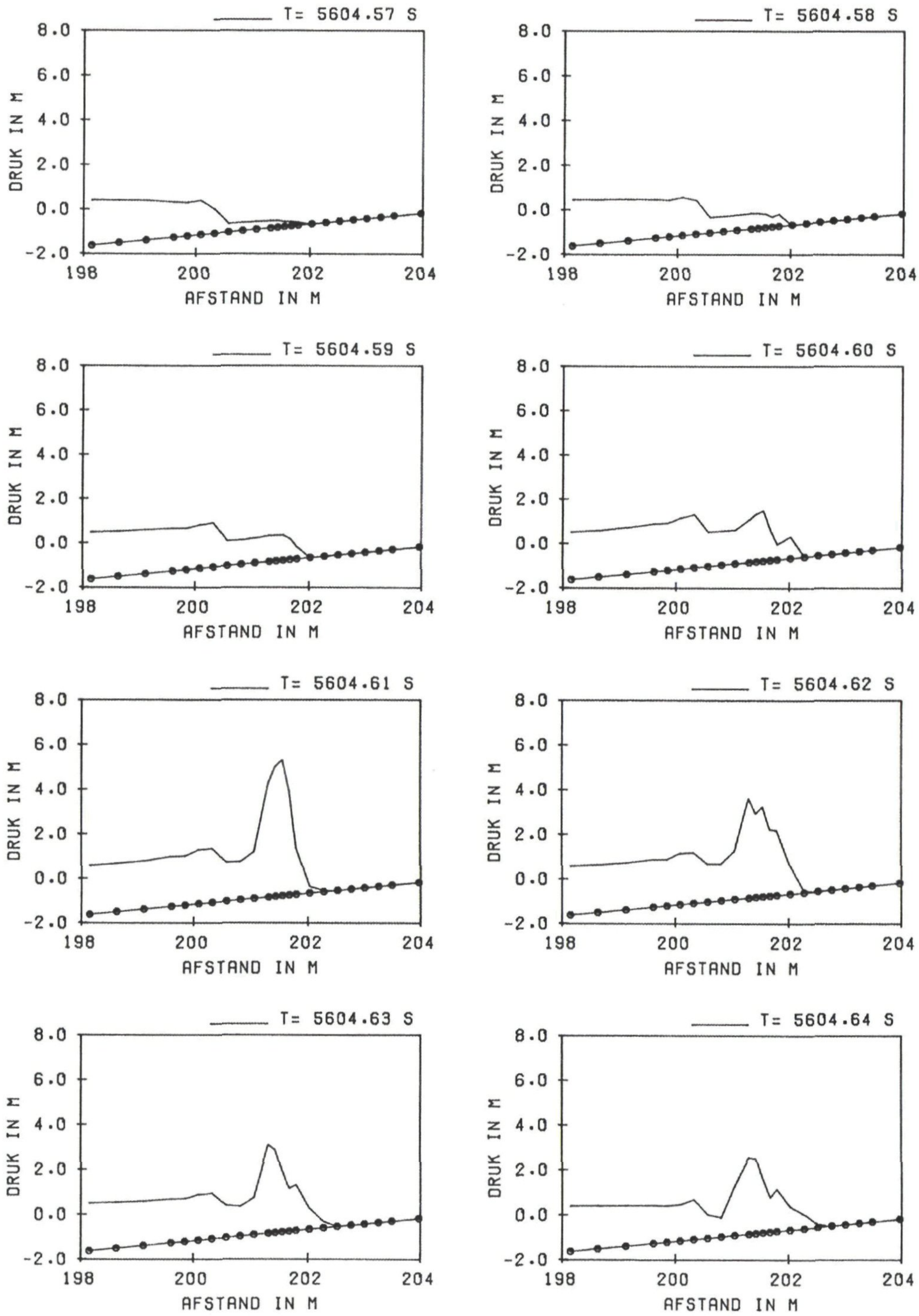

Figure 5-4 Example of a quick pressure variation on the slope (Run AS202)

5.4 Analysis of the strain

The next figure shows the recorded signal of the strain measuring devices. This is recorded in the AH108 test with waves of H=1.45 m and T=7.0 s. There is a high frequency signal disturbing the plot but the differences between the quasi-static load of changing water level on the slope and the dynamic load of the wave impact can be seen. Because the strain under wave impact is studied, this quasi-static and dynamic part are separated. By interpretation the quasi-static course is continued and the difference between the quasi-static part and dynamic part is visible. In the figure the negative strain means an extension at the underside of the revetment so a positive deflection downwards.

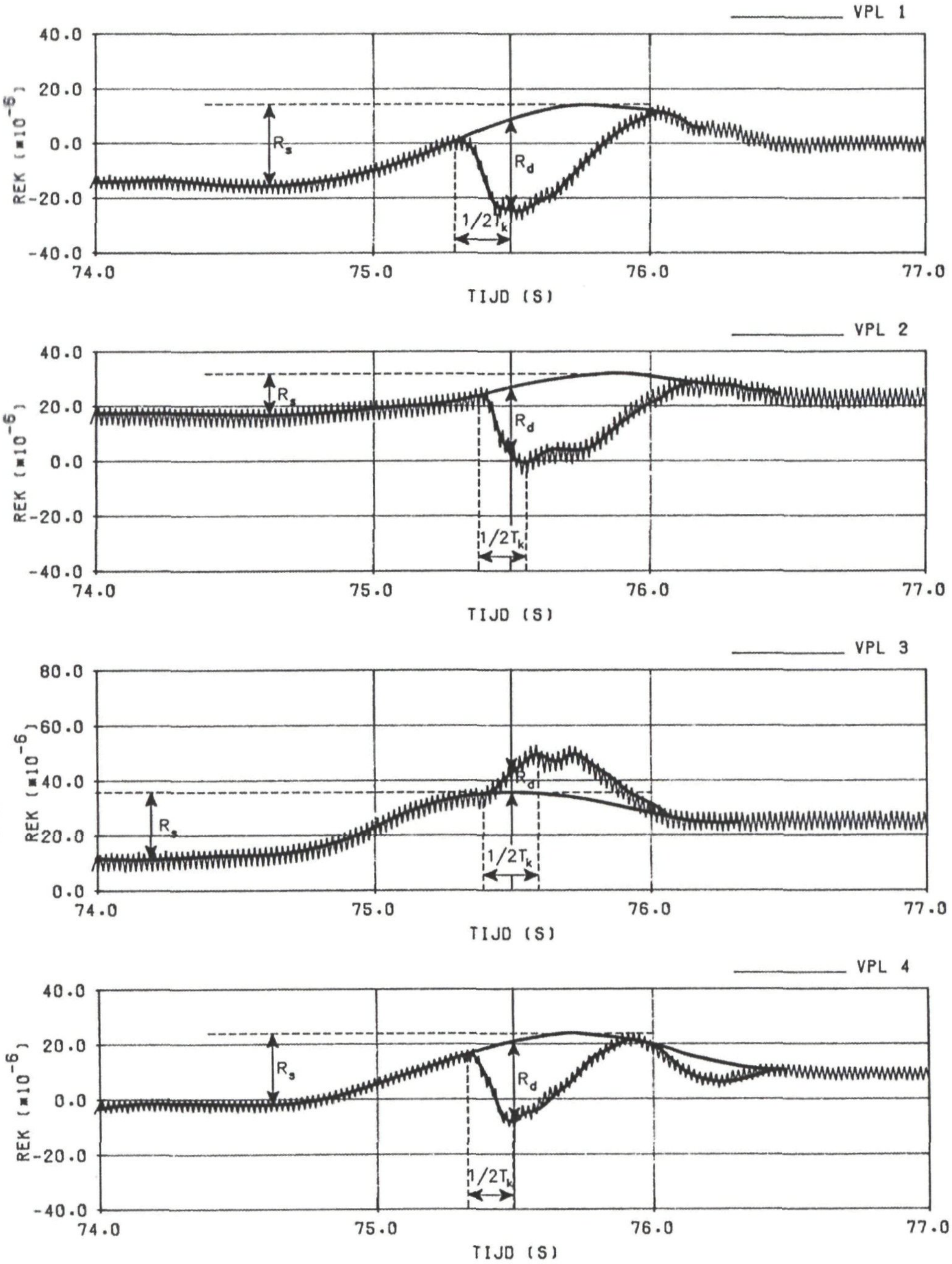

Figure 5-5 Example of the analysis of the strain signal (Run AHS108)

In the figure the different parts are displayed by R_d and R_s.

- strain amplitude of the quasi-static part (R_s)
- strain amplitude of the dynamic part (R_d)
- normative frequency of the dynamic part ($f_k=1/T_k$)

Furthermore the total strain is given; in Table 5-2 and Table 5-3 the numerical values are given. In de Waal (1993) is tried to calculate the dynamic part of the strain. In chapter seven is explained which formula is used to calculate the tension in the revetment. The parameters used in this formula is displayed here including the assumed values in the report.

- thickness of the asphalt layer (0.15m left part of the flume, 0.25m right part of the flume)

- modulus of elasticity (varying with asphalt temperature)
- stiffness of the subsoil (modulus of the subgrade) (100 MPa/m)
- symmetrical load

The result of the calculation is given in the tables and figures below.

Table 5-2 Calculated strain and measured dynamic strain

Proef	t	BEREKENDE REKKEN (* 10^{-6})								GEMETEN DYNAMISCHE REKKEN (* 10^{-6})							
		VPL								VPL							
	(s)	1	2	3	4	5	6	7	8	1	2	3	4	5	6	7	8
AS022	769	102	-22	-7	102	82	-3	20	82	23	2	-8	28	21	7	2	12
AS022	744	83	-5	2	83	73	6	22	73	23	10	-10	23	27	8	-4	21
AS022	594	124	12	-38	124	105	22	3	105	23	13	-15	20	21	8	-6	24
AH108	411	129	-18	-5	129	98	5	26	98	27	39	-18	18	42	-	18	40
AH108	75	126	4	-40	126	94	17	1	94	33	24	-9	26	45	8	10	36
AH108	453	98	-16	-2	98	75	2	22	75	42	19	8	35	42	10	11	33
AS117	374	84	18	11	84	69	24	27	69	24	18	14	36	34	25	0	25
AS117	219	95	32	-3	95	78	33	22	78	55	30	-1	41	54	26	38	36
AS117	309	59	8	37	59	58	16	46	58	42	24	8	44	46	19	26	52
AS202	3695	141	134	-53	141	134	119	1	134	60	58	60	57	90	49	30	88
AS202	3560	93	99	-57	93	85	79	-14	85	17	36	-22	13	32	35	0	13
AS202	5605	108	-33	13	108	73	-5	33	73	18	-14	21	31	38	0	23	17
AS202	5483	135	-11	-21	135	91	11	15	91	21	0	11	38	42	0	30	31
AS202	3539	99	-32	33	99	72	-5	45	72	16	4	38	45	75	3	45	33
AS203	4828	115	70	-39	115	96	63	2	96	65	17	38	-	49	9	60	64
AS203	1319	25	-46	106	25	32	-24	80	32	25	10	53	25	48	10	74	34
AS203	3540	97	-16	-4	97	65	3	18	65	54	10	38	-	49	10	35	60
AS203	1227	94	-15	1	94	65	3	21	65	56	31	-8	43	46	17	21	44
AS203	51	86	-3	9	86	64	10	25	64	28	25	-19	16	3	18	-10	7
AS025	81	90	-46	58	90	67	-15	62	67	28	-18	41	47	46	-21	56	15
AS025	151	89	15	29	89	77	23	42	77	41	21	-15	38	53	23	0	38
AS025	771	64	-42	70	64	52	-16	62	52	30	-8	23	31	46	17	13	40
AS025	207	92	19	-17	92	69	23	11	69	16	20	-3	19	38	17	8	38
AS025	728	77	46	-21	77	66	42	4	66	2	40	-9	8	22	33	-3	12

Table 5-3 Quasi-static strain and total strain

Proef	t	QUASI-STATISCHE REK (* 10^{-6})								TOTALE REK (* 10^{-6})							
		VPL								VPL							
	(s)	1	2	3	4	5	6	7	8	1	2	3	4	5	6	7	8
AS022	769	5	5	5	5	5	5	5	5	23	11	17	29	27	22	19	21
AS022	744	5	5	5	5	5	5	5	5	31	17	24	26	30	10	17	23
AS022	594	5	5	5	5	5	5	5	5	30	16	20	23	26	13	17	25
AH108	411	32	14	29	24	22	-	29	20	34	48	48	36	45	-	44	42
AH108	75	28	12	22	26	20	-	27	16	42	36	44	33	51	-	30	38
AH108	453	24	18	24	22	18	-	29	16	49	29	38	40	46	-	32	33
AS117	374	37	17	70	34	19	19	44	26	37	22	55	48	41	30	50	37
AS117	219	19	15	53	30	19	15	34	28	56	31	53	59	54	37	32	42
AS117	309	24	11	56	28	21	16	49	22	44	30	67	38	48	40	39	49
AS202	3695	33	28	28	40	38	18	23	30	126	66	71	119	101	58	30	88
AS202	3560	40	38	28	43	40	35	23	20	116	56	41	107	71	82	40	57
AS202	5605	16	17	29	23	18	11	20	20	35	26	48	41	40	21	40	20
AS202	5483	14	13	16	11	14	3	19	13	45	25	31	45	45	23	36	35
AS202	3539	45	18	29	23	15	8	18	17	45	35	70	53	77	18	60	40
AS203	4828	33	35	53	-	33	25	46	23	72	48	87	-	62	43	66	67
AS203	1319	56	40	30	35	20	20	21	22	75	67	111	44	66	40	76	39
AS203	3540	63	61	71	-	24	30	56	38	62	57	61	-	52	32	56	53
AS203	1227	30	21	53	38	25	13	39	28	55	34	78	45	49	27	51	41
AS203	51	13	10	20	14	12	10	20	14	26	43	50	20	21	36	49	21
AS025	81	9	16	8	9	9	15	11	11	29	37	56	56	56	37	58	31
AS025	151	12	10	25	13	16	11	20	11	38	25	56	39	53	33	45	45
AS025	771	8	10	10	11	9	11	11	8	44	23	48	51	56	30	27	51
AS025	207	5	5	20	8	9	7	15	6	38	30	45	30	45	34	39	42
AS025	728	8	5	15	8	9	6	12	9	18	47	43	30	28	39	41	28

The negative values of the strain in these tables represent a deflection of the revetment upwards so a compression at the underside of the revetment. The next first two graphs relate to the left side of the flume with a layer thickness of 0.15m and the last two graphs to the right side of the flume with 0.25m layer thickness.

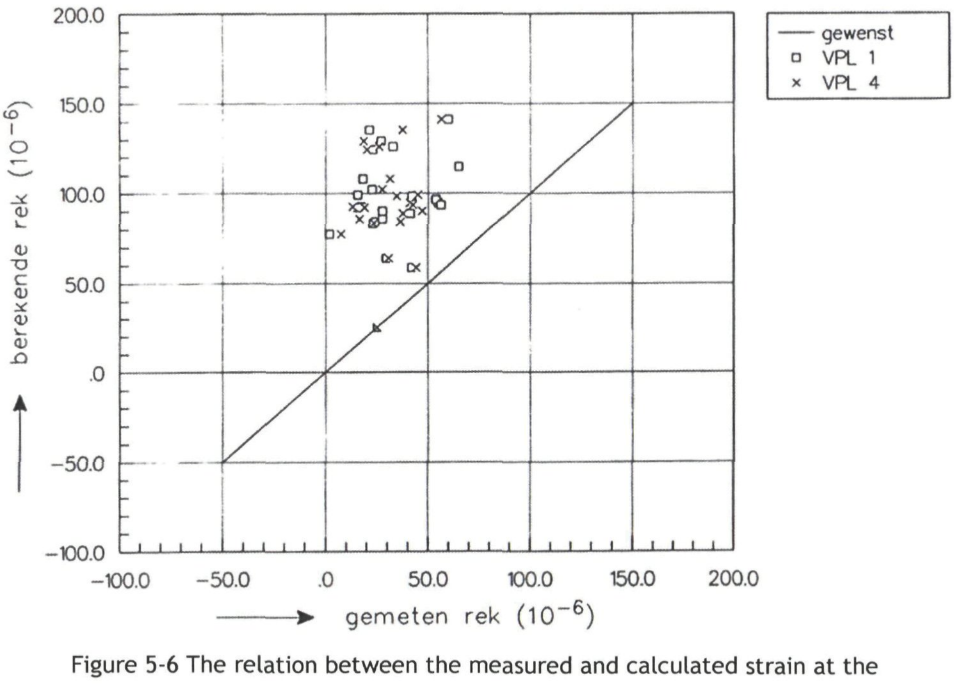

Figure 5-6 The relation between the measured and calculated strain at the left side of the flume (layer thickness of 15 cm)

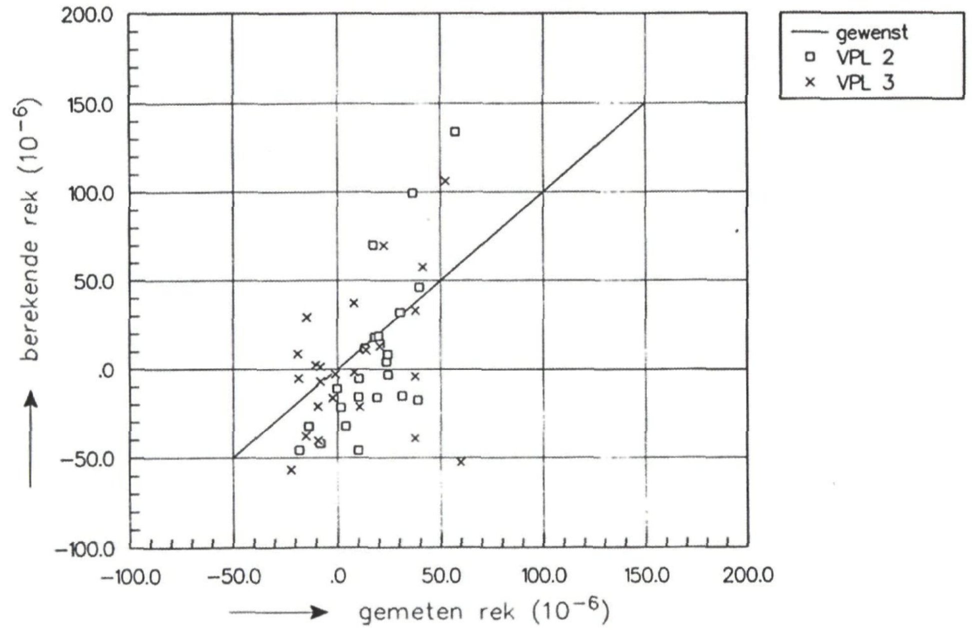

Figure 5-7 The relation between the measured and calculated strain at the left side of the flume (layer thickness of 15 cm)

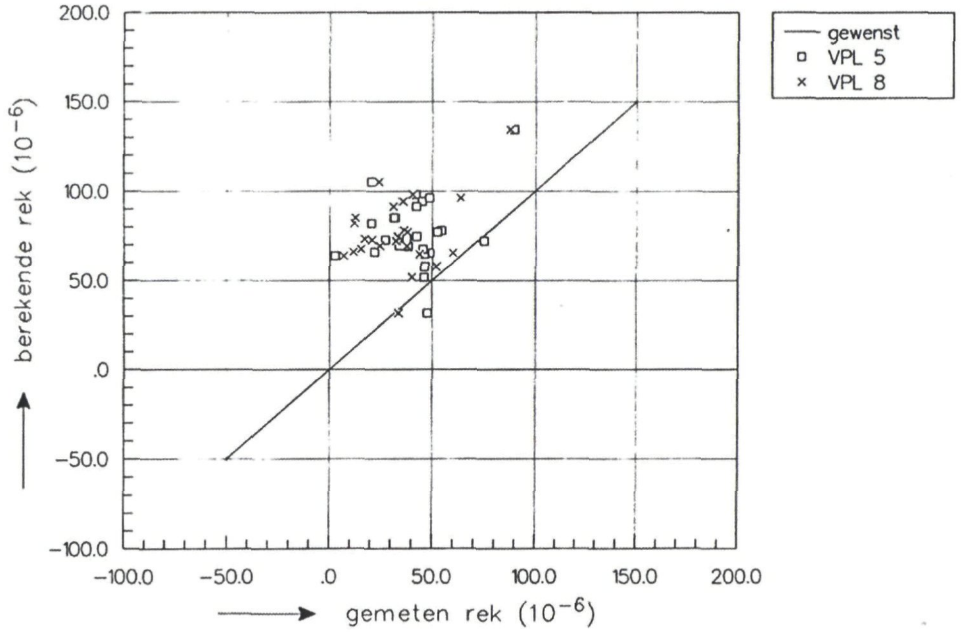

Figure 5-8 The relation between the measured and calculated strain at the right side of the flume (layer thickness of 25 cm)

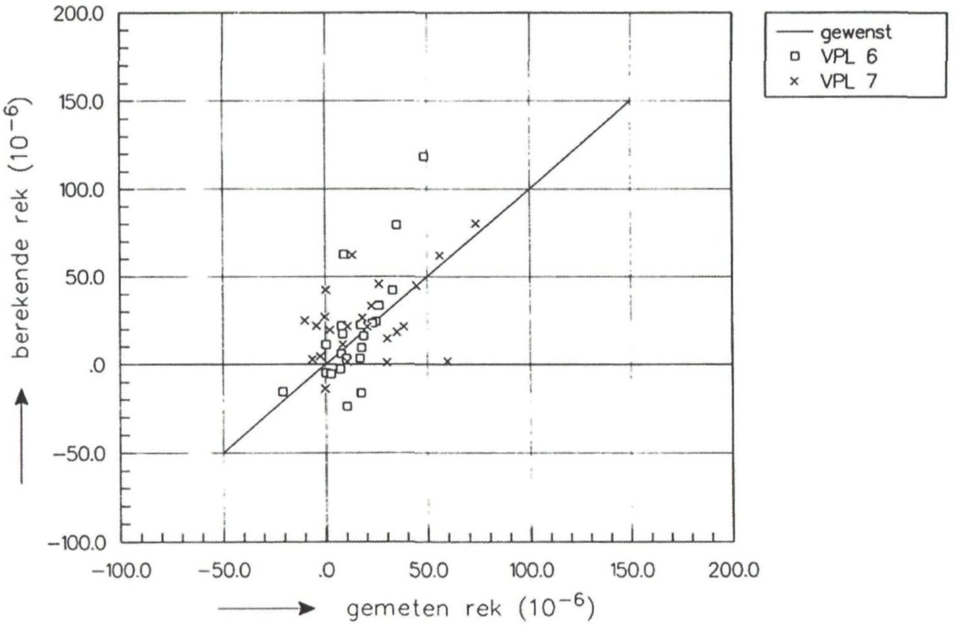

Figure 5-9 The relation between the measured and calculated strain at the right side of the flume (layer thickness of 25 cm)

As can be seen the measurements and the calculation do not agree with each other. In de Waal (1993) the uncertainties are mentioned:

- the symmetric load in the calculation is not in agreement with the measured load.
- the loading varies in time very quickly and the strain signal does not always follow the load signal. This can be caused by the different place of measuring; the pressure is measured on another place then the strain. Also, the modulus of elasticity is dependent on the frequency of the load and inertia of the layer can play a role.
- the wave load is not homogenous over the width of the flume. Most of the time the maximum impact occurs in the middle of the flume and at the borders the wave impact is less as mentioned in section 5.2.2.
- the peak value and the width of the prismatic load are highly dependent of the reference level. The limits of choosing the reference level are between 10% and 15%.
- the stiffness of the asphalt layer and the subsoil are not calculated very well. Adjusting these parameters will rather lead to a shift in the relation between measured and calculated strain than affecting the deviation of the values.
- the measured strain is divided in a quasi-static part and a dynamic part. By interpretation the difference is made. It is not clear whether this interpretation is physically correct.

De Waal (1993) concluded his analysis with the conclusion that there is almost no relation between the measured and calculated strain. The measured strain, in most of the cases, is lower than the calculated strain. There are many inaccuracies in the used parameters. De Waal recommends to search for the relation between the rising of the water level and the quasi-static component of the measured strain. Also the influence of the asymmetric loading and dynamic aspect should be quantified. The sensitivity of the used parameters to the calculation should be quantified.

5.5 References

DE WAAL, J.P. (1993) Gedrag van asfaltbekleding onder golfaanval, Relatie tussen belasting en rek (in Dutch)(Report H 1702), *DWW Rijkswaterstaat, Delft*

6 Conditions

When analyzing the measured and calculated strain one must realize that a lot of different aspects influence the strain in the revetment. In the literature review the loading part, the maximum impact pressure, is extensively treated. Also the width of the impact and the place of impact are dealt with. It is shown which equations are used in the program GOLFKLAP and on what research these equations are based.

In this reanalysis is chosen to use the same model which is used by de Waal (1993). Due to extensive testing of materials in the last fifteen years a better understanding of material behaviour is achieved. This concerns in particular the modulus of elasticity of asphaltic concrete (E) and the modulus of subgrade reaction (k). This knowledge will be used in this thesis to get new results from the same model. This model is derived from the guideline for application of asphalt in hydraulic engineering (TAW 1984) and explained in chapter seven.

Some of the schematizations of the model:

- the wave impacts are schematized as prismatic loads
- the system is schematized as a plate on springs
- the wave impact in time is schematized as a block pulse
- the prismatic wave load is the same over the width of the flume
- the strain is calculated by dividing the tension by the modulus of elasticity (linear-elastic behaviour)

In de Waal (1993) is recommended to perform sensitivity analysis. Because of the many uncertainties involved a statistical analysis is performed in this thesis. A well known statistical method is the Monte Carlo simulation. The Monte Carlo simulation is a stochastic simulation were all the possible outcomes of mathematical calculations with probability functions are simulated. The Monte Carlo simulation is used for many technical application and much information about this statistical method is available. This is the reason why this method is used in this thesis.

Some conditions for the simulation should be formulated. Some of the probability functions give information about the probability of occurrence in time and some give information about the probability of occurrence in space. The measured probability functions of chapter four, given by Derks and Klein Breteler (1992), give information about the probability of occurrence in time. The probability functions given in chapter four are the probability functions of the impact factor, the strain and the deflection. These probability functions are given for only one spot (for example, VPL 4). In chapter eight the probability function of the modulus of elasticity, the layer thickness and the modulus of the subgrade is derived. These probability functions give information about the variance of the material properties in space. Both probability functions in time and space are used in the Monte Carlo simulation. When the result of the Monte Carlo simulation is compared with the measurements to much variance is taken into account because at, for example, the spot where VPL 4 is installed there is only one layer thickness (h), one modulus of elasticity (E) and one modulus of the subgrade reaction (k). Because the exact values of these parameters at this spot are not known there probability functions are used.

There is another condition in the comparison between the measured and calculated strain. The impact factor distribution is given for the measured maximum wave impacts on the measuring beam placed in the middle of the flume. The distribution of the strain is given for, most of the times, VPL 1 or VPL 4. by comparing the simulation results with the measurements it is assumed that the maximum wave impacts are uniformly distributed over the width of the flume. So the impact factor distribution does give the impacts at the spot of the strain measuring device.

As shown in chapter five the strain is calculated for some test runs. In this thesis the same test runs are used. This because at first only for these test runs information about the strain was available and to limit the enormous amount of data.

6.1 References

DE WAAL, J.P. (1993) Gedrag van asfaltbekleding onder golfaanval, Relatie tussen belasting en rek (in Dutch)(Report H 1702), *DWW Rijkswaterstaat, Delft*

DERKS, H. AND KLEIN BRETELER, M. (1992) Gedrag van asfaltbekleding onder golfaanval, verslag modelonderzoek in Deltagoot, with annexes (in Dutch)(Report H 1480), *DWW Rijkswaterstaat, Delft*

TAW (1984) Leidraad voor toepassing van asfalt in de waterbouw (in Dutch), *Staatsuitgeverij, 's Gravenhage*

7 Monte Carlo Simulation; the theory

To reanalyze the experiment done in 1991 a Monte Carlo simulation is used. In this chapter is explained how the Monte Carlo simulation is used in probabilistic design. In chapter nine more details about the set-up of the Monte Carlo is given.

7.1 Monte Carlo in probability design

In the chapter "Probabilistic Design" of the literature review the reliability function is already mentioned. With this reliability function the reliability of an element can be calculated. The reliability of an element depends on the margin between the resistance to failure and the loads. The way this margin is calculated can differ per case. In the structural domain, the Joint committee on structural safety proposed a level-classification of the calculation methods. This classification includes the following three levels:

- Level III: The level III methods calculate the probability of failure, by considering the probability density functions of all strength and load variables. The reliability of an element is linked directly to the probability of failure.
- Level II: This level comprises a number of methods to determine the probability of failure and thus the reliability. It entails linearising the reliability function in a carefully selected point. These methods approximate the probability distribution of each variable by a standard normal distribution.
- Level I: At this level no failure probabilities are calculated. The level I calculation is a design method according to the standards, which consider an element sufficiently reliable if a certain margin is present between the representative values of the strength and the loads. This margin is created by taking so-called partial safety factors into account in the design.

In this thesis a level III calculation is performed.

7.1.1 Level III method

To calculate the probability of failure that part of the probability space which implies failure has to be defined. The joint probability density function of both strength and load has to be defined and with that knowledge the probability of failure can be determined by means of integration.

$$P_f = \iint_{z<0} f_{R,S}(R,S)\,dR\,dS$$

Usually the strength and the load are functions of one or more random variables. In such a case the reliability function can be written as:

$$Z = g(X_1, X_2, \ldots X_n)$$

The probability of failure can then be calculated with the integral:

$$P_f = \iint_{Z<0} \cdots \int f_{X_1,X_2,\ldots,X_n}(X_1, X_2, \ldots X_n)\,dX_1 dX_2 \ldots dX_n$$

This integral most of the times is determined numerically with the use of the Monte Carlo method.

7.2 Formula for calculating the strain

The Monte Carlo method is based on stochastic simulation. Because most of the parameters determining the strain in the revetment are stochastic, a stochastic simulation is executed. To execute the simulation first the probability functions of the parameters are formulated. After this formulation a random selected number which the computer generates is converted into a random number out of the probability density function. When all probability numbers are generated the numbers are put in the calculation of the strain of the revetment. In chapter nine this procedure is explained. In the next section the formula for calculating the maximum stress in the revetment is derived.

7.2.1 Maximum stress formula

This section starts with the summary of the guideline for the application of asphalt in hydraulic engineering (leidraad voor de toepassing van asfalt in de waterbouw, 1984). In the guideline (TAW, 1984) the deflection of the asphalt revetment is derived from formula used to determine the deflection of an elastic plate on a flexible subsoil. The flexible subsoil is represented by a system of spring-dashpots.

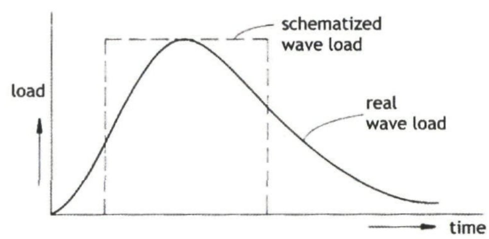

Schematization of the wave impact in time

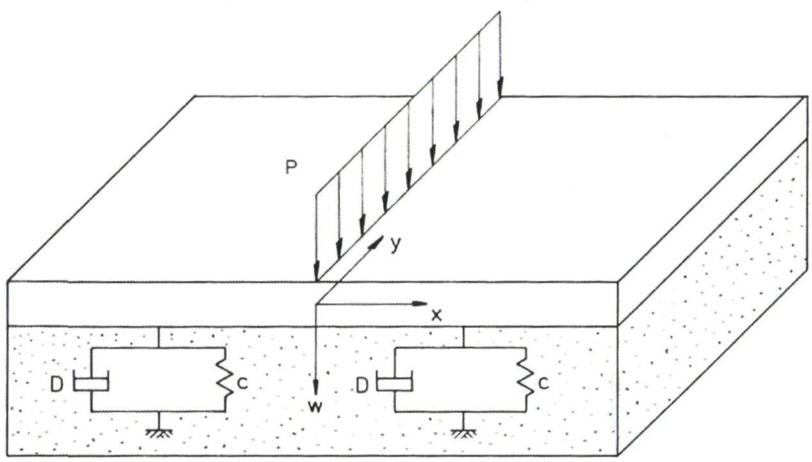

Schematization of the system

Figure 7-1 Schematization of the wave impact in time and the revetment with the subsoil

Because of the line load $P=\rho g q H_s$ (N/m^1) the deflection of the plate can be described with the differential equation:

$$K\frac{\partial^4 w}{\partial x^4}+M\frac{\partial^2 w}{\partial t^2}+D\frac{\partial w}{\partial t}+cw=0$$

with:

K	= E*I	
E	= stiffness modulus of asfalt	(N/m^2)
I	= moment of inertia $I=\frac{h^3}{12(1-\upsilon^2)}$	(m^3)
h	= thickness plate	(m)
ν	= Piossons constant for asphalt	(-)
M	= mass of the plate + contributing soil mass	(kg/m^2)
D	= damping of subsoil	(Ns/m)
c	= modulus of the subgrade reaction	(N/m^3)
w	= deflection of the plate	(m)
t	= time	(s)
x	= horizontal axis	(m)

In the calculation the plate is infinitely long in y direction so all derivatives in y direction are zero.

With Laplace transformation:

$$\overline{w}=\int_0^\infty we^{-st}dt$$

Follows:

$$K\frac{\partial^4 \overline{w}}{\partial x^4}+Ms^2\overline{w}+Ds\overline{w}+c\overline{w}=0$$

The solution:

$$\overline{w}=\frac{P}{8K\lambda^3 s}e^{-\lambda x}(\cos\lambda x+\sin\lambda x)$$

with:

$$\lambda=\beta\sqrt[4]{\left(\frac{s}{\gamma}\right)^2+\frac{s}{\delta}+1}$$

$$\beta=\sqrt[4]{\frac{c}{4K}}$$

$$\gamma=\sqrt{\frac{c}{M}}$$

$$\delta=\frac{c}{D}$$

By determining the Laplace-inverse the equation of the deflection is obtained. The terms $\frac{\partial w}{\partial t}$ and $\frac{\partial^2 w}{\partial t^2}$ will damp out to zero after some time. The way of damping is determined by the ratio to critical damping:

$$D = aD_{kr}$$

The critical damping:

$$D_{kr} = 2\sqrt{Mc}$$

Three different basic cases can be distinguished:

$D > D_{kr}$ damped supercritical

$D = D_{kr}$ damped critical

$D < D_{kr}$ damped subcritical

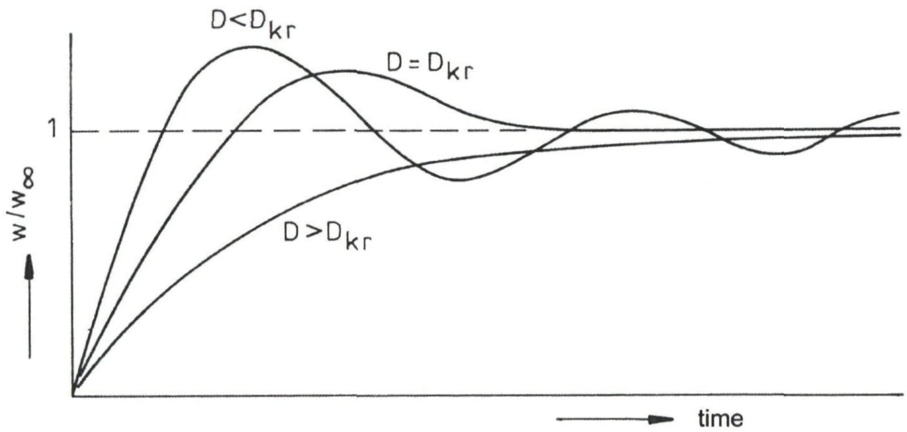

Figure 7-2 Different ways of damping

Now the Laplace inverse is determined in case there is no damping (D=0), so:

$$\lambda = \beta \sqrt[4]{\left(\frac{s}{\gamma}\right)^2 + 1}$$

when $t \to \infty$:

$$w_{x,\infty} = \lim_{s\to 0} s\bar{w} = \frac{P}{8K} \lim_{s\to 0} \frac{e^{-\lambda x}(\cos\lambda x + \sin\lambda x)}{\lambda^3} = \frac{P}{8K\beta^3} e^{-\beta x}(\cos\beta x + \sin\beta x)$$

with:

$$\beta = \sqrt[4]{\frac{c}{4K}}$$

In the guideline this formula is determined but nowadays the wave load is not schematized as a line load anymore but as a prismatic load. In 't Hart (2008) the result of the guideline is used to determine the deflection of a asphalt plate under prismatic loading. The result of 't Hart (2008) are displayed below.

The moment as function of x is derived from the deflection formula with:

$$m = K\frac{d^2w}{dx^2}$$

So the moment because of the line load is calculated by:

$$m_l(x) = \frac{P}{4\beta} e^{-\beta x}\left(\sin(\beta x) - \cos(\beta x)\right)$$

By considering the line load as a small part of the triangle load (P=q*dx) the moment of the prismatic load is derived by integrating over q(x):

$$m_q(x) = \int_{x=-z-x_0}^{x=z-x_0} \frac{q(x)}{4\beta} e^{-\beta x}\left(\sin(\beta x) - \cos(\beta x)\right)dx$$

with:

q(x)	p_{max}	(Pa)
z	$H_s/2$	(m)

The maximum pressure impact is defined as:

$$p_{max} = \rho_w g q H_s$$

Where:

ρ_w	density water	(kg/m^3)
g	acceleration of gravity	(=9,81 m/s^2)
q	impact factor, dependent on slope	(-)
H_s	wave height	(m)

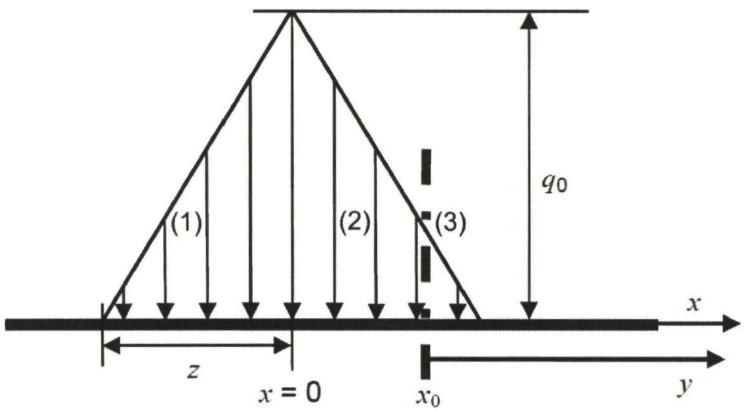

Figure 7-3 Schematization of the wave load divided in different sections

This integral is solved by splitting it up into different sections. For the situation as shown in Figure 7-3:

$$m_q(x_0) = \frac{q_0}{4\beta}\Big[\int_{y=-(z+x_0)}^{y=-x_0} (1+\frac{y+x_0}{z}) e^{(\beta y)}(\sin(-\beta y) - \cos(-\beta y))dy + \quad (1)$$

$$\int_{y=-x_0}^{y=0} (1-\frac{y+x_0}{z}) e^{(\beta y)}(\sin(-\beta y) - \cos(-\beta y))dy + \quad (2)$$

$$\int_{y=0}^{y=z-x_0} (1-\frac{y+x_0}{z}) e^{(-\beta y)}(\sin(\beta y) - \cos(\beta y))dy\Big] \quad (3)$$

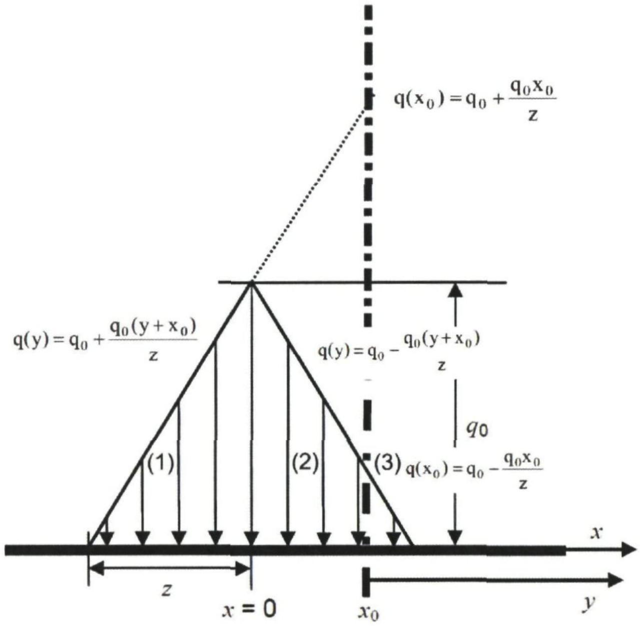

Figure 7-4 The integral vizualized

This integral is solved analytically which results in:

$$m_q(x_0) = \frac{q_0}{8\beta^2 \beta z}[-2\left[e^{-\beta x_0}\{\sin(\beta x_0) + \cos(\beta x_0)\}\right]$$
$$+\sin(\beta x_0)\{e^{\beta x_0} - e^{-\beta x_0}\}e^{-\beta z}\{\sin(\beta z) - \cos(\beta z)\}$$
$$+\cos(\beta x_0)\{e^{\beta x_0} + e^{-\beta x_0}\}e^{-\beta z}\{\sin(\beta z) + \cos(\beta z)\}]$$

In de Looff et al (2006) the stress distribution as function of x is given:

For x<z:

$$\sigma = -\frac{P_{max}}{8\beta^2 \beta z}\begin{bmatrix} -\sin(\beta x)\left\{e^{\beta x} - e^{-\beta x}\right\}e^{-\beta z}\{\cos(\beta z) - \sin(\beta z)\} + \\ \cos(\beta z)\left\{e^{\beta x} + e^{-\beta x}\right\}e^{-\beta z}\{\cos(\beta z) + \sin(\beta z)\} \\ -2e^{-\beta x}\{\sin(\beta x) + \cos(\beta x)\} \end{bmatrix}\frac{6}{h^2}$$

For x>z:

$$\sigma = -\frac{P_{max}}{8\beta^2 \beta z}e^{-\beta x}\begin{bmatrix} \cos(\beta x)\begin{Bmatrix} e^{\beta z}\{\cos(\beta z) - \sin(\beta z)\} + \\ e^{-\beta z}\{\cos(\beta z) + \sin(\beta z)\} \end{Bmatrix} \\ +\sin(\beta x)\begin{Bmatrix} e^{\beta z}\{\cos(\beta z) + \sin(\beta z)\} + \\ e^{-\beta z}\{\cos(\beta z) - \sin(\beta z)\} \end{Bmatrix} \\ -2\{\cos(\beta x) - \sin(\beta x)\} \\ \end{bmatrix}\frac{6}{h^2}$$

And the maximum stress which occurs under the load is calculated with (at x=0):

$$\sigma = \frac{p_{max}}{4\beta^2 \beta z}(1 - e^{(-\beta z)}(\cos(\beta z) + \sin(\beta z)))\frac{6}{h^2}$$

Where:

$$\beta = \sqrt[4]{\frac{3c(1-\nu^2)}{Sh^3}}$$

In de Waal (1993) the stress is divided by the modulus of elasticity to calculate the strain. This estimation is also used by Ruygrok (1994) where the measured strain in detail is compared with the calculated strain. Because of the good results in Ruygrok (1994) this estimation is also used in this thesis.

7.3 Using the maximum stress formula in the Monte Carlo simulation

To recalculate the strains calculated by de Waal (1993) (see section 5.4) the maximum stress formula of the foregoing section is used. In de Waal (1993) the strain for every measuring device is given (VPL 1-8). To recalculate the strain for every measuring device all the parameters are determined at the place of the measuring device. In the next chapter these parameters with there probability functions are derived.

7.4 References

BARDENDS F.B.J. (1980) Dynamics of elastic plates on a flexible subsoil. LGM-Mededelingen, deel 12, *Laboratorium voor Grondmechanica, Delft*

CUR (1997) CUR 190 "Probabilities in civil engineering, Part 1: Probabilistic design in theory", *CUR, Gouda*

DE LOOFF, A.K. ET AL (2004) Handleiding GOLFKLAP 1.2 (Report e038390) (in Dutch), *KOAC•NPC, Nieuwegein*

DE LOOFF, A.K. ET AL (2006) Golfklap a Model to Determine the Impact of Waves on Dike Structures with an Asphaltic Concrete Revetment, *Proceedings ICCE 2006, San Diego, USA*

DE WAAL, J.P. (1993) Gedrag van asfaltbekleding onder golfaanval, Relatie tussen belasting en rek (in Dutch)(Report H 1702), *DWW Rijkswaterstaat, Delft*

DEKKING, F.M. ET AL (2004) Probability and Statistics for the 21st Century, *Delft University of Technology, Delft*

RUYGROK, P.A. (1994) Dimensioneren van asfaltbekledingen op golfklappen, analyse van de relatie tussen golfbelasting en rekken (in Dutch)(Report CO-347160/17), *Grondmechanica Delft, Delft*

'T HART, R (2008) Scheur ten gevolge van golfbelasting in een al gescheurde asfaltbekleding (Report 435340-0004 v01) (in Dutch), *Stowa, Utrecht*

TAW (1984) Leidraad voor toepassing van asfalt in de waterbouw (in Dutch), *Staatsuitgeverij, 's Gravenhage*

8 Set-up of the probability functions

8.1 Introduction

In the formula for calculating the tension in the underside of the revetment many parameters have to be obtained. In this chapter these parameters are described with there probability functions. Difference is made in simulating in time and in space. In de Waal (1993) waves are selected at a certain moment in time and at that moment in time the strain is calculated for every strain measuring device, which is a calculation in space. To make a recalculation this is also done in this analysis. In the following sections a distinction is made between the probability function in space and in time. First the probability function of the maximum impact pressure is defined.

8.2 Maximum impact pressure and impact factor

The maximum pressure impact $p_{max} = \rho_w g q H_s$ is dependent on the wave height and the impact factor. The impact factor is used to account for the variation of wave height in time. The analysis of Führböter and Sparboom (1988) is used to compose a probability density function of the impact factor $q = \frac{p_{max}}{\rho g H_s}$. Führböter and Sparboom composed the probability function of the number of waves which create an impact together with the probability function of the intensity of the wave impact. The result is a log-normal distribution:

$$p(q) = \frac{1}{q\sqrt{2\pi}\beta} e^{-(\frac{(\ln(q)-\alpha)^2}{2\beta^2})}$$

With:

q impact factor

p(q) probability of occurrence of impact factor q

α,β parameters for the log-normal distribution

The mean and the variance are calculated with:

$$\mu = e^{\alpha + \frac{\beta^2}{2}}$$

$$\sigma^2 = e^{2\alpha+\beta^2}(e^{\beta^2} - 1)$$

μ the mean impact factor

σ^2 the variance of the probability function

Because the impact factor is log-normally distributed and the water density, the acceleration of gravity and the wave height are deterministic values the maximum impact pressure is log-normally distributed.

Führböter analyzed slopes of 1:4 and 1:6 only with regular waves in his experiment. However Grüne (1988) compared the data of Führböter and Sparboom (1988) with his own measurements at Wangerooge island (Germany) and concluded that also in real sea state conditions the maximum impact pressure is log-normal distributed. This is confirmed by Sparboom (1991). This means this log-normal distribution also can be used in the Delta flume experiment where regular waves and waves with a wave spectrum of Pierson-Moskowitz are used. However this log-normal distribution takes into account all the wave impacts which occur in the whole test run. To analyze the measured strain for only one wave impact only one impact factor belonging to that particular wave is used. The impact factor for each wave is stated in Table 8-2 as the S_f parameter. The test runs which are analyzed in this thesis and also are analyzed by de Waal (1993) are given in Table 8-1 (see also section 5.2.1 for the selection criteria).

Table 8-1 Selected runs

Date	Test Number	Spectrum Type or Regular waves	Hs, H	Tp, T
11-sep	AS 022	Regular	1.05	5.0
13-sep	AH 108	Regular	1.45	7.0
17-sep	AS 117	Regular	1.80	5.0
16-sep	AS 202	Pierson-Moskowitz	1.43	7.1
17-sep	AS 203	Pierson-Moskowitz	1.52	8.7
16-sep	AS 025	Pierson-Moskowitz	0.89	7.6

For each of these test runs some waves are selected to analyse.

Table 8-2 Maximum impact pressure and impact factor for each wave

Proef	h_t (m)	H (m)	T (s)	t (s)	p_{max} (kN/m^2)	S_f (-)
AS022	4.71	1.05	5.0	769	31.5	3.06
AS022	4.71	1.05	5.0	744	27.7	2.69
AS022	4.71	1.05	5.0	594	40.3	3.91
AH108	5.28	1.45	7.0	411	48.0	3.37
AH108	5.28	1.45	7.0	75	48.4	3.40
AH108	5.28	1.45	7.0	453	36.7	2.58
AS117	4.89	1.80	5.0	374	42.5	2.41
AS117	4.89	1.80	5.0	219	48.4	2.74
AS117	4.89	1.80	5.0	309	39.7	2.25
AS202	5.01	1.43	7.1	3695	97.5	6.95
AS202	5.01	1.43	7.1	3560	70.0	4.99
AS202	5.01	1.43	7.1	5605	59.4	4.24
AS202	5.01	1.43	7.1	5483	66.5	4.74
AS202	5.01	1.43	7.1	3539	54.9	3.91
AS203	5.10	1.52	8.7	4828	66.2	4.44
AS203	5.10	1.52	8.7	1319	56.9	3.82
AS203	5.10	1.52	8.7	3540	47.1	3.16
AS203	5.10	1.52	8.7	1227	45.3	3.04
AS203	5.10	1.52	8.7	51	41.1	2.75
AS025	5.21	.89	7.6	81	63.5	7.27
AS025	5.21	.89	7.6	151	47.9	5.48
AS025	5.21	.89	7.6	771	52.6	6.03
AS025	5.21	.89	7.6	207	45.3	5.19
AS025	5.21	.89	7.6	728	44.1	5.05

For each individual wave these values are used for calculating the strain. To calculate the differences in space the width of the impact area should be known. About the width in y-direction, as stated in de Waal (1993) the maximum impact pressure decreases to the border of the flume for the selected waves (see section 5.2.2). This because waves with a maximum impact at the middle of the wave flume (at DRO 15) are selected to analyze. The differences in maximum impact pressures are given in the graph below where in comparison to the mean value the local peak pressure is given with the standard deviation.

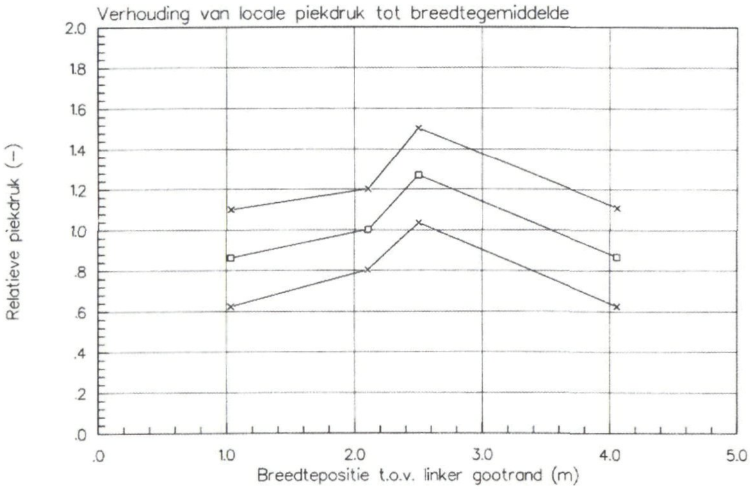

Figure 8-1 Pressure distribution over the width of the flume compared to the mean distribution

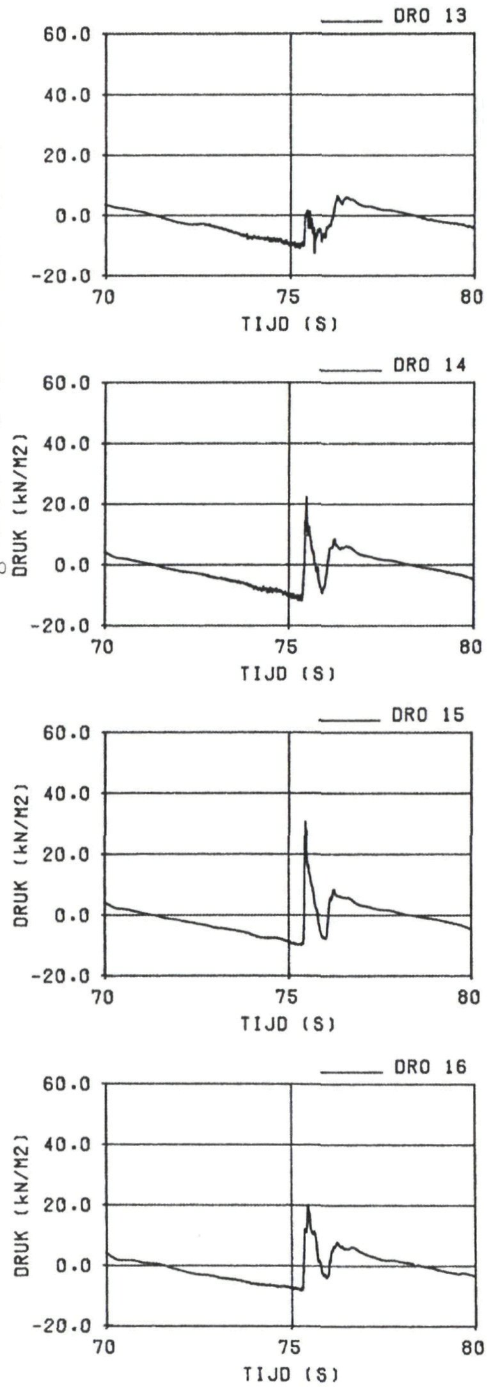

The impact pressure at the middle of the flume is almost 30% higher than the mean value of the impact pressure. Also the impact pressure at the border of the flume is about 15% lower than the mean value. The standard deviation of these values is about 20%. Also time record is given for the different pressure transducers where these differences are clearly shown. To take these differences into account the mean value of the impact is adapted. When the probability function of the maximum impact pressure for the whole test run has to be determined one has to know the probability function of the impact factor in time.

8.2.1 Impact factor distribution

8.2.1.1 AS022 Run Distribution

In Derks and Klein Breteler (1992) for each run the impact factor (vertical axis) is plotted with the probability of exceedance (see section 4.3.2). In Figure 8-2 the probability of exceedance of the impact factor of test run AS022 is given.

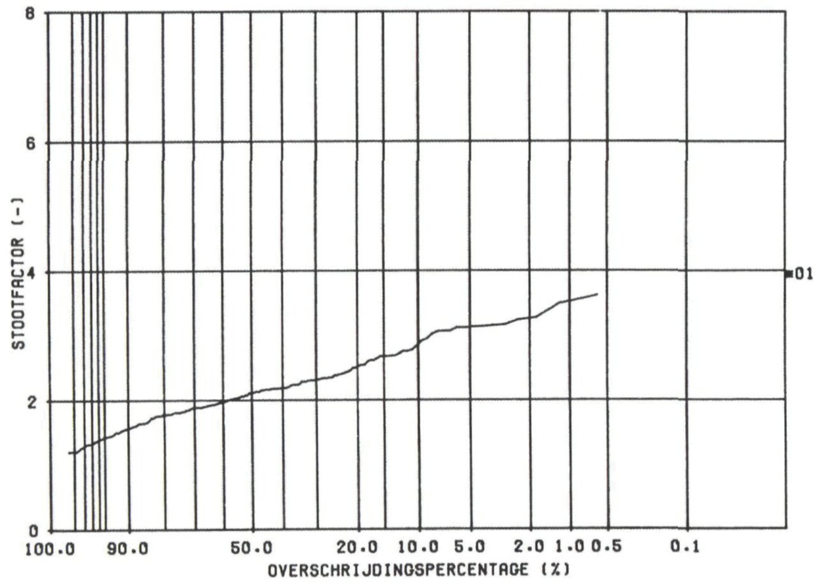

Figure 8-2 Exceedance percentage of the impact factor (Run AS022, DRO 11-19)

The data provided by this graph is used to determine the probability function of the impact factor for this test run. With interpolating this graph a table of values is obtained which is tested with the program Bestfit.

Table 8-3 The interpolated probabilities of the impact factor

Test series AS022			
Impact Factor	Probability of exceedance (%)	Probabilitty of non-exceedance (%)	Probability of non-exceedance
1.00	100.0	0.0	0.000
1.20	98.0	2.0	0.020
1.40	94.0	6.0	0.060
1.45	92.0	8.0	0.080
1.60	90.0	10.0	0.100
1.70	80.0	20.0	0.200
1.90	70.0	30.0	0.300
2.00	60.0	40.0	0.400
2.10	50.0	50.0	0.500
2.20	40.0	60.0	0.600
2.30	30.0	70.0	0.700
2.50	20.0	80.0	0.800
2.70	15.0	85.0	0.850
2.90	10.0	90.0	0.900
3.20	5.0	95.0	0.950
3.30	2.0	98.0	0.980
3.60	1.0	99.0	0.990
3.70	0.5	99.5	0.995
3.90	0.0	100.0	1.000

Bestfit uses the Chi-Square test and the Kolmogorov-Smirnov test to determine which probability distribution fits the data the best. In Table 8-4 the results of the Bestfit analysis are given.

Table 8-4 The results of the Bestfit analysis

Minimum=	1			
Maximum=	3.9			
Mode=	2.25			
Mean=	2.15075			
Std Deviation=	0.470199			
Variance=	0.221088			
Skewness=	0.576113			
Kurtosis=	3.971511			
Input Settings:				
Type of Fit:	Full Optimization			
Tests Run:	Chi-Square		K-S Test	
Best Fit Results				
Function	**Chi-Square**	**Rank**	**K-S Test**	**Rank**
Erlang(20.00,0.11)	1.72185	1	0.046793	3
Lognormal2(0.74,0.22)	1.815518	2	0.040562	1
Gamma(20.92,0.10)	1.840881	3	0.044779	2
Triang(1.00,1.91,3.90)	1.983831	4	0.144264	9
Lognormal(2.10,0.46)	2.082585	5	0.067068	6
Weibull(3.67,2.32)	2.390033	6	0.124985	8
Logistic(2.15,0.26)	2.530663	7	0.059042	4
Normal(2.15,0.47)	2.909264	8	0.068779	7

When both tests are considered the best fit is achieved by a lognormal2 distribution where the lognormal2(α,β) distribution is defined as:

$$f(x) = \frac{1}{x\sqrt{2\pi\beta^2}} e^{\frac{-(\ln(x)-\alpha)^2}{2\beta^2}}$$

The mean and the variance are calculated with:

$$\mu = e^{\alpha+\frac{\beta^2}{2}}$$

$$\sigma^2 = e^{2\alpha+\beta^2}(e^{\beta^2}-1)$$

μ the mean impact factor

σ^2 the variance of the probability function

The impact factor distribution for the AS022 run is defined as a lognormal2(0.74, 0.22) distribution with; μ=2.15 and σ^2=0.23

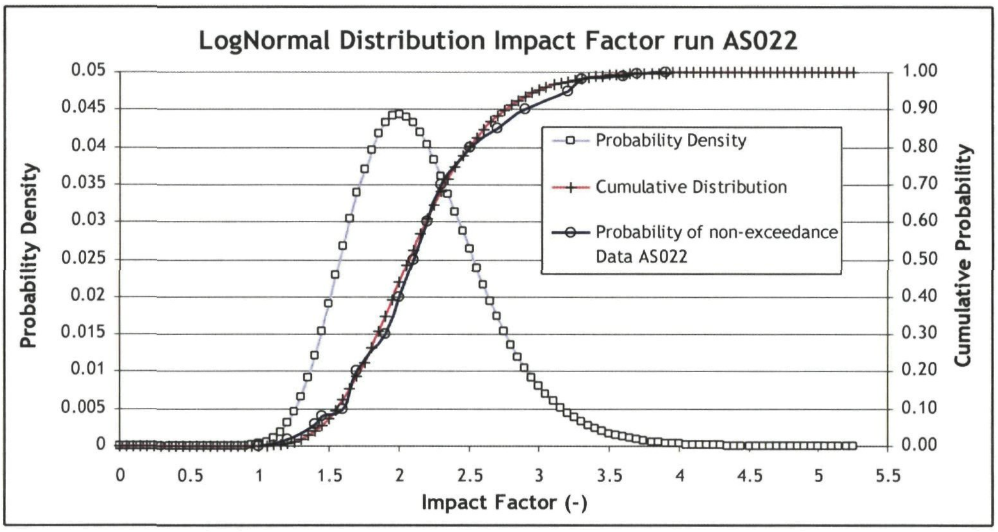

Figure 8-3 The fitted impact factor distribution for run AS022

8.2.2 Run AH108 Distribution

In Run AS117 regular waves were present. In the same way as for run AS022 the impact factor distribution is determined. The regular wave height is 1.45 meters with a wave period of 7.0 seconds.

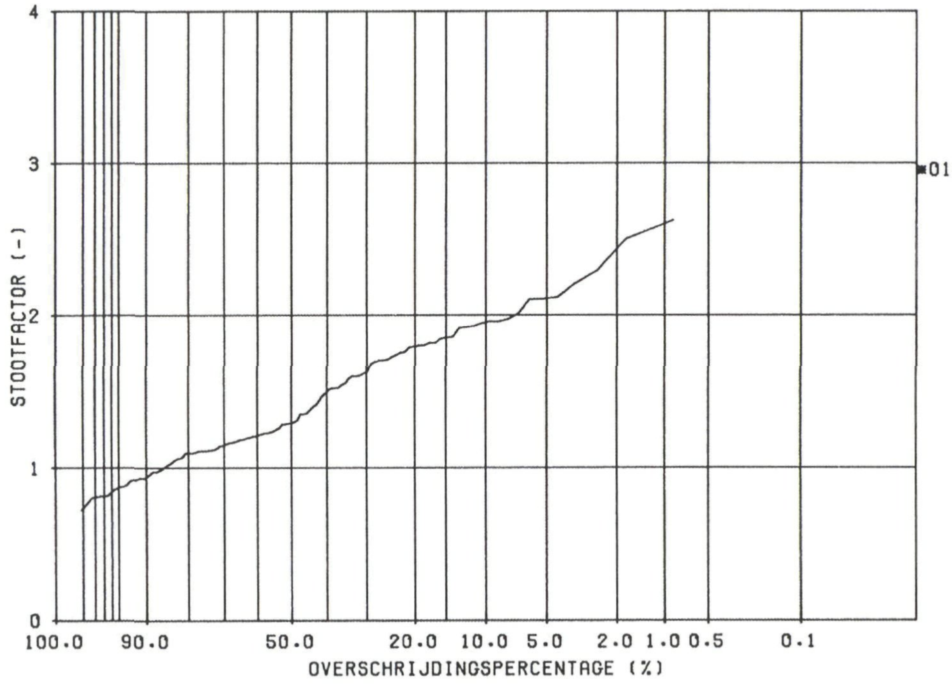

Figure 8-4 Exceedance percentage of the impact factor (Run AH108, DRO 9-17)

This graph is estimated in excel, by fitting, and again a lognormal distribution is found.

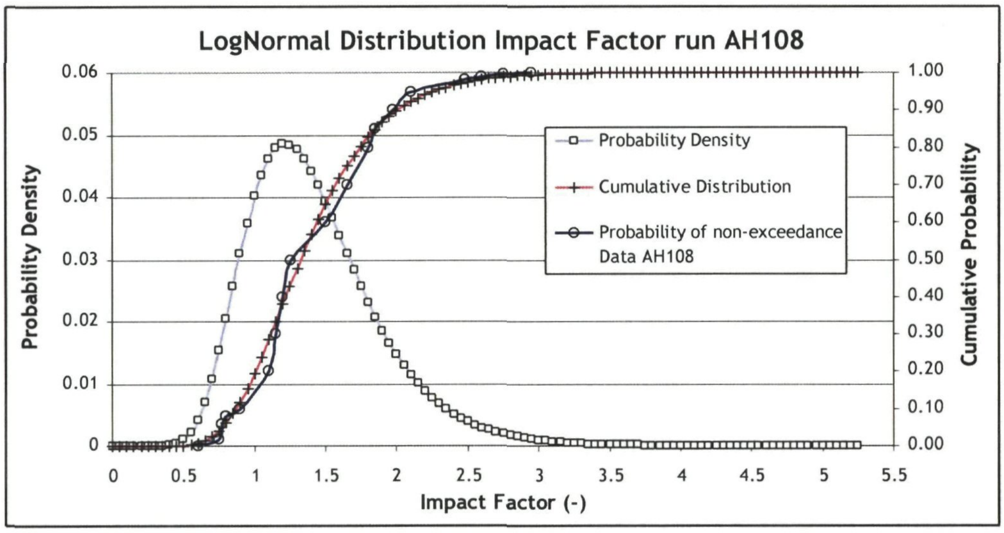

Figure 8-5 The fitted impact factor distribution for run AH108

The impact factor distribution for the AH108 run is defined as a lognormal2(0.30, 0.32) distribution with; μ=1.42 and σ^2=0.22.

8.2.3 Run AS117 Distribution

In Run AS117 also regular waves were present. In the same way as the foregoing runs the impact factor distribution is determined. The regular wave height is 1.80 meters with a wave period of 5.0 seconds.

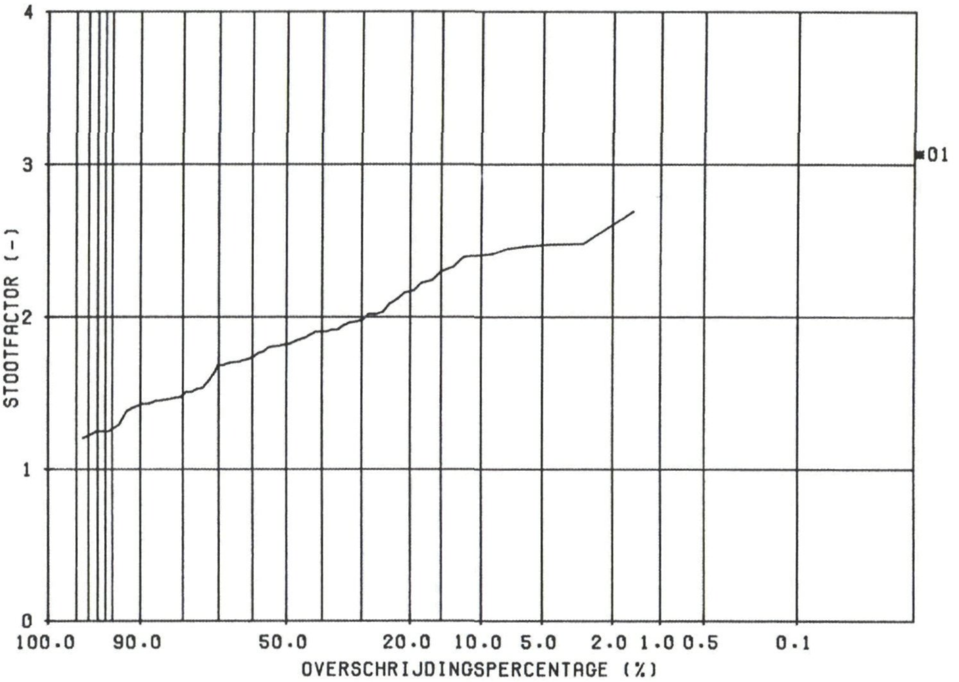

Figure 8-6 Exceedance percentage of the impact factor (Run AS117, DRO 11-18)

This graph is estimated in excel by fitting a lognormal distribution over this line.

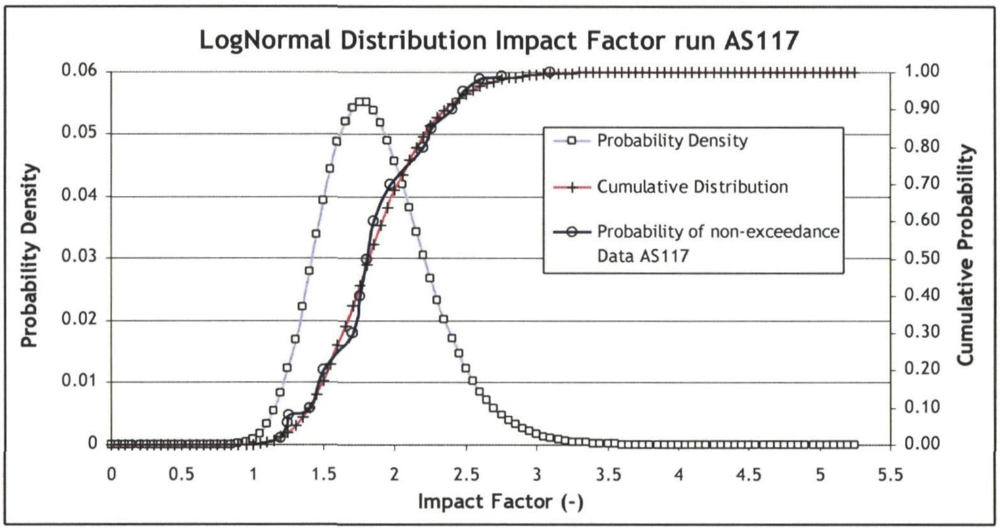

Figure 8-7 The fitted impact factor distribution for run AS117

The impact factor distribution for the AS117 run is defined as a lognormal2(0.61, 0.20) distribution with; μ=1.88 and σ^2=0.14.

8.2.4 Run AS202 Distribution

For run AS202 much higher impact factors are found. Here an irregular wave field is present with a Pierson-Moskowitz spectrum. The significant wave height is 1.43 meters and the peak period is 7.1 seconds.

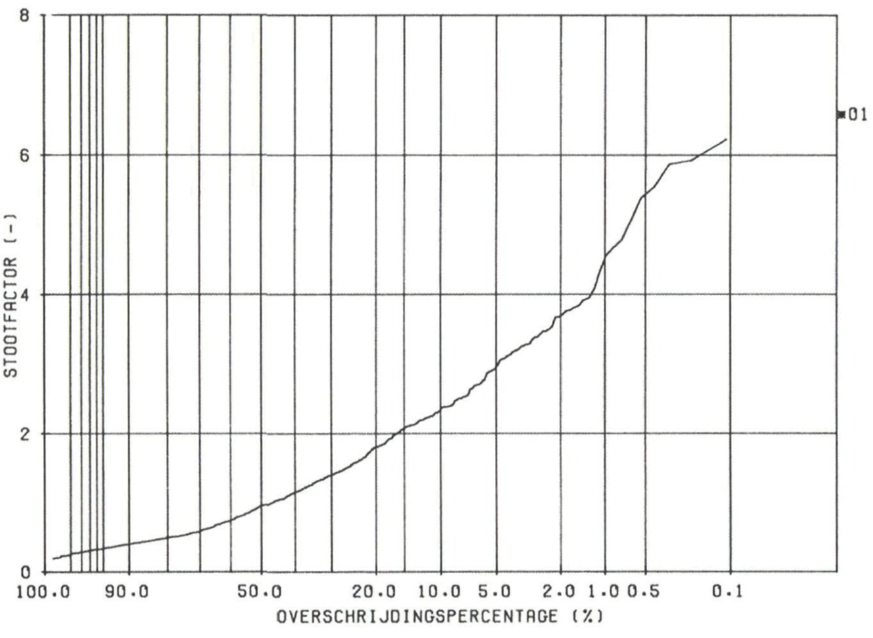

Figure 8-8 Exceedance percentage of the impact factor (Run AS202, DRO 8-19)

This data is also fitted with Bestfit and again a lognormal distribution is found. The parameters α and β Bestfit found were not in agreement with the real distribution so these are adapted to get a better fit.

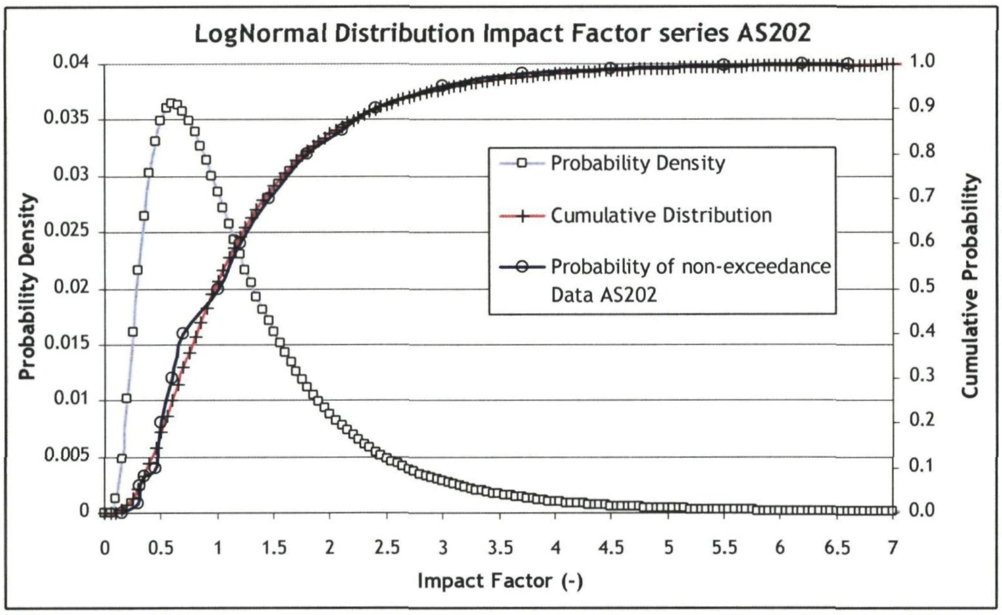

Figure 8-9 The fitted impact factor distribution for run AS202 (DRO 8-19)

The impact factor distribution for the AS202 run is defined as a lognormal2(0.00, 0.70) distribution with; μ=1.28 and σ^2=1.03. In the next figures the graphs of the impact factor distribution for the other test run.

8.2.5 AS203 Run Distribution

Here an irregular wave field is present with a Pierson-Moskowitz spectrum. The significant wave height is 1.52 meters and the peak period is 8.7 seconds.

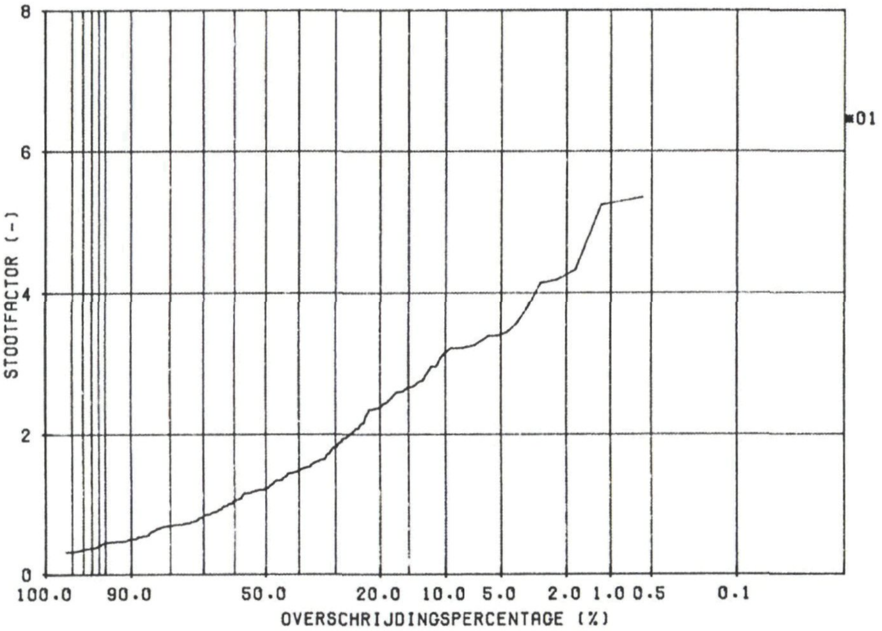

Figure 8-10 Exceedance percentage of the impact factor (Run AS203, DRO 8-19)

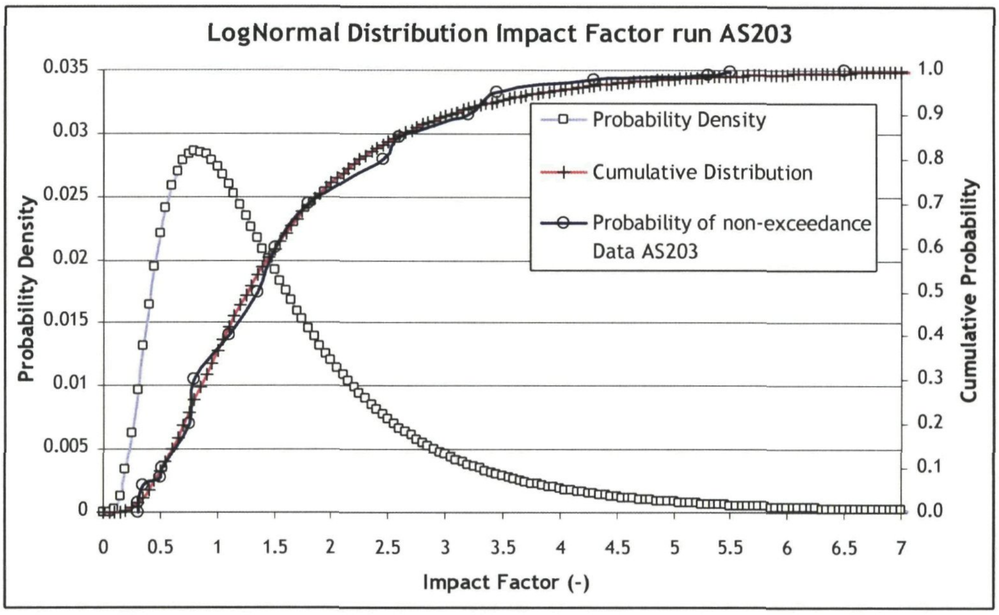

Figure 8-11 The fitted impact factor distribution for run AS203 (DRP 8-19)

The impact factor distribution for the AS203 run is defined as a lognormal2(0.26, 0.68) distribution with; μ=1.63 and σ^2=1.57.

8.2.6 AS025 Run distribution

Here an irregular wave field is present with a Pierson-Moskowitz spectrum. The significant wave height is 0.87 meters and the peak period is 7.6 seconds.

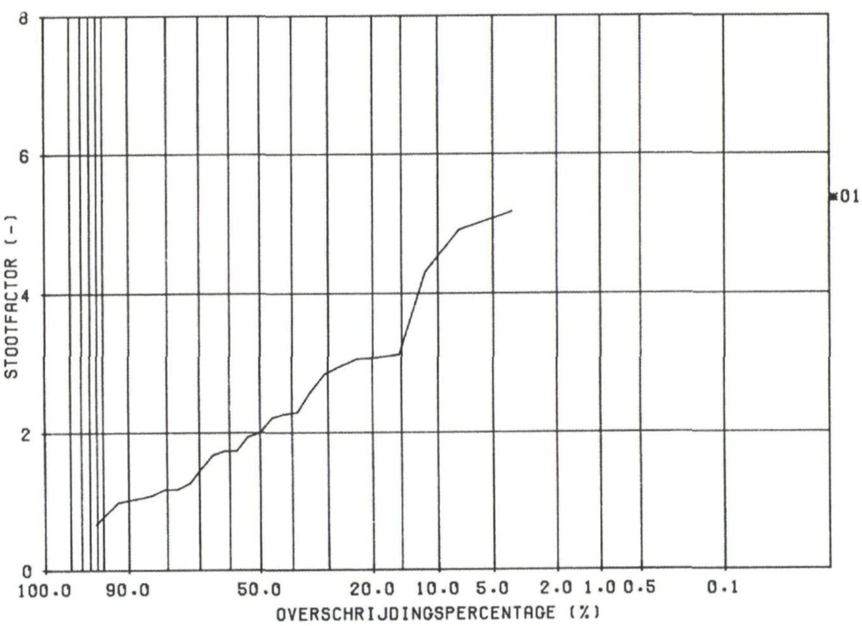

Figure 8-12 Exceedance percentage of the impact factor (Run AS025, DRO 9-17)

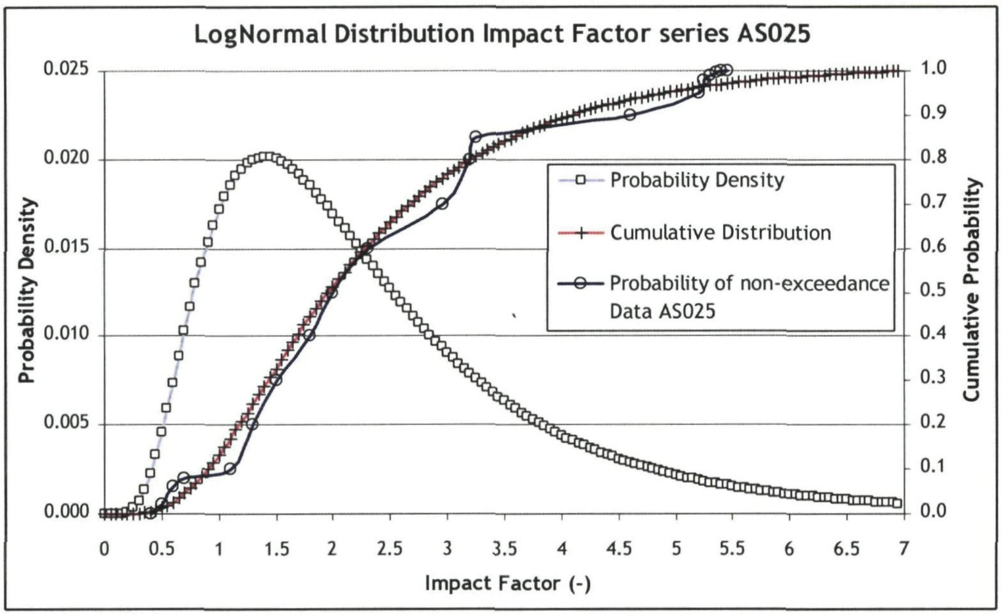

Figure 8-13 The fitted impact factor distribution for run AS025 (DRO 9-17)

The impact factor distribution for the AS025 run is defined as a lognormal2(0.70, 0.60) distribution with; μ=2.41 and σ^2=2.52.

8.2.7 Used maximum impact distribution

The next graph shows an example of the probability function of the maximum impact pressure for test run AS022 with a wave height of 1.05 m.

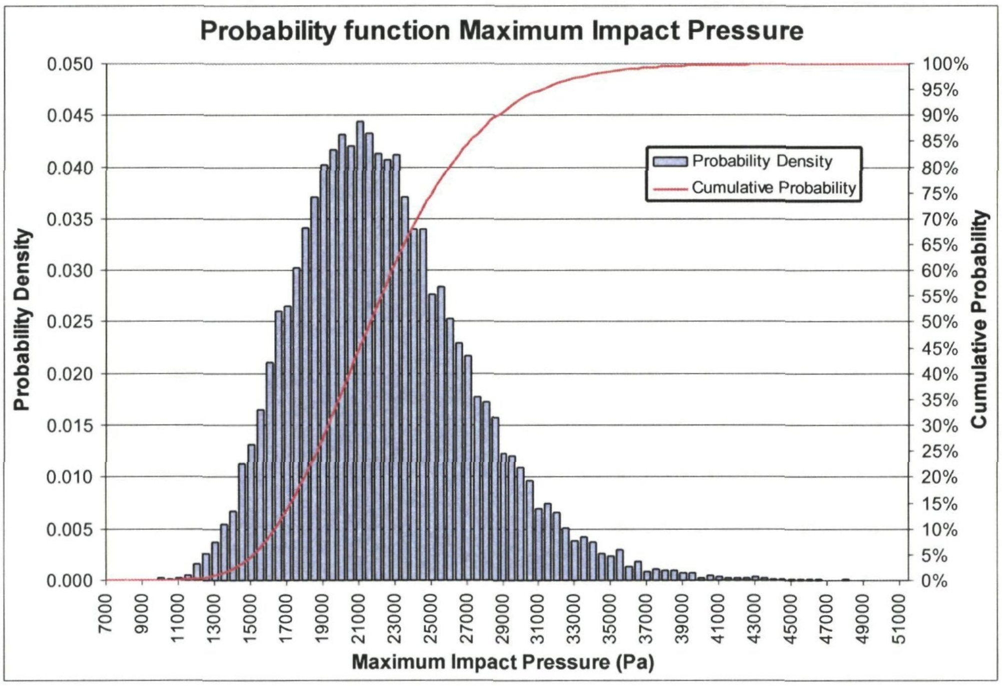

Figure 8-14 Example of a maximum impact pressure distribution used in the Monte Carlo simulation

8.3 Wave height

For every test run the wave height is know. Both tests with regular and irregular waves are selected. The following selection in runs is made (see section 5.2.1):

Table 8-5 The selected runs

Date	Test Number	Spectrum Type or Regular waves	Hs, H (m)	Tp, T (s)
11-sep	AS 022	Regular	1.05	5.0
13-sep	AH 108	Regular	1.45	7.0
17-sep	AS 117	Regular	1.80	5.0
16-sep	AS 202	Pierson-Moskowitz	1.43	7.1
17-sep	AS 203	Pierson-Moskowitz	1.52	8.7
16-sep	AS 025	Pierson-Moskowitz	0.89	7.6

In the Monte Carlo simulation the impact factor is used to take the variation in wave height into account. This means that the above stated values (Hs, H) are used for the wave height in the simulation.

8.4 Modulus of elasticity

In this section the modulus of elasticity of the asphalt revetment in the Delta flume is determined. Cores drilled out of the revetment are tested in a laboratory.

8.4.1 Laboratory data

In the Deltagoot 1991 experiment six cores are drilled out of the revetment. 24 beams are sawed out of these cores, two beams at the underside of the core and two at the upped side of the core and dynamical 3-point bending tests are executed. In Table 8-6 the used codes for the cores.

Table 8-6 Used codes in the laboratory

Gebruikte coderingen.					
Kern-code bij DWW	Kern-code bij NPC	Kern-hoogte ca. [mm]	Balk uit kern-laag	Balk-code E-init. bij NPC	Balk-code Vermoeiing bij NPC
H	BK0743	160	boven	HB1	HB3
			boven	HB2	HB4
			onder	HO1	HO3
			onder	HO2	HO4
I	BK0744	180	boven	IB1	IB3
			boven	IB2	IB4
			onder	IO1	IO3
			onder	IO2	IO4
J	BK0745	165	boven	JB1	JB3
			boven	JB2	JB4
			onder	JO1	JO3
			onder	JO2	JO4
K	BK0746	245	boven	KB1	KB3
			boven	KB2	KB4
			onder	KO1	KO3
			onder	KO2	KO4
L	BK0747	235	boven	LB1	LB3
			boven	LB2	LB4
			onder	LO1	LO3
			onder	LO2	LO4
M	BK0748	215	boven	MB1	MB3
			boven	MB2	MB4
			onder	MO1	MO3
			onder	MO2	MO4
K	(BK074	(245)	midden	KM1	
			midden	KM2	KM4
L	(BK074	(235)	midden	LM1	
			midden	LM2	
M	(BK074	(215)	midden	MM1	
			midden	MM2	

After sawing the beams from the cores, the left over is used to determine the mixture composition of the core. In Table 8-7 the result is given. First the grain size distribution is given, then the sand prism, the binder content, properties of the binder and voids percentage with densities.

Table 8-7 The properties of the asphalt cores, the laboratory results

netherlands pavement consultants

ONDERZOEKSRESULTATEN VAN ASFALTMONSTERS **(zaagrestanten van boorkernen Ø 250 mm): samenstelling, eigenschappen teruggewonnen bindmiddel en holle ruimte**

Projekt : 91523 "Deltagoot"
Soort asfaltbeton : waterbouwasfaltbeton

monster nr.[1] BK	H 743	I 744	J 745	K 746	L 747	M 748	....	....	gem.	s
korrelverdeling										
op C 31.5 (cum.%)	....	....	....	....	....	....	....	....	....	...
C 22.4	0,0	0,0	0,0	0,0	0,0	0,0	....	....	....	...
C 16	0,4	0,8	1,3	1,3	0,3	1,6	....	....	1,0	0,5
C 11.2	10,8	10,3	10,2	10,4	9,3	11,1	....	....	....	...
C 8	27,3	24,5	29,0	26,3	27,6	27,8	....	....	....	...
C 5.6	40,9	39,1	41,0	39,7	40,5	41,3	....	....	....	...
2 mm	49,9	48,2	49,7	48,2	49,3	49,4	....	....	49,1	0,7
63 µm	91,9	91,2	91,4	91,1	91,4	91,3	....	....	....	...
< 63 µm	8,1	8,8	8,6	8,9	8,6	8,7	....	....	8,6	0,3
zanddriehoek										
fraktie 2mm-500µm (%)	20,1	20,0	18,4	19,9	18,4	21,2	....	....	19,7	1,1
500-180µm	36,1	33,7	35,3	36,1	35,3	33,8	....	....	35,0	1,1
180- 63µm	43,8	46,3	46,3	44,0	46,3	45,0	....	....	45,3	1,2
bindmiddelgehalte										
(% "op")	6,5	6,7	6,4	6,6	6,5	6,6	....	....	6,6	0,1
eigenschappen terruggewonnen bindmiddel										
R&K (°C)	50,0	49,0	52,0	49,5	49,0	50,0	....	....	50,0	1,1
pen (0.1mm)	76	78	65	73	80	69	....	..	74	6
PI	-0,2	-0,3	-0,1	-0,4	-0,3	-0,4	....	....	-0,3	0,1
(asgehalte %) [3]	(0,2)	(0,1)	(0,3)	(0,2)	(0,3)	(0,5)				
holle ruimte										
dichth.ps.[2] (kg/m³)	2348	2353	2346	2335	2340	2349	....	....	2345	7[4]
dichth.meng. (kg/m³)	2423	2421	2422	2420	2420	2420	....	....	2421	1
holle ruimte (%)	3,1	2,8	3,1	3,5	3,3	2,9	....	....	3,1	0,3

The requirements of asphalt used in hydraulic engineering are stated in CROW (2005). The national Information and Technology Platform for Transport, Infrastructure and Public space (CROW) is a not-for-profit organization in which the government and businesses work together in pursuit of their common interests through the design, construction and management of roads and other traffic and transport facilities. This organisation formulates the requirements of asphalt and also the asphalt used in the Delta flume can be checked to these requirements. For hydraulic asphalt the requirements are:

- volume percentage of voids should be less then 5% of the total volume
- maximum deviation to the mean bitumen content should be less then 0.5% mass percentage
- maximum deviation of the grain size distribution in mass percentage should be less then:
    - C 22.4; 4%

- C16; 4%
- 2 mm; 5%
- 63 μm; 1%

All these requirement are fulfilled so the asphalt used in the Delta flume is indeed hydraulic asphalt according to the standard requirements.

The beams are placed in the test set-up in the way the strain will occur at the underside of the beam as it was in reality in the Delta flume. The experiment is repeated four times under different circumstances. Six beams are tested at 10 Hz with a temperature of 0°Celcius, six beams at 10 Hz with a temperature of 5°Celsius, six beams at 1 Hz with a temperature of 5°Celsius and six beams at 1 Hz with a temperature of 10°Celsius. Three different loadings are applied on the beams (under all temperatures and frequencies) to determine the initial modulus of elasticity. The results of the tests are regression parameters and modulus of elasticity.

Table 8-8 The regression parameters of the tested asphalt beams

Regressie parameters log(Nf)=log(k) - a*log(σ)			
Omstandigheden		Parameters	
fq [Hz]	temp [°C]	log(k)	a
9.8	0	5.3591	2.309
1.0	5	4.4440	3.515
9.8	5	6.4333	4.676
1.0	10	3.6847	2.977

Table 8-9 The testing conditions and testing results

Bepaling E-initieel										
	Proefomstandigheden				Proefresultaten					
Balk-code E-init.	fq [Hz]	temp [°C]	Fmin [N]	Fmax [N]	ampl. verpl. [mm]	rek [µm/m]	fasehoek [graden]	E-init. [MPa]	N-einde [-]	Offset bi proefeind [mm]
HB1	9.8	0	-30	-470	0.0055	41.4	12.2	11909	279	-0.067
IB1	9.8	0	-30	-470	0.0057	42.3	15.7	11643	279	-0.081
J02	9.8	0	-30	-470	0.0057	43.4	11.9	11173	279	-0.069
KB1	9.8	0	-30	-470	0.0074	54.5	15.8	9335	279	-0.097
LB1	9.8	0	-30	-470	0.0060	45.0	15.9	11068	279	-0.098
M02	9.8	0	-30	-470	0.0052	39.7	15.3	12096	279	-0.095
KM2	9.8	0	-30	-470	0.0054	40.4	13.9	12369	275	-0.075
Gemiddeld:					0.0058	43.8	14.4	11371	278	-0.083
Stand.dev.:					0.0007	4.7	1.6	938	1	0.013
HB2	1	5	-30	-330	0.0089	66.4	25.6	5075	191	-0.348
IB2	1	5	-30	-330	0.0085	64.3	28.7	5274	191	-0.407
J01	1	5	-30	-330	0.0067	51.2	23.9	6520	191	-0.206
KB2	1	5	-30	-330	0.0107	79.7	28.1	4528	191	-0.538
LB2	1	5	-30	-330	0.0093	70.4	28.1	4855	192	-0.515
M01	1	5	-30	-330	0.0077	59.1	27.2	5704	192	-0.392
Gemiddeld:					0.0087	65.2	26.9	5326	191	-0.401
Stand.dev.:					0.0013	8.9	1.7	645	0	0.110
H01	9.8	5	-30	-470	0.0067	51.3	19.7	9307	279	-0.166
I01	9.8	5	-30	-470	0.0076	57.5	19.7	8460	279	-0.225
JB2	9.8	5	-30	-470	0.0070	52.9	17.2	9310	279	-0.143
K01	9.8	5	-30	-470	0.0063	47.6	16.8	10269	279	-0.148
L01	9.8	5	-30	-470	0.0076	57.7	18.7	8544	279	-0.216
MB2	9.8	5	-30	-470	0.0069	52.0	18.3	9300	279	-0.193
Gemiddeld:					0.0070	53.2	18.4	9198	279	-0.182
Stand.dev.:					0.0005	3.5	1.1	599	0	0.032
H02	1	10	-30	-240	0.0083	63.6	36.0	3596	146	-0.540
I02	1	10	-30	-240	0.0090	68.2	35.5	3434	191	-0.601
JB1	1	10	-30	-240	0.0080	60.1	31.4	3958	191	-0.379
K02	1	10	-30	-240	0.0091	68.8	32.3	3541	146	-0.424
L02	1	10	-30	-240	0.0100	75.1	34.4	3269	192	-0.626
MB1	1	10	-30	-240	0.0099	75.0	33.8	3180	192	-0.685
Gemiddeld:					0.0090	68.5	33.9	3496	176	-0.542
Stand.dev.:					0.0007	5.5	1.6	252	21	0.109

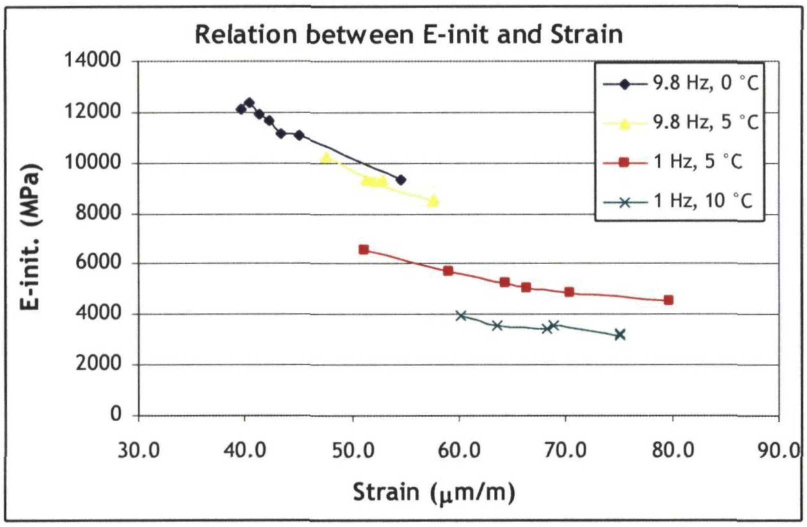

Figure 8-15 The relation between E-init and the strain from Table 8-9

The modulus of elasticity is calculated from the signal plots of the test. The difference in phase, the ratio between the load- and the strain amplitude determines the modulus of elasticity.

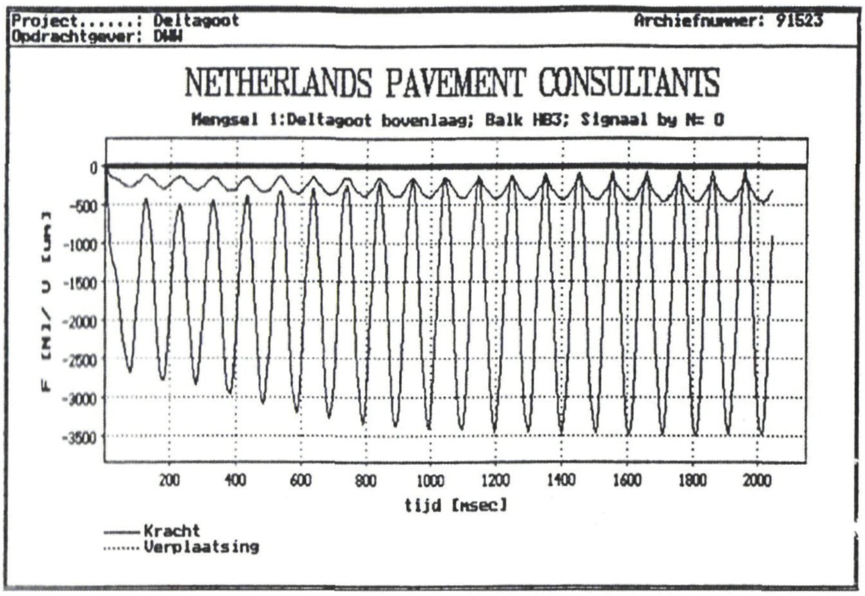

Figure 8-16 Example of a test signal, beam HB3

8.4.2 Mastercurve laboratory data

With the program Husaroad, a program used by KOAC•NPC to generate mastercurves from laboratory data, a mastercurve is obtained for different temperatures by using the above displayed data. In the program Husaroad the Huet-Sayegh model is used. Below this model this displayed with the parameters used to determine the mastercurve. The four main components in a model to simulate the behaviour of viscose-elastic material are:

E	modulus of elasticity - resistance of axial test piece against axial changes
G	shear modulus - resistance against changes in shape
K	bulk modulus - resistance against changes in volume
ν	Poisson's contraction coefficient - ratio between vertical and horizontal strain

The relations between these components are given by:

$$K=\frac{EG}{9G-3E}\qquad E=\frac{9KG}{G+3K}\qquad G=\frac{E}{2(1+\nu)}\qquad \nu=\frac{3KG}{2(G+3K)}$$

In Husaroad a choice is made to assume the bulk modulus as an elastic behaving component and the shear modulus as a viscose-elastic component.

Determination of Parameters in Model of Huet - Sayegh
using stiffnesses and phase angles as function of frequency and temperature

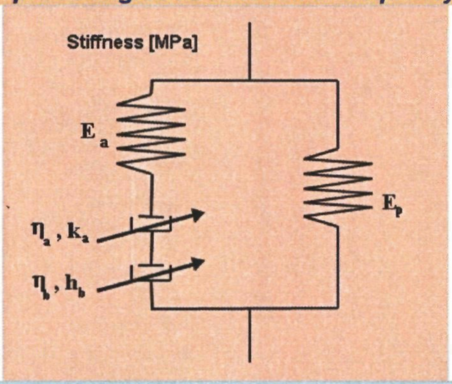

Load on element: $\varepsilon = \varepsilon_0 e^{i\omega t}$

General constitutive relation for mechanical elements:

$$\sigma = \{A\,\tau^{a-1}\,d^a/dt^a\}\varepsilon$$

Spring:	$A = E/\tau$	$a = 0$	$\sigma = E\,.\,\varepsilon = E\,.\varepsilon_0 e^{i\omega t}$
Linear dashpot	$A = \eta$	$a = 1$	$\sigma = \eta\,.\,\varepsilon' = \eta\,.\,i\omega\,.\,\varepsilon_0 e^{i\omega t}$
Variable dashpot:	$A = \eta$	$a = h$	$\sigma = \eta/\tau\,.\,(\tau^h\,d^h/d\tau^h)\,.\,\varepsilon = \eta/\tau\,.\,(i\omega\tau)^h\,.\,\varepsilon_0 e^{i\omega t}$

Specific assumptions in this model yield:
the same τ for both dashpots;
a constant factor between η_a and η_b

It appears that: $\eta_a = \tau\,.\,E_a/\delta$
$\eta_b = \tau\,.\,E_a$

As τ is a function of temperature, η_a and η_b depend on temperature.

The complex stiffness modulus in analytical form is:

$$E^*(\omega) = E_p + E_a/\left(1+\delta\,(i\omega\tau)^{-ka} + (i\omega\tau)^{-hb}\right)$$

with:
i is complex number ($i^2 = -1$)
ω is angular frequency of the sollicitation [rad/s], ω=2*π*frequency, dimension of frequency: [Hz]
E_p is elastic modulus in right branch (also stiffness at loading frequency zero) [MPa]
E_a is elastic modulus in left branch [MPa]
τ is characteristic time which is a function of temperature,
δ is proportionality factor between η_a and η_b
k_a is power for dashpot a
h_b is power for dashpot b

The result of using this model is a mastercurve for the cores drilled out of the Delta flume revetment.

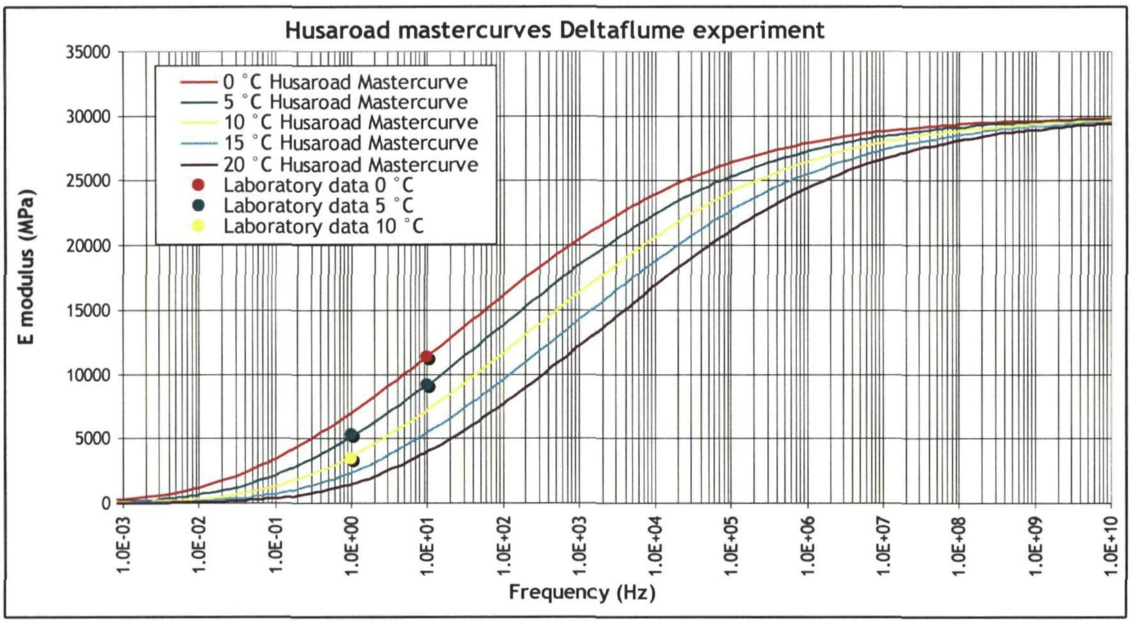

Figure 8-17 The calculated Husaroad mastercurves with laboratory data at different temperatures

With this mastercurve and the program Husaroad the modulus of elasticity for every temperature is calculated. At the end of this chapter the modulus of elasticity for the asphalt temperature of the Delta flume experiment is determined.

8.4.3 Recalculation using nomographs

It must be noted that these values of E-init should be validated, this because the 3-point bending test was in the starting phase of development in the year 1991. The development of the 3-point bending test is studied in the report de Looff (2003). In the calibration of the 3-point bending test it was discovered that there is some tolerance at the support of the beam. This tolerance results in measuring to much displacement of the beam which leads to an underestimation of the modulus of elasticity. The tolerance is higher at low temperatures and high frequencies of the loading signal. To cope with this problem the modulus of elasticity of the core samples will be recalculated. For this the "van der Poel's" nomograph is used in combination with the nomograph of Ugé. For more details about these nomographs reference is made to the Shell bitumen handbook, Schönian (1999).

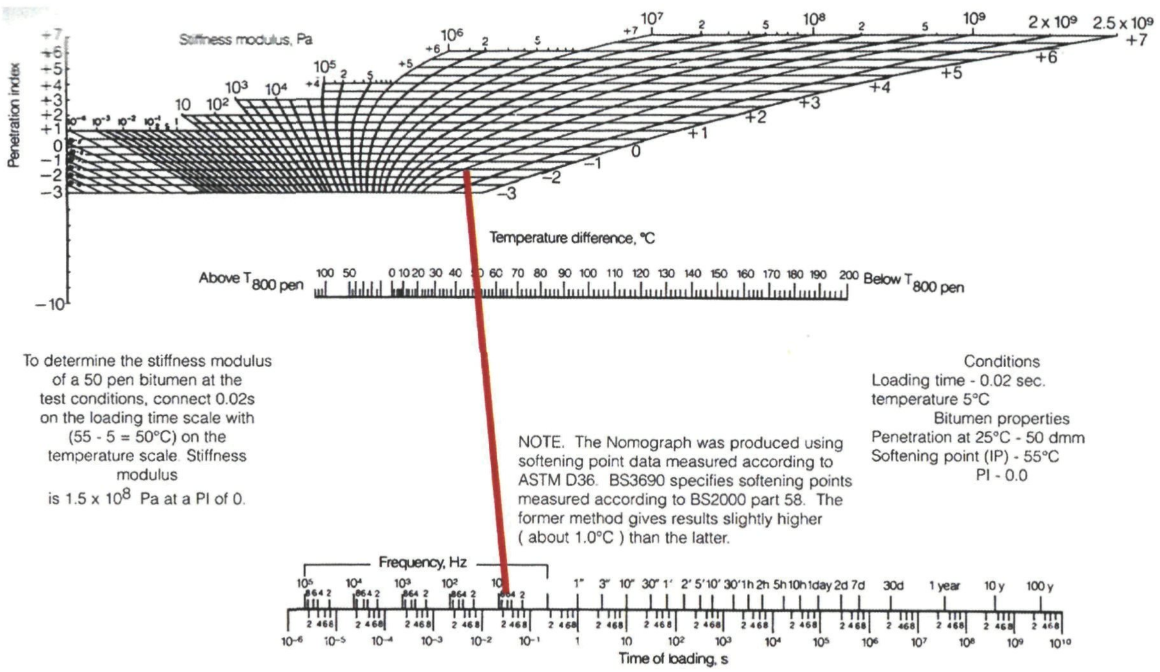

Figure 8-18 Van der Poel's Nomograph for determining the stiffness modulus of bitumens S_{bit} (Schönian 1999)

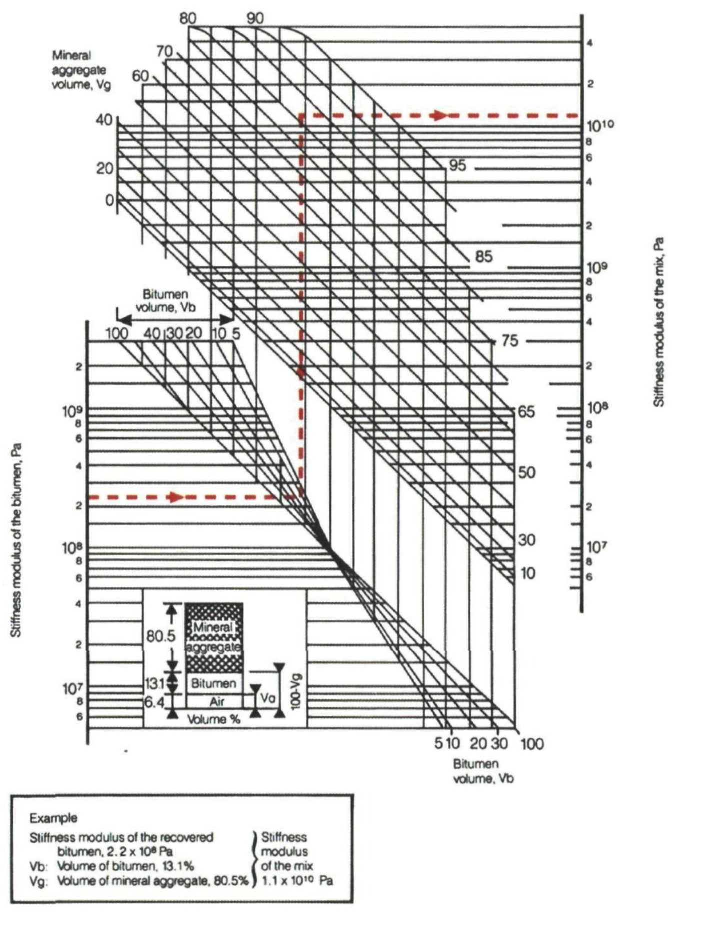

Ugé's Nomograph for determining the stiffness modulus S_{mix} for short loading times

Figure 8-19 Ugé's Nomograph for determining the stiffness modulus S_{mix} for short loading times (Schönian 1999)

The Shell company developed a program to deal with these nomographs without interpolating on paper. This program (Bands 2.0) is used to determine the stiffness modulus of the Delta flume cores. From Table 8-7 the percentage of stone, sand, filler and bitumen is determined. The percentages are averaged over all the cores because the differences are very small.

Table 8-10 Mixture composition in mass of the Delta flume cores

Grain distribution	Stone	49.1%
	Sand	42.3%
	Filler	8.6%
Total		100.0%
	Bitumen	6.6%
	Voids	3.1%
Total		109.7%

Total mixture composition	Stone	44.8%
	Sand	38.6%
	Filler	7.8%
	Bitumen	6.0%
	Voids	2.8%
Total		100.0%

Table 8-11 Mixture composition in volume of the Delta flume cores

Total mixture composition	Stone	40.17%
	Sand	35.26%
	Filler	7.75%
	Bitumen	14.29%
	Voids	2.83%
Total		100%

With the known volume percentage of the bitumen and the laboratory data with the softening point, the penetration index and penetration value the program Bands 2.0 is used to create mastercurves for different temperatures. This is shown in the next section.

8.4.4 Mastercurve nomograph data

In this section the program bands 2.0 is used to acquire a mastercurve. This mastercurve is generated to compare the Husaroad mastercurves with the data acquired by using a nomograph.

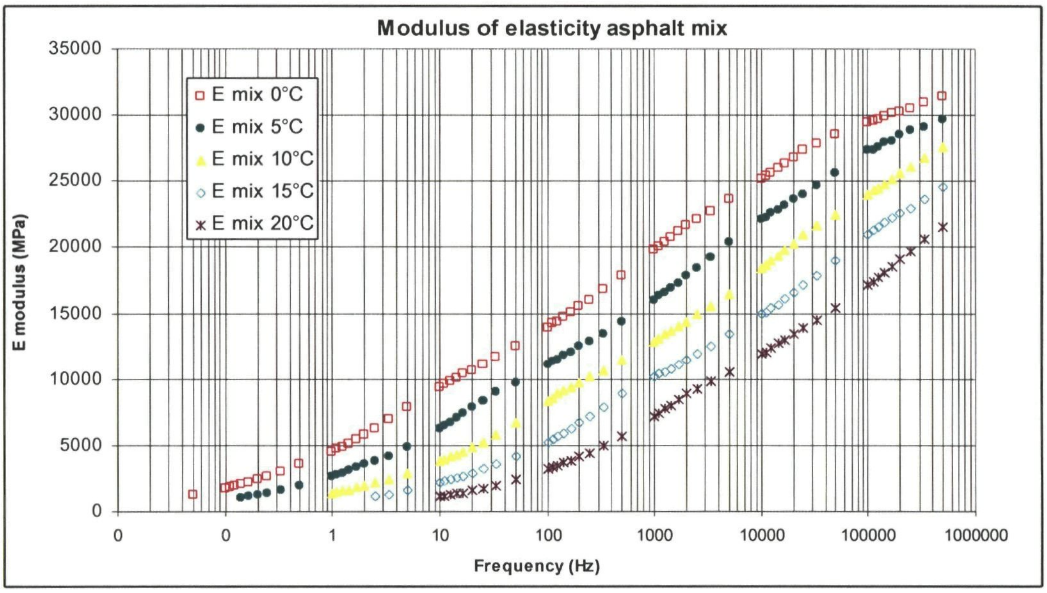

Figure 8-20 The calculated modulus of elasticity mastercurves with Bands 2.0

This graph shows a modulus of elasticity of about 32500 at high frequency what is a quite realistic value. This can be shown by comparing these mastercurves with the mastercurves generated with Husaroad.

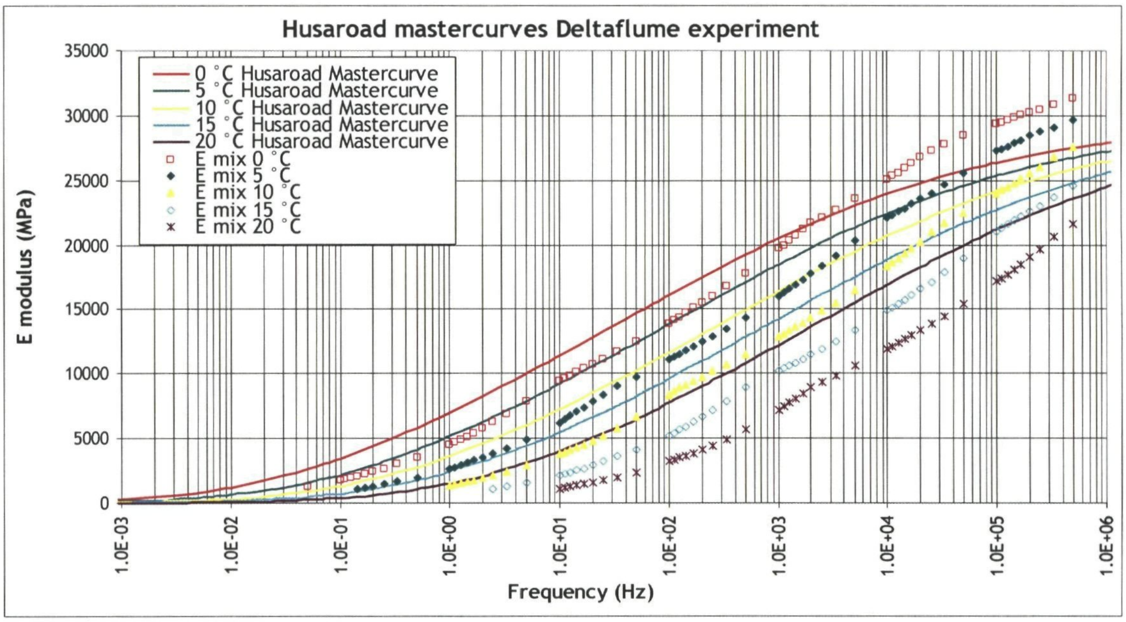

Figure 8-21 Comparison between the calculated mastercurves with Husaroad and Bands 2.0

8.4.5 Temperature correction

Because the modulus of elasticity is dependent on temperature it is corrected for the experimental conditions under which the test and measurements are performed. In de Waal (1993) this temperature correction is done, they are stated in Table 8-12.

Table 8-12 Asphalt temperature under testing conditions and the used modulus of elasticity of van de Waal (1993)

Proef	E_a (MPa)
AS022	1300
AS022	1300
AS022	1300
AH108	2040
AH108	2040
AH108	2040
AS117	3430
AS117	3430
AS117	3430
AS202	3430
AS202	3430
AS202	3430
AS202	3430
AS202	3430
AS203	3430
AS203	3430
AS203	3430
AS203	3430
AS203	3430
AS025	3430
AS025	3430
AS025	3430
AS025	3430
AS025	3430

Datum	Tijdstip	Temperatuur asfalt	
		Laagdikte 15 cm °C	Laagdikte 25 cm °C
11-9-1991	8.00	16,6	17,7
	16.00	14,0	15,6
12-9-1991	8.00	13,2	14,6
	12.00	12,9	14,2
	16.00	12,8	14,0
13-9-1991	8.00	12,7	13,4
	12.00	12,6	13,2
	16.00	12,5	13,0
16-9-1991	-	8,6	8,6
17-9-1991	-	8,6	8,6
18-9-1991	-	8,9	8,9
19-9-1991	-	8,7	8,7
20-9-1991	-	8,7	8,7
23-9-1991	-	8,7	8,7
24-9-1991	-	8,7	8,7
25-9-1991	-	8,7	8,7

Frequentie (1/s)	Temperatuur (°C)		
	8.6	13.0	16.5
5	3430	2040	1300
10	4350	2750	1800
15	5000	3270	2150
20	5530	3630	2440
25	5990	3920	2690

This data can be visualized in a mastercurve and compared with the Husaroad mastercurves calculated in section 8.4.2. In the next graphs the Husaroud mastercurve for 8.6°C, 13°C and 16.5°C are shown with the mastercurves of de Waal (1993).

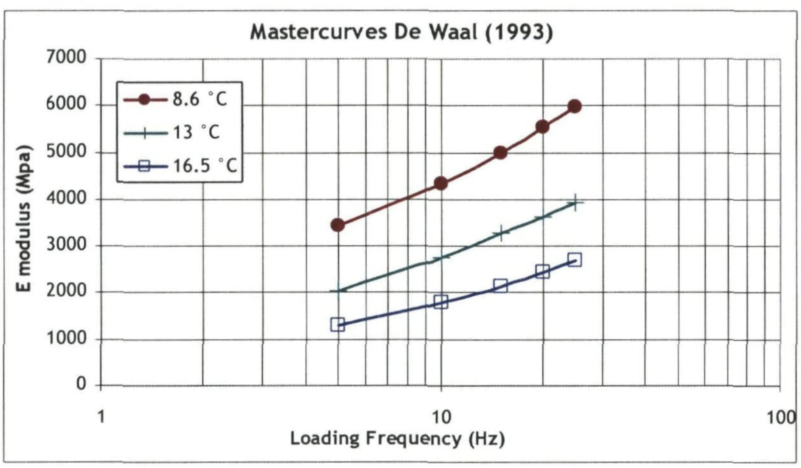

Figure 8-22 The used mastercurves of de Waal visualized

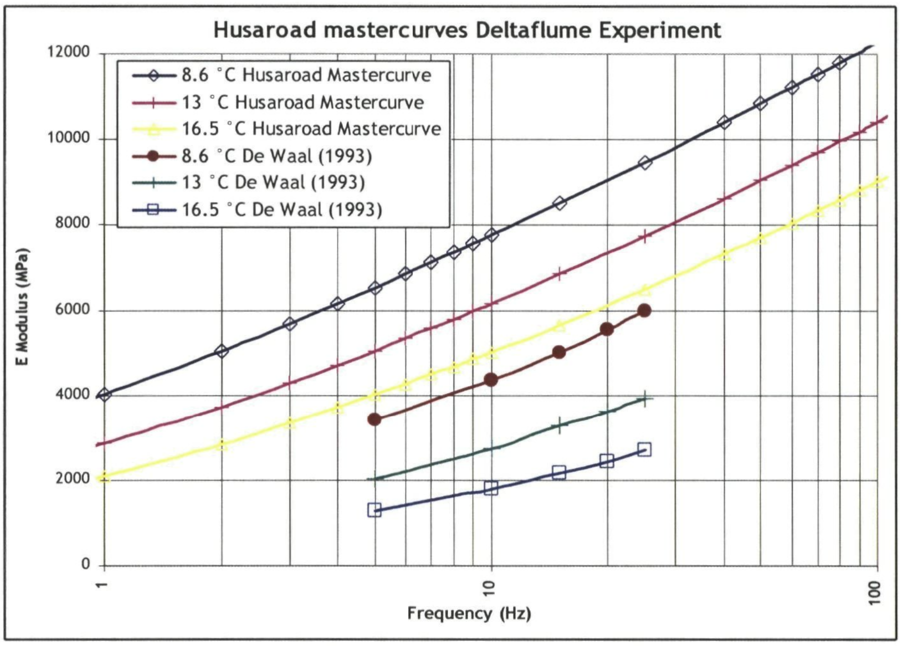

Figure 8-23 Comparison between the calculated mastercurves with Husaroad and the visualized mastercurves of de Waal

These mastercurves show a surprisingly big difference, the difference between these values is more than 3000 MPa. In Table 8-13 the values are stated.

Table 8-13 The values of the modulus of elasticity calculated with Husaroad compared with de Waal

E modulus	(MPa)	de Waal (1993)		E modulus	(MPa)	Husaroad	
Frequency (Hz)	8.6 °C	13 °C	16.5 °C	Frequency (Hz)	8.6 °C	13 °C	16.5 °C
5	3430	2040	1300	5	6540	5047	4006
10	4350	2750	1800	10	7761	6158	5018
15	5000	3270	2150	15	8509	6848	5656
20	5530	3630	2440	20	9053	7354	6127
25	5990	3920	2690	25	9481	7755	6502

The difference between the modulus of elasticity of de Waal (1993) and the calculated Husaroad elasticity can be the cause for the poor relation found in de Waal (1993) (see section 5.4). Furthermore results from an analysis done by P.A. Ruygrok in the year 1994, also on the Delta flume experiment of 1991, show much higher modulus of elasticity. One example is showed here to support the idea of a higher modulus of elasticity. In Figure 8-24 (Ruygrok 1994) the measured and calculated strain is given.

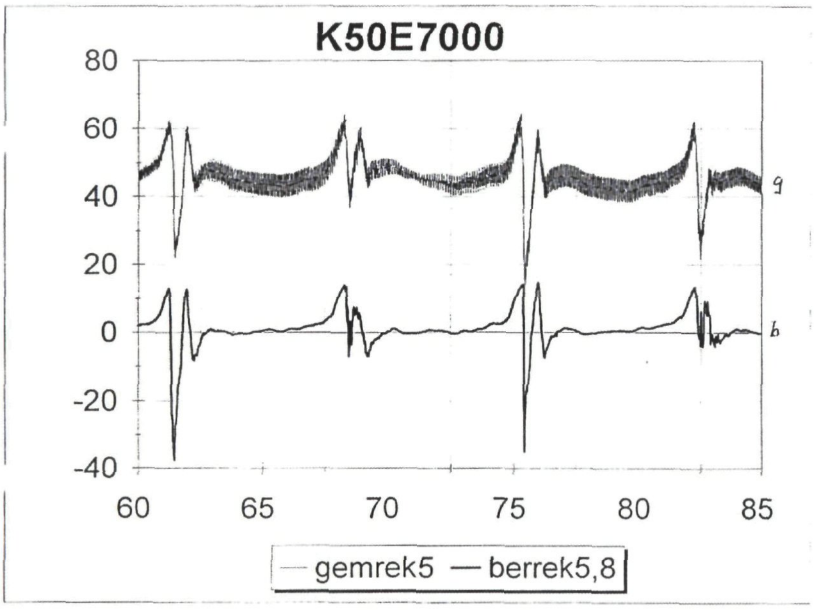

Figure 8-24 Measured and calculated strain compared from Ruygrok (1994)

As shown in Table 8-14 (Ruygrok 1994) the value of the modulus of elasticity is chosen to be 7.0 GPa at a temperature of 13 °C, which is, roughly, in agreement with a loading frequency of 17 Hz, calculated with Husaroad.

Table 8-14 Used parameter in Ruygrok (1994) for run AH108

golfhoogte	H_η	1.45	m	asf.temp.	T_a	13.0	°C
periode	t_η	7.0	s	watertemp.	T_w	<8>	°C
"steilheid"*	H/gt^2	3.0	$*10^{-3}$	veerconst.	k_{tl}	42	kN/m^3
rekenvariant dynamische belastingsfase (bijlage 8 A):							
asf.stijfh.	E_{asf}	7.0	GPa	veerconst.	k_{dy}	50	kN/m^3
rekenvariant traag-cyclische belastingsfase (bijlage 8 C):							
asf.stijfh.	E_{asf}	6.0	GPa	veerconst.	k_{tr}	40	kN/m^3

8.4.6 Modulus of elasticity used in the Monte Carlo simulation

As in shown in the foregoing sections the calculation of the modulus of elasticity done by de Waal differ al lot from the calculation in this thesis. Because of the good resemblance in Ruygrok (1994), much higher values than in de Waal (1993) will be used. In Ruygrok (1994) is stated that the loading frequency should be in between 10 and 15 Hz but looking to graphs of the impact in time the loading frequency can be much higher, so also higher values will be used in the Monte Carlo simulation. In the Monte Carlo simulation the modulus of elasticity belonging to a frequency of 20 Hz will be used.

Table 8-15 The modulus of elasticity which will be used in the Monte Carlo simulation

E modulus	(MPa)	Husaroad	
Frequency (Hz)	8.6 °C	13 °C	16.5 °C
5	6540	5047	4006
10	7761	6158	5018
15	8509	6848	5656
20	9053	7354	6127
25	9481	7755	6502

The values shown in Table 8-15 represent a mean value of a probability function. From Ashby (1987) it is assumed the probability density function of the modulus of elasticity is normal distributed as is shown in Figure 8-25 (Ashby 1987).

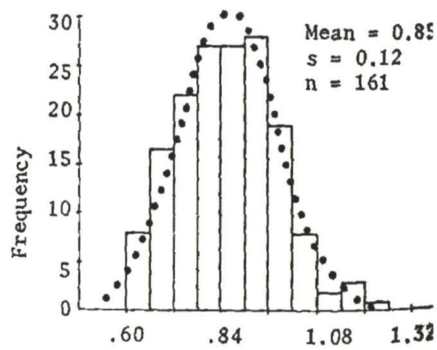

Figure 8-25 The normal distribution of the modulus of elasticity, from Ashby (1994)

In de Looff (2004) a safety assessment is performed on a dike section. In this assessment a comparison has been made between the modulus of elasticity data obtained by laboratory test on asphalt cores, with a normal distribution. The result shows that the modulus of elasticity is indeed normally distributed. Now also the coefficient of variation is determined. The modulus of elasticity is dependent on the temperature and frequency and looking to laboratory data the coefficient of variation also show this dependency (see also laboratory data section 8.4.1).

Table 8-16 Examples of coefficients of variation of the Delta flume beams

Frequency	9.8 Hz	1 Hz	9.8 Hz	1 Hz
Temperature	0 °C	5 °C	5 °C	10 °C
	E-init (MPa)	E-init (MPa)	E-init (MPa)	E-init (MPa)
	11909			
	11643	5075	9307	3596
	11173	5274	8460	3434
	9335	6520	9310	3958
	11068	4528	10269	3541
	12096	4855	8544	3269
	12369	5704	9300	3180
Mean	11370	5326	9198	3496
St Dev	1013	706	656	276
Coefficient of variation	8.9%	13.3%	7.1%	7.9%

This dependency is only shown for a very limited number of data and is not verified in this thesis. From field data it is know that the standard deviation of the modulus of elasticity of the revetment increases by increasing age. Because the asphalt revetment was very new (less than a year) when the experiment is executed it is assumed the coefficient of variation is low.

In the Monte Carlo simulation a normally distributed probability density function is used. Where the mean value depends on the asphalt temperature, so on the test run and on the loading frequency of the wave. In Ruygrok (1994) frequencies of 10 - 15 Hz are given, in this thesis a frequency of 20 Hz is used. The coefficient of variation is chosen to be 10% based on laboratory data and on the knowledge that the revetment was very new.

Table 8-17 Used modulus of elasticity

test	Temperature	E-modulus
AS022	16.5 °C	6127
AH108	13 °C	7354
AS117	8.6 °C	9053
AS202	8.6 °C	9053
AS203	8.6 °C	9053
AS025	8.6 °C	9053

An example of a modulus of elasticity distribution is given below for a mean value of 7000 MPa and a coefficient of variation with a value of 10%.

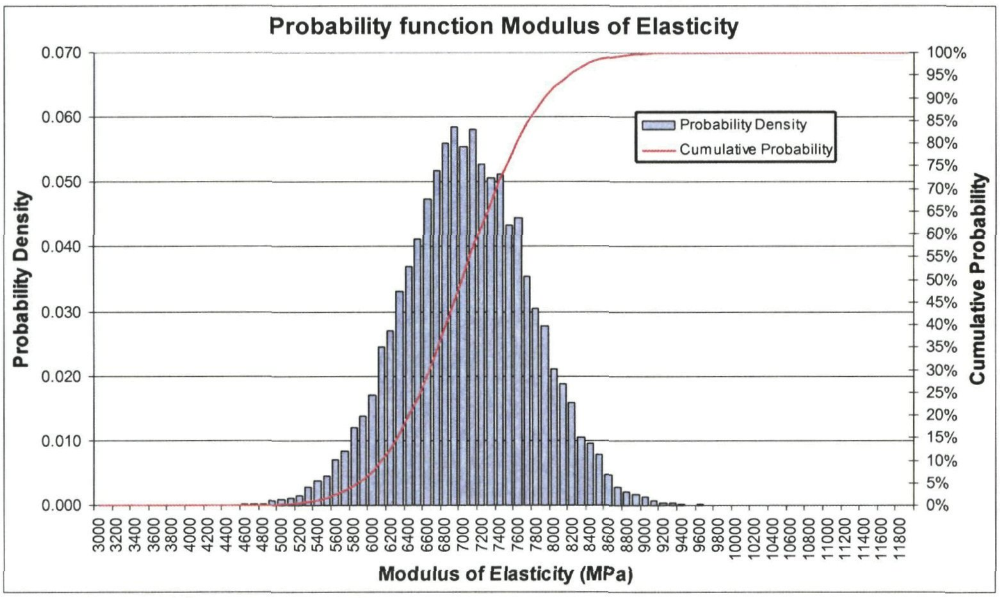

Figure 8-26 An example of the used normal distribution of the modulus of elasticity in the Monte Carlo simulation

8.5 Layer thickness

In this section the probability function of the layer thickness is determined. The cores sawed from the revetment are measured and the values are given in Table 8-18.

Table 8-18 The measured heights of the Delta flume cores

BOORKERNAFMETINGEN									
Boor-kern Code	Hoogte in mm				Diameter in mm				Opmerkingen
					Boven		Onder		
H	**150.6**	**160.4**	158.4	155.4	242.1	241.9	241.4	241.3	geen folie
I	**173.8**	**176.4**	180.6	174.0	244.9	244.6	242.0	242.0	folie (stratotester)
J	**164.3**	**153.1**	147.5	150.9	242.5	243.1	241.6	241.7	folie (stratotester)
K	**239.3**	**236.4**	231.2	226.4	244.5	243.4	243.0	241.7	folie (stratotester)
L	**236.0**	**229.4**	241.0	232.6	245.8	244.7	241.4	241.6	folie (stratotester)
M2	**198.4**	**207.0**	214.9	204.0	242.7	241.2	240.7	241.4	

The projected layer thickness was 15 cm at the left side and 25 cm at the right side of the flume (looking in wave direction). It is not known where on the slope these cores are drilled but it is assumed that the cores with codes H, I and J are drilled out of the 15 cm revetment and the other cores out of the 25 cm revetment.

Table 8-19 Measured heights of the Delta flume cores

Core Code	Height (mm)				Mean Core	Variance Core	Layer thickness of 15 cm	
H	150.6	160.4	158.4	155.4	156.2	3.7	Mean	162.1
I	173.8	176.4	180.6	174.0	176.2	2.7	St Dev	12.2
J	164.3	153.1	147.5	150.9	154.0	6.3	Coefficient of variation	7.6%
							Layer thickness of 25 cm	
K	239.3	236.4	231.2	226.4	233.3	4.9	Mean	224.7
L	236.0	229.4	241.0	232.6	234.8	4.3	St Dev	16.2
M2	198.4	207.0	214.9	204.0	206.1	6.0	Coefficient of variation	7.2%

Because only six values are available the mean values of the layer thickness are chosen at 15 cm and 25 cm. To check whether the layer thickness can be assumed as normally distributed, results of radar scans are used to check whether the distribution of the layer thickness is indeed normally distributed. Also a measure of the variation should be determined. The radar scans are performed on an asphalt revetment in the province of Groningen with a slope of 1:4. The length of the scanned revetment is 4.8 kilometres. The layer thickness is shown in the next graph normalized to a probability function.

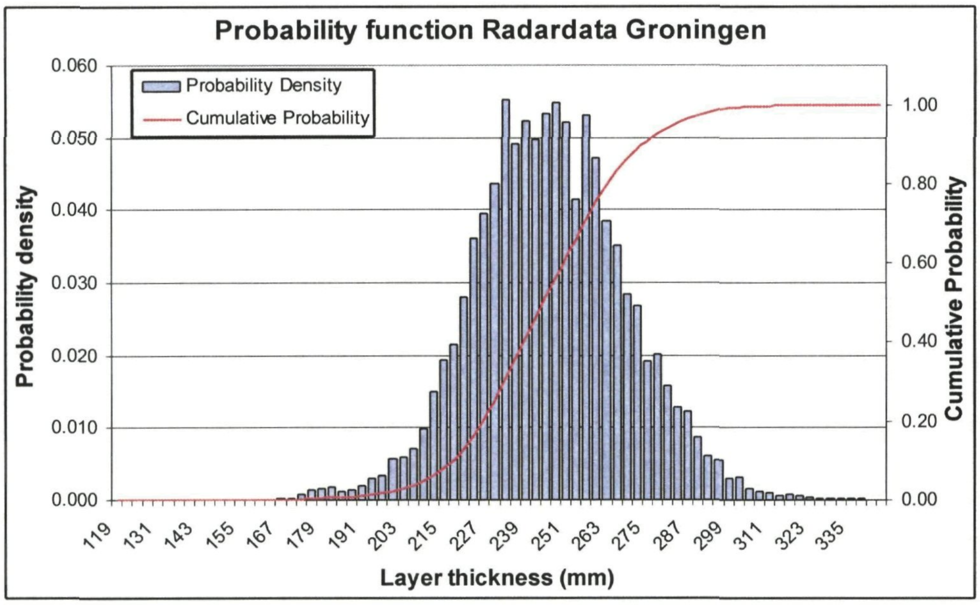

Figure 8-27 The probability function of measured data of a dike section in Groningen

The dataset produced to generate this figure is validated by the program Bestfit to check what kind of distribution the layer thickness follows. The result is shown in the next graph were the blue dots are the input data and the red line is fitted through this data.

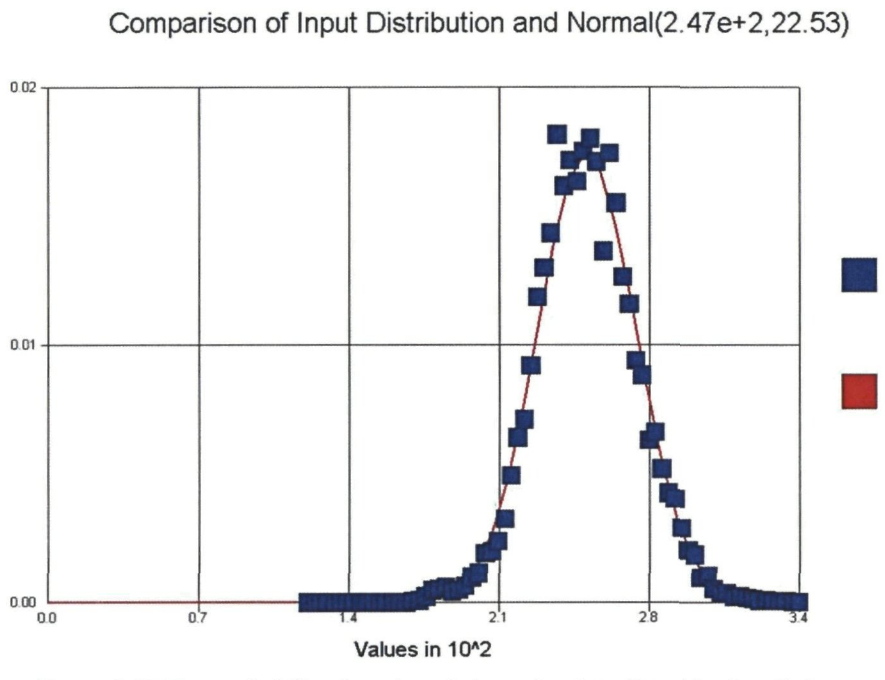

Figure 8-28 The probability function of the radar data fitted by Bestfit into a normal distribution

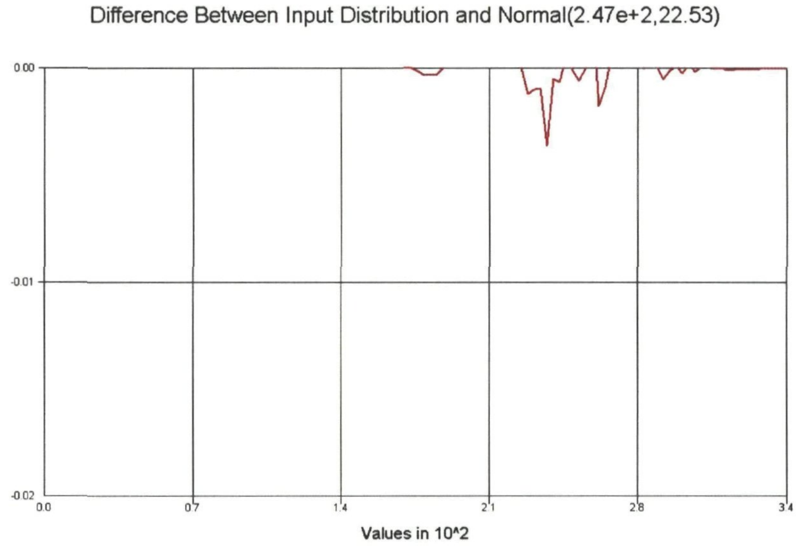

Figure 8-29 The differences between the radar data and the Bestfit fit

In the fitted graph a standard deviation of 22.52 mm is found instead of a deviation of 22.77 mm of the input data. The coefficient of variation is about 9%. Looking to other radar scans this coefficient is a little bit low so a coefficient of variation of 10% will be used for the layer thickness of the Delta flume asphalt revetment.

8.5.1 Used layer thickness in the Monte Carlo simulation

The used distribution of the layer thickness is a normal distribution with a mean value of 15 cm or 25 cm, with a coefficient of variation of 10%. The strain measuring device is placed into the revetment. In Derks and Klein Breteler (1992) the positions of the strain measuring devices are given. With these positions and with the knowledge that the surface of the revetment is positioned at (X-184.66)/4 the depth into the revetment is calculated. This is shown in Table 8-20.

Table 8-20 Positions of the strain measuring devices

Instrument Code	X (m)	Y (m)	Z (m)	Distance along slope with respect to DRO 15 (m)	Distance between underside revetment and strain measuring device (m)
DRO 15	201.550	2.500	4.222		
VPL 1	201.570	4.400	4.088	-0.0131	0.0147
VPL 2	202.050	3.800	4.219	0.4843	0.0253
VPL 3	201.080	3.800	3.980	-0.5147	0.0287
VPL 4	201.570	3.200	4.102	-0.0097	0.0282
VPL 5	201.590	1.800	4.005	-0.0138	0.0293
VPL 6	202.080	1.200	4.117	0.4887	0.0191
VPL 7	201.110	1.200	3.879	-0.5101	0.0235
VPL 8	201.590	0.600	3.998	-0.0179	0.0128

Because the strain measuring device is placed into the revetment the used layer thickness in the Monte Carlo simulation should be 12.6 or 22.9 cm. Below the probability function of a revetment with a layer thickness of 12.6 cm is given.

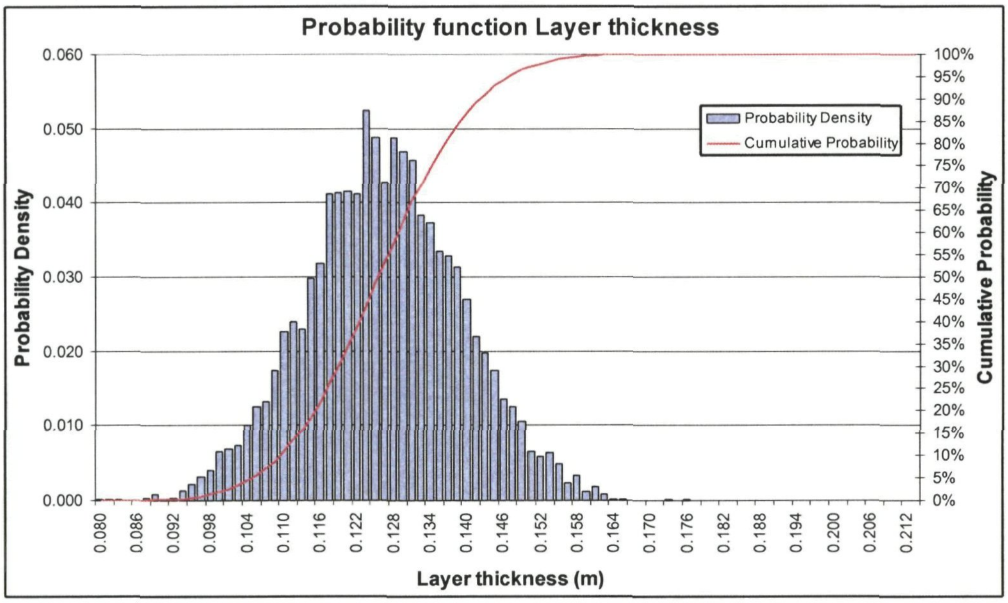

Figure 8-30 An example of a used distribution of the layer thickness in the *Monte Carlo simulation*

8.6 Modulus of the subgrade

In de Waal (1993) the stiffness of the subgrade (k) is chosen to be 100 MPa/m. In Ruygrok (1994) the modulus of the subgrade is determined and in this thesis the same procedure as in this report is followed. In Ruygrok (1991) the shear modulus and the modulus of elasticity of the subsoil is determined in combination with the Poisson modulus. The Poisson modulus is determined with a seismic cone which determines wave propagation speed.

$$\nu = 0.5\left(1 - \frac{1}{(C_p/C_s)^2 - 1}\right)^{0.5}$$

With:

C_p pressure wave propagation speed (in unsaturated soil) (m/s)

C_s shear wave propagation speed (m/s)

ρ_n density saturated soil (kg/m³)

The shear modulus is given by:

$$G = \rho_n C_s^2$$

The relation between these three parameter is given by:

$$E = 2(1+\nu)G$$

With:

E modulus of elasticity of the subsoil

G shear modulus

ν Poisson modulus

Table 8-21 Measurement results of the subsoil of the Delta flume experiment, from Ruygrok (1991)

nr.	pos.	a (m)	d (m)	C_p (m/s)	C_s (m/s)	ν	G (MPa)	E (MPa)
1	T	5.0	0.5	299	153	0.32	40	105
			1.5	302	162	0.30	45	116
8	T	5.0	1.0	333	168	0.33	47	127
			2.0	343	172	0.33	50	134
2	T	3.1	0.5	290	138	0.35	32	87
			1.5	305	147	0.31	36	98
7	T	3.1	1.0	310	161	0.31	45	117
			2.0	315	165	0.31	46	121
3	K	5.0	0.5	344	174	0.33	51	137
			1.5	348	165	0.35	45	123
6	K	5.0	1.0	329	160	0.32	48	127
			2.0	358	175	0.34	52	140
4	K	3.1	0.5	308	137	0.38	32	88
			1.5	359	146	0.40	36	102
5	K	3.1	1.0	-	-	-	-	-
			2.0	-	-	-	-	-
9	CR	2.0	1.0	355	163	0.37	45	124
			2.0	-	-	-	-	-

T = teenzijde
K = kruinzijde
a = afstand tot meetpunt C (op de hartlijn)
C = centrum (inslagpunt)
CR = rechts van C (taludopwaarts kijkend)

From Ruygrok (1991), where the investigation of the subsoil is described, is known that mean the relative density of the subsoil is estimated at 55%. The modulus of the subgrade (k) can be described by the formula, from Ruygrok (1992):

$$\begin{aligned} k(G_a,h_a,H,D_r,S) &= 198.6-22.6G_a-44h_a-87H+86D_r-16.5S+3.6G_a^2 \\ &-16.5G_ah_a+5.6G_aH-21G_aD_r+1.5G_aS-29h_a^2+60h_aH-164h_aD_r \\ &+16.6h_aS+12.8H^2-8.2HD_r+0.175HS+135D_r^2+0.43D_rS+0.54S^2 \end{aligned}$$

With:

k	modulus of the subgrade	(MPa)
h_a	layer thickness	(m)
D_r	relative density of the subsoil	(-)
H	wave height	(m)
S	impact factor	(-)
G_a	shear modulus of asphalt	(GPa)

This formula is evolved by using the finite element program PLAXIS and the mechanical system described in section 7.2.

The layer thickness is determined in section 8.5. The relative density of the subsoil is 55%. The wave height is given in section 8.3 and the impact factor in section 8.2. The shear modulus of asphalt is given in Table 8-22 where with acoustic sounding the properties of the revetment are determined. For more information is revered to Ruygrok (1991).

Table 8-22 Measured asphalt properties of the Delta flume cores, from Ruygrok (1991)

	positie (in m) taludopwaarts	c_s (m/s)	c_r (m/s)	c_p (m/s)	ν	G (GPa)	E (GPa)
I	2,2+ , R1	-	1667	3370	0,30	7,6	19,7
II	5,0+ , L1,5	(1670)	1650	3410	0,31	7,4	19,4
III	5,0+ , R1	(1744)	1700	3290	0,27	7,9	20,2
IV	6,3+ , L1,5		1545	3191	0,31	6,5	17,1

Legenda:
- positie ten opzichte van bodem, links of rechts uit de hartlijn (in m), taludopwaarts gezien
- aanname bij de conversie naar moduli: ρ = 2350 (kg/m³)
- deze waarden gelden voor frequenties > 4 kHz en temperatuur 19°C

The ratio between G and E of Table 8-22 can be used to determine the shear modulus of the revetment at lower temperatures and lower frequencies. In section 8.4.6 the modulus of elasticity of the revetment is determined for different temperatures. With these modulus of elasticity the shear modulus is calculated. The equivalent modulus of the subgrade (k_{eq}) is calculated with the formula of Ruygrok (1992) and the dynamic modulus of the subgrade (k_{dyn}) is taken to be 20% lower than the equivalent modulus of the subgrade. This because the course of the shear modulus (G_a) in time is dependent on the order of the amplitudes of the deformation. This means that the shear modulus of random vibrations is lower then the shear modulus of constant vibrations. For more information is referred to Ruygrok (1994).

Table 8-23 Calculated modulus of the subgrade per run

				D_r	layer thickness h			
				0.55	0.126	0.229	0.126	0.229
run	H, Hs (m)	E-modulus (MPa)	G_a (MPa)	s (-)	k_{eq} (MPa/m)	k_{eq} (MPa/m)	k_{dyn} (MPa/m)	k_{dyn} (MPa/m)
AS022	1.05	6127	2.45	2.15	123	114.0	98.3	91.2
AH108	1.45	7354	2.94	1.42	111	102.1	88.5	81.7
AS117	1.80	9053	3.62	1.88	98	91.6	78.7	73.3
AS202	1.43	9053	3.62	1.28	111	100.5	88.4	80.4
AS203	1.52	9053	3.62	1.63	106	96.9	84.6	77.6
AS025	0.89	9053	3.62	2.41	121	109.9	97.0	87.9

The values of Table 8-23 are used in the Monte Carlo simulation. The type of distribution is dependent on the distributions of the parameters used in the calculation of the modulus of subgrade reaction. An example of the probability function used in the Monte Carlo simulation is given in Figure 8-31.

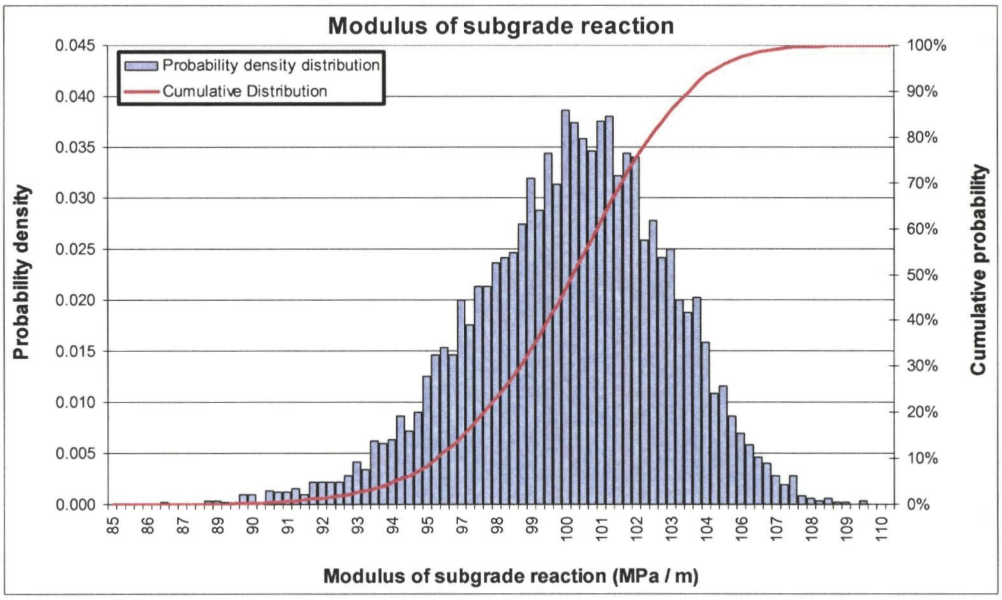

Figure 8-31 An example of a used distribution of the modulus of subgrade reaction in the Monte Carlo simulation

8.7 Width of the impact area

In de Waal (1993) the calculated width in x-vertical direction, along the slope, for every individual wave, for which the strain is calculated, is given (see section 5.2.2).

Table 8-24 Width of the impact area by de Waal (1993)

Proef	h_t (m)	H (m)	T (s)	t (s)	b (m)
AS022	4.71	1.05	5.0	769	1.29
AS022	4.71	1.05	5.0	744	1.55
AS022	4.71	1.05	5.0	594	1.34
AH108	5.28	1.45	7.0	411	1.26
AH108	5.28	1.45	7.0	75	1.08
AH108	5.28	1.45	7.0	453	1.25
AS117	4.89	1.80	5.0	374	1.72
AS117	4.89	1.80	5.0	219	1.64
AS117	4.89	1.80	5.0	309	2.42
AS202	5.01	1.43	7.1	3695	1.76
AS202	5.01	1.43	7.1	3560	1.35
AS202	5.01	1.43	7.1	5605	.94
AS202	5.01	1.43	7.1	5483	.95
AS202	5.01	1.43	7.1	3539	1.16
AS203	5.10	1.52	8.7	4828	1.45
AS203	5.10	1.52	8.7	1319	1.11
AS203	5.10	1.52	8.7	3540	1.00
AS203	5.10	1.52	8.7	1227	1.08
AS203	5.10	1.52	8.7	51	1.35
AS025	5.21	.89	7.6	81	1.04
AS025	5.21	.89	7.6	151	1.95
AS025	5.21	.89	7.6	771	1.14
AS025	5.21	.89	7.6	207	1.27
AS025	5.21	.89	7.6	728	1.55

This is also the only information which is available about the impact width. When a Monte Carlo simulation in time is performed the width of the wave impact is distributed as a Rayleigh distribution as done in the program GOLFKLAP. The only known relation of the width of the impact with the breaker parameter is according to measurements of Klein Breteler (2007). The results of Klein Breteler are used to check the difference with the Rayleigh distribution. It should be noted that Klein Breteler used 33% of the highest waves of the analyzed experiments. For more information is referred to Klein Breteler (2007).

According to Klein Breteler (2007), there is no relation between the width of the impact and the pressure height of the wave impact. However the width of the impact is dependent on the breaker parameter with the following relation (33% of the highest waves are analyzed):

$$\frac{B_{klap50\%2\%}}{H_s} = 0.96 - 0.11\xi_{op} \qquad \text{for } 1 \le \xi_{op} < 5.5$$

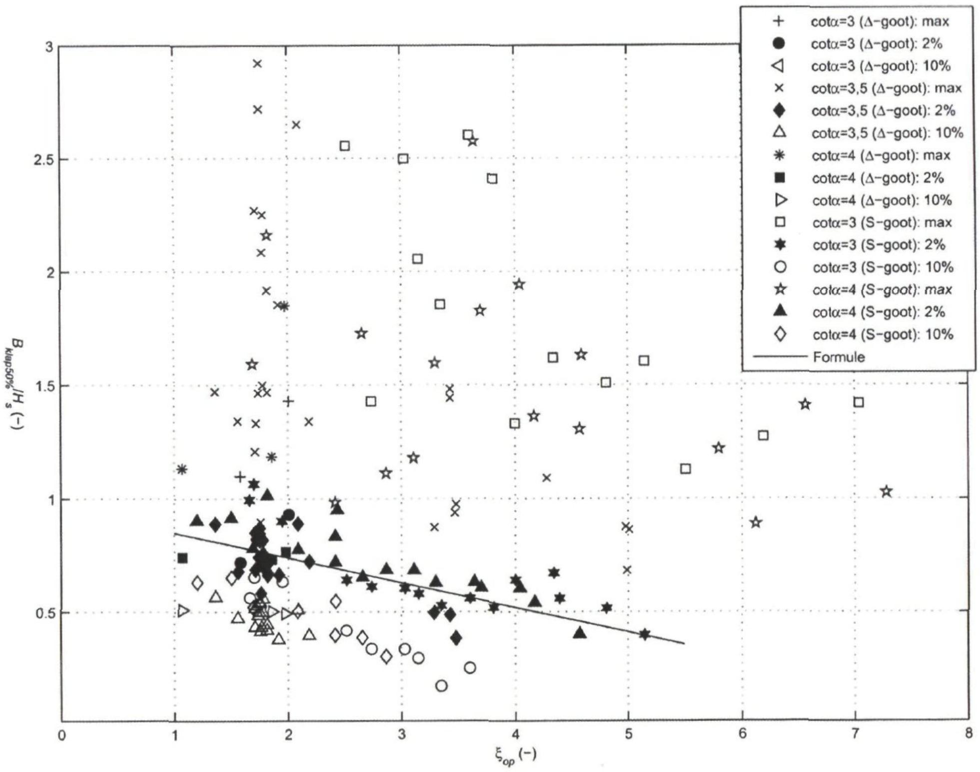

Figure 8-32 The relation between the breaker parameter and the width of the impact $B_{klap50\%2\%}$, from Klein Breteler (2007)

With $B_{klap50\%2\%}$ as the impact width, halfway the pressure height, with 2% probability of exceedance.

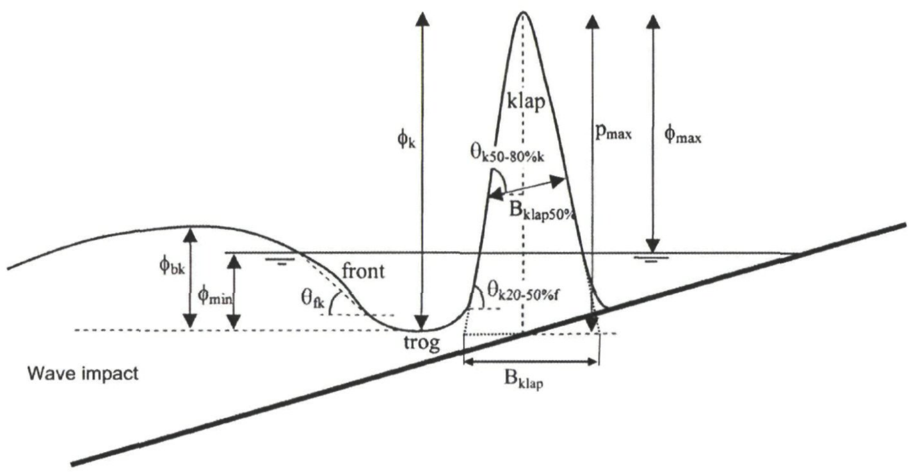

Figure 8-33 Definition used by Klein Breteler with extra parameter B_{klap} , from Klein Breteler (2006)

The width of the impact $B_{klap50\%2\%}$ is converted to the impact width at the base of the prismatic load (B_{klap}). The angle $\theta_{k20-50\%f}$ is used in combination with the maximum impact pressure to determine the parameter B_{klap}.

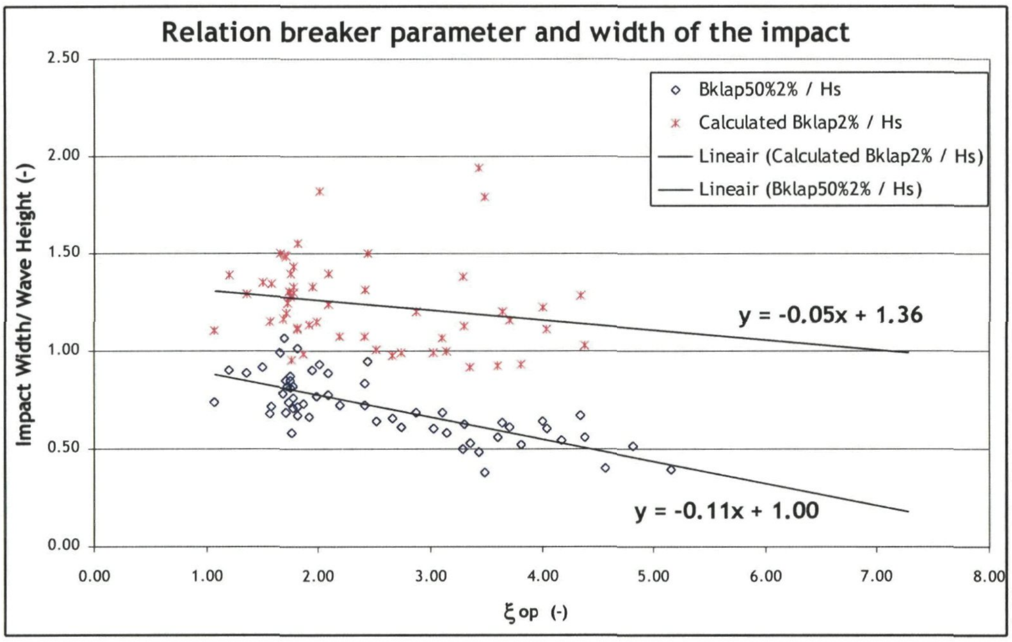

Figure 8-34 Relation between the breaker parameter and the width of the impact

8.7.1 Width of the impact area used in the simulation

The distribution shape used in GOLFKLAP is used in the simulation. This distribution is a Rayleigh distribution with a mode of z=0.5H and a mean value $\mu = z\sqrt{\frac{\pi}{2}}$.

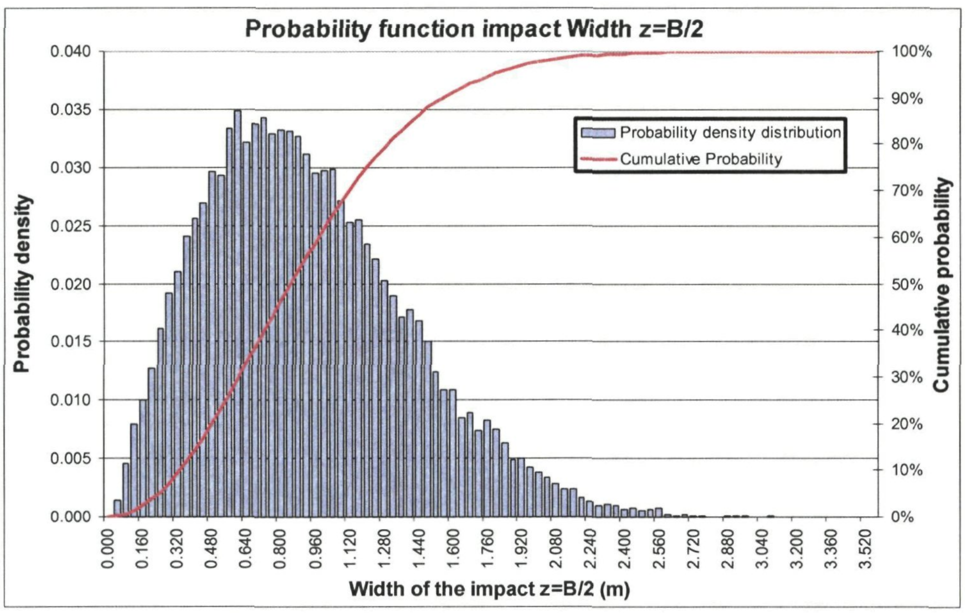

Figure 8-35 Example of the impact width distribution in the simulation for H=1m

When the formula put up by Klein Breteler is used the resulting z_{klap} is fairly in agreement with the formula used in GOLFKLAP. When the mode of the Rayleigh distribution is set to be z=0.5H then the distribution is wider than the distribution used in GOLFKLAP. This has been done so the deviation of the distribution does not have too much effect on the deviation of the results. The mean value in the Monte Carlo simulation is not affected much by this distribution.

Table 8-25 Recalculated width of impact with $2z_{klap}/H = 1.36\text{-}0.05\xi$

test	H	T	χ	ξ	B_{klap}/H	B_{klap}	z_{klap}
AS022	1.05	5.0	0.0042	1.52	1.28	1.35	0.67
AH108	1.45	7.0	0.0030	1.82	1.27	1.84	0.92
AS117	1.80	5.0	0.0073	1.16	1.30	2.34	1.17
AS202	1.43	7.1	0.0029	1.85	1.27	1.81	0.91
AS203	1.52	8.7	0.0020	2.20	1.25	1.90	0.95
AS025	0.89	7.6	0.0016	2.52	1.23	1.10	0.55

8.8 Poisson's contraction coefficient

The contraction coefficient used in de Waal (1993) is 0.38. The contraction coefficient is dependent on frequency and temperature. Depending on the model (Burgers, Huet Sayegh) which is used the coefficient varies between 0.5 for low frequencies and 0.3 for high frequencies. In Ruygrok (1991) the contraction coefficient of the asphalt revetment in the Delta flume is given. This is shown in Table 8-26 with ν as the contraction coefficient. These values are obtained by ultrasonic measurements.

Table 8-26 Measured asphalt properties of the Delta flume cores, from Ruygrok (1991)

	positie (in m) taludopwaarts	c_s (m/s)	c_r (m/s)	c_p (m/s)	ν	G (GPa)	E (GPa)
I	2,2+ , R1	-	1667	3370	0,30	7,6	19,7
II	5,0+ , L1,5	(1670)	1650	3410	0,31	7,4	19,4
III	5,0+ , R1	(1744)	1700	3290	0,27	7,9	20,2
IV	6,3+ , L1,5		1545	3191	0,31	6,5	17,1

Legenda:
- positie ten opzichte van bodem, links of rechts uit de hartlijn (in m), taludopwaarts gezien
- aanname bij de conversie naar moduli: ρ = 2350 (kg/m³)
- deze waarden gelden voor frequenties > 4 kHz en temperatuur 19°C

These values are valid for frequencies more then 4 kHz and a temperature of 19°C. It is not known which value exactly should be used. Therefore different runs of the Monte Carlo simulation are made to check the influence of the contraction coefficient of Poisson.

8.9 Summary

In this section the results of this chapter is summarized. The mean value with standard deviation and coefficient of variation for all the derived probability functions are given in Table 8-27.

Table 8-27 The Monte Carlo simulation input parameters summarized

				Mean	Standard deviation	Coefficient of variation	
All Tests	Symbol	Units	Distr Type	μ	σ	σ %	
layer thickness (right side, VPL 1-4)	h	m	Normal	0.126	0.0126	10%	
layer thickness (left side, VPL 5-8)	h	m	Normal	0.229	0.0229	10%	
poisson's contraction coefficient	ν	-	D	0.35			
Test AS022	Symbol	Units	Distr Type	μ	σ	σ %	
significant wave height	H, Hs	m	D	1.05			
half width prismatic load	z	m	Rayleigh	0.53			
modulus of elasticity	E	MPa	Normal	6127	612.7	10%	
				μ	σ	α	β
impact factor	q	-	Log-Normal	2.15	0.48	0.74	0.22
Test AH108	Symbol	Units	Distr Type	μ	σ	σ %	
significant wave height	H, Hs	m	D	1.45			
half width prismatic load	z	m	Rayleigh	0.73			
modulus of elasticity	E	MPa	Normal	7354	735.4	10%	
				μ	σ	α	β
impact factor	q	-	Log-Normal	1.42	0.47	0.3	0.32
Test AS117	Symbol	Units	Distr Type	μ	σ	σ %	
significant wave height	H, Hs	m	D	1.8			
half width prismatic load	z	m	Rayleigh	0.90			
modulus of elasticity	E	MPa	Normal	9053	905.3	10%	
				μ	σ	α	β
impact factor	q	-	Log-Normal	1.88	0.38	0.61	0.2
Test AS202	Symbol	Units	Distr Type	μ	σ	σ %	
significant wave height	H, Hs	m	D	1.43			
half width prismatic load	z	m	Rayleigh	0.72			
modulus of elasticity	E	MPa	Normal	9053	905.3	10%	
				μ	σ	α	β
impact factor	q	-	Log-Normal	1.28	1.02	0	0.7
Test AS203	Symbol	Units	Distr Type	μ	σ	σ %	
significant wave height	H, Hs	m	D	1.52			
half width prismatic load	z	m	Rayleigh	0.76			
modulus of elasticity	E	MPa	Normal	9053	905.3	10%	
				μ	σ	α	β
impact factor	q	-	Log-Normal	1.63	1.25	0.26	0.68
Test AS025	Symbol	Units	Distr Type	μ	σ	σ %	
significant wave height	H, Hs	m	D	0.89			
half width prismatic load	z	m	Rayleigh	0.45			
modulus of elasticity	E	MPa	Normal	9053	905.3	10%	
				μ	σ	α	β
impact factor	q	-	Log-Normal	2.41	1.59	0.7	0.6

8.10 References

Ashby, M.F. and Jones, D.R.H. (1987) Engineering Materials 1, An Introduction to there Properties and Applications, *Pergamon Press, Oxford*

CROW (2005) Standaard RAW Bepalingen (in Dutch), *CROW, Ede*

De Looff, A.K. (2002) Beoordeling Asfaltbekleding Lauwersmeerdijk en Eemshaven (Report 028292)(In Dutch), *Netherlands Pavement Consultants, Utrecht*

De Looff, A.K. (2003) Literatuurstudie Verificatiemetingen 3-Puntsbuigproef (Report 028126)(In Dutch), *Netherlands Pavement Consultants, Utrecht*

De Looff, A.K. (2004) Veiligheidsbeoordeling asfaltbekleding Houtribdijk - toetsing op treksterkte (Report e048163)(In Dutch), *KOAC•NPC, Nieuwegein*

de Waal, J.P. (1993) Gedrag van asfaltbekleding onder golfaanval, Relatie tussen belasting en rek (in Dutch)(Report H 1702), *DWW Rijkswaterstaat, Delft*

Derks, H. and Klein Breteler, M. (1992) Gedrag van asfaltbekleding onder golfaanval, verslag modelonderzoek in Deltagoot (in Dutch)(Report H 1480), *DWW Rijkswaterstaat, Delft*

Derks, H. and Klein Breteler, M. (1992) Gedrag van asfaltbekleding onder golfaanval, verslag modelonderzoek in Deltagoot, annex 1 (in Dutch)(Report H 1480), *DWW Rijkswaterstaat, Delft*

Führböter, A. and Sparboom, U. (1988) Full-Scale Wave Attack of Uniformly Sloping Sea Dykes, *Proceedings ICCE 1988, Malaga, Spain*

Grüne, J. (1988) Wave-induced Shock Pressures under Real Sea State Conditions, *Proceedings ICCE 1988, Malaga, Spain*

Johnson, R..A. (2000) Miller & Freund's Probability and Statistics for Engineers, *Prentice Hall International (UK) Limited, Sydney*

Klein Breteler, M. (2007) Validatie van GOLFKLAP (Report H4134) (in Dutch), *WL | Delft Hydraulics*

Klein Breteler, M. (2006) Kwantificering golfbelasting en invloed lange golven (Concept report H4421)(in Dutch), *WL | Delft Hydraulics*

Ruygrok, P.A. (1991) Parameterbepalingen voor het zand en de asfaltbekleding van het TAW A4 Dijkmodel in de Deltagoot (in Dutch)(Report CO-324970/7), *Grondmechanica Delft, Delft*

Ruygrok, P.A. (1992) Parameterstudie voor formulering van een equivalente effectieve veerconstante voor het plaat op veren model (in Dutch)(Report CO-336530/6), *Grondmechanica Delft, Delft*

Ruygrok, P.A. (1994) Dimensioneren van asfaltbekledingen op golfklappen, analyse van de relatie tussen golfbelasting en rekken (in Dutch)(Report CO-347160/17), *Grondmechanica Delft, Delft*

Schönian, E (1999) Shell Bitumen Hydraulic Engineering Handbook, *Shell International Petroleum Co. Ltd, London*

Sparboom, U. (1991) Full-Scale investigations on Wave Loadings of Sea Dyke Structures, *Proceedings 3rd International Conference on Coastal and Port Engineering in Developing Countries 1991, Mombasa, Kenia*

Versluis, A. (1991) 3-puntsbuigproeven aan balken van boorkernen uit de deltagoot (Report 91523-2 or DWW-504)(In Dutch), *Netherlands Pavement Consultants, Hoevelaken*

9 Simulation Set-up

9.1 Introduction

In this chapter first the set-up of the Monte Carlo simulation is explained. Then an example of the calculation procedure of the Monte Carlo simulation is given with the use of the program Maple.

9.2 Set up of the simulation

In the simulation the strain at the underside of the revetment is calculated. To calculate the strain a formula is used for calculating the maximum stress under prismatic loading (see section 7.2).

$$\sigma = \frac{p_{max}}{4\beta^2 \beta z}(1 - e^{(-\beta z)}(\cos(\beta z) + \sin(\beta z)))\frac{6}{h^2}$$

Where:

$$\beta = \sqrt[4]{\frac{3c(1-\nu^2)}{Eh^3}}$$

σ	= tension at the underside of the revetment	(Pa)
E	= modulus of elasticity of asfalt	(N/m^2)
I	= moment of inertia $I = \frac{h^3}{12(1-\nu^2)}$	(m^3)
h	= thickness plate	(m)
ν	= Piossons constant for asphalt	(-)
c	= spring constant subsoil	(N/m^3)
z	= base of the prismatic loading	(m)

The maximum pressure impact is defined as:

$$p_{max} = \rho_w g q H_s$$

Where:

ρ_w	density water	(kg/m^3)
g	acceleration of gravity	(=9,81 m/s^2)
q	impact factor, dependent on slope	(-)
H_s	wave height	(m)

The strain is calculated by dividing the tension by the modulus of elasticity.

In chapter eight the probability functions of the input parameters are determined. It is explained that a distinction in time and in space should be made which results in different calculations.

9.3 Probability function conversion

The Monte Carlo simulation is performed in the program Microsoft Office Excel 2003. First random numbers between 0 and 1 are created. The result is a uniform distribution between 0 and 1.

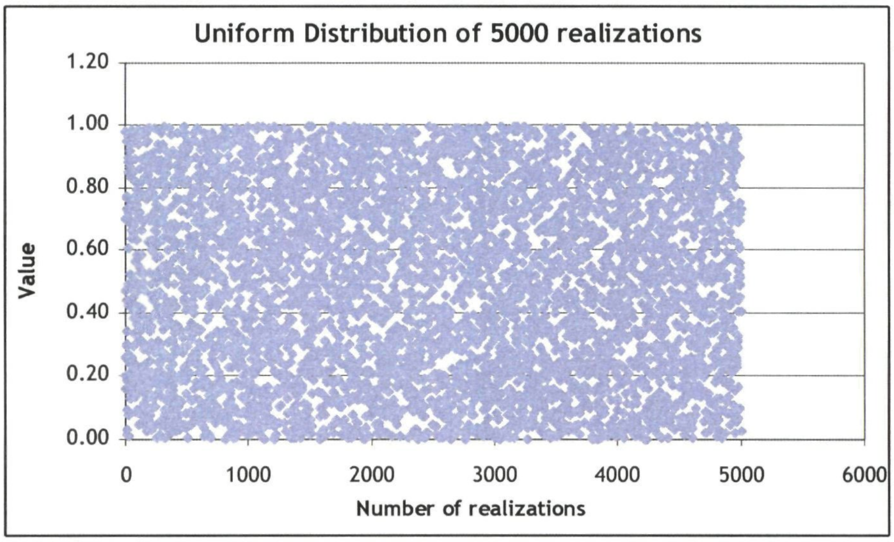

Figure 9-1 The uniform distribution of 5000 draws between 0 and 1

From this uniform distribution other distributions can be generated. The central limit theorem states that the sum of a large number of uniformly distributed variables is normally distributed (Dekking (2004)). Five times a summation of uniform distributions is shown in Figure 9-2 where the shape of a normal distribution already can be recognized.

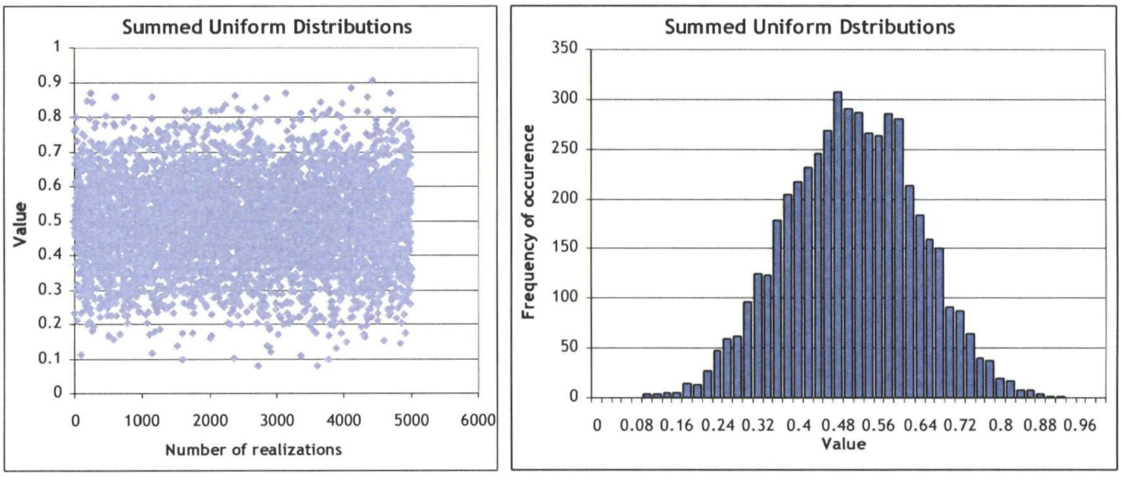

Figure 9-2 The summation of 5 uniform distributions between 0 and 1 with the frequency of occurence

By using transformation formulae from CUR (1997), normal and lognormal distributions are obtained. These transformation formulae are:

Normal distribution

$$x = \mu_x + \sigma_x \sqrt{-2\ln(x_{u,1})}\cos(2\pi\, x_{u,2})$$

Log-normal distribution

$$x = e^{\mu_x + \sigma_x \sqrt{-2\ln(x_{u,1})}\cos(2\pi\, x_{u,2})}$$

Rayleigh distribution

$$x = \sigma_x \sqrt{-2\ln(1 - x_{u,1})}$$

with:

μ_x mean value

σ_x standard deviation

$x_{u,1}$ random number from uniform distribution 1

$x_{u,2}$ random number from uniform distribution 2

9.4 Calculation example

In this section the Monte Carlo simulation is explained by making some calculations. The program Maple is used to get the results.

At first a random number will be chosen between 0 and 1 for two uniform distributions.

>

> $x1uniform1 := random_{uniform}(1)$

$$x1uniform1 := 0.9510535301$$

> $x1uniform2 := random_{uniform}(1)$

$$x1uniform2 := 0.1464863072$$

These two numbers can be put in the formulae for creating the normal distribution.

> $x1normal := \mu + \sigma\sqrt{-2\ln(x1uniform1)}\cos(2\pi\, x1uniform2)$

$$x1normal := \mu + 0.19182656\,\sigma$$

Then a choise can be made for what the mean value and the standard deviation of the normal distribution will be. For example the layer thickness of the asphalt revetment will be simulated as a normal distribution with a mean value of 0.15 m and a standard deviation of 10% so 0.015 m.

> $\mu := 0.15$

> $\sigma := 0.015$

> $x1normal := \mu + \sigma\sqrt{-2\ln(x1uniform1)}\cos(2\pi\, x1uniform2)$

$$x1normal := 0.1528774518$$

The result is one value of the normal distribution of the layer thickness. This can be repeated as many times desired creating an even amount of numbers of the normal distribution. In this example a choice is made for selecting another 9 numbers from the uniform distribution which are in the whole range between 0 and 1.

At first a random numbers will be chosen between 0 and 1 for two uniform distributions.

```
> x2uniform1:=random[uniform](1): x2uniform2:=random[uniform](1);
  x3uniform1:=random[uniform](1): x3uniform2:=random[uniform](1):
  x4uniform1:=random[uniform](1): x4uniform2:=random[uniform](1);
  x5uniform1:=random[uniform](1): x5uniform2:=random[uniform](1):
  x6uniform1:=random[uniform](1): x6uniform2:=random[uniform](1):
  x7uniform1:=random[uniform](1): x7uniform2:=random[uniform](1):
  x8uniform1:=random[uniform](1): x8uniform2:=random[uniform](1);
  x9uniform1:=random[uniform](1): x9uniform2:=random[uniform](1):
  x10uniform1:=random[uniform](1): x10uniform2:=random[uniform](1):
```

$$x2uniform2 := 0.4293926737$$

$x4uniform2 := 0.6759829338$

$x8uniform2 := 0.005862664913$

These number can be converted into nine values from the normal distribution.

> $x2normal := \mu + \sigma \sqrt{-2 \ln(x2uniform1)} \cos(2 \pi x2uniform2)$

$x2normal := 0.1238659930$

$x3normal := 0.1475915710$

$x4normal := 0.1382892125$

$x5normal := 0.1461260255$

$x6normal := 0.1563030905$

$x7normal := 0.1421484906$

$x8normal := 0.1728236629$

$x9normal := 0.1288688387$

$x10normal := 0.1358011716$

These numbers are normally distributed which can be vizualized by a histogram.

> $data := [x1normal, x2normal, x3normal, x4normal, x5normal, x6normal, x7normal, x8normal, x9normal, x10normal]$

$data := [0.1528774518, 0.1238659930, 0.1475915710, 0.1382892125, 0.1461260255, 0.1563030905, 0.1421484906, 0.1728236629, 0.1288688387, 0.1358011716]$

> $describe_{mean}(data)$

0.1444695509

> $describe_{standarddeviation}(data)$

0.01346768564

> $histogram(data, area = 1)$

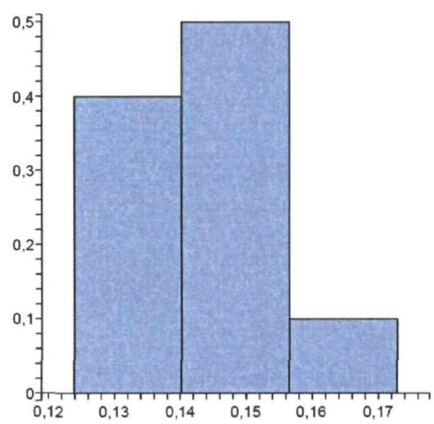

This example shows how a normal distributed density function is obtained. In this example just 10 values are used, in the Monte Carlo simulation 20000 values are used to reduce the relative error to less then 0.5%.

9.5 Visualizing the Excel sheet

In this section the Excel sheet used for the Monte Carlo simulation is visualized. The sheet is explained for each part and the sheet is divided into three different parts (1,2,3).

Number in red can be adjusted

Input parameters	Symbol	Units	Distr Type	Mean µ	Standard deviation σ	Coefficient of variation σ %	
maximum impact pressure	Pmax	Pa	Unknown				
significant wave height	H,Hs	m	D	1.05			
half width traingle load	z	m	Rayleigh	0.53			
density water	ρw	kg/m³	D	1000			
acceleration by gravity (1)	g	m/s²	D	9.81			
layer thickness	h	m	Normal	0.142	0.0142	10%	
modulus of elasticity	E	MPa	Normal	6127	612.7	10%	
poisson's contraction coefficient	ν	-	D	0.35			
				µ	σ	α	β
impact factor	q	-	Log-Normal	2.15	0.48	0.74	0.22

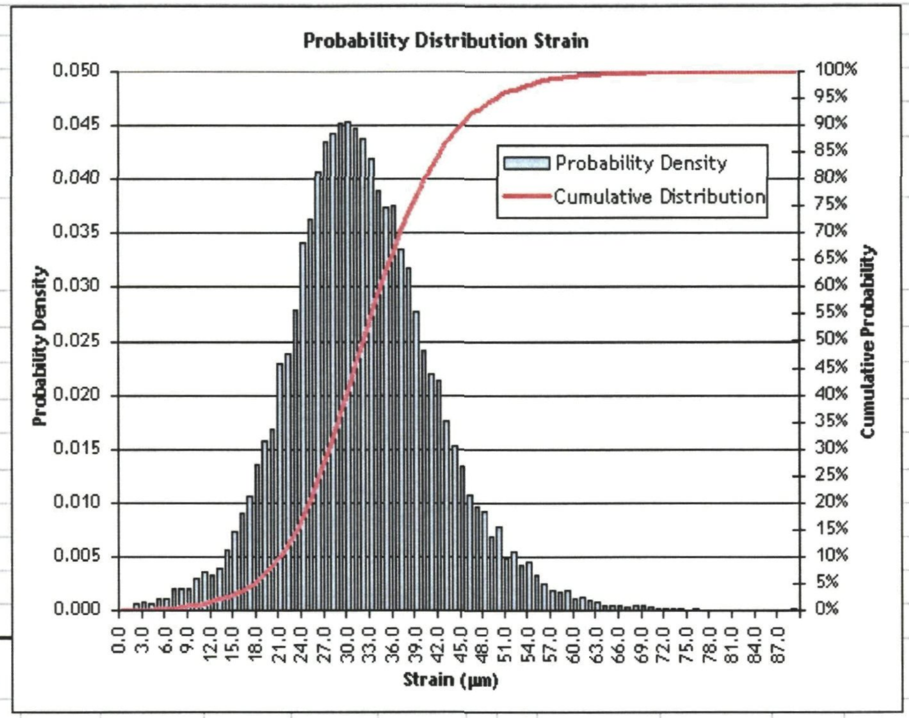

Count number of used cells	20017	20017	20008	20008	20000	20000	20000	20000	20000	20000	20000	20000
Mean value	0.50	0.50	2.15	0.14	98.86	6127	1.05	0.66	22132	1.98	191249	31.4
Standard Deviation	0.29	0.29	0.47	0.01	3.12	614	0.00	0.34	4889	0.16	59750	9.8
Count number of cell <0	0	0	0	0	0	0	0	0	0	0	0	0
Kurtosis (2)	-1.21	-1.21	0.71	0.06	0.15	-0.04	-2.00	0.36	0.71	0.61	0.84	0.89
Skewness	0.01	0.00	0.66	0.00	-0.35	-0.01	1.00	0.66	0.66	0.55	0.38	0.38
Standard error	0.0020	0.0020	0.0034	0.0001	0.0220	4.3403	0.0000	0.0024	34.5727	0.0012	422	0.0692
Relative error	0.41%	0.40%	0.16%	0.07%	0.02%	0.07%	0.00%	0.37%	0.16%	0.06%	0.22%	0.22%
	Uniform1	Uniform2	Log-Normal	Normal		Normal	D	Rayleigh	Log-Normal			
			q	h	c	E	H	z	Pmax	b	σ	ε
Tranformations	(-)	(-)	(-)	(m)	(MPa/m)	(MPa)	(m)	(m)	Pa	1/m	Pa	(-)
(3) 0.21	0.11	0.15	2.45	0.13	97.5	6.4E+03	1.05	0.295	25187	2.04	2.07E+05	32.1
0.45	0.19	0.34	2.39	0.14	97.6	5.2E+03	1.05	0.477	24656	2.10	2.21E+05	42.6
0.63	0.83	0.35	2.03	0.14	99.7	5.0E+03	1.05	0.485	20915	2.09	1.80E+05	36.1

Min	0.25		
Max	88.76		
Bin width	1.000	1.041	≈ projecte
Scale Check	1.000	85	≈ number o
	GPa		
Ga	2.27		
Dr	0.55		

	Bins	Frequentie	Scaled	Cumulatief
0	0.000	0	0.000	0
	1.000	2	0.000	0

The first part with number (1) is the part with input parameters. Here the parameters needed to determine the strain (see section 7.2) are given with there units. The distribution type with the mean value and standard deviation is given. The numbers in red can be adapted and these are the numbers which are determined in chapter eight. Part (2) gives the results of the 20000 cells of part (3). The mean value and standard deviation of (2) can be compared with part (1). Part (3) is the part where the probability functions are constructed. As explained in the foregoing sections 9.2 till 9.4 random selected numbers between zero and one are converted to numbers of a probability function. The probability functions into which they are converted are given above each column with there units. The last four columns of part (3) are constructed with the calculations explained in section 7.2. This results is a column where the strain is given.

A probability function of this column is constructed created by creating a histogram. First a bin width is defined and with the excel command "interval", or "frequency" in the English version, the number of times a value falls within this bin width is counted. When this is scaled to a total area of one the probability of occurrence of this value for 20000 cells is determined. Because no extreme value analysis is done the assumption is made that 20000 cells give reasonable results.

9.6 References

CUR (1997) CUR 190 "Probabilities in civil engineering, Part 1: Probabilistic design in theory", *CUR, Gouda*

DEKKING, F.M. ET AL (2004) KANSTAT, Probability and Statistics for the 21st Century, *Delft University of Technology, Delft*

10 Simulation results

10.1 Introduction

In this chapter the results of the simulation are displayed. First the strains calculated by de Waal (1993) are recalculated using the new parameter found in chapter eight. Next the probability functions which are obtained in chapter eight are used in the Monte Carlo simulation and are compared with the measured strains.

10.2 Comparison with de Waal (1993)

In de Waal (1993) some waves impacts are selected to analyze. The wave impacts are chosen from different runs of which some were performed with regular and some with irregular waves. In section 5.2 the criteria for selection are already discussed. The selected waves with the parameter are displayed in Table 10-1.

Table 10-1 Measured and calculated impact parameters by de Waal (1993)

Proef	h_t (m)	H (m)	T (s)	t (s)	p_{max} (kN/m^2)	s_f (-)	Δy (m)	b (m)	E_a (MPa)	R/O
AS022	4.71	1.05	5.0	769	31.5	3.06	-.04	1.29	1300	R
AS022	4.71	1.05	5.0	744	27.7	2.69	-.03	1.55	1300	R
AS022	4.71	1.05	5.0	594	40.3	3.91	.06	1.34	1300	R
AH108	5.28	1.45	7.0	411	48.0	3.37	-.03	1.26	2040	R
AH108	5.28	1.45	7.0	75	48.4	3.40	.06	1.08	2040	R
AH108	5.28	1.45	7.0	453	36.7	2.58	-.04	1.25	2040	R
AS117	4.89	1.80	5.0	374	42.5	2.41	.01	1.72	3430	R
AS117	4.89	1.80	5.0	219	48.4	2.74	.06	1.64	3430	R
AS117	4.89	1.80	5.0	309	39.7	2.25	-.15	2.42	3430	R
AS202	5.01	1.43	7.1	3695	97.5	6.95	.23	1.76	3430	O
AS202	5.01	1.43	7.1	3560	70.0	4.99	.25	1.35	3430	O
AS202	5.01	1.43	7.1	5605	59.4	4.24	-.12	.94	3430	O
AS202	5.01	1.43	7.1	5483	66.5	4.74	.01	.95	3430	O
AS202	5.01	1.43	7.1	3539	54.9	3.91	-.15	1.16	3430	O
AS203	5.10	1.52	8.7	4828	66.2	4.44	.16	1.45	3430	O
AS203	5.10	1.52	8.7	1319	56.9	3.82	-.40	1.11	3430	O
AS203	5.10	1.52	8.7	3540	47.1	3.16	-.04	1.00	3430	O
AS203	5.10	1.52	8.7	1227	45.3	3.04	-.05	1.08	3430	O
AS203	5.10	1.52	8.7	51	41.1	2.75	-.04	1.35	3430	O
AS025	5.21	.89	7.6	81	63.5	7.27	-.22	1.04	3430	O
AS025	5.21	.89	7.6	151	47.9	5.48	-.05	1.95	3430	O
AS025	5.21	.89	7.6	771	52.6	6.03	-.27	1.14	3430	O
AS025	5.21	.89	7.6	207	45.3	5.19	.06	1.27	3430	O
AS025	5.21	.89	7.6	728	44.1	5.05	.15	1.55	3430	O

Most of these values are measured and the shape of the impact pressure can be shown by looking to the recordings of the pressure transducers. The modulus of elasticity, the modulus of the subgrade and the layer thickness are not measured but calculated values. In this comparison first the calculated and measured values of the Waal (1993) are used and then the recalculated values of chapter eight are used. De Waal (1993) calculated the strain for all the strain measuring devices for waves impacting at DRO 15. In the formula for calculating the strain it is assumed that the wave impact is over the whole width of the wave flume (looking in wave direction). It is known that the impact at the sides of the flume is about 15% lower then the mean value of the impacts with a standard deviation of 20% and the impact in the middle of the flume is about 30% higher than the mean value. This is explained in section 5.2.2 and 8.2.

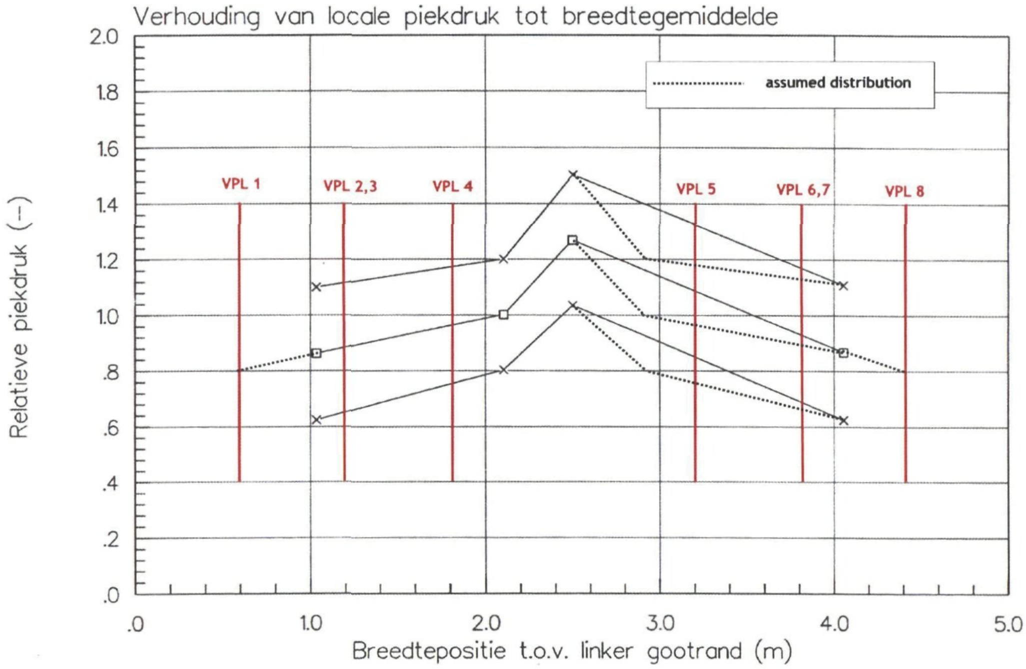

Figure 10-1 Pressure distribution over the width of the flume compared to the mean distribution

A 13% lower maximum impact pressure leads to 13% less strain. This means that the measured strain at VPL 1 should be 13% less than VPL 4 with a standard deviation of 20%. The distribution as shown in Figure 10-1 is given in Table 10-2 with the differences in percentage. These differences are not taken into account by de Waal (this section) but are used in the recalculated strains (section 10.3).

Table 10-2 The calculated spatial difference in distribution over the width of the flume

Maximum impact pressure distribution over the width of the flume		
DRO 15	1.27	100%
VPL 4,5	0.96	76%
VPL 2,3,6,7	0.88	69%
VPL 1,8	0.80	63%

VPL 2, 3 and 6,7 are placed down-slope and upslope of DRO 15 as is shown in Figure 10-2.

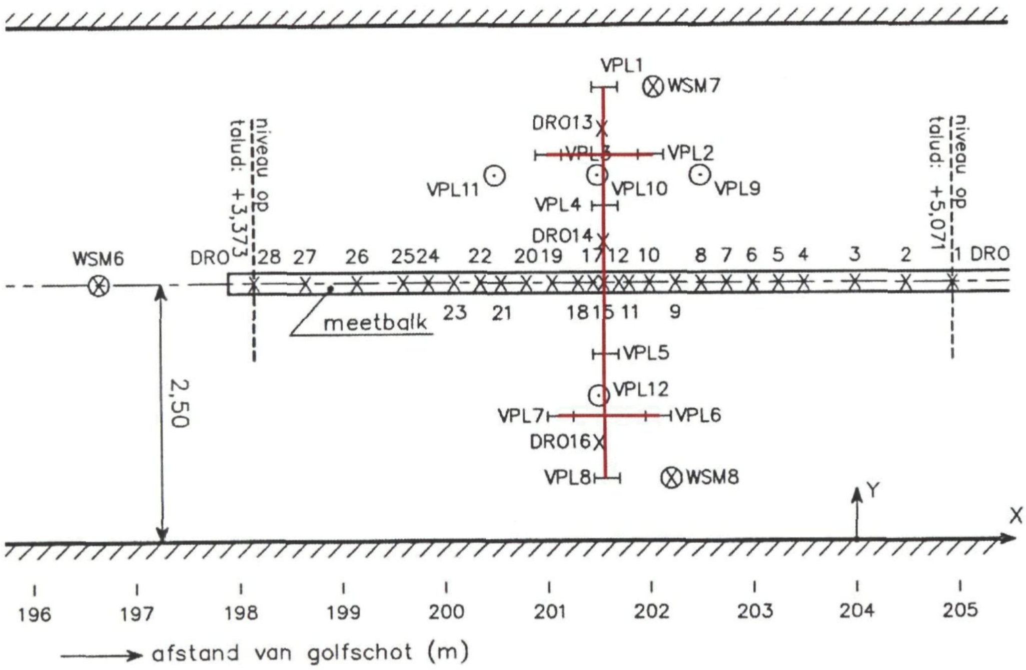

Figure 10-2 Top view of the measurement devices, the red line connects the used strain measuring devices and pressure transducers

To calculate the strain at VPL 2, 3, 6 and 7 the distance between the line through DRO 15 in Y direction should be known. In Table 10-3 this distance is given.

Table 10-3 Measured positions of pressure transducer DRO 15 and strain measuring devices VPL 1-8

Instrument Code	X (m)	Y (m)	Z (m)	Distance along slope with respect to DRO 15 (m)	Distance between underside revetment and strain measuring device (m)
DRO 15	201.550	2.500	4.222		
VPL 1	201.570	4.400	4.088	-0.0131	0.0147
VPL 2	202.050	3.800	4.219	0.4843	0.0253
VPL 3	201.080	3.800	3.980	-0.5147	0.0287
VPL 4	201.570	3.200	4.102	-0.0097	0.0282
VPL 5	201.590	1.800	4.005	-0.0138	0.0293
VPL 6	202.080	1.200	4.117	0.4887	0.0191
VPL 7	201.110	1.200	3.879	-0.5101	0.0235
VPL 8	201.590	0.600	3.998	-0.0179	0.0128

In section 7.2 the formula for calculating the strain is derived. With this formula the strain at some distance from the centre (down- or upslope) of the wave impact can be calculated. In the next maple sheet this strain is calculated and displayed in a graph with q_0 as maximum impact pressure.

```
> restart
```

At first the strain at the left part of the flume will be calculated (looking in wave direction) where the layer thickness of 15 cm is present

```
> h:=0.15;c:=100000000;nu:=0.38;E:=1300000000;rho:=1000;Hs:=1.05;z:=0.645;g
  =9.81;q:=3.06; Pmax:=rho*g*Hs*q;
```

$$h := 0.15$$
$$c := 100000000$$
$$\nu := 0.38$$
$$E := 1300000000$$
$$\rho := 1000$$
$$Hs := 1.05$$
$$z := 0.645$$
$$g := 9.81$$
$$q := 3.06$$
$$Pmax := 31519.53000$$

$$> b := \left(\frac{3\,c\,(1-\nu^2)}{E\,h^3}\right)^{\left(\frac{1}{4}\right)}$$

$$> \mathit{simplify}(b)$$

$$2.765627757$$

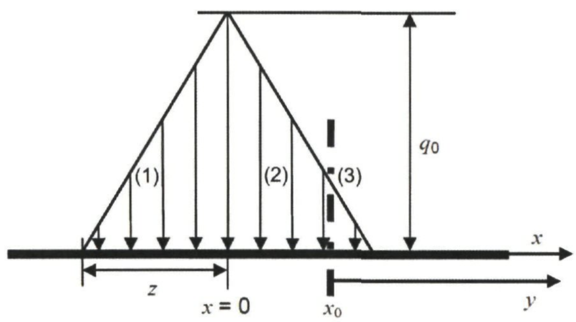

Formulae for the maximum tension under the load at x=0:

$$> sigmamax := \frac{Pmax\,(1 - e^{(-b\,z)}\,(\cos(b\,z) + \sin(b\,z)))\,\frac{6}{h^2}}{4\,b^2\,b\,z}$$

$$> \mathit{simplify}(sigmamax)$$

$$1.341919364\;10^5$$

$$> strain := \frac{sigmamax\;1000000}{E}$$

$$103.2245665$$

Formulae for the tension at x<z: (under the load)

$$> sigmaxz := -\frac{1}{8\,b^3\,z}\Big(Pmax\,(-\sin(b\,x)\,(e^{(b\,x)} - e^{(-b\,x)})\,e^{(-b\,z)}\,(\cos(b\,z) - \sin(b\,z))$$
$$+ \cos(b\,x)\,(e^{(b\,x)} + e^{(-b\,x)})\,e^{(-b\,z)}\,(\cos(b\,z) + \sin(b\,z)) - 2\,e^{(-b\,x)}\,(\sin(b\,x) + \cos(b\,x)))\,\frac{6}{h^2}\Big)$$

Formulae for the tension at z<x: (outside the loaded area)

$$sigmazx := -\frac{1}{8\,b^3\,z}\Big(Pmax\,e^{(-b\,x)}\,(\cos(b\,x)\,(e^{(b\,z)}\,(\cos(b\,z)-\sin(b\,z))+e^{(-b\,z)}\,(\cos(b\,z)+\sin(b\,z)))$$
$$+\sin(b\,x)\,(e^{(b\,z)}\,(\cos(b\,z)+\sin(b\,z))+e^{(-b\,z)}\,(\cos(b\,z)-\sin(b\,z)))-2\,(\cos(b\,x)+\sin(b\,x)))\,\frac{6}{h^2}\Big)$$

> $strainxz := \frac{sigmaxz\ 1000000}{E}$

> $strainzx := \frac{sigmazx\ 1000000}{E}$

> $x := 'x'$

```
Warning, the name changecoords has been redefined
```

> $F := plot(-strainxz, x = 0 .. z)$

> $G := plot(-strainzx, x = z .. 4.5)$

> $display(F, G)$

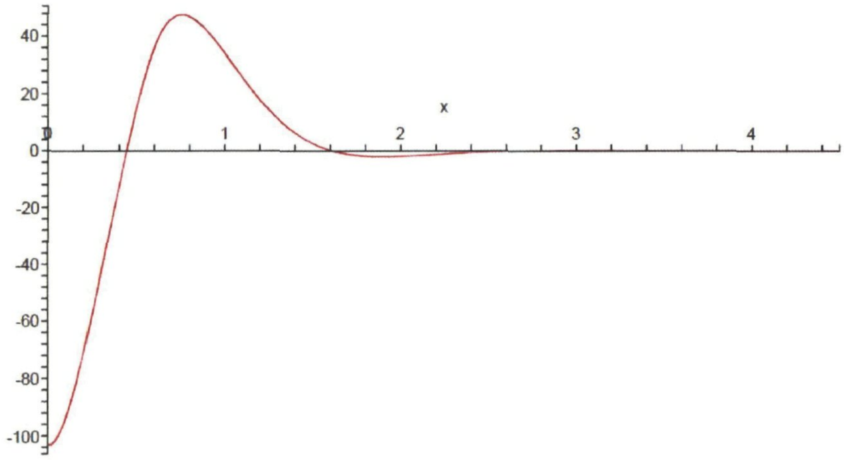

The result of this calculation is the strain at the underside of the revetment at x=0 of 103 μm. This is not in agreement with the measurements but in agreement with the calculated strain of de Waal (1993). The measured and the calculated strain are given in section 5.4 and here given again in

Table 10-4.

Table 10-4 Calculated strain and measured dynamic strain from de Waal (1993)

Proef	t	BEREKENDE REKKEN (* 10^{-6})								GEMETEN DYNAMISCHE REKKEN (* 10^{-6})							
		VPL								VPL							
	(s)	1	2	3	4	5	6	7	8	1	2	3	4	5	6	7	8
AS022	769	102	-22	-7	102	82	-3	20	82	23	2	-8	28	21	7	2	12
AS022	744	83	-5	2	83	73	6	22	73	23	10	-10	23	27	8	-4	21
AS022	594	124	12	-38	124	105	22	3	105	23	13	-15	20	21	8	-6	24
AH108	411	129	-18	-5	129	98	5	26	98	27	39	-18	18	42	-	18	40
AH108	75	126	4	-40	126	94	17	1	94	33	24	-9	26	45	8	10	36
AH108	453	98	-16	-2	98	75	2	22	75	42	19	8	35	42	10	11	33
AS117	374	84	18	11	84	69	24	27	69	24	18	14	36	34	25	0	25
AS117	219	95	32	-3	95	78	33	22	78	55	30	-1	41	54	26	38	36
AS117	309	59	8	37	59	58	16	46	58	42	24	8	44	46	19	26	52
AS202	3695	141	134	-53	141	134	119	1	134	60	58	60	57	90	49	30	88
AS202	3560	93	99	-57	93	85	79	-14	85	17	36	-22	13	32	35	0	13
AS202	5605	108	-33	13	108	73	-5	33	73	18	-14	21	31	38	0	23	17
AS202	5483	135	-11	-21	135	91	11	15	91	21	0	11	38	42	0	30	31
AS202	3539	99	-32	33	99	72	-5	45	72	16	4	38	45	75	3	45	33
AS203	4828	115	70	-39	115	96	63	2	96	65	17	38	-	49	9	60	64
AS203	1319	25	-46	106	25	32	-24	80	32	25	10	53	25	48	10	74	34
AS203	3540	97	-16	-4	97	65	3	18	65	54	10	38	-	49	10	35	60
AS203	1227	94	-15	1	94	65	3	21	65	56	31	-8	43	46	17	21	44
AS203	51	86	-3	9	86	64	10	25	64	28	25	-19	16	3	18	-10	7
AS025	81	90	-46	58	90	67	-15	62	67	28	-18	41	47	46	-21	56	15
AS025	151	89	15	29	89	77	23	42	77	41	21	-15	38	53	23	0	38
AS025	771	64	-42	70	64	52	-16	62	52	30	-8	23	31	46	17	13	40
AS025	207	92	19	-17	92	69	23	11	69	16	20	-3	19	38	17	8	38
AS025	728	77	46	-21	77	66	42	4	66	2	40	-9	8	22	33	-3	12

The strain for the other strain measuring devices can also be calculated.

The deflection at VPL 1 and 4 (x=0.03 m)

```
> x:=0.03:simplify(strainxz);
```

102.2904704

The deflection at VPL 2 (x=0.52 m):

```
> x:=0.52 :simplify(strainxz);
```

-19.50874284

The deflection at VPL 3 (x=0.48 m)

```
> x:=0.48:simplify(strainxz);
```

-9.619381901

```
> restart
```

Now at the right side of the revetment the strain will be calculated so the layer thickness is 25 cm

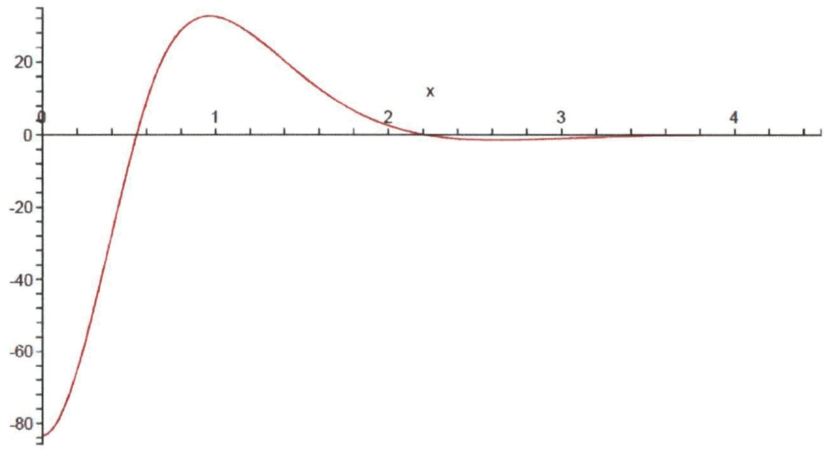

The strain at VPL 5 and 8 (x=0.05 m)

```
> x:=0.05:simplify(strainxz);
```

82.00695266

The strain at VPL 6 (x=0.55 m)

```
> x:=0.55: simplify(strainxz);
```

-1.056326296

The strain at VPL 7 (x=0.44 m)

```
> x:=0.44: simplify(strainxz);
```

19.60929558

These values are summarized in Table 10-5.

Table 10-5 The calculated strain, with used parameter of de Waal (1993) run AS022, t=769 s

Run	t	Calculated Strain (*10^-6)							
		VPL							
	(s)	1	2	3	4	5	6	7	8
AS022	769	102	-20	-10	102	82	-1	20	82

It should be noted that this table is the result of parameters used by de Waal (1993). Also for the other selected waves and runs the strain is recalculated.

```
> restart
```

Run AS022 time=744 seconds

At first the strain at the left part of the flume will be calculated (looking in wave direction) where the layer thickness of 15 cm is present

```
> h := 0.15
```

$h := 0.15$

$c := 100000000$

$\nu := 0.38$

$E := 1300000000$

$\rho := 1000$

$Hs := 1.05$

$z := 0.775$

$g := 9.81$

$q := 2.69$

$Pmax := 27708.34500$

2.765627757

```
Warning, the name changecoords has been redefined
```

```
> display(F, G)
```

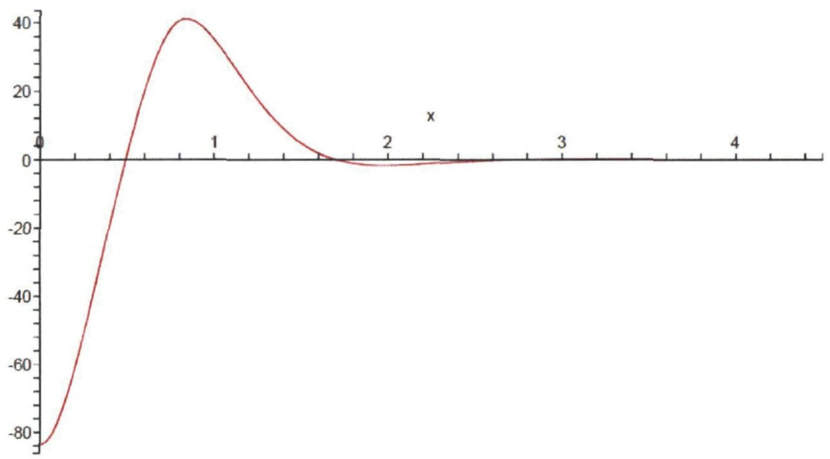

The deflection at VPL 1 and 4 (x=0.03 m)

```
> x:=0.03:simplify(strainxz);
```

82.97774610

The deflection at VPL 2 (x=0.52 m):

```
> x:=0.52 :simplify(strainxz);
```

-5.458697951

The deflection at VPL 3 (x=0.48 m)

```
> x:=0.48:simplify(strainxz);
```

2.458132370

```
> restart
```

Now at the right side of the revetment the strain will be calculated so the layer thickness is

25 cm

```
> h := 0.25
```

$$h := 0.25$$
$$c := 100000000$$
$$v := 0.38$$
$$E := 1300000000$$
$$\rho := 1000$$
$$Hs := 1.05$$
$$z := 0.775$$
$$g := 9.81$$
$$q := 2.69$$
$$Pmax := 27708.34500$$
$$1.885415891$$

```
Warning, the name changecoords has been redefined
> H := plot(-strainxz, x = 0 .. z)
> K := plot(-strainzx, x = z .. 4.5)
> display(H, K)
```

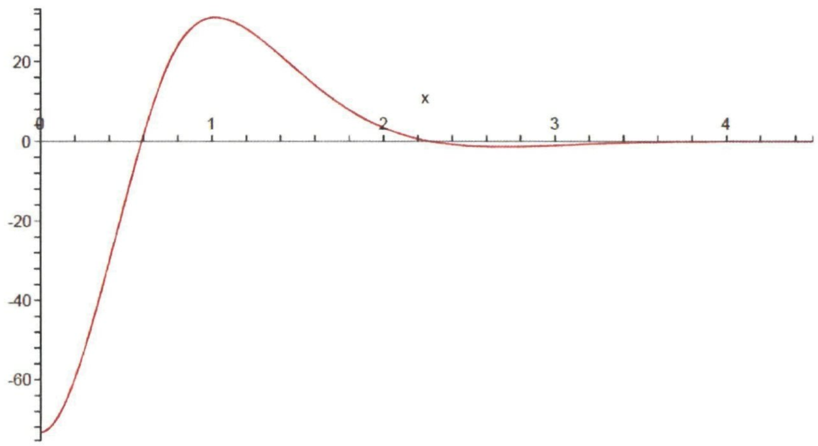

The strain at VPL 5 and 8 (x=0.05 m)

```
> x:=0.05:simplify(strainxz);
```

$$72.27567802$$

The strain at VPL 6 (x=0.55 m)

```
> x:=0.55: simplify(strainxz);
```

$$6.009481546$$

The strain at VPL 7 (x=0.44 m)

```
> x:=0.44: simplify(strainxz);
```

$$23.64448489$$

Table 10-6 Calculated strain, with used parameters of de Waal (1993)

Run	t	Calculated Strain (*10^-6)								Measured Strain (*10^-6)							
		VPL								VPL							
	(s)	1	2	3	4	5	6	7	8	1	2	3	4	5	6	7	8
AS022	769	102	-20	-10	102	82	-1	20	82	23	2	-8	28	21	7	2	12
AS022	744	83	-5	2	83	72	6	24	72	23	10	-10	23	27	8	-4	21
AS022	594	129	-21	-9	129	105	1	27	105	23	13	-15	20	21	8	-6	24
AH108	411	129	-18	-5	129	98	5	29	98	27	39	-18	18	42	-	18	40
AH108	75	131	-28	-16	131	94	0	22	94	33	24	-9	26	45	8	10	36
AH108	453	99	-14	-4	99	75	4	22	75	42	19	8	35	42	10	11	33
AS117	374	84	11	18	84	69	19	33	69	24	18	14	36	34	25	0	25
AS117	219	97	10	18	97	78	20	36	78	55	30	-1	41	54	26	38	36
AS117	309	64	20	25	64	62	27	37	62	42	24	8	44	46	19	26	52
AS202	3695	191	27	44	191	158	46	78	158	60	58	60	58	90	49	30	88
AS202	3560	146	-2	12	146	109	18	43	109	17	36	-22	13	32	35	0	13
AS202	5605	120	-19	-10	120	80	5	21	80	18	-14	21	31	38	0	23	17
AS202	5483	135	-21	-11	135	90	5	24	90	21	0	11	38	42	0	30	31
AS202	3539	115	-11	0	115	81	9	27	81	16	4	38	45	75	3	45	33
AS203	4828	137	3	16	137	105	21	44	105	65	17	38	-	49	9	60	64
AS203	1319	119	-13	-3	119	83	8	26	83	25	10	53	25	48	10	74	34
AS203	3541	97	-14	-6	97	65	4	18	65	54	10	38	-	49	10	35	60
AS203	1227	94	-12	-3	94	65	6	20	65	56	31	-8	43	46	17	21	44
AS203	51	86	-1	7	86	64	11	25	64	28	25	-19	16	3	18	-10	7
AS025	81	131	-18	-7	131	90	7	26	90	28	-18	41	47	46	-21	56	15
AS025	151	89	18	25	89	77	26	41	77	41	21	-15	38	53	23	0	38
AS025	771	110	-11	-1	110	77	8	25	77	30	-8	23	31	46	17	13	40
AS025	207	95	-5	4	95	69	10	25	69	16	20	-3	19	38	17	8	38
AS025	728	90	6	14	90	71	16	31	71	2	40	-9	8	22	33	-3	12

The calculated values are displayed in Figure 10-3 till Figure 10-6. These figures are (almost) the same as calculated by de Waal (1993) as shown in section 5.4. There is no explanation found for the differences.

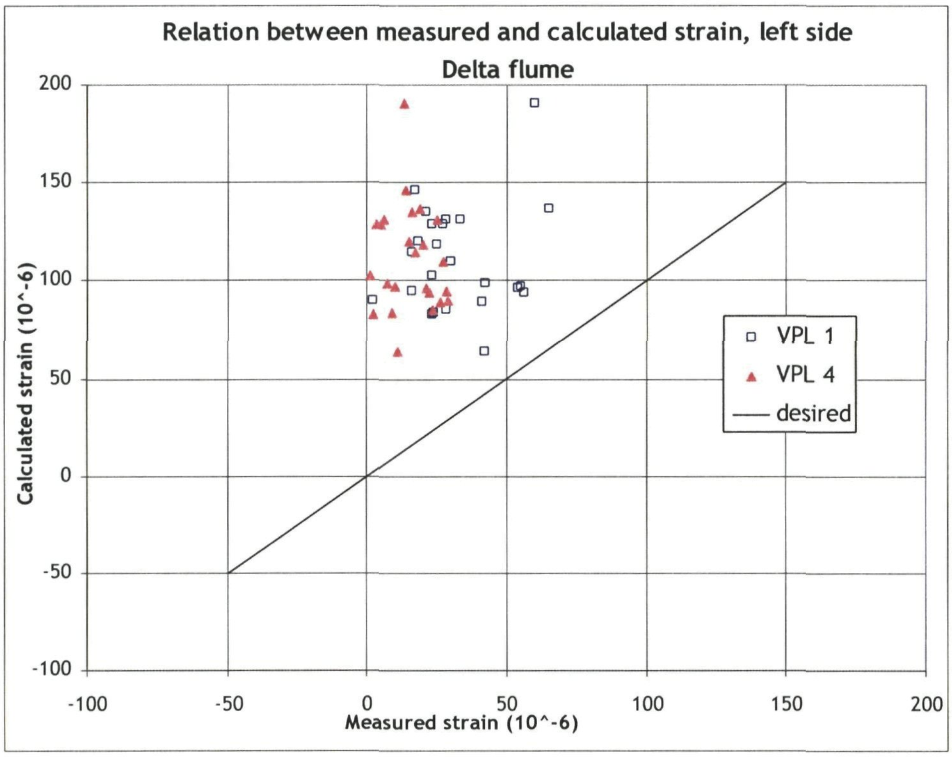

Figure 10-3 Relation between measured and calculated strain, left side of the flume. Used parameters of de Waal (1993)

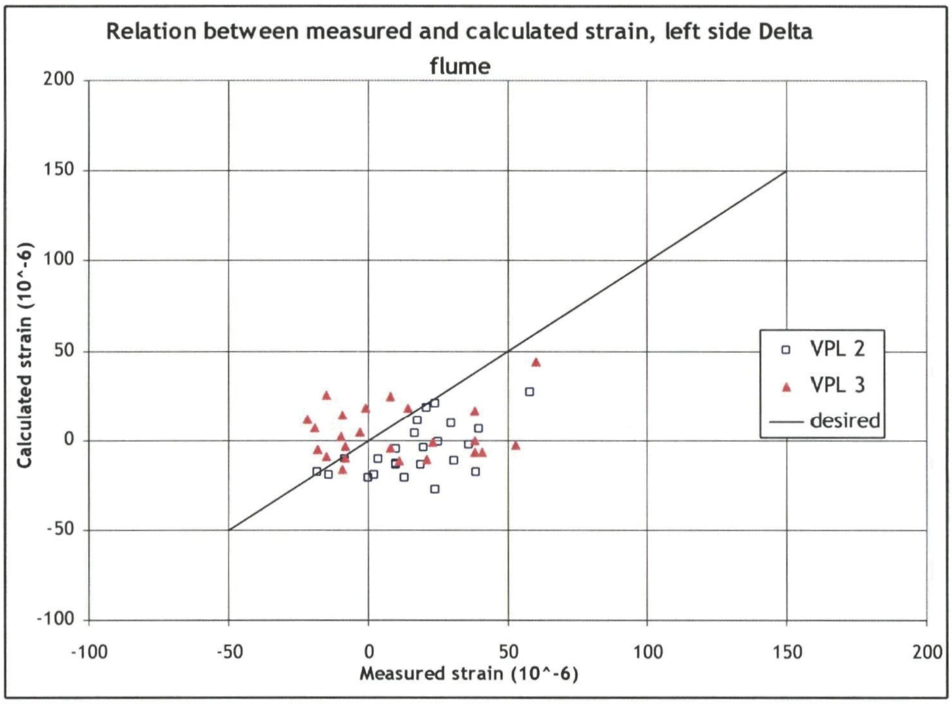

Figure 10-4 Relation between measured and calculated strain, left side of the flume. Used parameters of de Waal (1993)

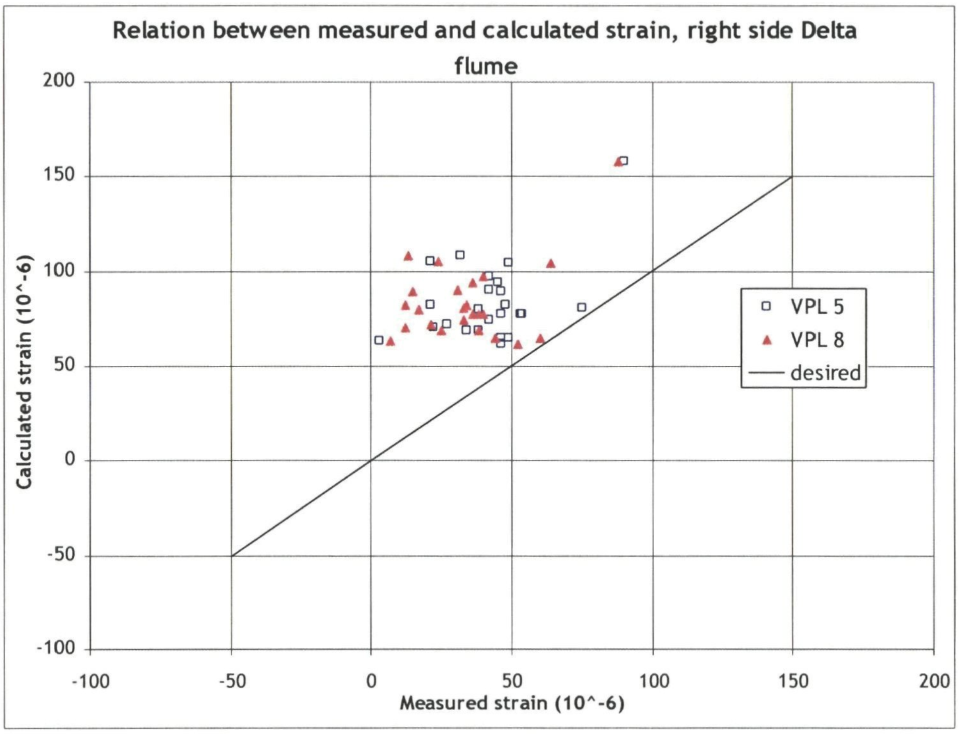

Figure 10-5 Relation between measured and calculated strain, right side of the flume. Used parameters of de Waal (1993)

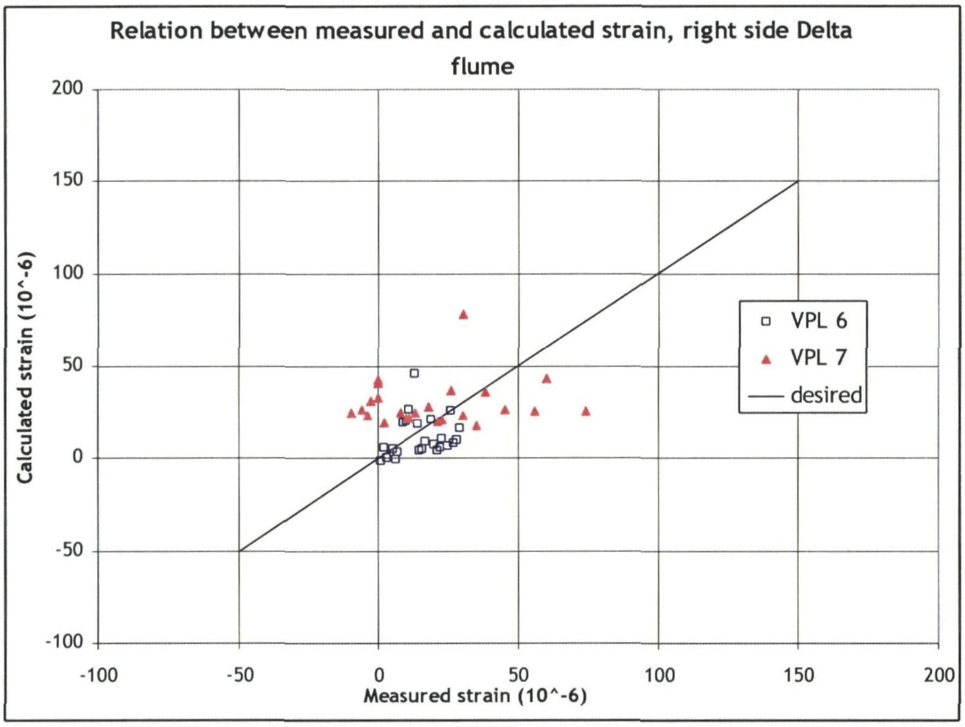

Figure 10-6 Relation between measured and calculated strain, right side of the flume. Used parameters of de Waal (1993)

10.3 Recalculation with new modulus of elasticity etc.

In this chapter the new values of the modulus of elasticity, the modulus of the subgrade and the layer thickness (see Table 8-27) are used to recalculate the strain. Also spatial difference is made by taking spatial difference of impact pressure into account as explained at the beginning of this section (Table 10-2)

Table 10-2 The calculated spatial difference in distribution over the width of the flume

Maximum impact pressure distribution over the width of the flume		
DRO 15	1.27	100%
VPL 4,5	0.96	76%
VPL 2,3,6,7	0.88	69%
VPL 1,8	0.80	63%

In chapter six and seven the schematization of the model is explained. One of the schematizations is that the prismatic load is assumed to be the same over the width of the flume. When calculating the strain for the specific place of the strain measuring devices this assumption will give no realistic results, this because it is known that the distribution of the impact pressure is not the same over the width of the flume. The strain at VPL 1 and VPL 8 is taken to be 37% lower than the calculated strain. VPL 4 and 5 are taken 24% lower than the calculated strain because the wave impacts occur at DRO 15 and the pressure decreases considerably when looking to the differences in impact pressure between DRO 15 and DRO 14. The distance between DRO 15 and VPL 4 or 5 is 0.7 m. The strain at VPL 2, 3, 6 and 7 are taken to be 31% lower than the calculated values. It should be noted that the standard deviation of the impact pressure is 20% so also the standard deviation of the strain is 20%. The result is given in Table 10-7.

Table 10-7 Recalculated strain, with new modulus of elasticity, layer thickness, modulus of the subgrade and spatial distribution

Run	t	Calculated Strain (*10^-6)								Measured Strain (*10^-6)							
		VPL								VPL							
	(s)	1	2	3	4	5	6	7	8	1	2	3	4	5	6	7	8
AS022	769	32	2	-1	38	27	11	10	23	23	2	-8	28	21	7	2	12
AS022	744	28	6	3	32	25	13	11	21	23	10	-10	23	27	8	-4	21
AS022	594	41	4	0	48	35	15	13	29	23	13	-15	20	21	8	-6	24
AH108	411	47	6	1	55	38	17	15	32	27	39	-18	18	42	-	18	40
AH108	75	46	1	-4	55	35	14	12	30	33	24	-9	26	45	8	10	36
AH108	453	36	4	1	42	29	13	12	25	42	19	8	35	42	10	11	33
AS117	374	39	17	14	46	35	23	21	29	24	18	14	36	34	25	0	25
AS117	219	45	18	14	53	39	24	23	33	55	30	-1	41	54	26	38	36
AS117	309	32	22	19	38	34	27	25	29	42	24	8	44	46	19	26	52
AS202	3695	90	41	32	106	80	53	49	68	60	58	60	58	90	49	30	88
AS202	3560	66	17	10	77	52	28	26	44	17	36	-22	13	32	35	0	13
AS202	5605	51	2	-3	60	37	15	13	31	18	-14	21	31	38	0	23	17
AS202	5483	58	2	-3	68	41	17	15	35	21	0	11	38	42	0	30	31
AS202	3539	50	7	2	59	38	18	16	32	16	4	38	45	75	3	45	33
AS203	4828	62	19	13	73	51	29	27	43	65	17	38	-	49	9	60	64
AS203	1319	52	6	1	61	39	18	16	33	25	10	53	25	48	10	74	34
AS203	3541	41	2	-1	49	30	13	11	26	54	10	38	-	49	10	35	60
AS203	1227	41	4	0	48	30	14	12	26	56	31	-8	43	46	17	21	44
AS203	51	38	10	6	45	31	17	15	26	28	25	-19	16	3	18	-10	7
AS025	81	57	5	-1	67	42	18	16	35	28	-18	41	47	46	-21	56	15
AS025	151	43	23	19	50	40	28	27	34	41	21	-15	38	53	23	0	38
AS025	771	48	7	2	57	36	17	15	31	30	-8	23	31	46	17	13	40
AS025	207	42	9	5	50	33	17	15	28	16	20	-3	19	38	17	8	38
AS025	728	41	15	11	49	35	21	19	42	2	40	-9	8	22	33	-3	12

Table 10-8 Used layer thickness and modulus of the subgrade

	ν	0.35				
	h	0.126	0.229	h	0.126	0.229
AS022	β	2.144	1.344	k	98.3	91.2
AH108	β	1.995	1.249	k	88.5	81.7
AS117	β	1.839	1.154	k	78.7	73.3
AS202	β	1.893	1.181	k	88.4	80.4
AS203	β	1.873	1.171	k	84.6	77.6
AS025	β	1.938	1.208	k	97.0	87.9

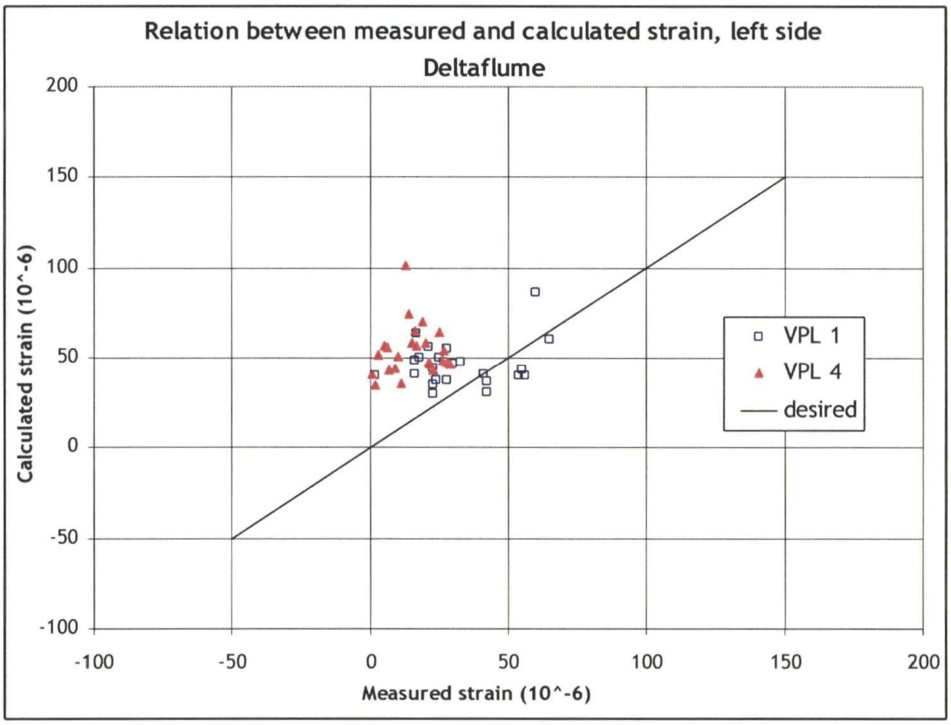

Figure 10-7 Relation between measured and recalculated strain, left side of the flume with new parameters

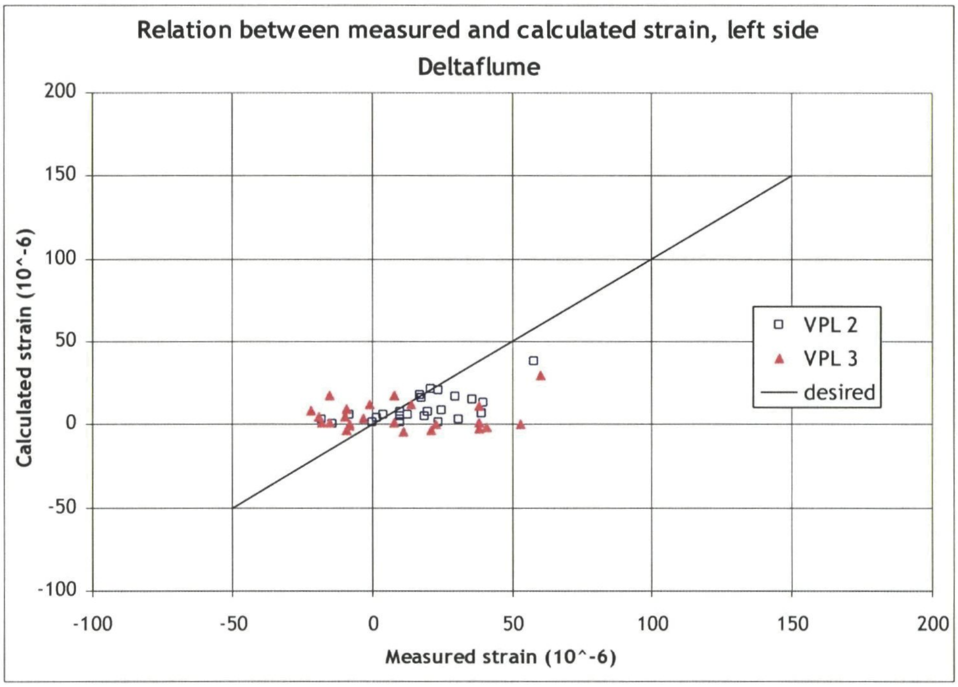

Figure 10-8 Relation between measured and recalculated strain, left side of the flume with new parameters

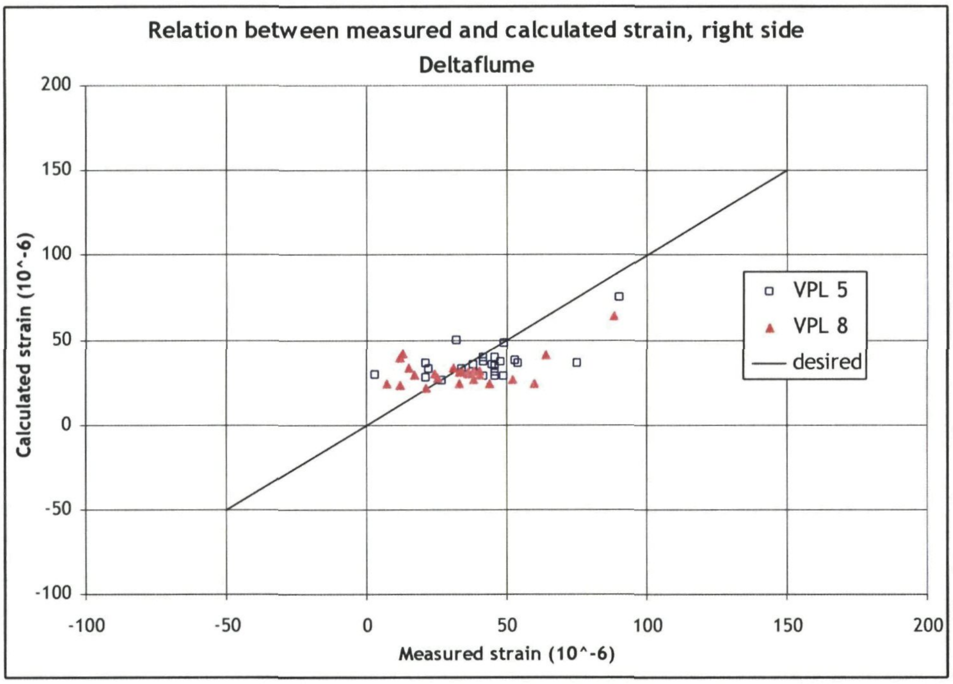

Figure 10-9 Relation between measured and recalculated strain, right side of the flume with new parameters

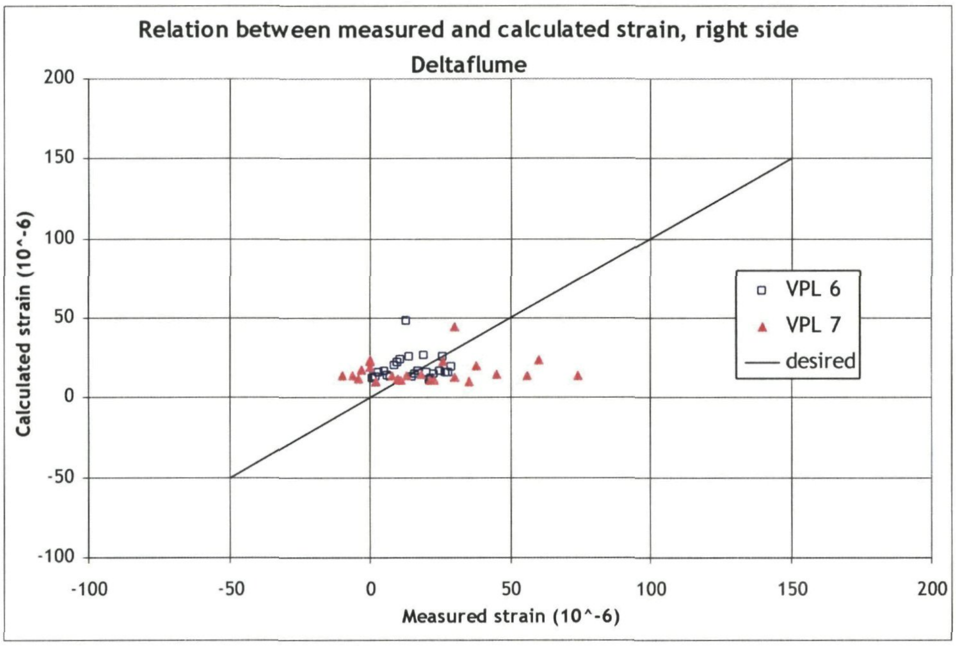

Figure 10-10 Relation between measured and recalculated strain, right side of the flume with new parameters

10.4 Result of the comparison with de Waal

As shown in the forgoing section the measured and calculated strain are more in agreement with each other by using other parameters. It looks like there is a horizontal tendency in Figure 10-8 till Figure 10-10. Because of this tendency the strain is compared to the impact pressure (Pmax) and to the impact width (z).

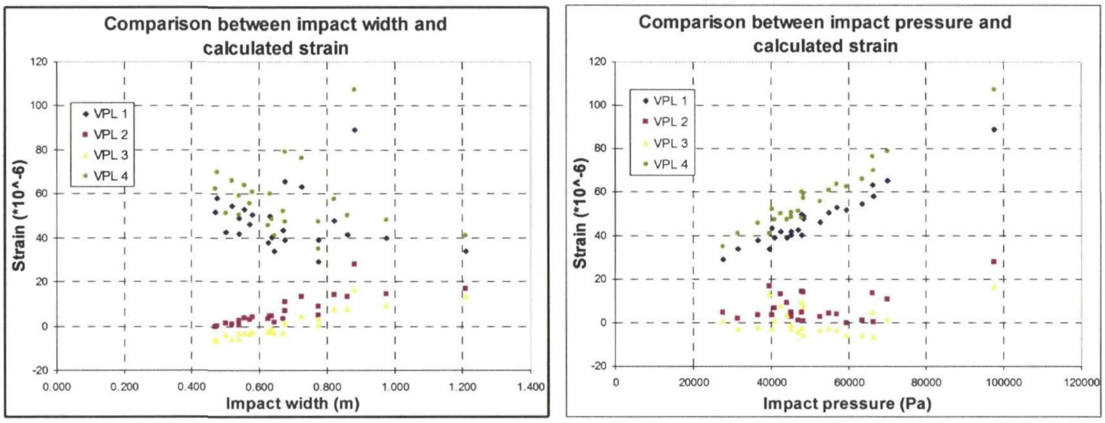

Figure 10-11 Relation between impact pressure, impact width and the strain, right side of the flume, data Table 10-7

The first figure shows a relation between the strain and the impact width. For the strain measuring devices VPL 2 and 3 this relation shows a stronger dependency. These two measuring devices are about half a meter away from the line of maximum pressure impact. The relation between the calculated strain and the impact pressure is shown in the second figure. The relation is stronger for the strain measuring devices which are placed at the line of maximum impact. Both tendencies cannot be found in the data of de Waal (1993).

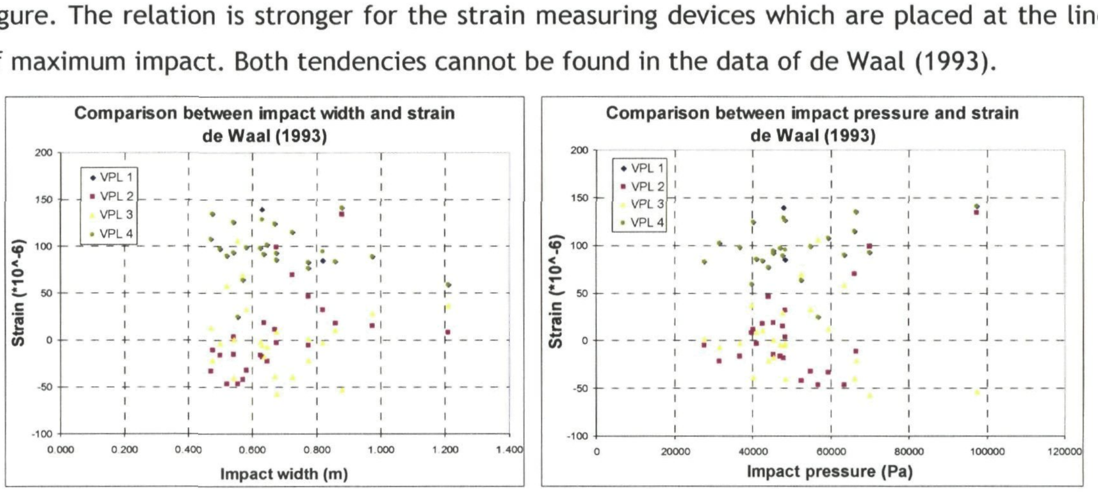

Figure 10-12 Relation between impact pressure, impact width and the strain, right side of the flume, calculated data by de Waal (1993) (

Table 10-4)

De Waal used the same formula so this difference was not expected. These tendencies also cannot be found in the measured data of the dynamic strain.

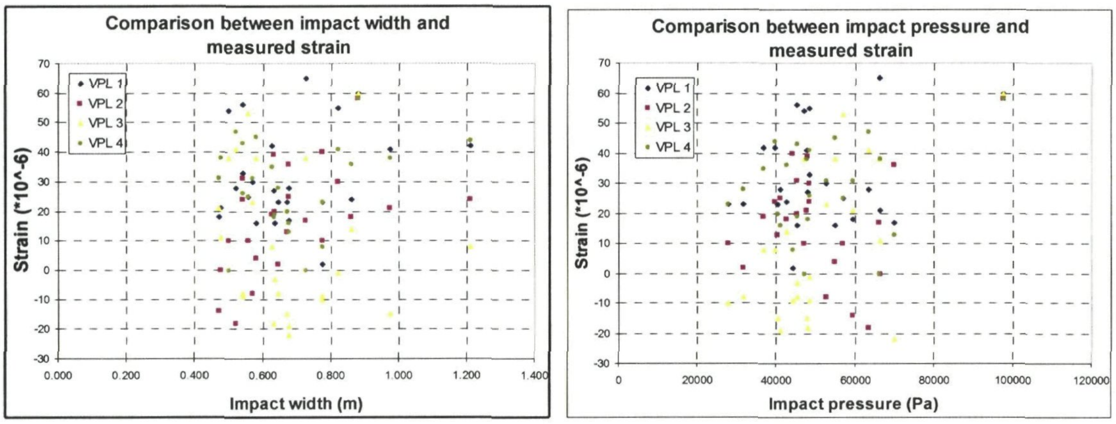

Figure 10-13 Relation between impact pressure, impact width and the strain, right side of the flume, measured data by the Waal (1993) (

Table 10-4)

The horizontal tendencies of Figure 10-8 till Figure 10-10 is caused by the limited variation of the width of the impact. According to Figure 10-13 there is no relation between the measured (dynamic) strain and the maximum impact pressure, looking to the physical processes one expects there is a relation. To compare Figure 10-13, the relation is also shown for the total strain given in de Waal (1993). So now no difference in dynamic and quasi-static strain is made.

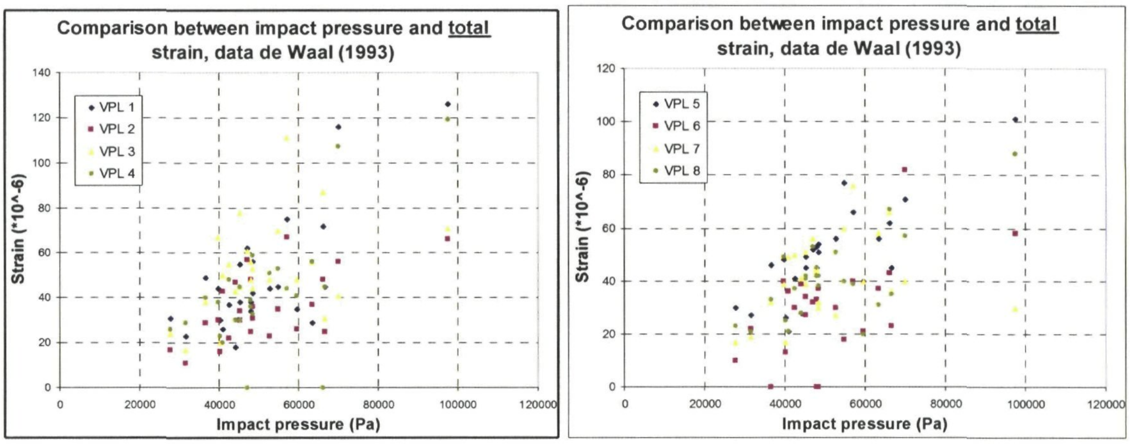

Figure 10-14 Relation between impact pressure, impact width and the total strain, measured data by the Waal (1993) (Table 5-3)

By comparing Figure 10-13 with Figure 10-14 it is clear that in the distinction de Waal makes between the total and the dynamic strain (see Figure 5-5) the dependency with the maximum impact pressure is lost.

The recalculated strains can be compared with the measured dynamic strains by subtraction. This in shown in Table 10-9 and Figure 10-15 till Figure 10-18.

Table 10-9 The recalculated strain compared to the measured dynamic strain

Run	t	Calculated - Measured strain (*10^-6)							
		VPL							
	(s)	1	2	3	4	5	6	7	8
AS022	769	11	0	5	13	8	2	6	12
AS022	744	6	-5	11	12	0	2	13	1
AS022	594	20	-10	12	32	17	4	16	7
AH108	411	23	-34	16	42	-1	-	-6	-6
AH108	75	16	-23	3	33	-6	3	-1	-4
AH108	453	-4	-16	-10	11	-11	0	-2	-7
AS117	374	18	-5	-6	14	4	-8	16	6
AS117	219	-7	-16	9	17	-12	-7	-21	-1
AS117	309	-8	-7	5	-3	-9	1	-6	-22
AS202	3695	29	-30	-44	49	-7	-11	6	-19
AS202	3560	49	-25	24	66	23	-15	19	32
AS202	5605	34	14	-27	31	1	11	-14	15
AS202	5483	37	0	-17	32	1	12	-19	5
AS202	3539	34	0	-40	16	-35	10	-33	0
AS203	4828	-2	-4	-33	-	5	13	-40	-19
AS203	1319	28	-6	-56	39	-7	3	-62	0
AS203	3541	-11	-9	-42	-	-17	-1	-27	-33
AS203	1227	-14	-28	5	8	-14	-7	-12	-17
AS203	51	11	-18	20	31	30	-6	21	20
AS025	81	27	19	-47	19	-4	33	-45	20
AS025	151	-1	-7	24	10	-13	-4	18	-5
AS025	771	16	11	-26	25	-9	-6	-3	-9
AS025	207	24	-15	2	30	-5	-6	2	-10
AS025	728	37	-31	13	39	13	-19	16	17
Mean Value		16	-10	-8	26	-2	0	-7	-1
Standard dev		17.54	14.21	24.95	15.95	13.69	10.86	22.53	15.54

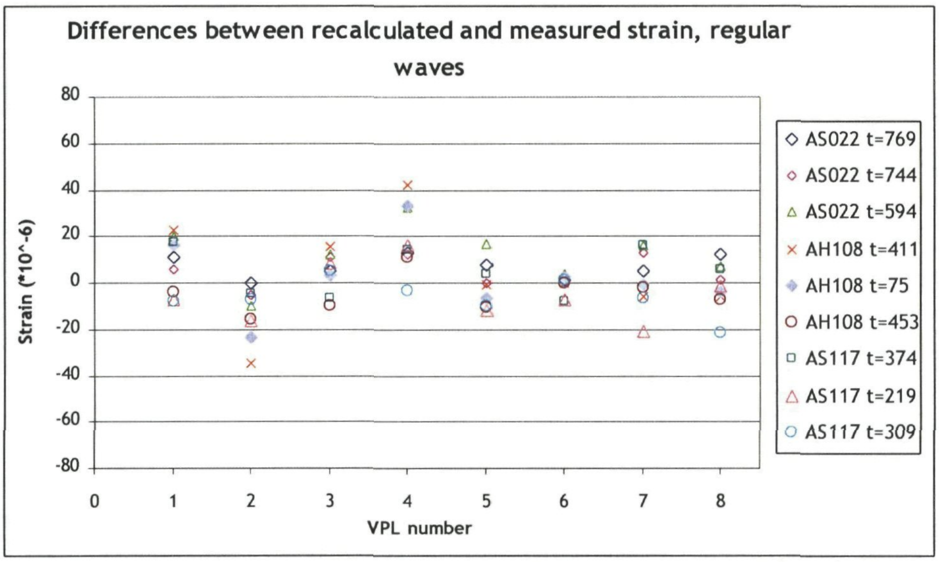

Figure 10-15 Differences between recalculated and measured strain, regular wave runs, per VPL

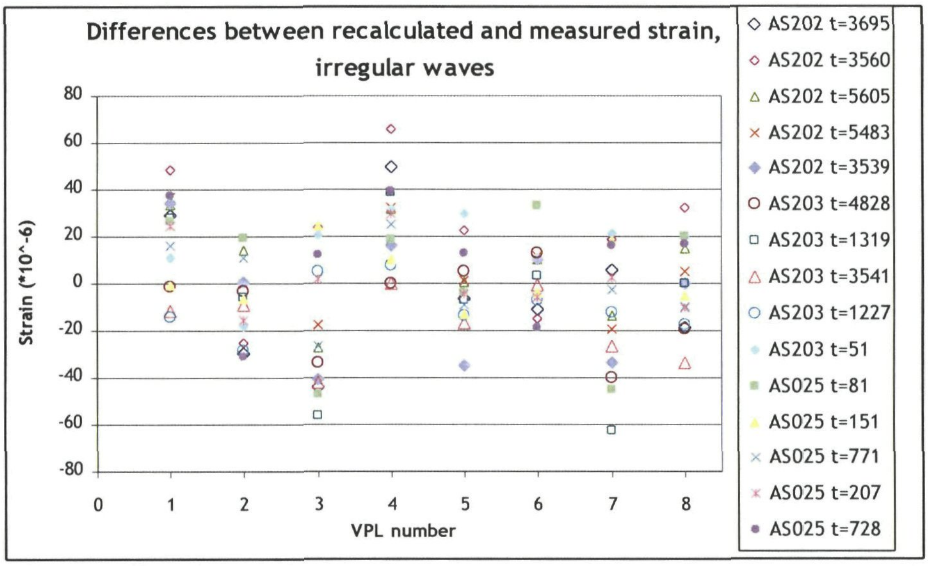

Figure 10-16 Differences between recalculated and measured strain, irregular wave runs, per VPL

The difference between Figure 10-15 and Figure 10-16 shows that the calculated strains for the regular wave runs are more in agreement with the measurements. This can be explained by the difference in strain signals between the signals under regular and irregular wave runs.

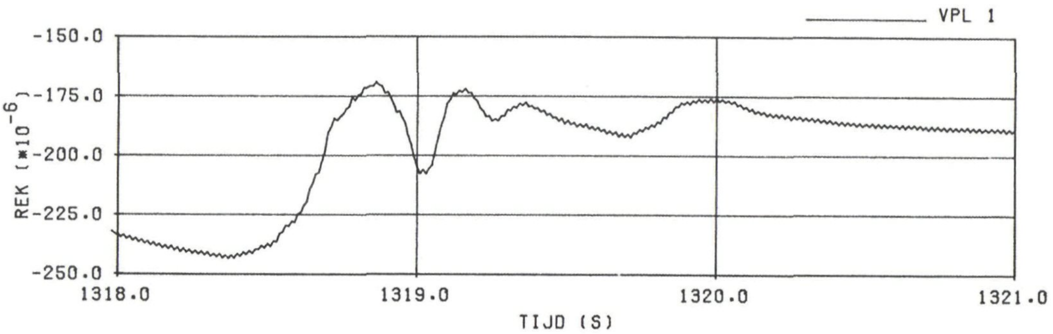

Figure 10-17 Example of a strain signal, (irregular) run AS203, t=1319

The strain signals under irregular wave loading show a more irregular pattern than the strain signal under regular wave loading. It is also more difficult to distinguish the dynamic part from the quasi-static part. The mean values of the differences are given in Figure 10-18.

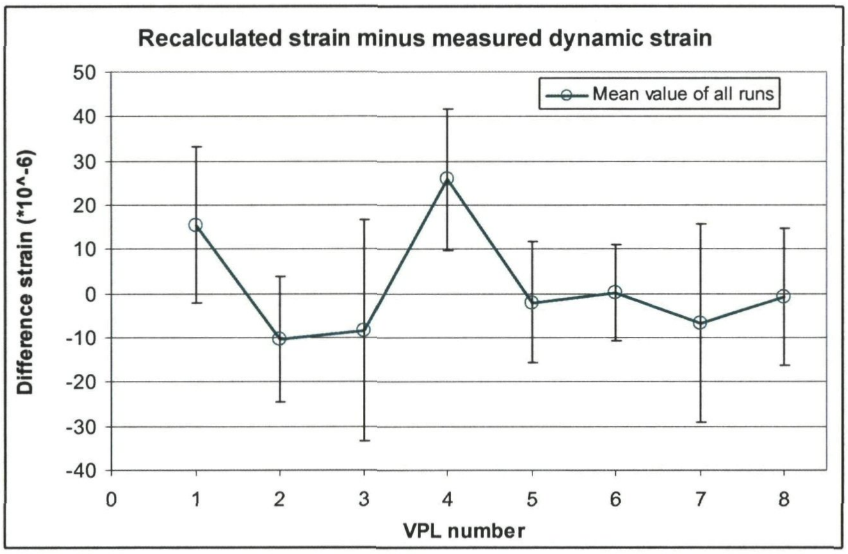

Figure 10-18 Mean value of the differences between recalculated and measured strain, with standard deviation, all wave runs, per VPL

The differences at the left side of the flume (VPL 1-4) are larger than at the right side of the flume. Maybe this shows differences between the functioning of the strain measuring devices. In chapter eleven some conclusions and recommendations for this part are stated.

In the next section the measuring signals are used again but now as a probability density function in comparison with the simulation results.

10.5 Comparison with Derks and Klein Breteler

In Derks and Klein Breteler (1992) the probability of exceedance of the strain amplitude is given for some of the strain measuring devices. In this section the result of the Monte Carlo simulation will be compared with the measurements. This is done, again, for the selected runs of de Waal (1993) (see section 5.2.1).

Table 10-10 Selected runs

Date	Test Number	Spectrum Type or Regular waves	Hs, H	Tp, T
11-sep	AS 022	Regular	1.05	5.0
13-sep	AH 108	Regular	1.45	7.0
17-sep	AS 117	Regular	1.80	5.0
16-sep	AS 202	Pierson-Moskowitz	1.43	7.1
17-sep	AS 203	Pierson-Moskowitz	1.52	8.7
16-sep	AS 025	Pierson-Moskowitz	0.89	7.6

10.5.1 Comparing the measurement with the simulation

10.5.1.1 Run AS022 VPL 4

The run AS022 exceedance percentage of the strain amplitude for strain measuring device VPL 4 is given in Figure 10-19. The strain amplitude is given for the maximum wave impacts on pressure transducer 11-19.

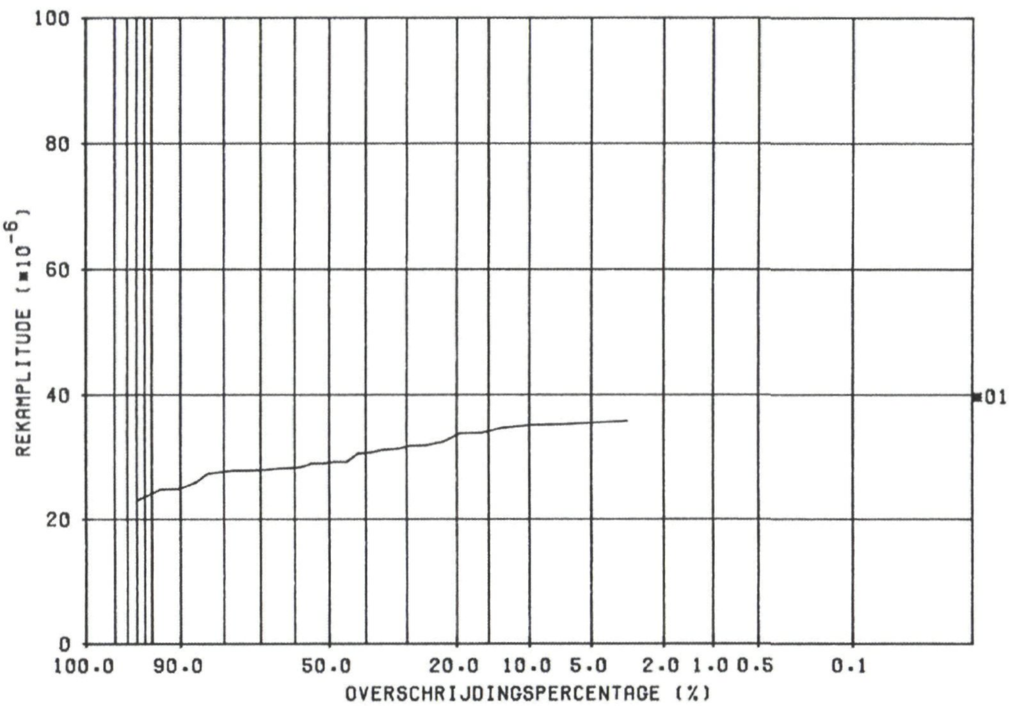

Figure 10-19 Exceedance percentage of the strain amplitude (Run AS022, VPL 4, for maximum wave impacts at DRO 11-19)

This measured data is fitted into a lognormal distribution with a mean value of 30.26 and a standard deviation of 4.26.

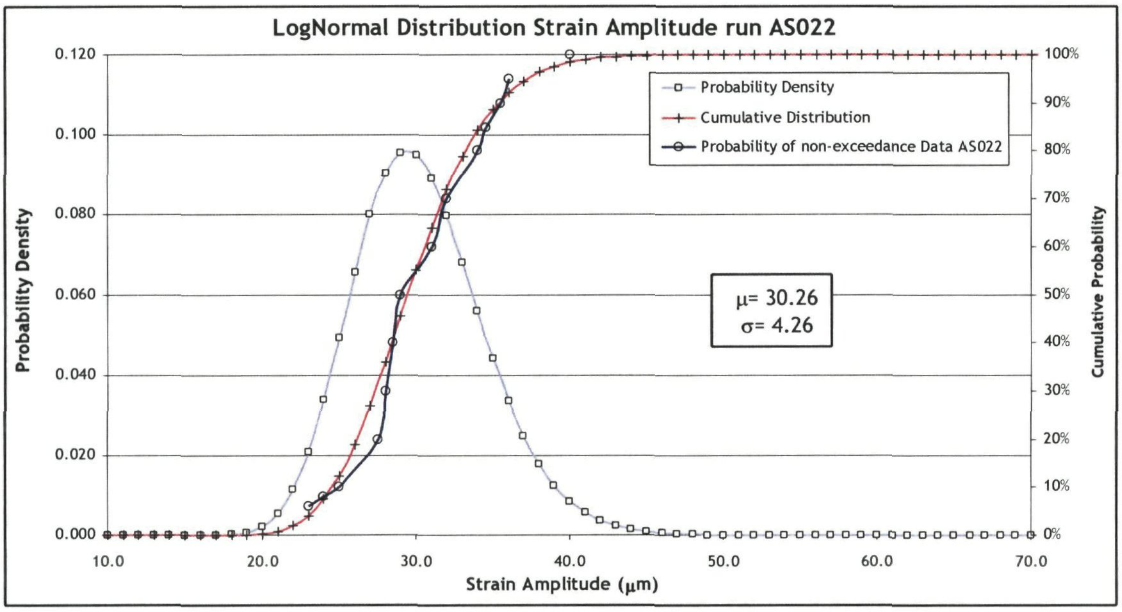

Figure 10-20 Comparison between the measured and the fitted strain amplitude distribution (Run AS022, VPL 4, for maximum wave impacts at DRO 11-19)

In the experiment for this run regular waves are used. The temperature of the asphalt was about 16.5°C so the modulus of elasticity should be chosen at 6127 MPa (see section 8.4.6). The mean value of the measured strain is 30.3 (μm) with this in mind a Monte Carlo simulation is performed.

Table 10-11 Used input and output of the Monte Carlo simulation, run AS022

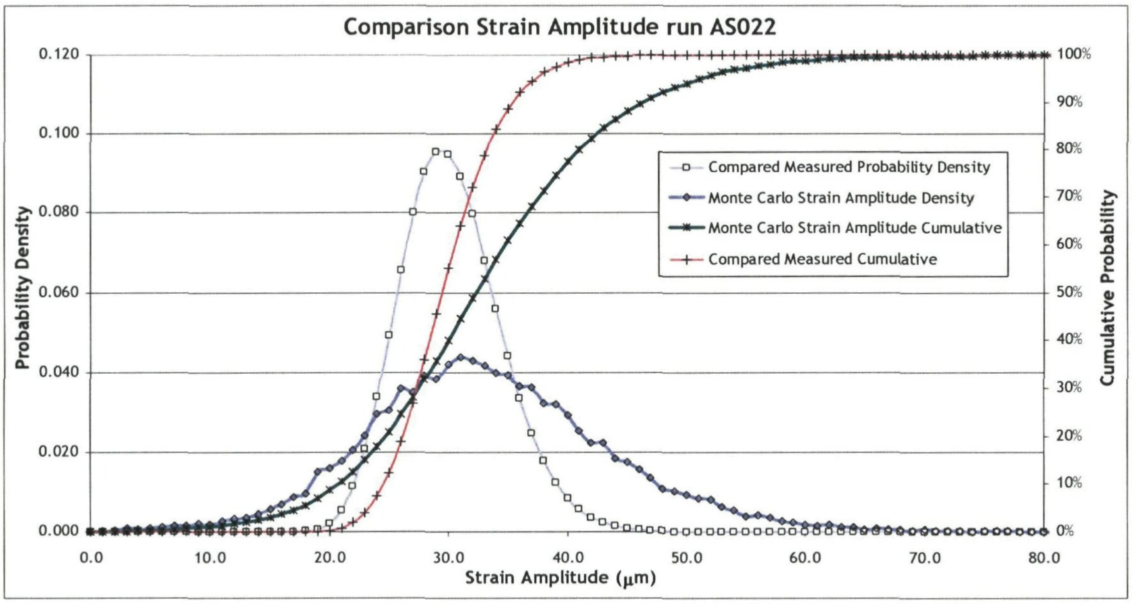

Figure 10-21 Comparison between the measured and calculated strain, run AS022, VPL 4

The mean value of the strain is 32.8 (μm) whereas the mean value of the experiment measurement was 30.3 (μm). It should be noted that this comparison is made only for one strain measuring device namely VPL 4 whereas in the Monte Carlo simulation no calculation for a specific point in space is made. The modulus of elasticity, the modulus of the subgrade and the layer thickness do take the differences in space into account. This can be an explanation for the differences in deviation. Now Poisson's contraction coefficient will be varied to look what the influence of this coefficient is.

Table 10-12 The influence of the contraction coefficient to the calculated strain

Contraction Coefficient Influence			
Contraction Coefficient	0.45	0.35	0.3
Strain	ε	ε	ε
μ	34.5	32.9	32.5
σ	10.8	10.2	10.3
σ %	31%	31%	32%

The differences are not much so in the simulation the other runs are performed with the contraction coefficient as a constant value of 0.35.

10.5.1.2 Run AH108 VPL 1

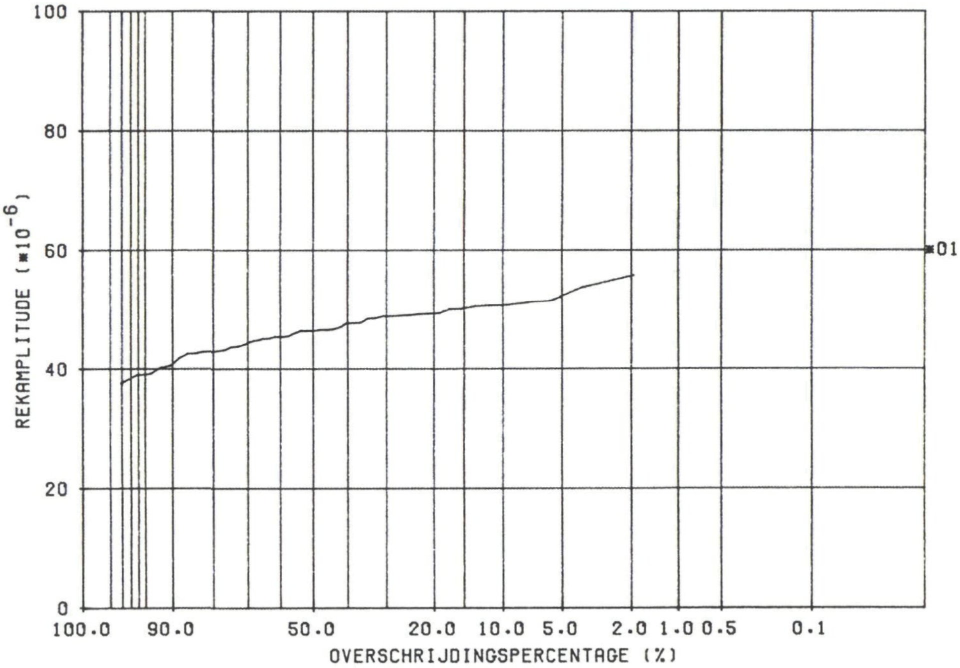

Figure 10-22 Exceedance percentage of the strain amplitude (Run AH108, VPL 1, for maximum wave impacts at DRO 9-17)

Run AH108 consisted of regular waves. The graph of the strain amplitude is fitted into a lognormal distribution with a mean value of 47.20 (μm) and a standard deviation of 4.26. This is shown in Figure 10-23.

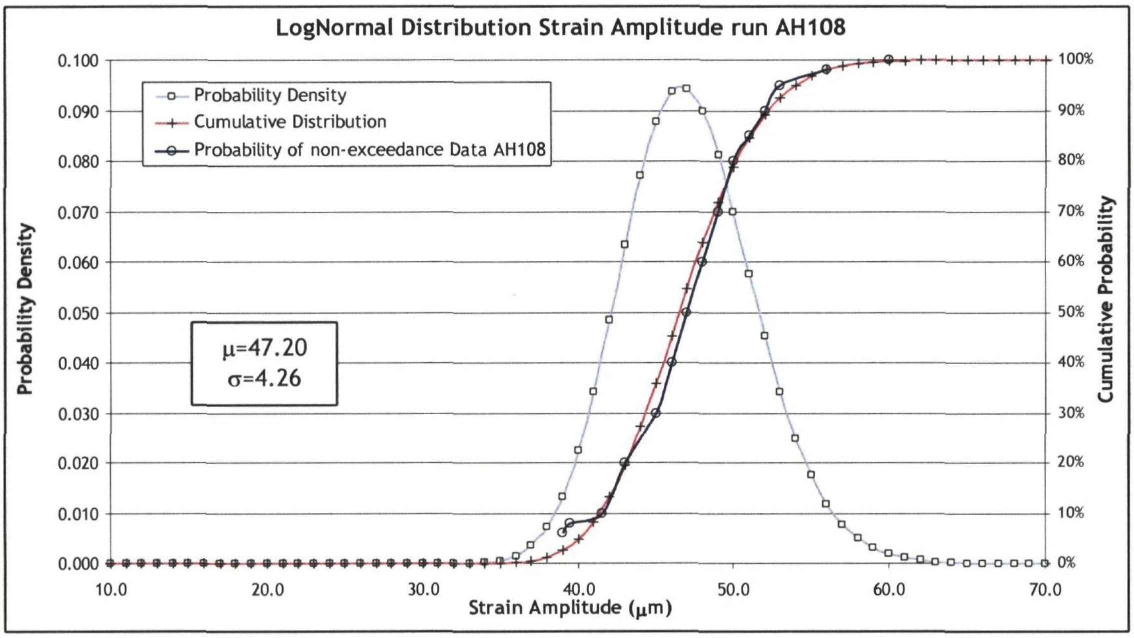

Figure 10-23 Comparison between the measured and the fitted strain amplitude distribution (Run AH108, VPL 1, for maximum wave impacts at DRO 9-17)

With the known distribution of the strain amplitude the simulation is performed and the distributions are compared with each other. The main difference between this run and run AS022 is the modulus of elasticity, the impact factor and the wave height.

Table 10-13 Used input and output of the Monte Carlo simulation, run AH108

Input AH108				Mean	Standard deviation	Coefficient of variation	
Input parameters	**Symbol**	**Units**	**Distr Type**	μ	σ	σ %	
significant wave height	H,Hs	m	D	1.45			
half width prismatic load	z	m	Rayleigh	0.725			
density water	ρω	kg/m³	D	1000			
acceleration by gravity	g	m/s²	D	9.81			
layer thickness	h	m	Normal	0.126	0.0126	10%	
modulus of elasticity	E	MPa	Normal	7354	735.4	10%	
poisson's contraction coefficient	ν	-	D	0.35			
				μ	σ	α	β
impact factor	q	-	Log-Normal	1.42	0.47	0.3	0.32
Output AH108				Mean	Standard deviation	Coefficient of variation	
Output parameter	**Symbol**	**Units**	**Distr Type**	μ	σ	σ %	
Strain	ε	mm		28.1	11.6	41%	
Pmax	Pmax	Pa	Log-Normal	20193	6648	33%	

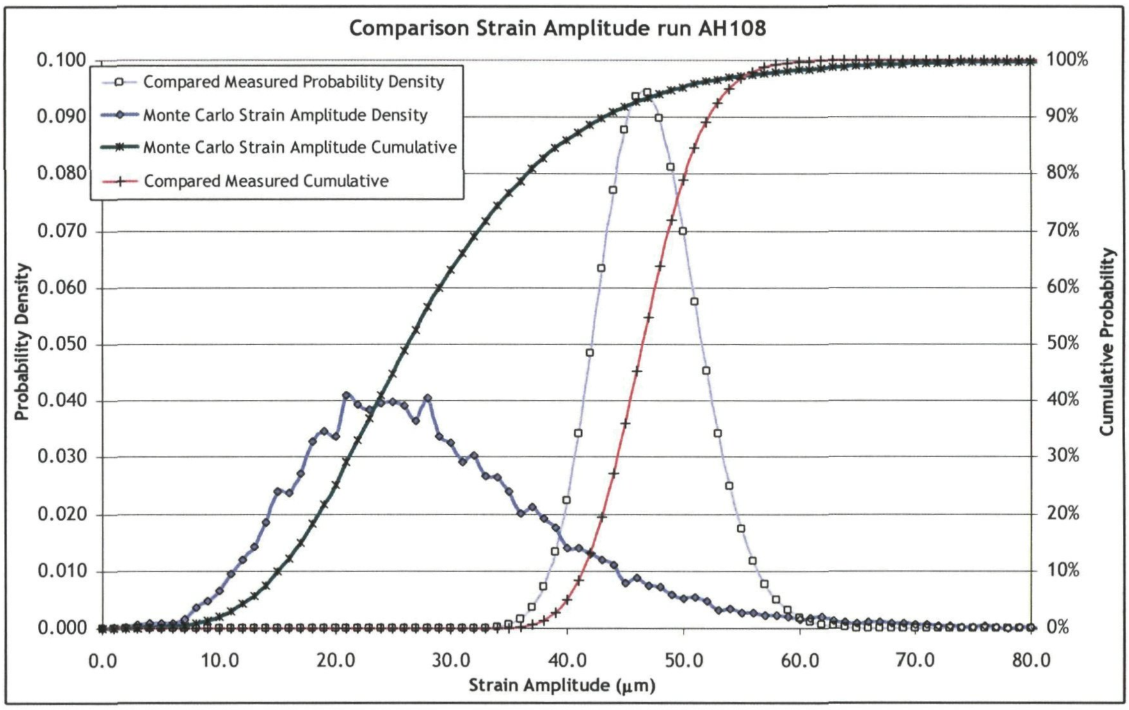

Figure 10-24 Comparison between the measured and calculated strain, run AH108, VPL 1

10.5.1.3 Run AS117 VPL 4

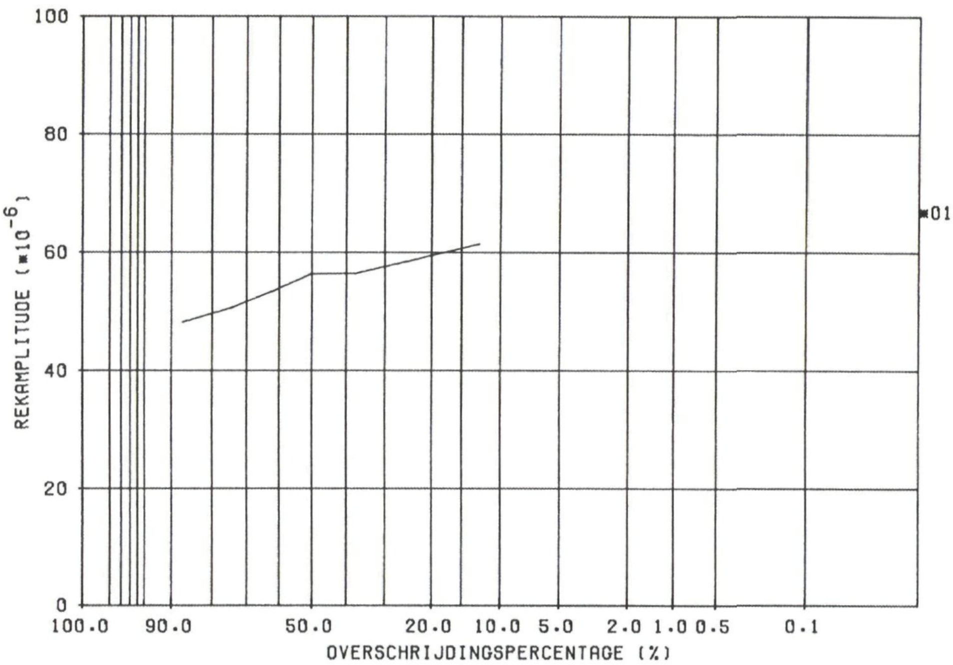

Figure 10-25 Exceedance percentage of the strain amplitude (Run AS117, VPL 4, for maximum wave impacts at DRO 11-18)

Again regular waves are used in this experiment run. The data is fitted into a lognormal distribution. This distribution is used to compare with the output of the simulation.

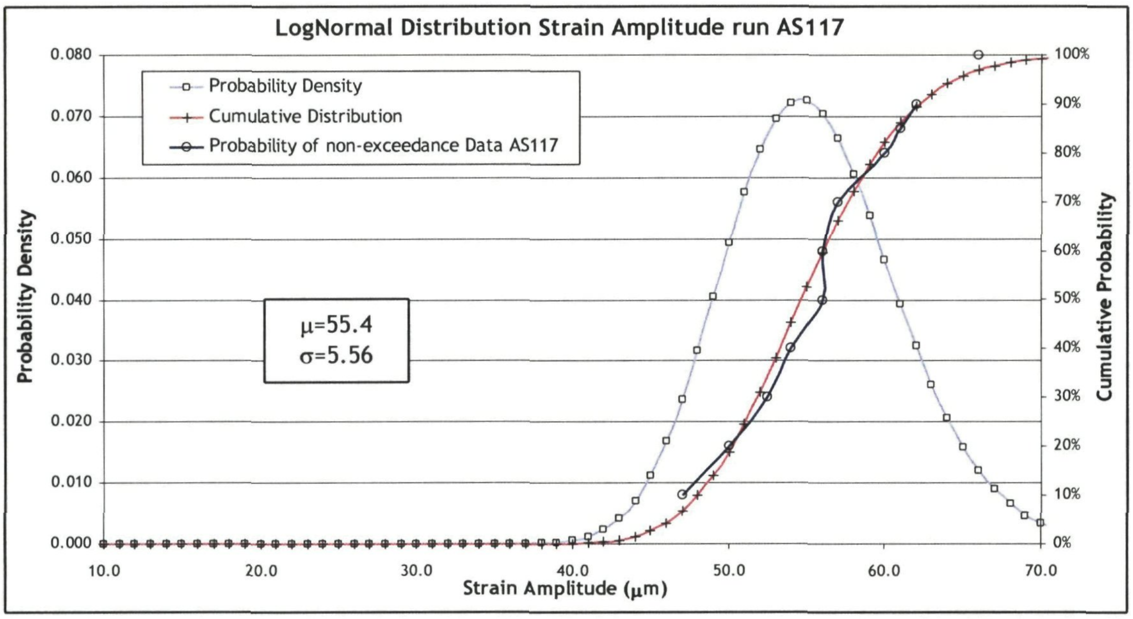

Figure 10-26 Comparison between the measured and the fitted strain amplitude distribution (Run AS117, VPL 4, for maximum wave impacts at DRO 11-18)

In this run again the modulus of elasticity, the impact factor and the wave height are adapted to the new temperature and measurements.

Table 10-14 Used input and output of the Monte Carlo simulation, run AS117

Input AS117				Mean	Standard deviation	Coefficient of variation	
Input parameters	**Symbol**	**Units**	**Distr Type**	**μ**	**σ**	**σ %**	
significant wave height	H,Hs	m	D	1.8			
half width prismatic load	z	m	Rayleigh	0.9			
density water	ρω	kg/m³	D	1000			
acceleration by gravity	g	m/s²	D	9.81			
layer thickness	h	m	Normal	0.126	0.0126	10%	
modulus of elasticity	E	MPa	Normal	9053	905.3	10%	
poisson's contraction coefficient	v	-	D	0.35			
				μ	σ	α	β
impact factor	q	-	Log-Normal	1.88	0.38	0.61	0.2
Output AS117				Mean	Standard deviation	Coefficient of variation	
Output parameter	**Symbol**	**Units**	**Distr Type**	**μ**	**σ**	**σ %**	
Strain	ε	mm		42.7	13.7	32%	
Pmax	Pmax	Pa	Log-Normal	33156	6704	20%	

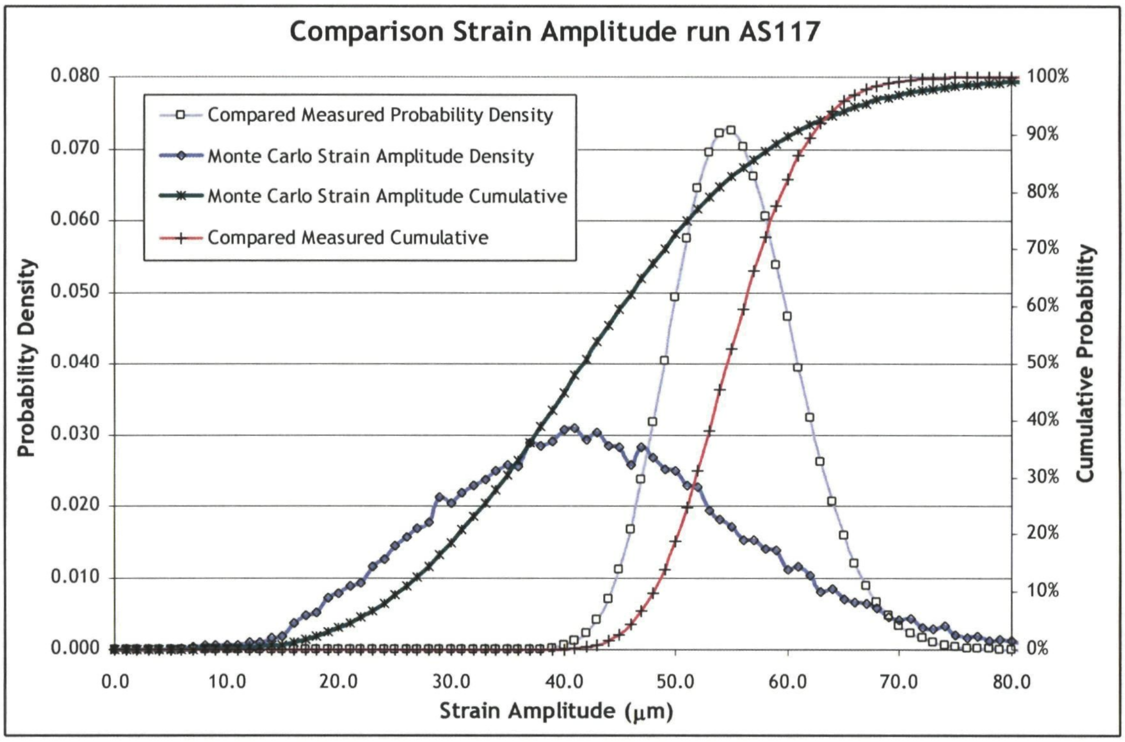

Figure 10-27 Comparison between the measured and calculated strain, run AS117, VPL 4

10.5.1.4 Run AS202 VPL 1

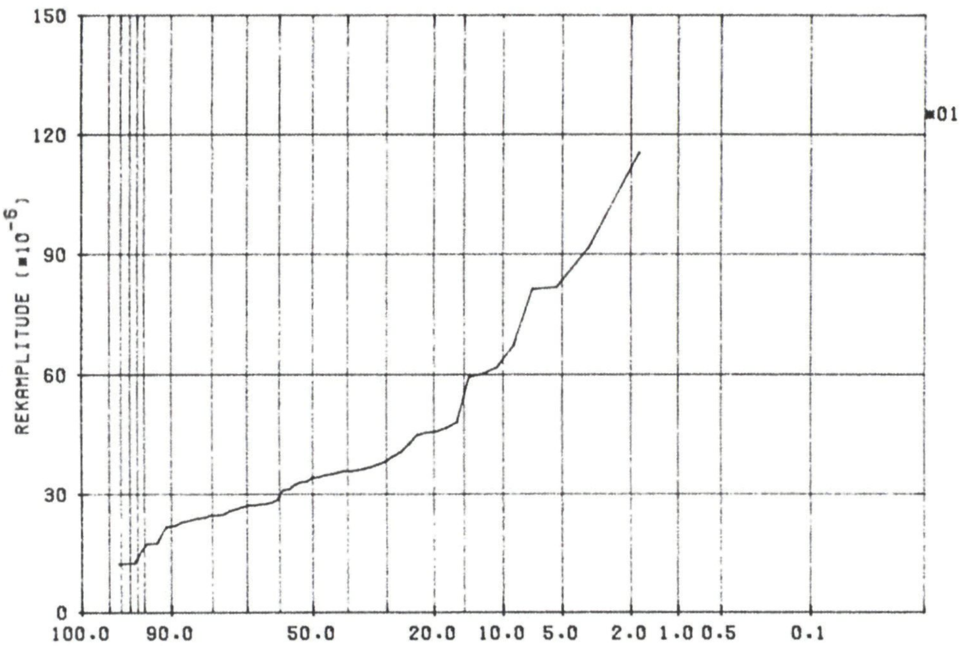

Figure 10-28 Exceedance percentage of the strain amplitude (Run AS202, VPL 1, for maximum wave impacts at DRO 8-19)

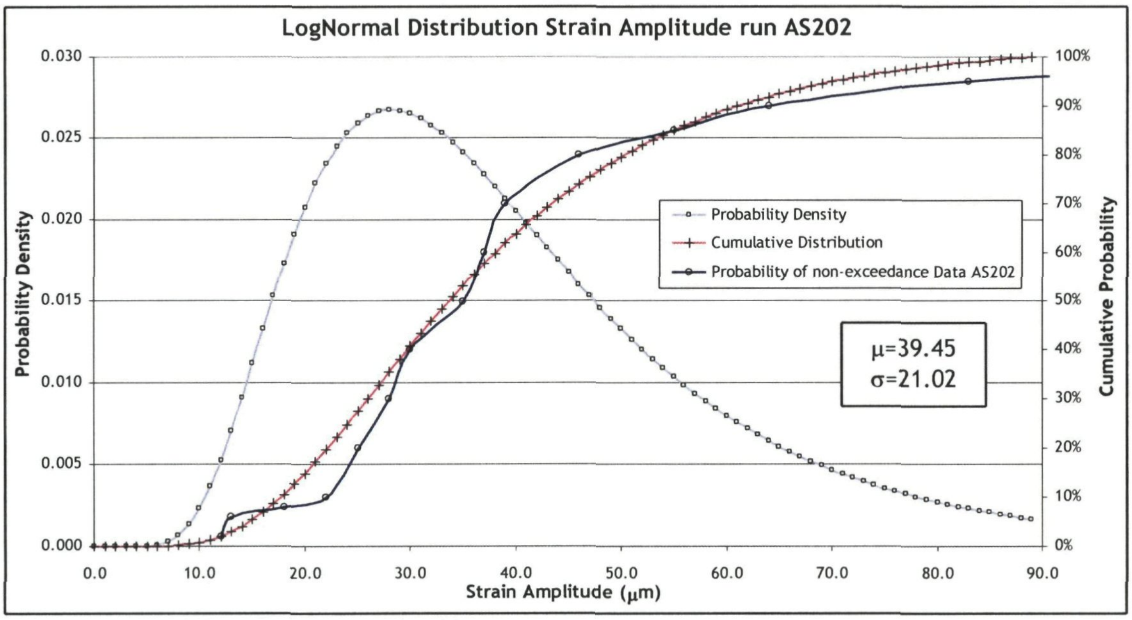

Figure 10-29 Comparison between the measured and the fitted strain amplitude distribution (Run AS202, VPL 1, for maximum wave impacts at DRO 8-19)

In the experiment irregular waves are used in this run. The temperature of the asphalt was about 8.6°C so the modulus of elasticity is chosen at 9053 MPa. The wave height is 1.43 m and the mean value of the measured strain at VPL 1 is 39.5 (μm).

Table 10-15 Used input and output of the Monte Carlo simulation, run AS202

Input AS202				Mean	Standard deviation	Coefficient of variation	
Input parameters	**Symbol**	**Units**	**Distr Type**	**μ**	**σ**	**σ %**	
significant wave height	H,Hs	m	D	1.43			
half width prismatic load	z	m	Rayleigh	0.715			
density water	ρω	kg/m³	D	1000			
acceleration by gravity	g	m/s²	D	9.81			
layer thickness	h	m	Normal	0.126	0.0126	10%	
modulus of elasticity	E	MPa	Normal	9053	905.3	10%	
poisson's contraction coefficient	ν	-	D	0.35			
				μ	**σ**	**α**	**β**
impact factor	q	-	Log-Normal	1.28	1.02	0	0.7
Output AS202				Mean	Standard deviation	Coefficient of variation	
Output parameter	**Symbol**	**Units**	**Distr Type**	**μ**	**σ**	**σ %**	
Strain	ε	mm		23.2	21.0	91%	
Pmax	Pmax	Pa	Log-Normal	17847	14253	80%	

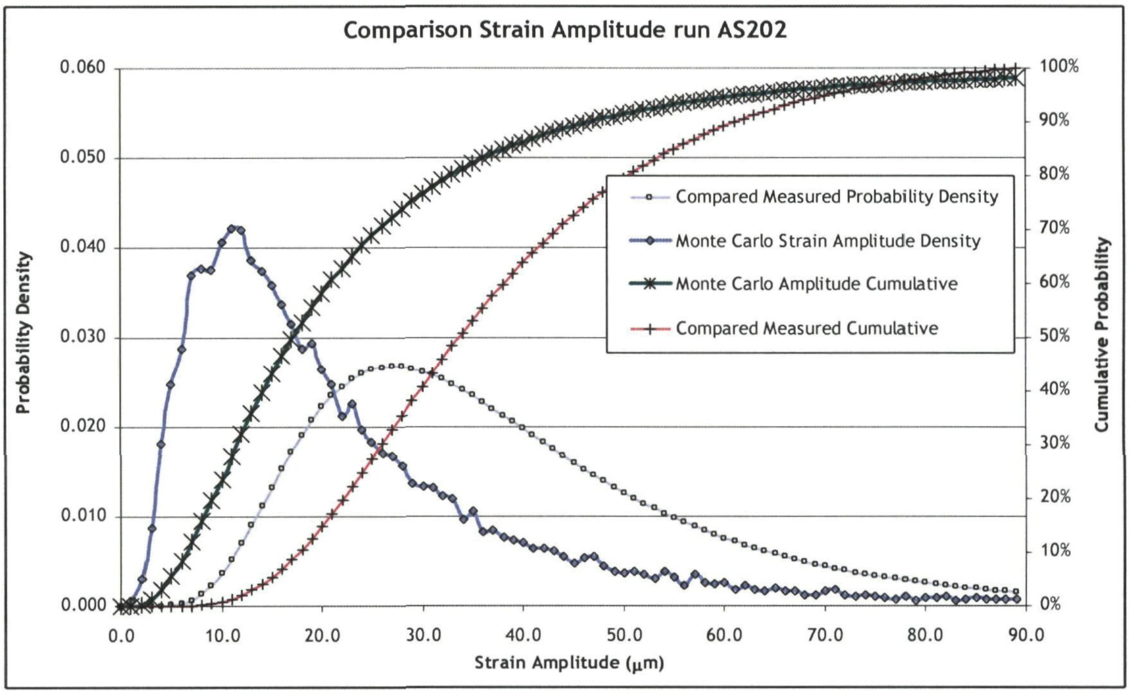

Figure 10-30 Comparison between the measured and calculated strain, run AS202, VPL 1

10.5.1.5 Run AS203 VPL 1

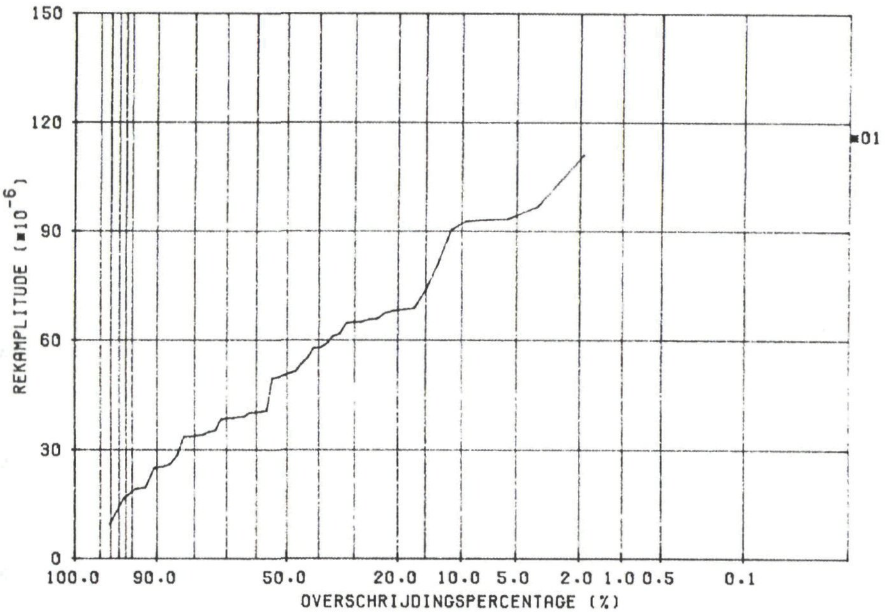

Figure 10-31 Exceedance percentage of the strain amplitude (Run AS203, VPL 1, for maximum wave impacts at DRO 8-19)

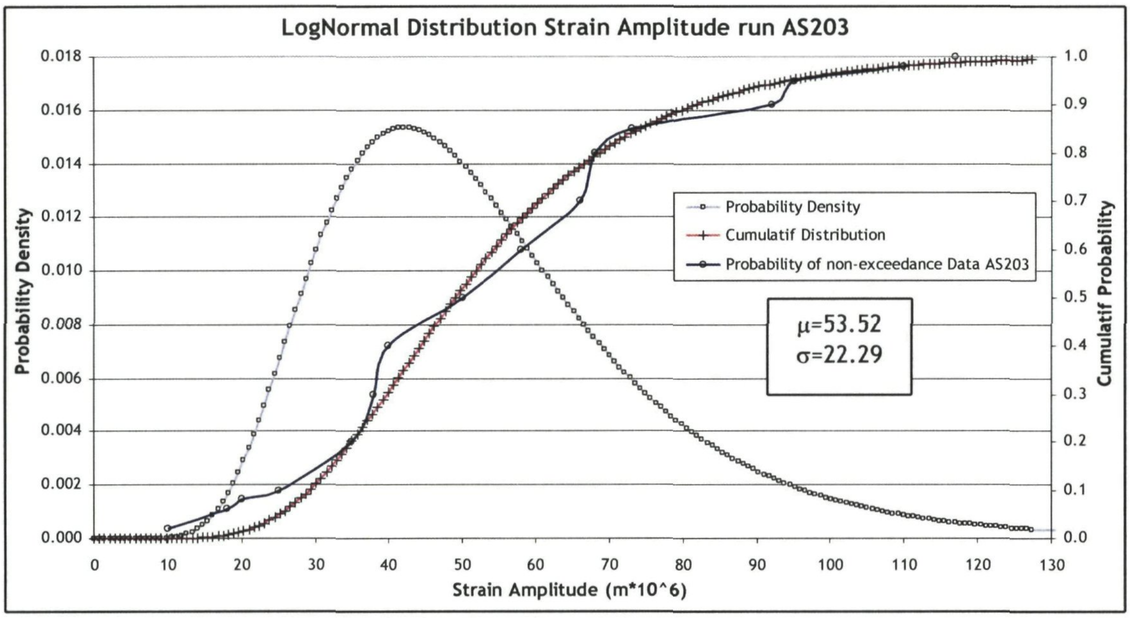

Figure 10-32 Comparison between the measured and the fitted strain amplitude distribution (Run AS203, VPL 1, for maximum wave impacts at DRO 8-19)

In the experiment irregular waves are used in this run. The temperature of the asphalt was about 8.6°C so the modulus of elasticity is chosen at 9053 MPa. The wave height is 1.52 m. The mean value of the measured strain at VPL 1 is 53.5 (μm).

Table 10-16 Used input and output of the Monte Carlo simulation, run AS203

Input AS203				Mean	Standard deviation	Coefficient of variation	
Input parameters	Symbol	Units	Distr Type	μ	σ	σ %	
significant wave height	H,Hs	m	D	1.52			
half width prismatic load	z	m	Rayleigh	0.76			
density water	ρω	kg/m³	D	1000			
acceleration by gravity	g	m/s²	D	9.81			
layer thickness	h	m	Normal	0.126	0.0126	10%	
modulus of elasticity	E	MPa	Normal	9053	905.3	10%	
poisson's contraction coefficient	ν	-	D	0.35			
				μ	σ	α	β
impact factor	q	-	Log-Normal	1.63	1.25	0.26	0.68
Output AS203				Mean	Standard deviation	Coefficient of variation	
Output parameter	Symbol	Units	Distr Type	μ	σ	σ %	
Strain	ε	mm		32.4	28.7	89%	
Pmax	Pmax	Pa	Log-Normal	24472	19080	78%	

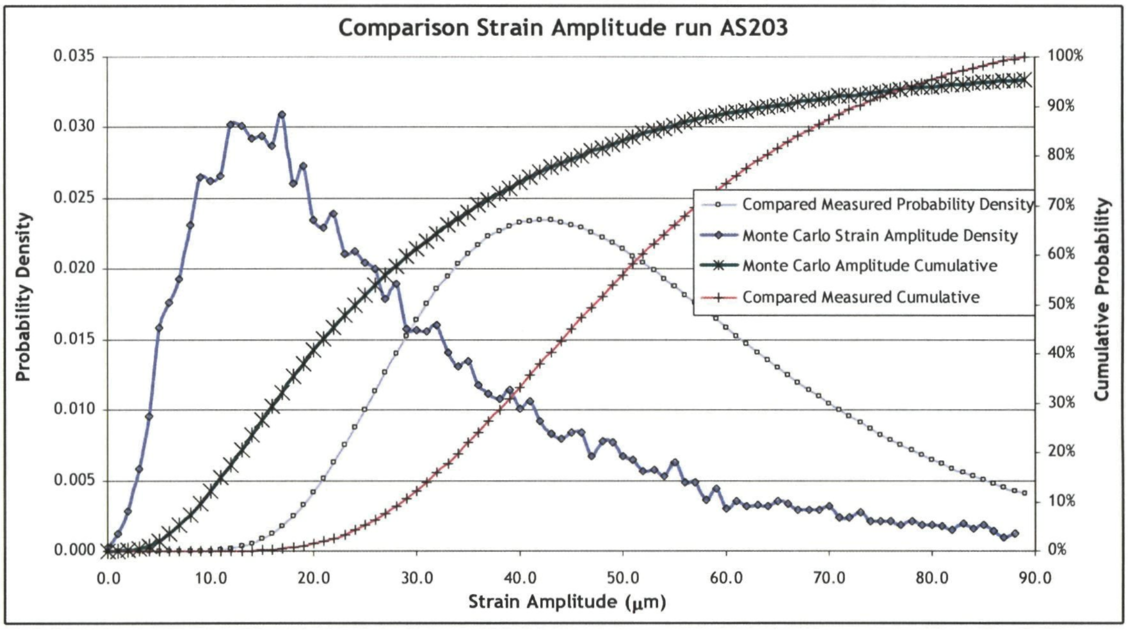

Figure 10-33 Comparison between the measured and calculated strain, run AS203, VPL 1

10.5.1.6 Run AS025 VPL 3

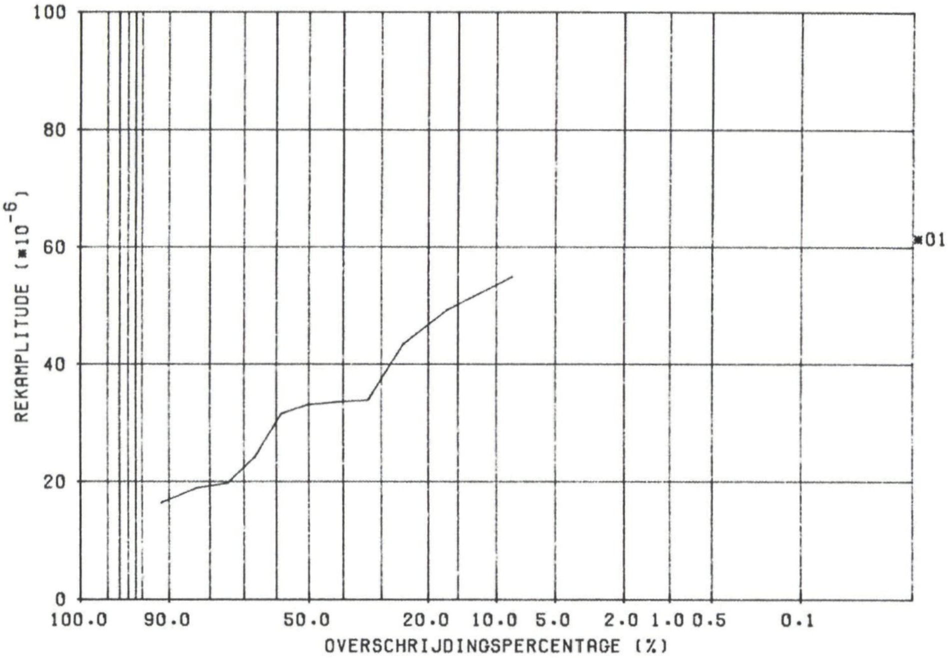

Figure 10-34 Exceedance percentage of the strain amplitude (Run AS025, VPL 3, for maximum wave impacts at DRO 9-17)

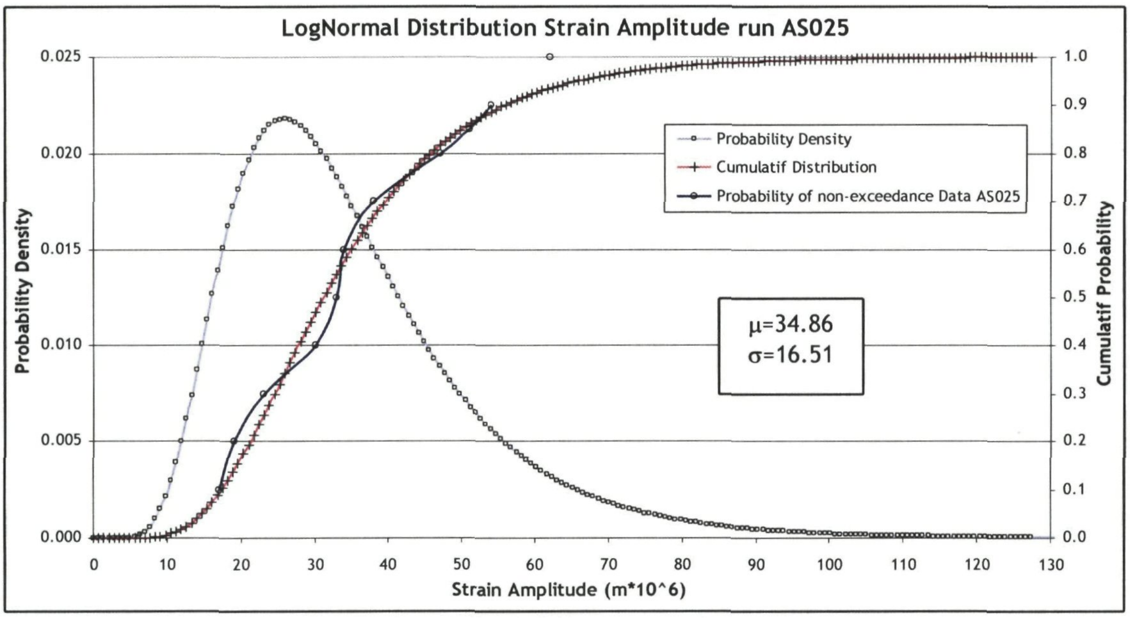

Figure 10-35 Comparison between the measured and the fitted strain amplitude distribution (Run AS025, VPL 3, for maximum wave impacts at DRO 9-17)

In the experiment irregular waves are used in this run. The temperature of the asphalt was about 8.6°C so the modulus of elasticity is chosen at 9053 MPa. The wave height is 0.89 m. The mean value of the measured strain at VPL 3! (some distance upslope from other strain measuring devices) is 34.9 (μm).

Table 10-17 Used input and output of the Monte Carlo simulation, run AS025

Input AS025				Mean	Standard deviation	Coefficient of variation	
Input parameters	Symbol	Units	Distr Type	μ	σ	σ %	
significant wave height	H,Hs	m	D	0.89			
half width prismatic load	z	m	Rayleigh	0.445			
density water	ρω	kg/m³	D	1000			
acceleration by gravity	g	m/s²	D	9.81			
layer thickness	h	m	Normal	0.126	0.0126	10%	
modulus of elasticity	E	MPa	Normal	9053	905.3	10%	
poisson's contraction coefficient	ν	-	D	0.35			
				μ	σ	α	β
impact factor	q	-	Log-Normal	2.41	1.59	0.7	0.6
Output AS025				Mean	Standard deviation	Coefficient of variation	
Output parameter	Symbol	Units	Distr Type	μ	σ	σ %	
Strain	ε	mm		26.3	19.7	75%	
Pmax	Pmax	Pa	Log-Normal	21135	13919	66%	

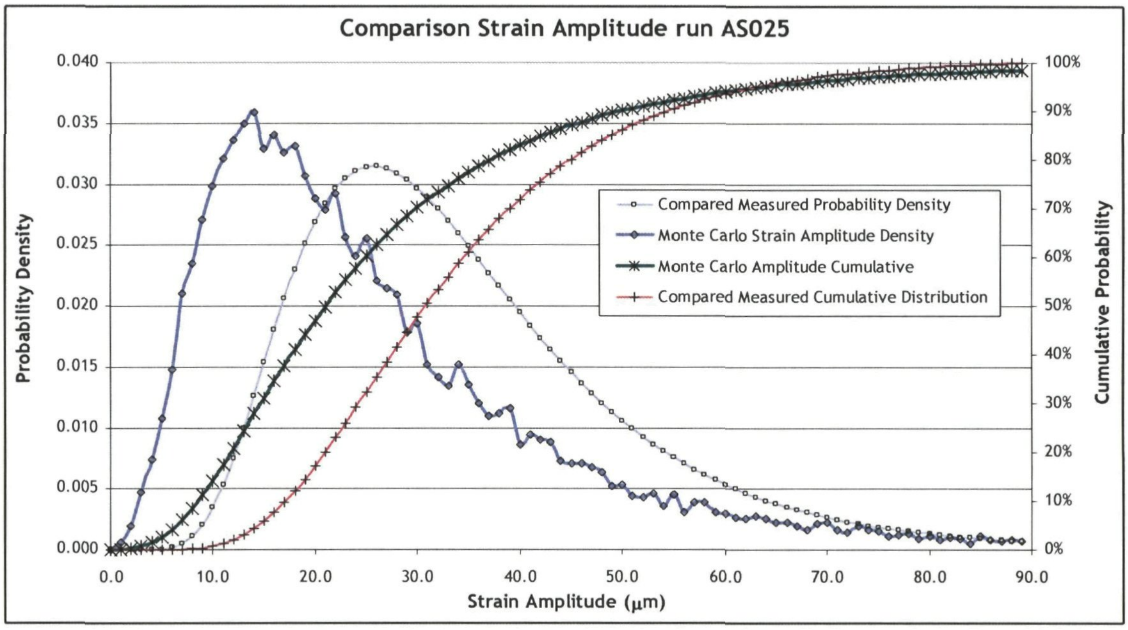

Figure 10-36 Comparison between the measured and calculated strain, run AS025, VPL 3!

10.6 Summary

Table 10-18 Summary of the measured and calculated strains for test runs AS022, AH108, AS117, AS202, AS203, AS025

	Calculated	Measured			Calculated	Measured	
Symbol	mean	mean	unit	Symbol	mean	mean	unit
	Test AS022				Test AS202		
H, Hs	1.05		m	H, Hs	1.43		m
h	0.126		m	h	0.126		m
E	6127		MPa	E	9053		MPa
q	2.15		-	q	1.28		-
ε	32.8	30.3	μm	ε	23.2	39.5	μm
	Test AH108				Test AS203		
H, Hs	1.45		m	H, Hs	1.52		m
h	0.126		m	h	0.126		m
E	7354		MPa	E	9053		MPa
q	1.42		-	q	1.28		-
ε	28.1	47.2	μm	ε	23.2	53.5	μm
	Test AS117				Test AS025		
H, Hs	1.8		m	H, Hs	0.89		m
h	0.126		m	h	0.126		m
E	9053		MPa	E	9053		MPa
q	1.88		-	q	2.41		-
ε	42.7	55.4	μm	ε	26.3	34.9	μm

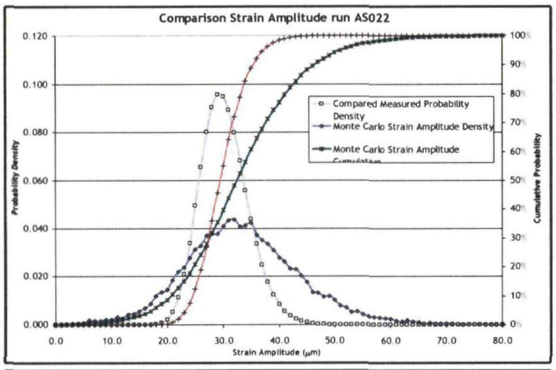
Comparison Strain Amplitude run AS022
Compared Measured Probability Density
Monte Carlo Strain Amplitude Density
Monte Carlo Strain Amplitude Cumulative
Probability Density
Cumulative Probability
Strain Amplitude (μm)

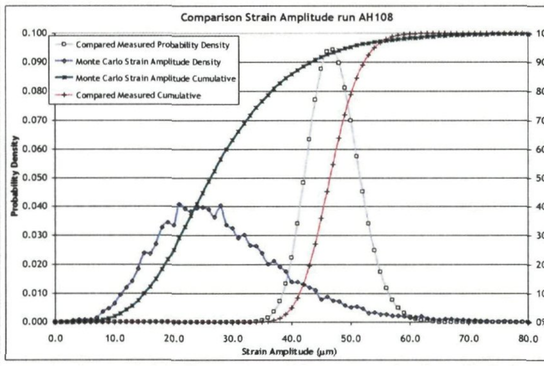
Comparison Strain Amplitude run AH108
Compared Measured Probability Density
Monte Carlo Strain Amplitude Density
Monte Carlo Strain Amplitude Cumulative
Compared Measured Cumulative
Probability Density
Cumulative Probability
Strain Amplitude (μm)

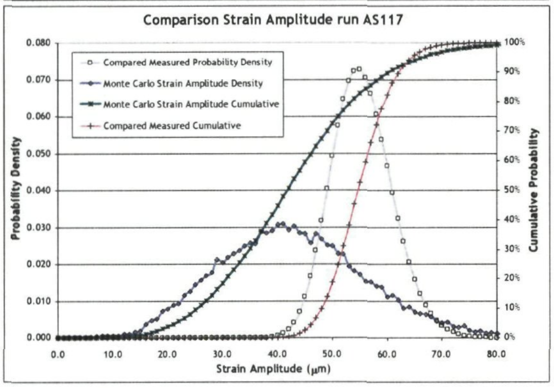
Comparison Strain Amplitude run AS117
Compared Measured Probability Density
Monte Carlo Strain Amplitude Density
Monte Carlo Strain Amplitude Cumulative
Compared Measured Cumulative
Probability Density
Cumulative Probability
Strain Amplitude (μm)

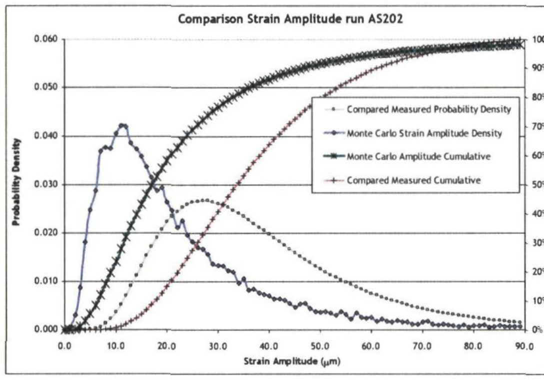
Comparison Strain Amplitude run AS202
Compared Measured Probability Density
Monte Carlo Strain Amplitude Density
Monte Carlo Amplitude Cumulative
Compared Measured Cumulative
Probability Density
Cumulative Probability
Strain Amplitude (μm)

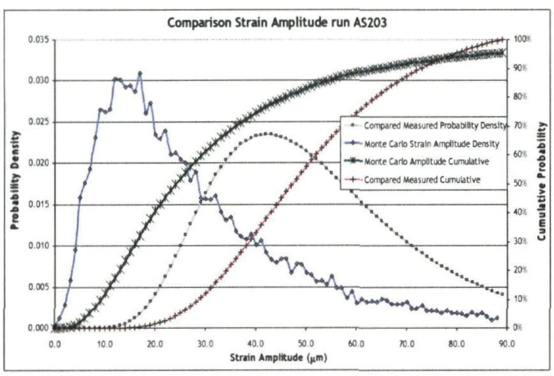
Comparison Strain Amplitude run AS203
Compared Measured Probability Density
Monte Carlo Strain Amplitude Density
Monte Carlo Amplitude Cumulative
Compared Measured Cumulative
Probability Density
Cumulative Probability
Strain Amplitude (μm)

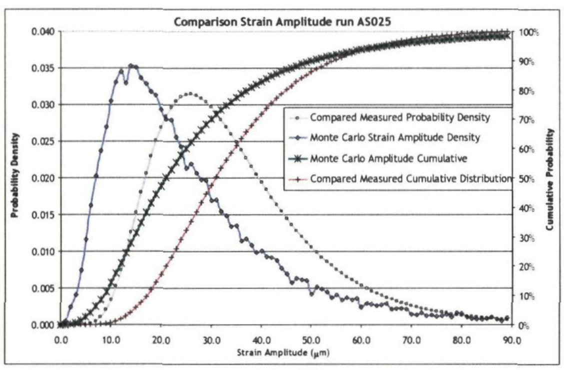
Comparison Strain Amplitude run AS025
Compared Measured Probability Density
Monte Carlo Strain Amplitude Density
Monte Carlo Amplitude Cumulative
Compared Measured Cumulative Distribution
Probability Density
Cumulative Probability
Strain Amplitude (μm)

10.7 Results of the comparison with Derks and Klein Breteler

In this section the influence coefficient for the input parameters are determined. With the influence coefficients (α^2) the simulation results are analyzed. The influence coefficient gives the influence of the variance of a probability function to the variance of the calculated probability function.

10.7.1 Influence coefficients

To calculate the influence coefficient the partial derivative of the formula for calculating the strain is calculated. This is done with maple and the maple sheets are given below with b=β and where pmaxdiff is the partial derivative of the strain formula with respect to Pmax.

Formula for the maximum tension under the prismatic load (x=0)

$$> sigmamax := \frac{pmax\,(1 - e^{(-b\,z)}\,(\cos(b\,z) + \sin(b\,z)))\,\frac{6}{h^2}}{4\,b^3\,z}$$

Formula for the maximum strain under the prismatic load (x=0)

$$> strain := \frac{sigmamax}{E}$$

$$strain := \frac{3\,pmax\,(1 - e^{(-b\,z)}\,(\cos(b\,z) + \sin(b\,z)))}{2\,b^3\,z\,h^2\,E}$$

To calculate the influence of each parameter to the total strain the influence coefficients can be calculated. To calculate the influence coefficient the formula for the maximum strain should be differentiated for each parameter. First the strain formula is differentiated for pmax.

$$> pmaxdif := \frac{\partial}{\partial pmax}\left(\frac{3\,pmax\,(1 - e^{(-b\,z)}\,(\cos(b\,z) + \sin(b\,z)))}{2\,b^3\,z\,h^2\,E}\right)$$

$$pmaxdif := \frac{3\,(1 - e^{(-b\,z)}\,(\cos(b\,z) + \sin(b\,z)))}{2\,b^3\,z\,h^2\,E}$$

$$> hdif := \frac{\partial}{\partial h}\left(\frac{3\,pmax\,(1 - e^{(-b\,z)}\,(\cos(b\,z) + \sin(b\,z)))}{2\,b^3\,z\,h^2\,E}\right)$$

$$hdif := -\frac{3\,pmax\,(1 - e^{(-b\,z)}\,(\cos(b\,z) + \sin(b\,z)))}{b^3\,z\,h^3\,E}$$

$$> zdif := \frac{\partial}{\partial z}\left(\frac{3\,pmax\,(1 - e^{(-b\,z)}\,(\cos(b\,z) + \sin(b\,z)))}{2\,b^3\,z\,h^2\,E}\right)$$

$$zdif := -\frac{3\,pmax\,(1 - e^{(-b\,z)}\,(\cos(b\,z) + \sin(b\,z)))}{2\,b^3\,z^2\,h^2\,E} + \frac{3\,pmax\,(b\,e^{(-b\,z)}\,(\cos(b\,z) + \sin(b\,z)) - e^{(-b\,z)}\,(-\sin(b\,z)\,b + \cos(b\,z)\,b))}{2\,b^3\,z\,h^2\,E}$$

$$> bdif := \frac{\partial}{\partial b}\left(\frac{3\,pmax\,(1 - e^{(-b\,z)}\,(\cos(b\,z) + \sin(b\,z)))}{2\,b^3\,z\,h^2\,E}\right)$$

$$bdif := -\frac{9\,pmax\,(1 - e^{(-b\,z)}\,(\cos(b\,z) + \sin(b\,z)))}{2\,b^4\,z\,h^2\,E} + \frac{3\,pmax\,(z\,e^{(-b\,z)}\,(\cos(b\,z) + \sin(b\,z)) - e^{(-b\,z)}\,(-\sin(b\,z)\,z + \cos(b\,z)\,z))}{2\,b^3\,z\,h^2\,E}$$

$$> Edif := \frac{\partial}{\partial E}\left(\frac{3\,pmax\,(1 - e^{(-b\,z)}\,(\cos(b\,z) + \sin(b\,z)))}{2\,b^3\,z\,h^2\,E}\right)$$

$$Edif := -\frac{3\,pmax\,(1 - e^{(-b\,z)}\,(\cos(b\,z) + \sin(b\,z)))}{2\,b^3\,z\,h^2\,E^2}$$

These derivatives are used in excel to calculate the influence coefficient. The coefficients are normalized with respect to the sum of the coefficients so the sum of the coefficients is one. With the derivative of β or bdif the influence of β is calculated. The influence of the layer thickenss (h), the modulus of the subgrade reaction (k) and the modulus of elasticity is calculated by taking the derivative of β. This is shown in the maple sheets below where bkdif is the partial derivative of β to k.

$$> b1 := \left(\frac{3\,k\,(1 - v^2)}{E\,h^3}\right)^{\left(\frac{1}{4}\right)}$$

$$b1 := 3^{(1/4)}\left(\frac{k\,(1 - v^2)}{E\,h^3}\right)^{(1/4)}$$

$$> bnudif := \frac{\partial}{\partial v}\left(3^{\left(\frac{1}{4}\right)}\left(\frac{k\,(1 - v^2)}{E\,h^3}\right)^{\left(\frac{1}{4}\right)}\right)$$

$$bnudif := -\frac{3^{(1/4)}\,k\,v}{2\left(\frac{k\,(1 - v^2)}{E\,h^3}\right)^{(3/4)} E\,h^3}$$

$$> bkdif := \frac{\partial}{\partial k}\left(3^{\left(\frac{1}{4}\right)}\left(\frac{k\,(1 - v^2)}{E\,h^3}\right)^{\left(\frac{1}{4}\right)}\right)$$

$$bkdif := \frac{3^{(1/4)}\,(1 - v^2)}{4\left(\frac{k\,(1 - v^2)}{E\,h^3}\right)^{(3/4)} E\,h^3}$$

$$> bhdif := \frac{\partial}{\partial h}\left(3^{\left(\frac{1}{4}\right)}\left(\frac{k\,(1-\nu^2)}{E\,h^3}\right)^{\left(\frac{1}{4}\right)}\right)$$

$$bhdif := -\frac{3\;3^{(1/4)}\,k\,(1-\nu^2)}{4\left(\frac{k\,(1-\nu^2)}{E\,h^3}\right)^{(3/4)} E\,h^4}$$

$$> bEdif := \frac{\partial}{\partial E}\left(3^{\left(\frac{1}{4}\right)}\left(\frac{k\,(1-\nu^2)}{E\,h^3}\right)^{\left(\frac{1}{4}\right)}\right)$$

$$bEdif := -\frac{3^{(1/4)}\,k\,(1-\nu^2)}{4\left(\frac{k\,(1-\nu^2)}{E\,h^3}\right)^{(3/4)} E^2\,h^3}$$

In the next subsections the calculated coefficients according to the procedure given above are given in tables.

Table 10-19 The calculated influence coefficients for run AS022

	Normal		Normal	Rayleigh	Log-Normal		
f =>	h	k	E	z	Pmax	β	ε
Run AS022	(m)	(MPa/m)	(MPa)	(m)	Pa	1/m	(-)
Mean value	0.1260	99.89	6120	0.66	22136	2.17	33.0
Standard Deviation	0.01259	3.19	617	0.34	4929	0.18	10.3
d ε/df	-587.28		-0.0060	-4.02	0.00167	-35.30	
(d ε/df)*σ	-7.39		-3.73	-1.38	8.24	-6.38	sum
((d ε/df)*σ)²	54.63		13.89	1.90	67.84	40.70	179
α	0.55		0.28	0.10	-0.62	0.48	sum
α²	0.31		0.08	0.01	0.38	0.23	1
d β/df	-12.3913	0.0052	0.000074				
(d β/df)*σ	-0.1560	0.0166	0.0458				sum
((d β/df)*σ)²	0.0243	0.0003	0.0021				0.0267
α	0.9544	-0.1018	-0.2805				sum
α²	0.9109	0.0104	0.0787				1
							sum
Total α²	0.512	0.002	0.096	0.011	0.379		1

The layer thickness is the main cause of the standard deviation of the strain followed by the maximum impact pressure. The variation coefficient of the layer thickness is 10%. When the variation coefficient is 8% the impact pressure is the main parameter influencing the standard deviation.

Table 10-20 The calculated influence coefficients for run AS022 with a variation coefficient of 8% for the layer thickness

	h	k	E	z	Pmax	sum
Total α²	0.402	0.003	0.114	0.012	0.468	1

Table 10-21 The calculated influence coefficients for run AH108

	Normal		Normal	Rayleigh	Log-Normal		
f =>	h	k	E	z	Pmax	β	ε
Run AH108	(m)	(MPa/m)	(MPa)	(m)	Pa	1/m	(-)
Mean value	0.1260	89.53	7349	0.91	20235	2.02	28.2
Standard Deviation	0.01264	3.10	729	0.47	6633	0.17	11.7
$d\,\varepsilon/df$	-490.46		-0.0042	-12.35	0.00153	-36.19	
$(d\,\varepsilon/df)^*\sigma$	-6.20		-3.07	-5.84	10.13	-6.15	sum
$((d\,\varepsilon/df)^*\sigma)^2$	38.43		9.41	34.10	102.58	37.77	222
α	0.42		0.21	0.39	-0.68	0.41	sum
α^2	0.17		0.04	0.15	0.46	0.17	1
$d\,\beta/df$	-12.0567	0.0057	0.000072				
$(d\,\beta/df)^*\sigma$	-0.1524	0.0175	0.0528				sum
$((d\,\beta/df)^*\sigma)^2$	0.0232	0.0003	0.0028				0.0263
α	0.9394	-0.1081	-0.3253				sum
α^2	0.8825	0.0117	0.1058				1
							sum
Total α^2	0.323	0.002	0.060	0.153	0.461		1

Table 10-22 The calculated influence coefficients for run AS117

	Normal		Normal	Rayleigh	Log-Normal		
f =>	h	k	E	z	Pmax	β	ε
Run AS117	(m)	(MPa/m)	(MPa)	(m)	Pa	1/m	(-)
Mean value	0.1260	78.33	9055	1.12	33183	1.85	42.8
Standard Deviation	0.01255	2.11	912	0.59	6708	0.15	13.6
$d\,\varepsilon/df$	-734.11		-0.0051	-21.45	0.00139	-62.91	
$(d\,\varepsilon/df)^*\sigma$	-9.21		-4.66	-12.58	9.35	-9.66	sum
$((d\,\varepsilon/df)^*\sigma)^2$	84.84		21.68	158.19	87.44	93.28	445
α	0.44		0.22	0.60	-0.44	0.46	sum
α^2	0.19		0.05	0.36	0.20	0.21	1
$d\,\beta/df$	-11.6605	0.0063	0.000070				
$(d\,\beta/df)^*\sigma$	-0.1463	0.0132	0.0638				sum
$((d\,\beta/df)^*\sigma)^2$	0.0214	0.0002	0.0041				0.0256
α	0.9136	-0.0825	-0.3982				sum
α^2	0.8346	0.0068	0.1586				1
							sum
Total α^2	0.365	0.001	0.082	0.355	0.196		1

Table 10-23 The calculated influence coefficients for run AS202

	Normal		Normal	Rayleigh	Log-Normal		
f =>	h	k	E	z	Pmax	β	ε
Run AS202	(m)	(MPa/m)	(MPa)	(m)	Pa	1/m	(-)
Mean value	0.1260	89.15	9055	0.90	17936	1.91	23.3
Standard Deviation	0.01267	5.15	906	0.47	14674	0.16	21.4
d ε/df	-401.20		-0.0028	-7.85	0.00141	-30.12	
(d ε/df)*σ	-5.08		-2.53	-3.66	20.69	-4.93	sum
((d ε/df)*σ)²	25.82		6.40	13.43	427.91	24.26	498
α	0.23		0.11	0.16	-0.93	0.22	sum
α²	0.05		0.01	0.03	0.86	0.05	1
d β/df	-12.0438	0.0057	0.000072				
(d β/df)*σ	-0.1526	0.0292	0.0655				sum
((d β/df)*σ)²	0.0233	0.0009	0.0043				0.0284
α	0.9050	-0.1734	-0.3884				sum
α²	0.8191	0.0301	0.1509				1
							sum
Total α²	0.092	0.001	0.020	0.027	0.860		1

Table 10-24 The calculated influence coefficients for run AS203

	Normal		Normal	Rayleigh	Log-Normal		
f =>	h	k	E	z	Pmax	β	ε
Run AS203	(m)	(MPa/m)	(MPa)	(m)	Pa	1/m	(-)
Mean value	0.1260	85.38	9045	0.95	24167	1.89	31.9
Standard Deviation	0.01256	5.68	906	0.50	18382	0.16	27.4
d ε/df	-544.15		-0.0038	-12.30	0.00142	-42.45	
(d ε/df)*σ	-6.83		-3.44	-6.15	26.08	-6.79	sum
((d ε/df)*σ)²	46.68		11.80	37.78	680.38	46.12	823
α	0.24		0.12	0.21	-0.91	0.24	sum
α²	0.06		0.01	0.05	0.83	0.06	1
d β/df	-11.9142	0.0059	0.000071				
(d β/df)*σ	-0.1496	0.0333	0.0648				sum
((d β/df)*σ)²	0.0224	0.0011	0.0042				0.0277
α	0.8991	-0.2001	-0.3893				sum
α²	0.8084	0.0400	0.1516				1
							sum
Total α²	0.102	0.002	0.023	0.046	0.827		1

Table 10-25 The calculated influence coefficients for run AS025

	Normal		Normal	Rayleigh	Log-Normal		
f =>	h	k	E	z	Pmax	β	ε
Run AS025	(m)	(MPa/m)	(MPa)	(m)	Pa	1/m	(-)
Mean value	0.1260	98.71	9055	0.56	20953	1.96	25.9
Standard Deviation	0.01268	6.42	902	0.29	13810	0.17	19.3
d ε/df	-451.75		-0.0031	9.71	0.00136	-26.27	
(d ε/df)*σ	-5.73		-2.83	2.82	18.76	-4.40	sum
((d ε/df)*σ)²	32.84		8.03	7.96	351.97	19.40	420
α	0.28		0.14	-0.14	-0.92	0.21	sum
α²	0.08		0.02	0.02	0.84	0.05	1
d β/df	-12.3543	0.0053	0.000074				
(d β/df)*σ	-0.1567	0.0337	0.0668				sum
((d β/df)*σ)²	0.0246	0.0011	0.0045				0.0302
α	0.9023	-0.1943	-0.3848				sum
α²	0.8141	0.0378	0.1481				1
	h	k	E	z	Pmax		sum
Total α²	0.116	0.002	0.026	0.019	0.838		1

From the tables becomes clear that the variation of the maximum impact pressure causes the most of the variation of the strain. Especially for the runs with irregular waves this variation of the maximum impact pressure is dominating. This is also the reason why the shape of the distribution function of the strain is alike the shape of the impact factor distribution (the *impact factor distribution determines the impact pressure distribution*).

10.7.2 Measured strain

The cumulative probability of non-exceedance of the strain is given for maximum wave impacts at a range of pressure transducers. This means that when a wave impact hits one of the transducers, a certain time interval (0.7T, starting at 0.3T before time of impact), is captured. Then at this same time interval the maximum strain amplitude of the strain measuring device is given. So when a wave impact hits DRO 8, a time interval is set up and the strain signals of the strain measuring devices are recorded.

Table 10-26 Distance between the pressure transducers along slope

Instrument Code	X (m)	Z (m)	X,DROn-X,DROn+1	Z,DROn-Z,DROn+1	distance to next DRO along slope	distance to DRO 15 along slope
DRO8	202.520	4.488	0.240	0.084	0.25	1.01
DRO9	202.280	4.404	0.250	0.061	0.26	0.75
DRO10	202.030	4.343	0.240	0.061	0.25	0.50
DRO11	201.790	4.282	0.120	0.030	0.12	0.25
DRO12	201.670	4.252	0.120	0.030	0.12	0.12
DRO15	201.550	4.222	0.120	0.031	0.12	
DRO17	201.43	4.191	0.120	0.030	0.12	0.12
DRO18	201.31	4.161	0.250	0.060	0.26	0.25
DRO19	201.06	4.101				0.50

In Table 10-3 the distance along slope between DRO 15 and VPL 3 is given. The distance between DRO 8 and VPL 3 is about 1.5m. This means when the wave impacts at DRO 8 the strain 1.5m down-slope is measured. This example shows that a large part of the measured strains can be caused by a quasi-static pressure variation.

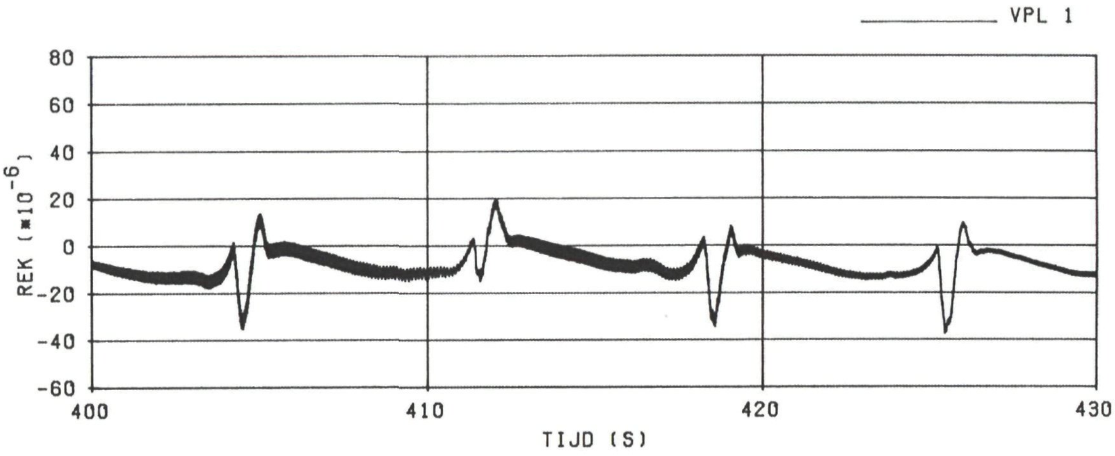

Figure 10-37 Measured strain at maximum wave impact, run AH108

In Figure 10-37 a strain signal in time is given. When the method of de Waal (1993) is used (see Figure 5-5) to make a distinction between dynamic and quasi-static strain the resulting measured (dynamic) strain would be less for some of the wave impacts. One solution to this problem is to reduce the time interval of 0.7T. This time interval should be, looking to this strain signal between 0.1-0.2 times the wave period T. The time interval is dependent on the time of impact so also this relation can be searched for. When subtracting the dynamic strain of Table 5-2 from the total strain in Table 5-3 one sees that a large part of the total strain consists of a quasi-static part.

Table 10-27 Total measured strain minus the absolute value of the dynamic strain

Total measured Strain - Dynamic strain (*10^-6)							
1	2	3	4	5	6	7	8
0	9	9	1	6	15	17	9
8	7	14	3	3	2	13	2
7	3	5	3	5	5	11	1
7	9	30	18	3	-	26	2
9	12	35	7	6	-	20	2
7	10	30	5	4	-	21	0
13	4	41	12	7	5	50	12
1	1	52	18	0	11	-6	6
2	6	59	-6	2	21	13	-3
66	8	11	61	11	9	0	0
99	20	19	94	39	47	40	44
17	12	27	10	2	21	17	3
24	25	20	7	3	23	6	4
29	31	32	8	2	15	15	7
7	31	49	-	13	34	6	3
50	57	58	19	18	30	2	5
8	47	23	-	3	22	21	-7
-1	3	70	2	3	10	30	-3
-2	18	31	4	18	18	39	14
1	19	15	9	10	16	2	16
-3	4	41	1	0	10	45	7
14	15	25	20	10	13	14	11
22	10	42	11	7	17	31	4
16	7	34	22	6	6	38	16

In Ruygrok (1994) the difference in quasi-static strain and dynamic strain is taken into account by adjusting the modulus of the subgrade. The relation between the quasi-static and dynamic strain is taken to be $k_{dyn}=1.5*k_{quasi\text{-}static}$. An example of using the $k_{quasi\text{-}static}$ value for run AS117 is given in

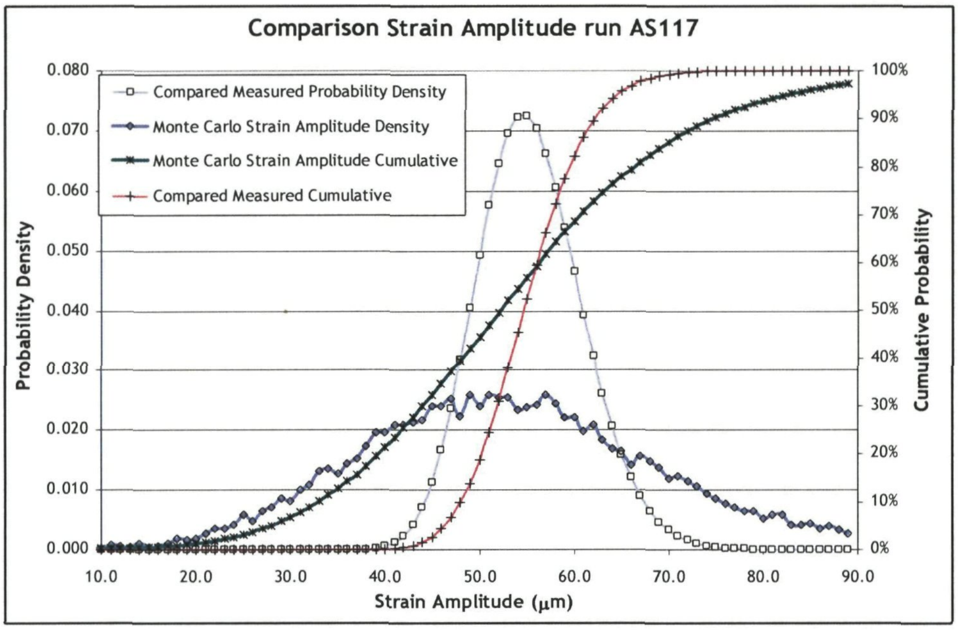

Figure 10-38 Comparison between the measured and calculated strain, run AS117, VPL 4, adapted k value

Another reason for the differences between the measurements and the calculation could be in the deviation of the impact factor distribution. The impact factor distribution is only given for maximum wave impact at a range of pressure transducers, for example DRO 9 - DRO 17. The question is what the difference would be when the impact factor distribution of only DRO 15 was known. No information in other reports is available so it is hypothesized that the deviation of the distribution can be less for one pressure transducer. Because the simulation is sensitive for the distribution of the maximum impact pressure more information of this distribution is needed.

In chapter eleven statements and conclusions are given.

10.8 References

CUR (1997) CUR 190 "Probabilities in civil engineering, Part 1: Probabilistic design in theory", *CUR, Gouda*

DE WAAL, J.P. (1993) Gedrag van asfaltbekleding onder golfaanval, Relatie tussen belasting en rek (in Dutch)(Report H 1702), *DWW Rijkswaterstaat, Delft*

DERKS, H. AND KLEIN BRETELER, M. (1992) Gedrag van asfaltbekleding onder golfaanval, verslag modelonderzoek in Deltagoot (in Dutch)(Report H 1480), *DWW Rijkswaterstaat, Delft*

RUYGROK, P.A. (1994) Dimensioneren van asfaltbekledingen op golfklappen, analyse van de relatie tussen golfbelasting en rekken (in Dutch)(Report CO-347160/17), *Grondmechanica Delft, Delft*

11 Conclusions and recommendations

The conclusions in this chapter are divided into three different parts. In the first part conclusions are stated with respect to the recalculation of the strains calculated by de Waal. In the seconds part conclusions are stated about the strains simulated with the Monte Carlo method. In the last part conclusions and recommendations are given with respect to this investigation and further research.

11.1 Conclusions recalculation

In the recalculation a better agreement between the measured and calculated strain is obtained. When the calculation performed by de Waal is compared with the recalculation some conclusions of the results can be made:

- the model gives good results for the calculation of the <u>dynamic</u> strain. This is confirmed by Ruygrok (1994)
- when the strain signal is studied an irregular character is found. This irregular character makes modelling the strain difficult
- the recalculated modulus of elasticity used in the calculation is much higher
- the recalculated modulus of the subgrade is lower
- the strain measuring devices are placed at about 2 cm above the base in the revetment and therefore a lower layer thickness is taken into account
- the relation between the maximum impact pressure and the strain is lost in the calculation of de Waal, the recalculation show a relation between maximum impact pressure and the strain
- the differences between the measured and calculated strains are larger for runs where irregular waves are used than where regular waves are used
- at the right side of the flume the strains are more comparable than at the right side of the flume
- over the width of the flume, there is a spatial difference of the impact pressure. When this spatial difference is taken into account the relation between calculation and measurements improves (although the model cannot be applied according to the schematizations).
- it is difficult to divide the dynamic strain and the quasi-static strain from each other
- by dividing the dynamic strain and the quasi-static strain the relation with the maximum impact pressure is lost
- the recalculated values of the strain show less deviation than the measured values

11.2 Conclusions Monte Carlo simulation

After the comparison with de Waal where the measurement and the calculation are fairly in agreement with each other, the results of the Monte Carlo simulation are surprising. There are large differences between the distributions of the measured and calculated strain and in general the measured strains are larger than the calculated strains.

The differences between measured and simulated strains are caused by:

- the distribution function of the impact factor is measured in the middle of the flume while the strain is given for VPL 1, 3 or 4
- the distribution function of the impact factor is given for a range of pressure transducers, not for one specific transducer, and only for maximum wave impacts. The effect of using the distribution of one pressure transducer is not known.
- the measured strain is given for maximum wave impacts at the range of the pressure transducers. The dynamic strain is calculated and the total strain is given. This explanation is confirmed by the fact that the calculated strains are lower than the measured strains

Conclusions regarding the simulation:

- the simulation is sensitive to the impact factor distribution, more information about this distribution is needed
- the measured shape of the distribution function of the strain is in agreement with the shape of the simulated distribution function
- the deviation of the calculated strain is more than the deviation of the measured strain
- the modulus of the subgrade reaction can be used to take the differences between the dynamic strain and quasi-static strain into account

11.3 General conclusions

Conclusions regarding the model:

- the model gives good results for the calculation of the dynamic strain. This is also confirmed by Ruygrok (1994)
- more insight into the difference between dynamic strain and quasi-static strain is needed
- the impact factor distribution of GOLFKLAP is in agreement with the impact factor distributions found in this thesis

Recommendations:

- the effect of a wave load which is not symmetrical still has to be investigated
- when a stochastic approach is used in analysing the experiment one should have information for all the observation in the experiment and not only for maximum wave impacts
- also information about the distribution over the width of the flume is needed
- the modulus of the subgrade can be used for making differences in between the dynamic and quasi-static strain
- the influence of the quasi-static strain should be investigated. If the influence of the quasi-static is important for the damage by fatigue this part of the strain should also be taken into account

12 References

Ashby, M.F. and Jones, D.R.H. (1987) Engineering Materials 1, An Introduction to there Properties and Applications, *Pergamon Press, Oxford*

Bardends F.B.J. (1980) Dynamics of elastic plates on a flexible subsoil. LGM-Mededelingen, deel 12, *Laboratorium voor Grondmechanica, Delft*

CROW (2005) Standaard RAW Bepalingen (in Dutch), *CROW, Ede*

CUR (1997) CUR 190 "Probabilities in civil engineering, Part 1: Probabilistic design in theory", *CUR, Gouda*

De Looff, A.K. (2002) Beoordeling Asfaltbekleding Lauwersmeerdijk en Eemshaven (Report 028292)(In Dutch), *Netherlands Pavement Consultants, Utrecht*

De Looff, A.K. (2003) Literatuurstudie Verificatiemetingen 3-Puntsbuigproef (Report 028126)(In Dutch), *Netherlands Pavement Consultants, Utrecht*

De Looff, A.K. (2004) Veiligheidsbeoordeling asfaltbekleding Houtribdijk - toetsing op treksterkte (Report e048163)(In Dutch), *KOAC•NPC, Nieuwegein*

de Looff, A.K. et al (2004) Handleiding GOLFKLAP 1.2 (Report e038390) (in Dutch), *KOAC•NPC, Nieuwegein*

de Looff, A.K. et al (2006) Golfklap a Model to Determine the Impact of Waves on Dike Structures with an Asphaltic Concrete Revetment, *Proceedings ICCE 2006, San Diego, USA*

de Waal, J.P. (1993) Gedrag van asfaltbekleding onder golfaanval, Relatie tussen belasting en rek (in Dutch)(Report H 1702), *DWW Rijkswaterstaat, Delft*

Dekking, F.M. Et Al (2004) Probability and Statistics for the 21st Century, *Delft University of Technology, Delft*

Derks, H. and Klein Breteler, M. (1992) Gedrag van asfaltbekleding onder golfaanval, verslag modelonderzoek in Deltagoot, with annexes (in Dutch)(Report H 1480), *DWW Rijkswaterstaat, Delft*

Führböter, A. and Sparboom, U. (1988) Full-Scale Wave Attack of Uniformly Sloping Sea Dykes, *Proceedings ICCE 1988, Malaga, Spain*

Grüne, J. (1988) Wave-induced Shock Pressures under Real Sea State Conditions, *Proceedings ICCE 1988, Malaga, Spain*

Johnson, R..A. (2000) Miller & Freund's Probability and Statistics for Engineers, *Prentice Hall International (UK) Limited, Sydney*

Klein Breteler, M. (2007) Validatie van GOLFKLAP (Report H4134) (in Dutch), *WL | Delft Hydraulics*

Klein Breteler, M. (2006) Kwantificering golfbelasting en invloed lange golven (Concept report H4421)(in Dutch), *WL | Delft Hydraulics*

Ruygrok, P.A. (1991) Parameterbepalingen voor het zand en de asfaltbekleding van het TAW A4 Dijkmodel in de Deltagoot (in Dutch)(Report CO-324970/7), *Grondmechanica Delft, Delft*

Ruygrok, P.A. (1992) Parameterstudie voor formulering van een equivalente effectieve veerconstante voor het plaat op veren model (in Dutch)(Report CO-336530/6), *Grondmechanica Delft, Delft*

Ruygrok, P.A. (1994) Dimensioneren van asfaltbekledingen op golfklappen, analyse van de relatie tussen golfbelasting en rekken (in Dutch)(Report CO-347160/17), *Grondmechanica Delft, Delft*

Schönian, E (1999) Shell Bitumen Hydraulic Engineering Handbook, *Shell International Petroleum Co. Ltd, London*

Sparboom, U. (1991) Full-Scale investigations on Wave Loadings of Sea Dyke Structures, *Proceedings 3rd International Conference on Coastal and Port Engineering in Developing Countries 1991, Mombasa, Kenia*

'T HART, R (2008) Scheur ten gevolge van golfbelasting in een al gescheurde asfaltbekleding (Report 435340-0004 v01) (in Dutch), *Stowa, Utrecht*

TAW (1984) Leidraad voor toepassing van asfalt in de waterbouw (in Dutch), *Staatsuitgeverij, 's Gravenhage*

VAN VLEDDER, G. PH. (1990) Literature survey to wave impacts on dike slope (Report H976), *Delft hydraulics, Delft*

VERSLUIS, A. (1991) 3-puntsbuigproeven aan balken van boorkernen uit de deltagoot (Report 91523-2 or DWW-504)(In Dutch), *Netherlands Pavement Consultants, Hoevelaken*